AN ABSTRACT OF THE THESIS OF

Shaun F. Kelly for the degree of Doctor of Philosophy in Civil Engineering presented on January, 9, 1998. Title: Non-convective Ion Movement in Unsaturated Porous Media.

Redacted for Privacy

Abstract approved. _____

John S. Selker

Ion movement in porous media is of broad interest in engineering, science and agriculture. In agriculture, crystalline fertilizer may be applied to the surface of a soil or other media and physically shielded from surface applied water to minimize leaching and conserve fertilizers. This dissertation explored the basic underlying physical processes of this practice whereby coupled ion-water movement results from the addition of salts to the surface of a hydrostatic unsaturated porous medium. Experiments were conducted where KBr and NaBr salts were placed at the surface of sealed columns filled with a peat:vermicultite (1:1 by volume) container medium at initial water contents of 4.0, 2.5 or 1.0 g_{H20} /g_{media}. Bromide and water distributions were determined in replicated columns after 5, 10, 25 and 120 days. Diffusion rates increased with increasing water content. Differences in the hygroscopicity and solubility of KBr and NaBr affected the distribution of water and diffusion rates. Redistribution of water was most apparent at low water content. At high water content, water redistribution was affected by solution density gradients. Using an analytical solution to the Fickian diffusion model gave useful diffusion estimates at medium water contents but was of limited predictive value in the high and low water content media. Effective diffusion coefficients calculated for Br^- in

the medium at 2.5 g_{H20} /g_{media} ranged from 2.7 - 4.6 $\cdot 10^{-10} \cdot m^2$ /sec which is 3 to 9 times less than the diffusion coefficient in water alone. Experiments showed that salts at high concentrations in unsaturated porous media induce significant water vapor flow caused by large gradients in osmotic potential. Existing theories of water vapor diffusion and aqueous electrolyte thermodynamic theory were combined to model the observed water vapor flow and validated using experimental data previously published by Wheeting, (1925). Finally, a complete model was developed describing the simultaneous diffusion of salts, water vapor and liquid water flow. The model was implemented numerically and verified using experimental data. It was shown that the model correctly accounted for the coupled liquid-vapor-salt transport process and that these processes significantly affect the quantity and distance of salt entering the media.

Non-convective Ion Movement in Unsaturated Porous Media

by

Shaun F. Kelly

A THESIS

submitted to

Oregon State University

in partial fulfillment of
the requirements for the
degree of

Doctor of Philosophy

Presented January 9, 1998
Commencement June, 1998

Doctor of Philosophy thesis of Shaun F. Kelly presented on January 9, 1998

APPROVED:

Redacted for Privacy

Major Professor, representing Civil Engineering

Redacted for Privacy

Head of Department of Civil, Construction and Environmental Engineering

Redacted for Privacy

Dean of Graduate School

I understand that my thesis will become part of the permanent collection of Oregon State University libraries. My signature below authorizes release of my thesis to any reader upon request.

Redacted for Privacy

Shaun F. Kelly, Author

ACKNOWLEDGMENT

The author wishes to acknowledge Agricultural Research Foundation for financial support of parts of this thesis.

CONTRIBUTION OF AUTHORS

Dr. John S. Selker and Dr. Jim Green assisted in the interpretation of the data and preparation of the manuscript entitled "Fertilizer Diffusion in Container Medium". The laboratory analyses were performed in the laboratory of Dr. Jim Green.

TABLE OF CONTENTS

TABLE OF CONTENTS (Continued)

Page

TABLE OF CONTENTS (Continued)

Page

LIST OF FIGURES

LIST OF FIGURES (Continued)

LIST OF FIGURES (Continued)

Figure Page

LIST OF TABLES

LIST OF APPENDIX FIGURES

LIST OF APPENDIX FIGURES (Continued)

LIST OF APPENDIX TABLES

DEDICATION

This thesis is dedicated to Maria, Jasper and Seth.

Non-convective Ion Movement in Unsaturated Porous Media

Chapter 1. Introduction

1.1 Background

Horticultural crop production, including orchards, vineyards, nurseries and greenhouses use traditional production systems where unprotected fertilizer is moved in solution with applied water through and beyond the plant root zone often resulting in leaching losses that contaminate ground and surface waters. The recent increased awareness of protecting water quality is recognized by the horticultural industry and many solutions have been proposed and are already practiced. Current solutions include; timing of fertilizer application (Hershey et al., 1982), collection and treatment of runoff, and reduction of water use by using drip irrigation and irrigation scheduling (Ticknor and Green, 1987). Production systems are currently being designed at Oregon State University to minimize leaching losses by physically shielding the fertilizer from applied surface water. These systems rely on processes other than bulk convection to get the fertilizer ions to the plant roots where uptake occurs. The "Closed Insulated Pallet System" (CIPS) and the "Conserver" are two systems that use the idea of shielding the fertilizer from applied surface water.

CIPS is a plant production system currently being evaluated at Oregon State University for container grown nursery crop production. As shown in Figure 1, upward movement of bulk water from a reservoir below the plant container through a capillary

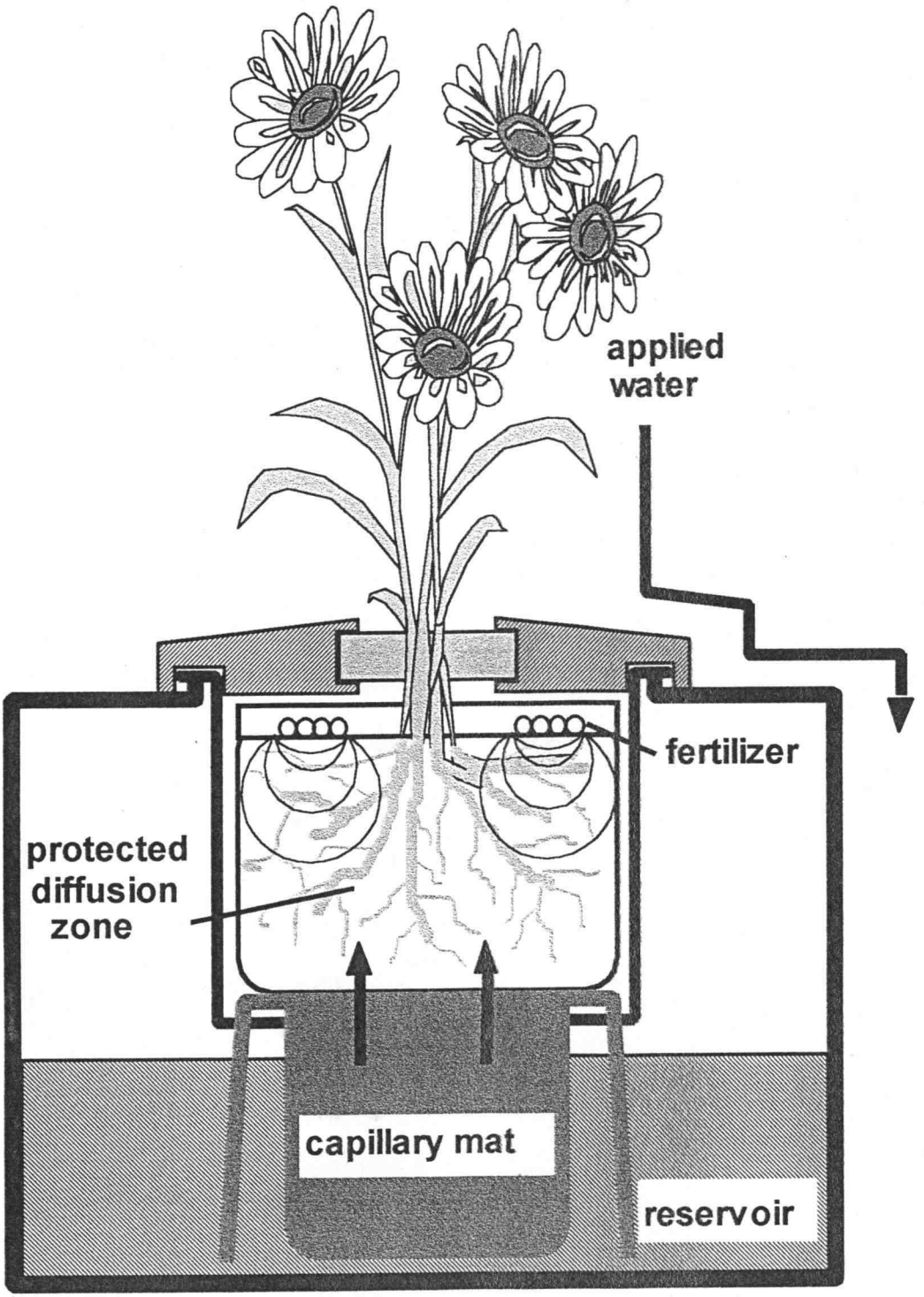

Figure 1. Closed Insulated Pallet System (CIPS).

mat to the media at the bottom of the plant container is one characteristic of CIPS. Water is drawn upward by the matric potential of the media and subsequently removed by the transpiring plant through roots distributed in the media. The sealed upper surface of the media provides a no flux boundary and a shielded root zone. The system is referred to as "plant driven" because plant growth and transpiration dictate the water flux through the systems.

Another characteristic of CIPS is the placement of fertilizer. At planting time enough fertilizer is applied to the upper media surface to satisfy the plants nutrient needs until the plant is removed from CIPS. The plant roots take up fertilizer ions as they move downward through the media. The flux of ions is driven in part by diffusion and chemical potentials set up through solute concentration gradients and adsorption in the media. Ideally, the downward ion flux through the media should be equal to plant uptake of ions. Since one objective of CIPS is to minimize waste nutrients (i.e. maximize nutrient use), it is preferable that fertilizer ions remain in the media. If the flux of fertilizer ions exceeds plant uptake and adsorption capacity of the media, movement of ions into the CIPS water supply reservoir could occur. Conversely, if ion movement is insufficient, plant development may be delayed or stunted.

Consideration of "plant-driven" movement of water and fertilizer uptake in CIPS led to the concept of a "protected diffusion zone" for conservation of fertilizer in traditional open intensive crop production systems. Fertilizer can be protected in CIPS or similarly in the Conserver in an open production system (Fig. 2). The Conserver is a moisture-impermeable fertilizer compartment with vertically extended side-walls enclosing a diffusion zone protected from the water flow pathways associated with

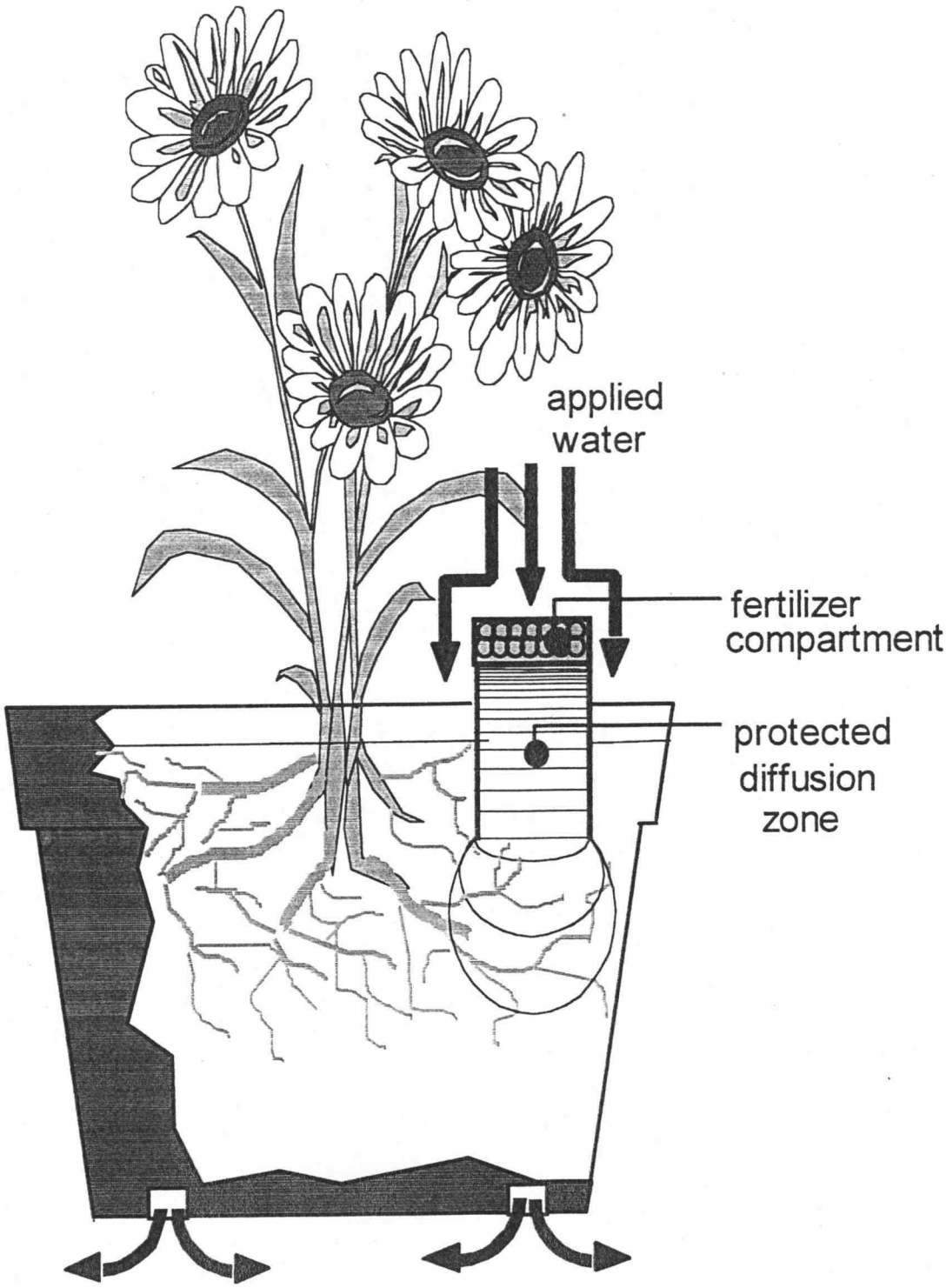

Figure 2. Conserver.

evaporation and leaching. In June 1991, Briggs Nursery, Olympia WA and Oregon State University initiated research to determine feasibility of conserving fertilizer within a protected diffusion zone. Results from this research suggest that the movement of nitrate within the protected diffusion zone is between rates reported for diffusion in pure water, 1.9×10^{-5} cm^2 sec^{-1} at 25°C (Erdey-Gruz, 1974) and values for diffusion in field soils, 10^{-6}-10^{-7} cm^2 sec^{-1} (Barber, 1974). In CIPS and in the Conserver with a peat:vermiculite media, the observed effective diffusion coefficient for NO_3^- has been approximately 2.0×10^{-6} cm^2 sec^{-1} (Blackburn, 1992). At this rate, in the absence of root uptake, 37% of the nitrate diffuses beyond the 6-inch length of the protected diffusion zone over a one year period. Nitrate and potassium were observed moving faster in the regions of higher moisture content. With plants in the system, roots were observed growing into the protected diffusion zone and intercepting the nutrients before leaving the Conserver. When applying fertilizer within a protected zone, a plant's total fertilizer requirement can be met by direct root contact and interception of fertilizer as it exits the Conserver.

To characterize nitrate fertilizer movement, nitrates in particular, in a protected diffusion zone, this dissertation focuses on the movement of the Br^-, bromide. Bromide is frequently used to characterize the movement of nitrate in soils because concentrations are easily determined by using a selective ion electrode and it doesn't undergo chemical transformations like nitrate. By using a conservative tracer like bromide, there are no chemical transformations occurring in the media and nitrate movement will tend to be overestimated. This will lead to a more conservative estimate concerning leaching potential of nitrate. Diffusion rates of anions have been observed to vary depending on initial ion concentration and soil water content (Klute and Letey, 1958; Patil et al., 1963;

Olsen et al., 1965; Schaff and Skogley, 1982; Barber, 1984). Establishment of the reliability of the Conserver and the CIPS systems in production settings requires the development of an engineering model to predict fertilizer movement. This model should include the effects of moisture content, media, and fertilizer amount on the rate of movement of fertilizer within the protected diffusion zone.

1.2 Related Applications to this Research

This research is directed to develop further understanding of ion movement in CIPS and the Conserver. But more broadly, it has applications in other including soil fertility, dispersion of placed fertilizer and salt movement in soils.

The rate of fertilizer movement to the root is sometimes more limiting than the actual quantity of fertilizer that is available (Massee et al., 1977). Diffusion is the major process affecting P and K movement to plant roots in many soils. Diffusion affects the availability of P and K in a soil, and differences in availability between soils are probably due to diffusion rates (Barber et al., 1963).

Geraldson (1990) concluded that intensive tomato production systems that depend on fertilizer concentration gradients in the media to provide nutrients have advantages over fertigation systems, where fertilizer is applied to the root environment through irrigation. Fertilizer concentration gradients provide a range of N and K concentrations to better meet plant uptake demands at different stages of growth. Fertigation systems, on the other hand, provide homogeneous ionic concentrations of N and K in the root environment that cannot always meet differential plant uptake demands and are more vulnerable to nutrient deficiency as compared to gradient fertilizer systems (Geraldson,

1990). With gradient fertilizer systems it has also been shown that root specialization occurs with tomatoes in response to unequal fertilizer distribution in the root environment. Roots in areas with high concentrations of nutrients will preferably take up nutrients and roots in areas of low nutrient concentrations will preferably take up water (Sonneveld and Voogt, 1990).

This research began with the following questions relating to the design of CIPS and the Conserver. How fast does the fertilizer move and how can we prevent it from reaching the reservoir in CIPS? What are the factors affecting fertilizer movement in the Conserver and what are the design limits affected by the ion movements? These questions query the same principle, that of non-convective ion movement in unsaturated porous media. If the problem of describing non-convective ion movement in unsaturated porous media is solved, then the specific questions relating to CIPS and the Conserver will have been solved.

Since non-convective ion movement in unsaturated porous media is a broad topic, the scope of this thesis is focused on examining ion movement in conditions similar to the conditions that are found in the CIPS and Conserver environments. This thesis is limited to the following conditions: (1) There is no bulk convection of ions (i.e. no external water flows created by application of water); (2) The media to be considered will be restricted to horticultural media likely to be used in horticultural production systems such as 50% peat: vermiculite; (3) The moisture contents of the media to be considered will be within the range necessary for production, between "field capacity" and about 20 kPa tension; (4) Bromide is the representative anion to be considered for reasons discussed in the previous section.

The scope is further focused by solving for the most conservative engineering design, or "worst case" scenario. In looking at the CIPS, one design goal concerning ion movement is to keep fertilizer ions out of the reservoir but still provide enough for plant growth. Keeping this design goal in mind leads one to the worst case scenario where there is no plant uptake of fertilizer ions, no transformations of ions and no interaction between the ions and the particles that make up the porous media. Therefore, the most useful information for design of CIPS and the Conserver may be found through column experiments examining bromide movement in unsaturated porous media without plants.

The general goal of this research is to find the rate of ion movement in the absence of convection in porous media and the mechanisms that control this rate. This goal is to be achieved through laboratory column experiments and mathematical modeling of the phenomena. The modeling and laboratory experiments are designed to be complementary. Mathematical models are used to design relevant column experiments and the column experiments provide the models with the appropriate coefficients and observed phenomena to be modeled.

Chapter I provides a general description of the CIPS and the Conserver and serves as an introduction for the entire thesis. Chapter II, *Theory and Concepts,* is a general literature review for the entire thesis covering ion movement, diffusion, water potentials and movement and time-domain reflectometry. Chapter III, *Fertilizer diffusion in container media*, presents experimental evidence for the importance of vapor driven processes in ionic movement. The effects of media, moisture content, ion concentration and species on movement are investigated. Estimates of Fickian diffusion coefficients are obtained, and the need for more rigorous analysis is shown. In Chapter IV, *Osmotically*

driven water vapor transport in unsaturated soil, it is shown how osmotic potentials in the presence of high salt concentrations can cause significant water vapor movement in soils. In Chapter V, *Modeling ion diffusion and osmotic water vapor transport in unsaturated porous media,* concepts and theory of ion movement are quantified through combinations of mass balance and diffusion equations. Chapters III, IV and V will be presented as separate, standalone manuscripts. Chapter VI serves as the conclusion for the entire thesis and is followed by a comprehensive Bibliography and Appendices.

Chapter 2. Theory and Concepts

This chapter is a general literature review for the entire thesis covering ion diffusion, solute movement, water transport, and the use of time domain reflectometry techniques in unsaturated porous media. It will lay out the groundwork of this thesis by presenting the most relevant up to date literature which will serve as the basis for laboratory techniques, experimental design, analysis of the data and modeling.

2.1 Ion Diffusion

The transport processes involved in the movement of ions in a porous media are generally known as diffusion and convection. Diffusion and convection are important natural processes intensively studied in nearly every branch of science. As a result, many different definitions, mathematical notations and transport theories with varying degrees of complexity and rigor have been developed to suit the intended application. Diffusion is usually treated on two levels: a molecular level which considers the individual ions or at the macroscopic level which is geared more towards applications.

Simple molecular theories have been developed to calculate diffusion coefficients, which depend solely on the viscosity of the solvent and diameter of the solute molecules when the size of the solute molecule is greater than the solvent molecule (Einstein 1908). Rigorous theories on the molecular level make use of the kinetic theory of gases. The "dusty gas model" is a recently developed theory that clarifies many of the problems of past theories including the nature of the total diffusive flux of a system and the nature of

the coupling between the diffusive and viscous fluxes (Cunningham and Williams 1980). Techniques of non-equilibrium statistical thermodynamics can provide, in principle, methods for calculating transport properties from basic molecular properties (Tyrrell 1984). These rich and relatively complex theories of diffusion have not generally been embraced by scientists in the study of ion transport processes in soils. The level of rigor most useful for solving ion transport processes in soils is on the macroscopic level. The rest of this section on ion movement will be limited to a review of these processes on a macroscopic level rather than a molecular level unless necessary. In the field of soil science and agronomy, it is generally accepted that diffusion results from the net movement of ions by thermal motion resulting from the existence of a concentration gradient and convection results from conveyance of the ion as a result of motion of the solution, (Olsen and Kemper 1968), and is sometimes referred to as viscous flux, viscous flow or advection. It has long been realized that osmotic pressure can be looked upon as the driving force in diffusion phenomena (Einstein 1908). Diffusion can also be looked upon as the result of the distribution of osmotic pressure (related to chemical potential) in the solution, the mobility of the ion in solution and the irregular motions of the solute molecules produced by thermal molecular movement. Superimposing these processes leads to a general theory of Brownian movement or diffusion.

2.1.1 Fick's Laws

Diffusion can be considered to be a 'flow' taking place under the influence of a 'force'; in the case of ion diffusion the forces are the gradients of concentration. Analogies

to this are heat flow (Fourier's law) and electrical flow (Ohm's law) (Tyrrell 1984). Fick's first law describes ionic diffusion and is shown here in one dimension:

$$J_i = -D_i \frac{dC_i}{dx} \qquad [1]$$

where J_i is the flux or flux density of ion species i in units of mass, or moles, per unit area per unit time across a defined reference plane perpendicular to the direction of flow in the x-direction; D_i is the diffusion coefficient of ion species i in units of length squared per unit time; C_i is the concentration in mass, or moles of ion species i per unit volume. The negative sign arises because diffusion occurs in the direction opposite to that of increasing concentration. Fick's first law is useful for steady state analysis of diffusion process. Eq. [1] is valid only for an isotropic media, whose structure and diffusion properties, D_i are the same at all points along the x-direction. The diffusion coefficient is typically considered to be constant and independent of the ion concentration.

First formulated in 1855 by direct analogy with Fourier's equations of heat conduction, Fick's second law is commonly regarded as the diffusion law or differential equation of diffusion (Tyrrell 1984; Crank 1975). It is useful for solving diffusion problems in transient conditions. Fick's second law may be derived from the first law in conjunction with the continuity equation or conservation of mass (Crank 1975; Olsen and Kemper 1968). Fick's second law in one dimension is:

$$\frac{dC_i}{dt} = \frac{d}{dx}\left(D_i \frac{dC_i}{dx} \right) \qquad [2]$$

where t is the time. If the diffusion coefficient is constant with position Eq. [2] may be written

$$\frac{dC_i}{dt} = D_i \frac{d^2C_i}{dx^2} \qquad [3]$$

If the diffusion coefficient is time dependent and not a function of the other variables (i.e. where $D_i=f(t)$), a new time scale, T, may be introduced such that $dT=f(t)dt$. The diffusion equation may then be written:

$$\frac{dC_i}{dT} = \frac{d^2C_i}{dx^2} \qquad [4]$$

which is the same form as Eq. [2] where D_i is equal one. This form of the diffusion equation is useful when analytical solutions are needed when the diffusion coefficient is a function of time (Crank 1975).

Many analytical solutions to the diffusion equation, Eq. [2] can be found in Crank (1975). A solution of interest in the present study is the case of the semi-infinite medium, where a constant ion concentration, C_i is present at one end at all times,

$$C_i = C_{i,0}, \quad x=0, \quad t>0, \qquad [5]$$

and where the initial ion concentration throughout the media is zero.

$$C_i = 0, \quad x>0, \quad t=0, \qquad [6]$$

A solution to Eq. [3] for these conditions is found in Crank, 1975.

The function *erfc* is the complementary error function. This solution is plotted in Figure 3.

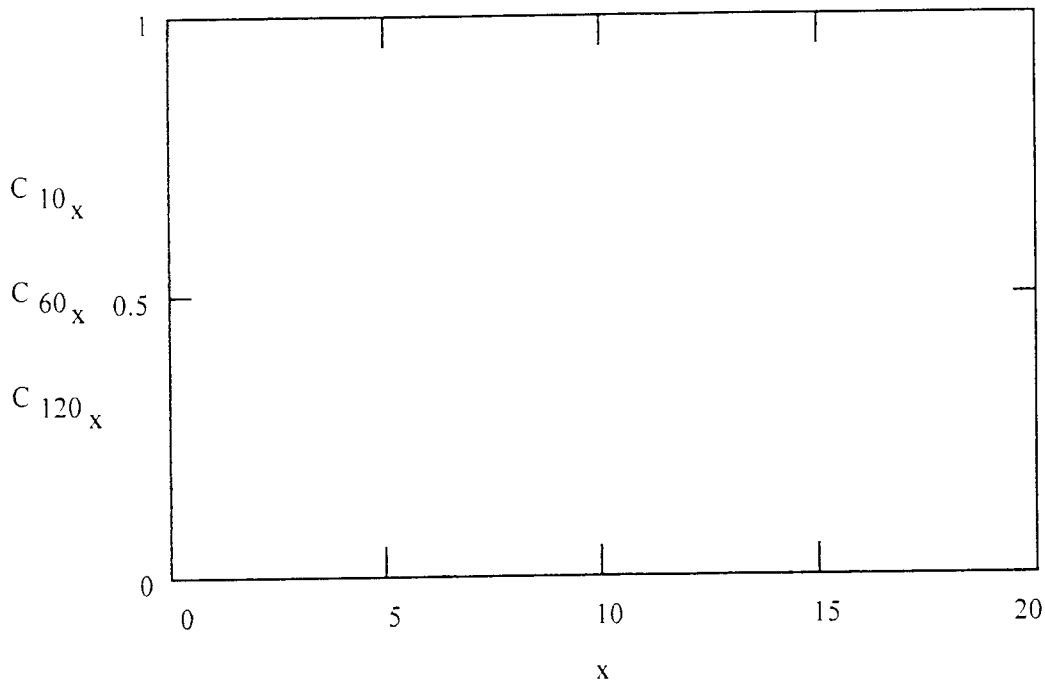

Figure 3. Solution of the diffusion equation in a semi-infinite medium. Di = 2.5 x 10-6 cm2/sec. x is the distance diffused in cm, C10, C60, C120 are the relative concentrations Ci/C0 at times of 10,60 and 120 days.

In many instances the diffusion coefficient cannot be considered constant, for certain special cases it is possible to obtain solutions for variable D_i (Crank 1975). These solutions are limited in application and more difficult to handle. When using the diffusion equation to solve for D_i, it is usually easier to choose experimental conditions such that the variation of the coefficients is sufficiently small so that Eq. [3] may be used. Alternatively steady state conditions may be devised to determine D_i using Fick's first law, Eq. [1] (Tyrrell 1984).

One can obtain different diffusion coefficients for the same ion depending on how the diffusion coefficient is determined. Measurement of diffusion coefficients using two

solutions with the same ion species but with different initial concentrations is termed interdiffusion coefficients or mutual diffusion coefficients (Tyrrell 1984). Concurrent movement of ions of like charge in the opposite direction is sometimes termed intradiffusion (Kemper and Olsen 1968) Concurrent movement of ions of opposite charge in the same direction is termed "salt diffusion" or counter-diffusion (Kemper and Olsen 1968). If it were possible to label some ions in a solution, without otherwise changing its properties and to follow its motion through the unlabelled molecules, D_i would be a self-diffusion coefficient. In studies of ion diffusion in soils many researchers have measured the self-diffusion coefficient of ions using radio-labeled ions (e.g. Patil, et al., 1963; Phillips and Brown 1964; Olsen et al., 1965; Nye, 1966; Mott and Nye, 1968).

2.1.2 Diffusion of Ions in Soil

Fick's first law for steady state diffusion, Eq. [1] can be rewritten using the following notation.

$$\frac{\Delta M}{\Delta t} = -DA\frac{\Delta C}{\Delta x} \qquad [7]$$

ΔM is the mass (or moles) diffusing in time Δt; t is the time; D is the diffusion coefficient [length^2/time]; A is the cross sectional area through which diffusion occurs [length^2]; C is the concentration of the ion in solution [mass/length^3]; x is the distance diffused [length]. When ions diffuse through water in soil or other porous media, ion diffusion is affected by pore geometry, physical properties and chemical interactions.

The charge on an ion affects how the ion will diffuse through the soil. Cations may be adsorbed weakly at the cation exchange sites on clay minerals and actually

participate in diffusion on the clay surfaces. Anions on the other hand are either repelled, not adsorbed or if they are adsorbed, the sites are sufficiently few that they do not contribute to diffusion (Kemper and Olsen, 1968). When a salt diffuses through the soil both anions and cations may diffuse concurrently through the soil and electroneutrality must be maintained leading to electrically coupled ion movement (Rhue, 1992).

To account for pore geometry, physical properties and chemical interactions Eq. [7] is modified by altering the diffusion coefficient to obtain an effective diffusion coefficient, D_p.

$$D_p = -D \cdot \left(L / L_e\right)^2 \cdot A \cdot \theta \cdot \alpha \cdot \gamma \qquad [8]$$

L is the macroscopic distance between two points; L_e is the actual distance through which the ions diffuse; θ is the volumetric water content; α is the relative mobility or fluidity of water, D is the self-diffusion coefficient of the ion in water; and γ is the anion exclusion factor. The diffusion equation can thus be written as,

$$\frac{\partial C}{\partial t} = \frac{-D_p}{\theta} \frac{\partial^2 C}{\partial x^2} \qquad [9]$$

To account for adsorption of cations in soil, it is useful to relate the adsorbed ions and ions in solution by an instantaneous, reversible, linear adsorption isotherm described by

$$C_s = K_d \cdot C \qquad [10]$$

C_S is the concentration of ion adsorbed to the soil [mass/length^3] and K_d is the slope of the isotherm. The diffusion equation including adsorption is written as

$$\frac{\partial C}{\partial t} = \frac{-D_p \quad \partial^2 C}{(\theta + \rho_b K_d)\,\partial x^2} \qquad [11]$$

where ρ_b is the soil bulk density.

2.1.2.1 Buffer Capacity

The soil buffer power, b' has been defined in the literature as the total amount of diffusible ion (solution plus sorbed) per unit volume of soil required to increase the solution concentration by one unit (Van Rees et al. 1990). This is sometimes referred to as the "capacity factor" and the divisor of the effective diffusion coefficient described in Eq. [11]

$$b' = \theta + \rho_b \cdot K_d \qquad [12]$$

Olsen et al. (1964) measured a capacity factor for diffusion of phosphorous in silty clay loam soils and found that the varied from 100-300. These results demonstrated the necessity of measuring a capacity factor when effective diffusion coefficients are to be measured by transient methods (Olsen et al. 1964). Methods for calculating the capacity factor for ions other than phosphorous have not been developed.

2.1.2.2 Tortuosity, $(L/L_e)^2$

When diffusion takes place through water in a soil several geometric factors must be considered. The major effects of the geometric factors are illustrated in the simplified pore shown in Figure 4. The porosity of the solid is $S=x_1/A$. The cross-sectional area

available for diffusion perpendicular to the direction of diffusion is x_2, which, from geometry of the solid, is equal to $x_1(L/L_e)$. Therefore the total area available for diffusion

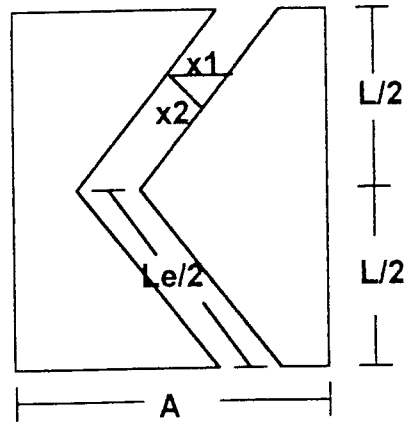

Figure 4. Simplified block of porous media adapted from Porter et al. (1960).

is $x_1(L/L_e)/A=S(L/L_e)$. The actual distance through which diffusion takes place is L_e, so Δx in a porous media is larger by the factor L_e/L. Because the length is increased and the area is reduced the factor L/L_e occurs twice in definition of the effective diffusion coefficient of Eq. [8]. L/L_e is often referred to as the tortuosity or the impedance factor, *f*. Porter et al. (1960) reported that this factor varies from 0.15 at 1 bar suction and even as low as 0.04 at lower water contents. Tortuosity in saturated soils has been reported from 0.35 to 0.53 (Palmer and Blanchar 1980).

2.1.2.3 Viscosity of Water

The viscosity of water increases with decreasing distance from a clay surface (Olsen and Kemper 1968). To account for this effect on the diffusion coefficient the

relative mobility or fluidity of the water, α can be determined. Porter et al. (1960) estimated α in soil to be about 0.8 at 1/3 bar suction Although, greater viscosity near the particle surfaces accounted for an appreciable reduction in diffusion, it was not considered a major factor when compared to the decreasing moisture content.

Viscosity has been found to be inversely proportional to the diffusion coefficient Einstein (1908). Diffusion coefficients can be directly calculated from the molecular size and the viscosity of the solution from the following equation.

$$D = \frac{RT}{N} \cdot \frac{1}{6\pi\eta\rho} \qquad [13]$$

where R is the universal gas constant; T is the absolute temperature, N is Avogadro's number; η is the solution viscosity and ρ is the solute molecule radius. This equation, which is identical to Stokes law, shows that ions with smaller hydrated radius will have a proportionally higher self diffusion coefficient in a given fluid.

2.1.2.4 Anion Exclusion, γ

Repulsion of anions in soil or clay can exclude ions from some of the smaller pores and even larger pores with narrow films of water connecting them. This exclusion of pathways is accounted for by decreasing the effective diffusion coefficient by a factor, γ. For many soils the effect of this interaction on the diffusive movement of ions will be fairly small and γ will be near unity (Porter 1960). Cations are not thought to be excluded from the flow pathways in this manner due to exchange with a mobile fraction on the particle surface (Olsen and Kemper 1968).

2.1.2.5 Water Content

The effect of water content on the diffusion rates of ions in soil has been studied extensively. For Ca-saturated systems Porter (1960) found that the transmission factors for diffusion of chloride (ratio of diffusion the soil to that in pure water) directly proportional to the water content. These factors varied from 0.310 to 0.027 depending on the soil moisture and the soil texture. Schaff and Skogley (1982) found that soil moisture significantly influenced the diffusion of Mg, K and Ca.

2.1.3 Methods of Measuring Diffusion Coefficients in Porous Media

Most methods of measuring diffusion coefficients in porous media are based on transient experiments. Eq. [9] is used by establishing appropriate boundary conditions. The concentrations of the diffusing ions are monitored either at selected time intervals or at a given time at discrete sampling distances. Destructive sampling techniques have been carried out by Saxena et al. (1974) to study the effect of pore size on diffusion of 2-4-D. Brown et al. (1963) used a quick freeze technique and a refrigerated micro-time to section a diffusion cell into 50 μ sections. The subsequent sections were analyzed for a radioisotope tracer.

Radio-labelled tracers were one of the first techniques used to measure the self-diffusion coefficients in soils. Klute and Letey (1958) measured the diffusion of $Rb^{86}Cl$ in columns packed with 75 and 200μ glass beads. The technique utilizes two half cells filled with glass beads. One half cell is saturated with non-labelled RbCl and the other half cell is saturated with radio-labelled $Rb^{86}Cl$. The half-cells are placed together and diffusion is allowed to proceed for a predetermined amount of time until they are

separated and analyzed. Similar techniques were utilized by Phillips and Brown (1964) with Rb^{86}, Graham-Bryce (1963) using radio-labelled Rb^{+},Sr^{+}, and K^{+} and Mott and Nye (1968) using radio-labelled Sr^{+}.

Another technique widely utilized to measure diffusion makes use of an ion exchange resin. Vaidyanathan and Nye (1966) and Baligar (1984) use a method to measure bulk diffusion using a resin exchange paper which acts as a sink at zero concentration when it is placed in contact with the soil. Schaff and Skogley (1982) used a H-saturated resin sink to measure the bulk diffusion of K^{+}, Mg^{++}, and Ca^{++}. Diffusion coefficients can also be derived from measurements of electrical conductivity of the media with the diffusing solute in it (Palmer and Blanchar 1980; Conkling and Blanchar 1989; Conca and Wright 1990). Other methods include use of miniature ion selective electrodes to monitor solute concentration in the porous matrix.

2.2 Water Movement in Unsaturated Porous Media

The basic equation used to model water movement in rigid, homogeneous, isotropic, one-dimensional, isothermal unsaturated porous media is formulated from Richard's equation (1931).

$$\frac{\partial \theta}{\partial t} = \frac{\partial}{\partial z}\left[D(\theta)\frac{\partial \theta}{\partial z}\right] - \frac{\partial K(\theta)}{\partial z} - S_r \qquad [14]$$

θ is volumetric soil water content, t is time, z vertical direction (positive upward), $D(\theta)$ is soil water diffusivity function, $K(\theta)$ is hydraulic conductivity function, and S_r is a sink

or source term. The soil water diffusivity in Eq. [14] may be replaced by the quotient of the hydraulic conductivity divided by the differential soil water capacity,

$$D(\theta) = \frac{K(\theta)}{C(\theta)} \qquad [15]$$

where

$$\text{differential soil water capacity} = C(\theta) = \frac{\partial \theta}{\partial h} \qquad [16]$$

and h is the soil water tension, so that Eq. [14] may also be written as,

$$\frac{\partial \theta}{\partial t} = \frac{\partial}{\partial z}\left[K(\theta)\frac{\partial h}{\partial z}\right] - \frac{\partial K(\theta)}{\partial z} - S_r \qquad [17]$$

2.3 Solute Transport: Advective-Dispersion Equation

The Advective Dispersion Equation (ADE), also called the Convective-Dispersion Equation (CDE) is used as the basis to describe solute transport in porous media.

2.3.1 Scope of Application

Solutes: pesticides, dissolved organics, nitrates, bacteria, viruses, fertilizer, heavy metals. Most aquifer contamination originates in the vadose zone. Often the complicated processes in the vadose zone are considered as a source term for transport in the saturated zone in the vertical direction, although in some cases horizontal transport may be significant.

The ADE assumes the solutes are hydrodynamically inactive. i.e. concentrations are so small that density induced flow is ignored. The flow field is known a priori, or is modeled parallel to transport by use of a flow model. Richard's equation yields heads from which specific flowrates are calculated by means on Darcy's Law. The ADE requires average pore water velocities obtained by dividing specific flowrates by the effective porosity or volumetric water content, θ. For the above reason the transport equation or ADE is less predictive than the flow equation.

2.3.2 Derivation of the Advection-Dispersion Equation

The derivation that follows is found in Bear (1972) and uses vector and tensor notation to derive a general equation in three dimensions. An overview of the derivation is as follows.

1. Use a mass balance on a representative elemental volume (REV) to obtain a solute mass conservation equation in three dimensions.
2. Look at the flux term at a microscopic and macroscopic level to identify transport processes and add these processes into the solute conservation equation.
3. Add in chemical reactions (decay and absorption) to obtain the ADE in three dimensions.

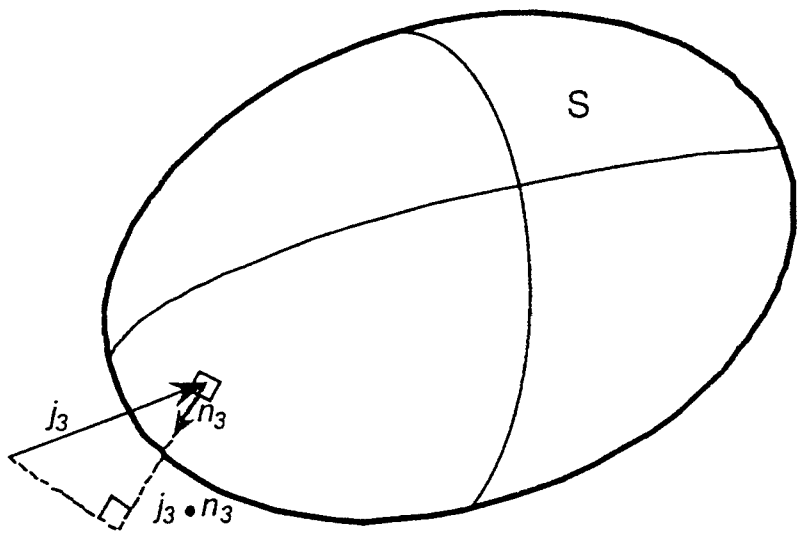

Figure 5. Mass balance on a representative elemental volume (REV) mass in the volume.

2.3.2.1 Solute mass conservation equation.

A mass balance over the REV (Figure 5) requires that the total flux into the REV is equal to the change of stored mass in the REV. That is, the dot product of the three dimensional flux vector, $\mathbf{j}_3$, and the unit normal vector, $\mathbf{n}_3$, over the boundary surface, S, and sources and sinks, σ equals the time rate of change in storage of mass inside the REV. C is the total mass of solute per unit volume in the volume and $\partial C/\partial t$ is the time rate of change of solute mass. This mass balance is shown in Eq. [18].

$$-\oint_S (\mathbf{j}_3 \cdot \mathbf{n}_3)\, dS + \int_V \sigma\, dV = \int_V \frac{\partial C}{\partial t}\, dV \qquad [18]$$

A flux across the surface and into the volume is defined as being negative. The first term in Eq. [18] is the mass entering into the volume as a flux through the surface. The second term is the source/sink term or the mass of solute generated or decayed per unit time in the volume. The third term on the right hand side of Eq. [18] is the time rate of change of To simplify Eq. [18] we will transform the first surface integral into a volume integral to correspond with the latter volume integrals by means of the Gauss Divergence Theorem, Eq. [19].

$$\oint_S (\mathbf{k} \cdot \mathbf{n}) dS = \int_V (\nabla \cdot \mathbf{k}) dV \qquad [19]$$

So we find,

$$\oint_S (\mathbf{j}_3 \cdot \mathbf{n}_3) dS = \int_V (\nabla_3 \cdot \mathbf{j}_3) dV \qquad [20]$$

then substituting Eq. [20] into Eq. [18] to obtain three volume integrals

$$-\int_V (\nabla_3 \cdot \mathbf{j}_3) dV + \int_V \sigma dV = \int_V \frac{\partial C}{\partial t} dV \qquad [21]$$

which can rearranged as

$$\int_V \left[(\nabla_3 \cdot \mathbf{j}_3) + \frac{\partial C}{\partial t} - \sigma \right] dV = 0 \qquad [22]$$

Since the volume is considered arbitrary, this requires that the integrand under the volume integral is zero for all points which leads to the solute mass conservation equation in three dimensions.

Change in storage with time = Fluxes into (-) and out + sources and sinks

$$\frac{\partial C}{\partial t} = -(\nabla_3 \cdot \mathbf{j}_3) + \sigma \qquad [23]$$

2.3.2.2 Flux term, $\mathbf{j}_3$.

Next we will consider the flux term, $\mathbf{j}_3$, at a microscopic and macroscopic level to identify the transport processes of convection, diffusion and dispersion and show how these transport processes can be added into the solute conservation of mass equation to obtain the advective-dispersion equation.

2.3.2.2.1 Microscopic Phenomena

If we look at the transport phenomena on a microscopic level between pores (Figure 6), we can identify two processes, convection (advection) and molecular diffusion, which is a random process described by Fick's Law.

2.3.2.2.1.1 Convective Transport

The rate of convective mass flow through the area, dA, at point $\mathbf{x}_3$ is the dot product of the three dimensional fluid velocity vector, $\mathbf{u}_3$ and the unit normal vector, $\mathbf{n}_3$ to the area, dA, all multiplied by the concentration of solute in the fluid, c. The solute concentration has units of mass of solute per unit volume of fluid,

$$\begin{matrix}\text{convective mass} \\ \text{transport through dA}\end{matrix} = (\mathbf{u}_3 \cdot \mathbf{n}_3)c\ dA = (\mathbf{j}_{conv} \cdot \mathbf{n}_3)dA \qquad \left[\frac{\text{mass}}{\text{time}}\right] \qquad [24]$$

where the convective mass flux, $\mathbf{j}_{conv}$, is defined as.

$$\mathbf{j}_{conv} = \mathbf{u}_3 c \qquad \left[\frac{\text{mass}}{\text{time} \times \text{area}}\right] \qquad [25]$$

2.3.2.2.1.2 Diffusive Transport

Fick's Law states that the net rate of diffusive mass transport is proportional to the negative gradient of concentration normal to the area, dA. Therefore,

$$\begin{matrix}\text{diffusive mass} \\ \text{transport through } dA\end{matrix} = -D\frac{\partial c}{\partial \mathbf{n}_3} dA = -D(\nabla_3 c \cdot \mathbf{n}_3) dA \qquad \left[\frac{\text{mass}}{\text{time}}\right] \qquad [26]$$

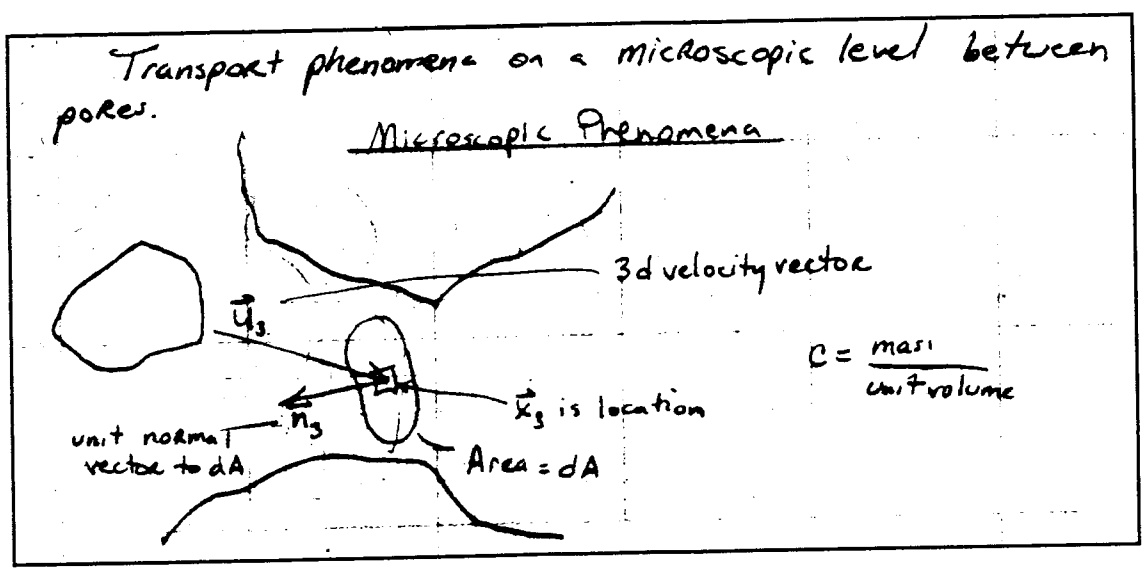

Figure 6. Microscopic transport phenomena in a pore

$$-D(\nabla_3 c \cdot \mathbf{n}_3)dA = (\mathbf{j}_{diff} \cdot \mathbf{n}_3)dA \qquad \left[\frac{\text{mass}}{\text{time}}\right] \qquad [27]$$

where the diffusive mass flux, $\mathbf{j}_{diff}$, is defined by Eq.[28].

$$\mathbf{j}_{diff} = -D\nabla_3 c \qquad \left[\frac{\text{mass}}{\text{time} \times \text{area}}\right] \qquad [28]$$

D, is the diffusion coefficient, which is the proportionality constant described in Fick's Law and ∇_3 is a vector quantity.

The total microscopic scale flux, $\mathbf{j}_3$, is the sum of both the convective, $\mathbf{j}_{conv}$, and diffusive, $\mathbf{j}_{diff}$, mass fluxes.

$$\mathbf{j}_3 = \mathbf{j}_{conv} + \mathbf{j}_{diff} = \mathbf{u}_3 c - D\nabla_3 c \qquad [29]$$

The three-dimensional vector, $\mathbf{j}_3$, represents the mass flux of solute at an point in space.

2.3.2.2.2 Macroscopic Phenomena

We can look at the total solute flux, $\mathbf{j}_3$, on a macroscopic scale to understand how dispersion arises. On a macroscopic scale, the total solute flux, $\mathbf{j}_3$, is the sum the convective flux, $\mathbf{j}_{conv}$, the flux due to molecular diffusion, $\mathbf{j}_{diff}$, and the flux due to mechanical dispersion, $\mathbf{j}_{disp}$. Where the diffusive flux and the dispersive flux are both modeled by a random Fickian process analogous to Fick's Law. The particular flow path of the fluid depends on physical properties of the porous matrix structure and the volumetric fluid content or effective porosity contributing to flow. On a macroscopic scale, this gives rise to fluids moving at different velocities and a solute particle will travel with a velocity either faster or slower than the average fluid velocity depending on

the flowpath followed. Therefore, to introduce dispersion into the ADE we need to calculate average fluid velocities and solute concentrations and local deviations from these averages.

$$\mathbf{u}_3 = \overline{\mathbf{u}_3} + \delta\mathbf{u}_3 \qquad [30]$$

$$c = \bar{c} + \delta c \qquad [31]$$

Averages are denoted by over bars and the deviations from the average are denoted by δ. We substitute Eqs. [30] and [31] into the flux equation derived on a microscopic scale, Eq. [29].

$$\mathbf{j}_3 = (\overline{\mathbf{u}_3} + \delta\mathbf{u}_3)(\bar{c} + \delta c) - D\nabla_3(\bar{c} + \delta c) \qquad [32]$$

$$\mathbf{j}_3 = \overline{\mathbf{u}_3 c} + \overline{\mathbf{u}_3}\delta c + \delta\mathbf{u}_3\bar{c} + \delta\mathbf{u}_3\delta c - D\nabla_3\bar{c} - D\nabla_3\delta c \qquad [33]$$

To obtain a volume averaged flux we multiply the right side of Eq. [33] by the fraction of the volume taking part in the flow which is the volumetric water content, θ, and take averages of all terms.

$$\overline{\mathbf{j}_3} = \theta(\overline{\overline{\mathbf{u}_3 c}} + \overline{\overline{\mathbf{u}_3}\delta c} + \overline{\delta\mathbf{u}_3\bar{c}} + \overline{\delta\mathbf{u}_3\delta c} - \overline{D\nabla_3\bar{c}} - \overline{D\nabla_3\delta c}) \qquad [34]$$

To simplify Eq. [34] we note that the following terms are equal to zero.

$$\overline{\overline{\mathbf{u}_3}\delta c} = \overline{\delta\mathbf{u}_3\bar{c}} = \overline{D\nabla_3\delta c} = 0 \qquad [35]$$

This is because by definition an average of the deviation terms defined by Eqs. [30] and [31] have to equal zero and if we multiply the deviation by a constant as in the terms in

Eq.[35], the result of the average is still zero. The total flux is then expressed as the sum of three separate fluxes.

$$\overline{\mathbf{j}_3} = \theta(\overline{\overline{\mathbf{u}_3 c}} + \overline{\delta\mathbf{u}_3 \delta c} - \overline{D\nabla_3 \bar{c}}) \quad [36]$$

$$\text{convective flux} = \mathbf{j}_{conv} = \theta\overline{\overline{\mathbf{u}_3 c}} \quad [37]$$

$$\text{diffusive flux} = \mathbf{j}_{diff} = -\theta\overline{D\nabla_3 \bar{c}} \quad [38]$$

$$\text{dispersive flux} = \mathbf{j}_{disp} = \overline{\theta\delta\mathbf{u}_3 \delta c} \quad [39]$$

Therefore, it is shown that the process of describing the spatially variable velocity by an average velocity introduces dispersion into the equations. Dispersion is due to correlations between variations in solute concentrations and fluid velocities. Physically, the dispersive flux is due to variable pore size, the velocity profile in a pore, and tortuous flow channels (Figure 7).

It is not practical to measure fluid velocities and solute concentrations on a macroscopic scale to determine the velocity variations and concentration variations. In practice, dispersion "looks" much like a diffusion process so it is often mathematically modeled as a random Fickian process analogous to diffusion.

$$\mathbf{j}_{disp} = \theta\overline{\delta\mathbf{u}_3 \delta c} = -\theta\mathbf{D}_3 \nabla_3 c \quad [40]$$

This is justified if the velocity variations of a particle will experience the whole range of possible velocities. $\mathbf{D}_3$ is the second rank dispersion tensor. $\mathbf{D}_3$ is always anisotropic even if flow is isotropic. Dispersion in the longitudinal direction (in the direction of flow) is always much greater than in the transverse direction. It is usually

possible to align the coordinate system (and thereby $\mathbf{D}_3$) in the direction of flow, so that $\mathbf{D}_3$ is symmetric with no off diagonal components.

Total flux may now be written using Eqs.[36] and [40] where all concentrations, c, and velocities, $\mathbf{u}_3$, now represent averages throughout the REV to remove overbars.

$$\mathbf{j}_3 = \theta \mathbf{u}_3 c - \theta(D + \mathbf{D}_3)\nabla_3 c \qquad [41]$$

Now recall the solute mass conservation equation, Eq[23], and substitute for the total flux

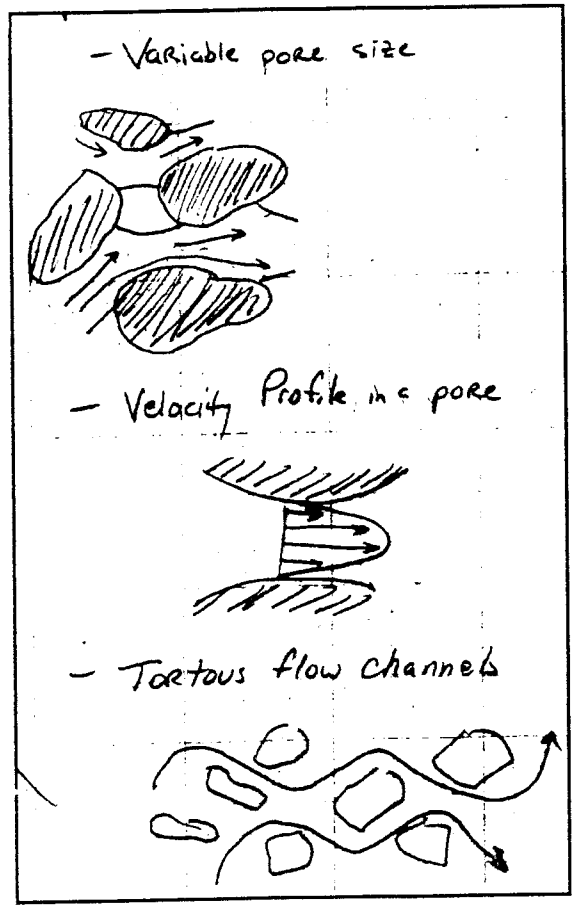

Figure 7. Physical processes affecting the dispersive flux

given by Eq.[41].

$$\frac{\partial C}{\partial t} = -\nabla_3\left(\theta \mathbf{u}_3 c - \theta(D + \mathbf{D}_3)\nabla_3 c\right) + \sigma \qquad [42]$$

or,

$$\frac{\partial C}{\partial t} + \nabla_3(\theta \mathbf{u}_3 c) - \nabla_3\left(\theta(D + \mathbf{D}_3)\nabla_3 c\right) - \sigma = 0 \qquad [43]$$

Equation [43] is the solute transport equation for the REV defined in **Error! Reference source not found.**. It includes terms for the time rate of change of solute, transport by advection, molecular diffusion, mechanical dispersion and internal sources or sinks of solute in the REV with dimensional units expressed in rates per unit volume.

2.3.2.3 Dispersion coefficients

In this section we will look more closely at dispersion coefficients.. The dispersion tensor in three dimensions

$$\mathbf{D}_3 = \begin{bmatrix} D_{xx} & D_{yx} & D_{zx} \\ D_{xy} & D_{yy} & D_{zy} \\ D_{xz} & D_{yz} & D_{zz} \end{bmatrix} \qquad [44]$$

If $\mathbf{D}_3$ is aligned with the velocity as is usually the case then

$$\mathbf{D}_3 = \begin{bmatrix} D_x & 0 & 0 \\ 0 & D_y & 0 \\ 0 & 0 & D_z \end{bmatrix} \qquad [45]$$

Taking the transverse dispersion coefficients to be equal, the dispersion tensor is commonly represented as

$$\mathbf{D}_2 = \begin{bmatrix} D_L & 0 \\ 0 & D_T \end{bmatrix} \qquad [46]$$

D_L is the longitudinal dispersion in the direction of the flow field and D_T is the transverse dispersion perpendicular to the flow field with units of length^2 per unit time. D_L is typically ten times the value of D_T.

Longitudinal dispersivity, α_L and transverse dispersivity, α_T with units of length are defined in relation to the average pore water velocity in the longitudinal direction, u.

$$\begin{aligned} D_L &= \alpha_L |u| \\ D_T &= \alpha_T |u| \end{aligned} \qquad [47]$$

Dispersion coefficients are rarely known a priori, but the following rules of thumb are commonly used in solute transport problems to estimate dispersivity..

$$\frac{\alpha_L}{\sqrt{k}} \approx 25 \text{ to } 50 \qquad [48]$$

$$\frac{\alpha_T}{\alpha_L} \approx 0.1 \qquad [49]$$

Dispersivity is scale dependent and the random Fickian model does not fully describe the dispersion process because dispersion is not a random process. Values of longitudinal dispersivity measured in laboratory column experiments are usually on the order of one centimeter, but in the field using tracer experiments they are found to be much larger than laboratory measurements (Kinzelbach, 1986, p.201). Scaling of dispersivity is due to increased heterogeneity and small scale variations in permeability that are found in the field.

The relationship between molecular diffusion, dispersion and pore water velocity is expressed in terms of the dimensionless Peclet number, defined analogous to heat transfer problems. The Peclet number is calculated as the ratio between the average pore water velocity, u, times a characteristic length expressed as the mean grain size, d, to the molecular diffusion coefficient, D as in Eq. [50].

$$\mathrm{Pe} = \frac{ud}{\mathrm{D}} \qquad [50]$$

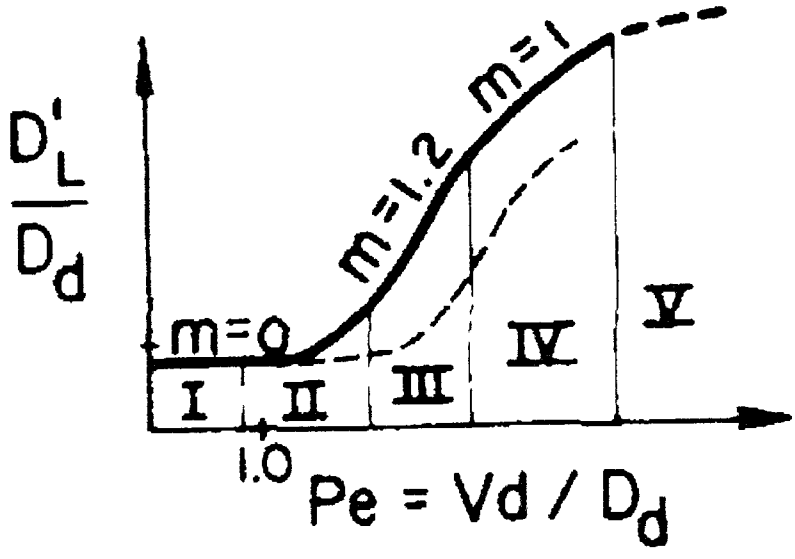

Figure 8. Relationship between molecular diffusion and convective dispersion (after Pfannkuch (1963) and Saffman (1960) as found in Bear (1972), Fig. 10.4.1, p 607.

Using methods of dimensional analysis it has been shown that the coefficient of hydrodynamic dispersion, $\mathbf{D}_3$ which includes the effects of both diffusion and dispersion, is related a function of the Peclet number. The curve shown in Figure 8 can be divided into several zones. In Zone I, molecular diffusion dominates, Pe<0.4. In this zone the

velocity is such that the time of travel through a pore is equal to or greater than the time required for diffusion of the solute. In Zone II, molecular diffusion is of the same order of magnitude as dispersion, $0.4 < Pe < 5$, and diffusion processes are as important as dispersion processes. In Zone III, $5 < Pe < 10$, the main spreading is due to mechanical dispersion combined with transverse molecular diffusion, and transverse diffusion reduces longitudinal dispersion. In Zone IV, $Pe \geq 10$, mechanical dispersion dominates and diffusion is negligible. In Zone V, mechanical dispersion is important, but because of the high pore water velocity, the effects of inertia and turbulence may no longer be neglected.

Molecular diffusion coefficients, D for solutes in pure water are readily found in most handbooks, but in porous media these diffusion coefficients are reduced due to tortuosity, porosity, media structure and water content. To account for these effects in porous media, an effective diffusion coefficient, D_e is used where D_e for typical ions range from 10^{-9} to 10^{-14} m^2/sec. So , for dispersion to dominate we need $Pe > 5$ for a sandy soil, with a mean grain diameter, $d = 1 \times 10^{-3}$ m and $D_e = 10^{-11}$ m^2/sec using Eq. [50] one finds a pore water velocity needs to be greater than about 5×10^{-8} m/sec (1.6 m/year) to neglect the effects of diffusion on the longitudinal spreading of the solute.

2.3.2.4 Chemical reactions, solute decay and adsorption

Many solutes can undergo chemical reactions in porous media. Terms that account for solute decay and reversible adsorption of solutes onto the solid matrix of the porous media can be added into the transport equation. A first order decay reaction is where solute gain or loss is proportional to its concentration as described by Eq. [51],

$$\frac{dC}{dt} = -\lambda C = \sigma = \text{source or sink} \qquad [51]$$

where λ is the proportionality constant, C is the total solute concentration and all other variables are previously defined.

The simplest case of reversible adsorption of solute onto the solid matrix of the porous media can be accounted for using a linear adsorption isotherm where we consider solute concentrations in both the liquid and solid phase. The total solute concentration in the porous matrix, C is the sum of the concentrations in the liquid and the solid phase. For

$$C = \rho_b c_s + \theta c \qquad [52]$$

where ρ_b is the bulk density of the porous media with units [mass dry media per total volume], c_s is the solute concentration adsorbed on the porous media with units [mass of solute adsorbed per mass of dry media], θ is the volumetric water content with units [volume of water per total volume], C is the solute concentration in the liquid phase with units [mass of solute in liquid phase per volume of water] and c is the total solute concentration with units [mass total solute per total volume]. For the case of a linear isotherm,

$$c_s = k_d c \qquad [53]$$

where k_d is the proportionality constant relating the adsorbed solute to the solute concentration in the media. Substituting Eq. [53] into Eq.[52] to express the total concentration in terms of the liquid solute concentration.

$$C = \rho_b k_d c + \theta c \qquad [54]$$

$$C = (\rho_b k_d + \theta)c \qquad [55]$$

$$C = \left(1 + \frac{\rho_b k_d}{\theta}\right)c\theta \qquad [56]$$

$$C = Rc\theta \qquad [57]$$

where R is the retardation factor defined as

$$R = 1 + \frac{\rho_b k_d}{\theta} \qquad [58]$$

First order decay and solute adsorption can now be added into the solute transport equation defined in Eq.[43].

$$\frac{\partial(Rc\theta)}{\partial t} + \nabla_3(\theta \mathbf{u}_3 c) - \nabla_3\left(\theta(D + \mathbf{D}_3)\nabla_3 c\right) + \lambda R\theta c - \sigma = 0 \qquad [59]$$

Equation [59] is the advection dispersion equation expressed in three dimensions and can be simplified if we assume θ is constant in space and time, then divide Eq. [59] by $R\theta$ to obtain

$$\frac{\partial c}{\partial t} + \nabla_3\left(\frac{\mathbf{u}_3}{R} c\right) - \nabla_3\left(\left(\frac{D + \mathbf{D}_3}{R}\right)\nabla_3 c\right) + \lambda c - \frac{\sigma}{R\theta} = 0 \qquad [60]$$

When $P_e > 10$ dispersion processes dominate solute spreading and diffusion is negligible.

$$\frac{\partial c}{\partial t} + \nabla_3\left(\frac{\mathbf{u}_3}{R} c\right) - \nabla_3\left(\frac{\mathbf{D}_3}{R}\nabla_3 c\right) + \lambda c - \frac{\sigma}{R\theta} = 0 \qquad [61]$$

The advection dispersion equation is often expressed in one dimension by further assumptions that the fluid velocities are known, the retardation factor and the dispersivity are constant in space and time.

$$\frac{dc}{dt} + \frac{u}{R}\frac{dc}{dx} - \frac{D_L}{R}\frac{d^2c}{dx^2} + \lambda c - \frac{\sigma}{R\theta} = 0 \qquad [62]$$

If the fluid velocity is moving in the x-direction we can look at solute spreading in two dimensions by examining the effects of transverse dispersion using Eq. [63].

$$\frac{dc}{dt} + \frac{u}{R}\frac{dc}{dx} - \frac{D_L}{R}\frac{d^2c}{dx^2} - \frac{D_T}{R}\frac{d^2c}{dy^2} + \lambda c - \frac{\sigma}{R\theta} = 0 \qquad [63]$$

When the ADE is expressed as Eqs. [63] and [64] the advantage of expressing solute adsorption in terms of the retardation factor is seen. If there is no adsorption, then the retardation factor, R in the denominator is equal to 1. If there is adsorption present, the retardation factor in the denominator is greater than 1 which tends to decrease the apparent solute velocity, u/R and the apparent dispersion D_L/R. The effect of the retardation factor on the solution to the ADE is to make the solute plume appear to advance and spread out more slowly which is what would be expected if some solute were adsorbed to the porous matrix.

2.4 Time Domain Reflectometry

During the last decade, the use of time domain reflectometry, (TDR) to monitor soil water content and salinity has increased rapidly in agriculture, forestry, engineering and environmental studies. This increase was facilitated by numerous advances in automated signal interpretation, probe and instrument technology and conceptual

understanding, making what was once an exotic technique commonplace. TDR has been found to be a relatively non-destructive, quick, easily automated and non-nuclear method to measure both moisture content and bulk electrical conductivity of soils. Calibration for measurements of volumetric moisture content is consistent across a wide range of soil types, densities and conductivities. Measurements can be made *in situ,* which require installation of two or more wires or rods into the soil to act as a parallel transmission line.

An instrument commonly used for electric and communication cable testing, known as a time domain reflectometer transmits step shaped electromagnetic pulses down the parallel rods where they are reflected back to the TDR instrument and recorded. The characteristics of the reflected signal depend on the dielectric property and conductivity of the soil surrounding the parallel rods. The pulse travel time and signal attenuation determined from the reflected signal is proportional to the apparent dielectric constant of the soil, K_a and the bulk soil electrical conductivity,σ, respectively. Experimental correlation and theoretical analysis have further shown that there exists a unique relationship between these two measured parameters and the volumetric moisture content and pore water salinity. This relationship is the basis for TDR measurements of soil water and salinity measurements in soil.

2.4.1 Dielectric properties of soil

The dielectric properties of a media are described by the complex permittivity, which consists of both a real and imaginary component. Throughout this discussion the dielectric constant refers to the real part of the complex permittivity. A discussion of complex permittivity or the dielectric constant is provided in Von Hippel (1954). In the

contest of TDR measurements, the real part is controlled by volumetric water content and the imaginary part is a function of bulk soil conductivity (Dalton and van Genuchten, 1986; Campbell, 1990).

The dielectric properties of a soil are dependent on the water content and the measurement frequency. That it is dependent on the water content is readily apparent from the large differences between the dielectric constants of the major constituents of soil at 300 MHz and 25C, which are 1.0 for air, 3-5 for major soil minerals and 77.5 for water (Von Hippel, 1954). The relationship between the dielectric properties and the frequency are not as apparent as the dielectric property and water content.

The dielectrics of soil have been studied from DC up to frequencies of 10 GHz. At low frequencies dielectric constant was observed to be approximately inversely proportional to the frequency (Smith-Rose, 1933) and levels off at a frequency of about 10 MHz to values ranging from 5 to 27 depending on the water content of the soil (Hoekstra and Delany, 1974; Patterson and Smith, 1980). In clay soils dielectric constants have been measured to be greater than 100 at 1 MHz dropping to about 50 at 50 MHz (Campbell, 1990; Smith-Rose, 1933). At lower frequencies the dielectric properties are affected by ionic conductivity of the soil and show considerable variation between soil types even at similar water contents (Campbell, 1990).

At frequencies between about 10 MHz up to 1 GHz, the dielectric constant appears to be solely dependent on the water content and independent of frequency and soil type (Hoekstra and Delaney, 1974; Hipp, 1974; Patterson and Smith, 1980; Campbell, 1990). At frequencies above 1 GHz the dielectric constant is again dependent on the frequency. Von Hippel (1954), tabulated a series of dielectric measurements made

on a sand, loam and clay soil at various water contents which shows a marked decrease in dielectric constant between 100 MHz and 10 GHz. Hoekstra and Delaney (1974) measured the dielectric constant of a Goodrich clay from 100 MHz to 26 GHz and found a significant decrease at frequencies over 1 GHz due to the dielectric relaxation of bulk water in the soil which occurs at about 8 GHz.

2.4.2 Measurement of soil water content

Numerous methods to measure the dielectric properties of a media are described in Von Hippel (1954). 'Fringe' capacitance techniques have been used to measure dielectric properties of soils to determine soil moisture content (Thomas, 1965; Birchak 1974). More recently techniques using rectangular or open-ended waveguides have been developed for non-destructive measurement of dielectric properties (Sphicopoulos et al., 1985). A portable dielectric probe (Brundfeldt, 1987) has recently been evaluated and found suitable for making soil moisture measurements of the order of 1 cm in thickness (Brisco et al., 1992). Although time domain reflectometers had been used for years for cable testing, the first measurements of dielectrics in the time domain were made on alkyl alcohols to determine the high and low frequency dielectric constant, the relaxation time and the dielectric loss (Fellner Feldegg, 1971).

The time domain reflectometer generally consists of a pulse generator which produces a fast rise time voltage step (typically rise time approx. 20 ps, amplitude approx. 250 mV), a sampling head and display/recording unit (an oscilloscope or similar display). The pulse from the step generator travels along a coaxial line, which typically has a characteristic impedance of 50 ohms, until it meets a discontinuity or change in

impedance where part of the signal is reflected along the line back to the sampling head where it produces an additional signal which is displayed on the oscilloscope. When a dielectric substance is placed in the coaxial line the reflected signal yields information about its complex permittivity. The reflected signal has traditionally been analyzed in the time domain using Fourier transformations of the reflected pulses (Arcone and Wills, 1986; Hoekstra and Delaney, 1974; Bertolini et al., 1990). The reflected signal can also be analyzed by using a non-Fourier approach by using the travel time approach. This is the approach used almost universally when making soil moisture and bulk conductivity measurements (Topp et al., 1980; Dalton et al., 1985; Dalton and van Genuchten, 1986).

Soil water content measurements using TDR were first determined by placing soil in 1.0 and 0.33 m coaxial lines (Topp et al., 1980). Four mineral soils were tested and found to be almost independent of texture, bulk density, temperature and salt content. The sample to be measured is placed in the transmission line, either in the coaxial cable or in the case with *in situ* soil moisture measurements the coaxial cable is terminated by parallel transmission rods, which are placed into the sample. The time delay between reflections originating at the front and the back of the sample are then determined by linear extrapolation from the signal. The apparent dielectric constant K_a is then calculated from the following simple formula,

$$K_a = \left(\frac{ct_d}{2L}\right)^2 \qquad [64]$$

where: t_d is the time delay, c is the propagation velocity of an electromagnetic pulse in free space (3.0×10^8 m/sec), and l is the length of the probe.

The most expedient procedure for calculating the volumetric moisture content of measurements made in the soil has been to indirectly correlate the apparent dielectric constant to soil moisture using regression (Wobschall, 1977; Topp et al. 1980). The regression equation determined by Topp et al. (1980) for parallel transmission rods in soil is

$$q_v = (-530 + 292K_a - 5.5K_a^2 + 0.043K_a^3) / 10{,}000 \qquad [65]$$

with a reported accuracy of measurement of about 0.01 m^3m^{-3}. This relationship which is widely used has recently been verified by Dalton (1992) and Zegelin (1992) for most mineral soils and conditions except for soils high in organic content (Herkelrath et al., 1991).

Ansoult (1987) developed a statistical relationship between the dielectric constant and volumetric moisture content. Herkelrath et al. (1991) found that a linear relationship existed between the volumetric moisture content and the inverse of the apparent velocity that is consistent with a simple series model of air-water-soil arranged in series along the waveguide. Most recently Dirkson and Dasberg (1993) found that a theoretical model based on the Maxwell-DeLoor dielectric mixing model improved calibration over a wider range of soils by including the bound water as a fourth phase.

Shortly following the work of Topp et al. (1980), numerous advances in measurement techniques and technology appeared. Vertically installed transmission lines with discontinuities were found to successfully determine moisture content with depth (Topp et al. 1981(a) and (b); Topp and Davis 1985). A portable TDR probe with parallel transmission lines of 30, 15 and 12.5 cm long was designed to be used with the Tektronix

1502 (a rugged, fairly inexpensive, commercial cable tester) (Topp et al., 1984). Kachanoski et al. (1990) used 20 cm long probes to determine three dimensional water flow in a laboratory column. The maximum probe length is a function of water content and electrical conductivity and minimum practical probe length is 10 cm (with the Tektronix 1502) (Dalton and van Genuchten, 1986).

Most TDR methods utilize a balun between the coaxial connector of the instrument and the parallel transmission line inserted into the soil. The function of the balun is two-fold: (i) to change an electrical field from balanced to unbalanced and (ii) to match lines with different impedances (Spaans and Baker, 1993). The use of two-wire probes without a balun has been found to give water content results consistent with probes with a balun (Stein and Kane, 1983; Authors personal experience). It is thought that there is greater risk of encountering stray voltages if a balun is omitted (Zegelin et al. 1989). Therefore, Zegelin et al. (1989) developed improved fifteen-cm long 3 and 4 wire field probes for improved signal analysis and elimination of the balun. Simple inexpensive baluns were developed for two wire probes (Spaans and Baker, 1993).

Recently considerable effort has been placed on automating and multiplexing TDR systems for continuous monitoring of soil water contents at multiple locations (Baker and Allmaras, 1990; Heimovaara and Bouten, 1990; Herkelrath et al., 1991; Wraith and Baker, 1991). Heimovaara and Bouten (1990) present an algorithm to automate the calculation of the travel time from the TDR trace using a "tangent method". Various commercial systems are available that use proprietary algorithms to interpret the trace are TRASE by Soilmoisture Equipment and IRAMS by CPN and Campbell Scientific using the Tektronix 1502 series cable tester.

2.4.3 Theory

Step-shaped electromagnetic pulses are transmitted down a transmission line. When the pulse encounters a discontinuity or changes in impedance in the transmission line a portion of that signal is reflected back down the line where the resulting waveform is recorded. The propagation velocity, v can be determined from the signal. This propagation velocity depends on the dielectric properties of the materials surrounding the transmission line.

If a transmission line is formed by inserting parallel rods into the soil, the dielectric properties of the soil can be determined. The dielectric properties of the soil can thus be determined. The dielectric properties of the soil are strongly correlated to the volumetric moisture content. The dielectric constant of water, air and soil at 25°C are respectively; K_{water}=80, K_{air}=1 and K_{soil}=2-7. Small increases in soil water content increases the apparent dielectric constant of the bulk soil.

The following equations are developed from a distributed circuit transmission line analysis of Ramo et al. (1984). The same result can be found starting from Maxwell's equations and electromagnetic theory. Consider a length of line dz having a distributed inductance L per unit length and a distributed capacitance C per unit length as shown in Figure 9. The length dz then has inductance Ldz and capacitance Cdz. At high frequencies the conductance and resistance in the line can be ignored. The change in voltage across this line is equal to the product of the inductance and the time rate of change of the current, I. The voltage change along the line at any instant is the length times the rate of change of voltage per unit length as in Eq. [66]

$$\text{voltage change} = V - (V + \frac{\partial V}{\partial z} dz) = -(\frac{\partial V}{\partial z} dz) = Ldz \frac{\partial I}{\partial t} \quad [66]$$

$$\frac{\partial V}{\partial z} dz = -(Ldz) \frac{\partial I}{\partial t} \quad [67]$$

Similarly, the change in current along the line is equal to the product of the capacitance and the time rate of change of voltage. The change in current along the line at any instant is the length times the rate of change of current per unit length as in Eq. [68].

$$\text{current change} = I - (I + \frac{\partial I}{\partial z} dz) = -(\frac{\partial I}{\partial z} dz) = (Cdz) \frac{\partial V}{\partial t} \quad [68]$$

$$\frac{\partial I}{\partial z} dz = -(Cdz) \frac{\partial V}{\partial t} \quad [69]$$

The differential length *dz* can be canceled in Eqs. [67] and [69] to obtain the

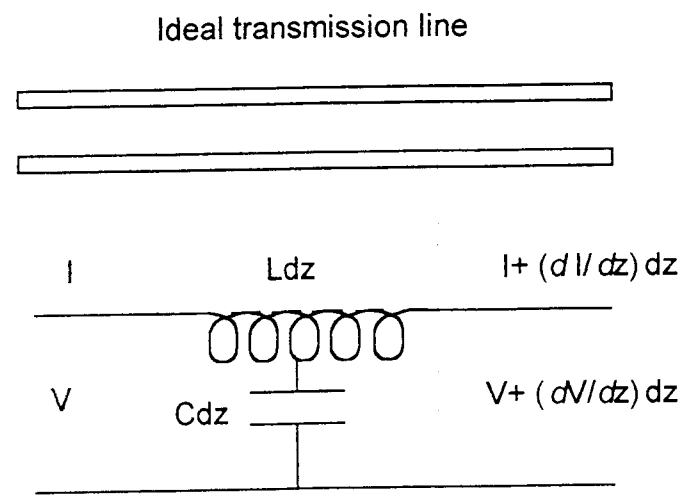

Figure 9. Ideal transmission line with a distributed load.

telegraphist's equations.

$$\frac{\partial V}{\partial z} = -L\frac{\partial I}{\partial t} \qquad [70]$$

$$\frac{\partial I}{\partial z} = -C\frac{\partial V}{\partial t} \qquad [71]$$

Eqs. [70] and [71] can be combined to form a wave equation by differentiating Eq. [70] with respect to distance and Eq. [71] with respect to time to obtain the following

$$\frac{\partial^2 V}{\partial z^2} = -L\frac{\partial^2 I}{\partial t \partial z} \qquad [72]$$

$$\frac{\partial^2 I}{\partial t \partial z} = -C\frac{\partial^2 V}{\partial t^2} \qquad [73]$$

Substitute Eq. [72] into Eq. [73] one obtains

$$\frac{\partial^2 V}{\partial z^2} = LC\frac{\partial^2 V}{\partial t^2} \qquad [74]$$

This is the classical form of the wave equation having solutions that demonstrate propagation of a wave in the z direction with velocity, v

$$v = \frac{1}{\sqrt{LC}} \qquad [75]$$

For the specific transmission line of infinite length in Figure 10, the capacitance per unit length and the inductance per unit length is found to be (Ramo et al. 1984).

$$C = \frac{\pi\varepsilon}{\cosh^{-1}(s\ d)} \quad \left[\frac{\text{Farads}}{\text{meter}}\right] \qquad [76]$$

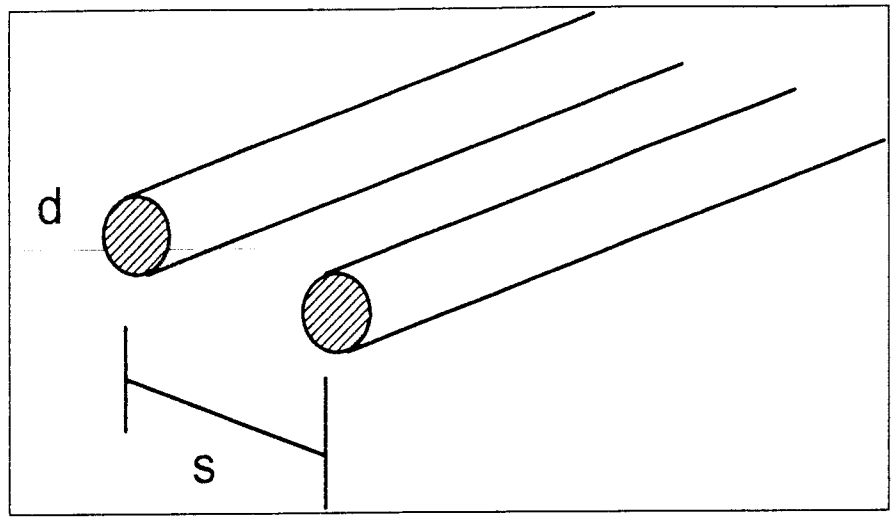

Figure 10. Dimensions of the parallel transmission line.

$$L = \frac{\mu}{\pi}\cosh^{-1}(s/d) \quad \left[\frac{\text{Siemens}}{\text{meter}}\right] \qquad [77]$$

Substituting Eq.[76] and Eq.[77] into Eq.[75] gives a propagation velocity which is independent of line geometry and only dependent on the permittivity, ε and the permeability, μ of the media surrounding the transmission line. The permittivity and permeability are defined from relationships between electric flux density, **D** and electric field, **E**, and magnetic flux density, **B** and magnetic field, **H** (Von Hippel, 1954).

$$\mathbf{D} = \varepsilon\mathbf{E} = \varepsilon_0\varepsilon_r\mathbf{E} \qquad [78]$$

$$\mathbf{B} = \mu\mathbf{H} = \mu_0\mu_r\mathbf{H} \qquad [79]$$

In free space, the permittivity and permeability are ε_0 = 8.854 x10^{-12} F/m and μ_0=4πx10^{-7} H/m and ε_r and μ_r are the relative permittivity and relative permeability of the media surrounding the transmission line. From Eq. [75] the propagation velocity of a wave in air along the transmission line is 3.0 x 10^8 m/s which is exactly the speed of light, c.

Now if we consider a TDR probe as shown in Figure 10. The apparent dielectric constant, K_a or relative permittivity, ε_r is defined by,

$$K_a = \varepsilon_r = \frac{\varepsilon}{\varepsilon_0} \qquad [80]$$

and the relative permeability is defined by,

$$\mu_r = \frac{\mu}{\mu_0} \qquad [81]$$

The electromagnetic propagation velocity, v from Eq.[75] is

$$v = \frac{1}{\sqrt{\varepsilon\mu}} = \frac{1}{\sqrt{\varepsilon_0\mu_0}} \cdot \frac{1}{\sqrt{\varepsilon_r\mu_r}} = \frac{c}{\sqrt{\varepsilon_r\mu_r}} \qquad [82]$$

Furthermore, if it is assumed that the soil is not magnetically active (i.e. μ_r=1), then the electromagnetic propagation velocity depends only on the dielectric properties of the media surrounding the probe.

$$v = \frac{c}{\sqrt{\varepsilon_r}} = \frac{c}{\sqrt{K_a}} \qquad [83]$$

The mechanical pulse velocity along the probe is determined from the time it takes for the pulse to travel from the start of the probe to the end and back again.

$$v = \frac{2L}{t_d} \qquad [84]$$

Eqs. [83] and [84] can be combined to form

$$K_a = \left(\frac{ct_d}{2L}\right)^2 \qquad [85]$$

which is the result stated by Topp et al. (1980). In practice it is usually easier to determine the travel time of any given probe in air, t_{air} and in soil, t_{soil} to determine the apparent dielectric constant from the following relationship.

$$K_a = \left(\frac{t_{soil}}{t_{air}}\right)^2 \qquad [86]$$

The apparent refractive index, n_a is then calculated as the square root of K_a following Heimovaara (1993), which is the ratio of the velocity of the pulse in air, c=2.998 x 10^8 m/s, to the apparent velocity of the pulse in the soil.

$$n_a = \frac{t_{soil}}{t_{air}} \qquad [87]$$

The apparent velocity has been shown to be inversely related to volumetric moisture content (Herkelrath et al. 1991; Heimovaara 1993). The use of the apparent refractive index is a convenient method to develop calibration curves.

2.4.4 Measurement of bulk electrical conductivity

In this section, the theory and methods of measuring bulk soil electrical conductivity using TDR are presented. Analysis using the distributed load circuit shown

in Figure 9 was used by Dalton (1984) to derive an expression for the bulk soil electrical conductivity, σ.

$$\sigma = \left(\frac{\sqrt{\varepsilon}}{120 \cdot L \cdot \pi} \right) \ln\left(\frac{V_t}{V_r} \right) \quad [88]$$

where V_t transmitted voltage, V_r is the reflected voltage as shown in Figure 11, L is the length of the probe, and ε is the dielectric constant of the soil. Analysis of this method using electrolyte solutions and probes of varying length found a good linear correlation to conductivity but it was found to be about 25% smaller than the theoretical value (Dalton, 1992). Using TDR to measure both water content and bulk electrical conductivity one can calculate soil salinity according to Rhoades et al. (1976).

$$\sigma = \sigma_w \theta T + \sigma_s \quad [89]$$

Where σ is the bulk soil electrical conductivity, θ is the volumetric soil water

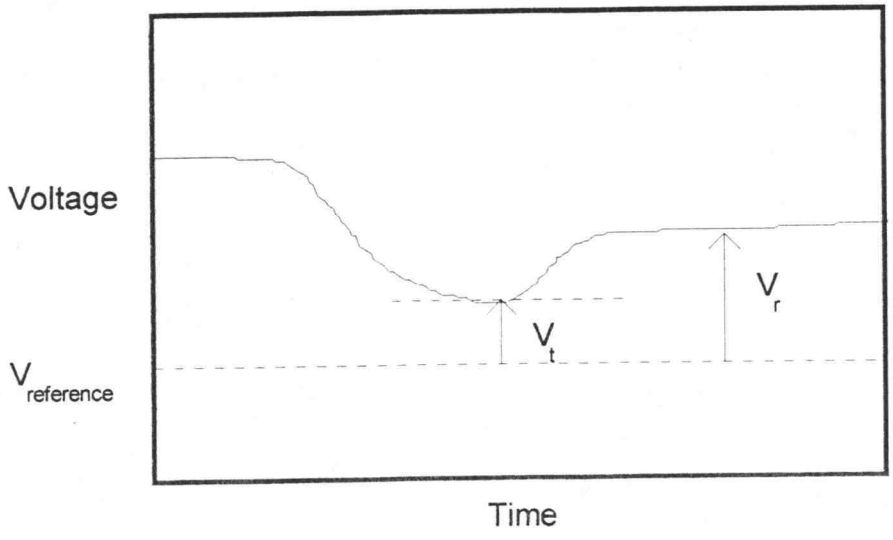

Figure 11. Measurement of Vt and Vr from the TDR trace.

content, σ_w is the pore water salinity, σ_s is the mineral phase surface conductance and T is a tortuosity factor. Estimates of pore water salinity can then be obtained when given values of σ_s and T are known for a particular soil. Using a signal pulse of 250 mV, common in most TDR instrumentation, limits measurement of to soils with pore electrical conductivities less than 14 - 20 dS/m depending on soil water content (Dalton and van Genuchten, 1986).

Determination of the bulk soil electrical conductivity can also be found using a lumped circuit analysis where the probe and soil together have a lumped characteristic impedance, Z_l. This analysis is usually given in terms of the reflection coefficient, ρ, which is the ratio of the transmitted voltage to the return voltage. The reflection coefficient can also be given in terms of the cable impedance Z_0 and the load impedance Z_l (Tektronix, 1989),

$$\rho = \left(\frac{Z_l - Z_0}{Z_l + Z_0} \right) \qquad [90]$$

By using the reflection coefficient, ρ, after all possible reflections have taken place, the impedance of the soil and probe can be calculated when the impedance of the line is known, $Z_0 = 50$ ohms.

$$Z_l = Z_0 \left(\frac{1 + \rho}{1 - \rho} \right) \qquad [91]$$

The resistance of the soil is then dependent on the probe geometry and introducing a cell constant for the specific probe to obtain an explicit expression for the bulk soil electrical conductivity.

$$\sigma = \frac{K}{Z_0}\left(\frac{1-\rho}{1+\rho}\right) \qquad [92]$$

Independent measurements of bulk soil electrical conductivity and measurements made using Eq. [92] have shown excellent correlation (Dalton, 1990).

TDR techniques are a very valuable method for the simultaneous measurement of water content and salinity in soils. Interpretation of waveforms, frequency domain analysis and improved understanding of measurements is an intensive area of research today.

Chapter 3. Fertilizer Diffusion in Container Medium[1]

3.1 Abstract

The process of fertilizer diffusion was examined using KBr and NaBr salts placed at the of columns filled with a container medium at initial water contents of 4.0, 2.5 or 1.0 g/g (mass of water/mass of medium). Columns were sealed to create a Protected Diffusion Zone (PDZ) shielding the system from water infiltration and evaporation. Bromide and water distributions were determined after 5, 10, 25 and 120 days. Using a Fickian diffusion model, effective diffusion coefficients calculated for Br^- in the medium at 2.5 g/g ranged from 2.7 - 4.6 $\cdot 10^{-6} \cdot$ $cm^2 \cdot sec^{-1}$ which is 3 to 9 times less than the diffusion coefficient in water alone. Diffusion rates increased with increasing medium water content. Differences in the hygroscopicity and solubility of KBr and NaBr affected the distribution of water and diffusion rates in the columns. Redistribution of water was driven to a significant degree by vapor phase transport, caused by large gradients in osmotic potential and was most apparent at low water contents. At high water contents, water redistribution was affected by solution density gradients in the system. This significantly complicates the mathematical modeling of the system, which renders a simple Fickian diffusion model of limited predictive value in the high and low water content media.

---

[1] Published as:

Kelly, S. F., J. L. Green, and J. S. Selker. Fertilizer Diffusion in Container Medium. *J. Amer. Soc. Hort. Sci.* 122(1):122-128. 1997.

3.2 Introduction

In intensive nursery crop production systems, fertilizer often moves with applied water through and beyond the plant root zone and has the potential to contaminate ground and surface waters. The importance of protecting water quality is recognized in the horticulture industry and numerous solutions have been proposed and implemented. Current practices include optimization of the timing of fertilizer application (Hershey and Paul, 1982; Biernbaum, 1992; Cox, 1993;), collection and treatment of runoff (Alexander, 1993), and reduction of water and fertilizer use through drip irrigation and scheduling (Ticknor and Green, 1987; Kabashima, 1993). The "Closed Insulated Pallet System" (CIPS) and the "Conserver" are two systems currently being investigated to minimize leaching losses by placing fertilizer in a PDZ in the media to shield it from gravitational flow of surface applied water (Green and Schnekenburger, 1992; Green et al., 1993a; Green et al., 1993b; Rost, 1995; Green, 1995). Understanding the process of diffusion from these concentrated fertilizer sources is important for incorporating a PDZ into commercial production systems to minimize environmental impact yet sustain economic plant growth.

Agricultural research on diffusion has focused on diffusion of nutrients toward plant roots in natural soils (Barber et al., 1963; Olsen and Kemper, 1968; Nye and Tinker, 1977; Bhadoria et al., 1991). Although many researchers have reported increased diffusion rates with an increase in water content (Klute and Letey, 1958; Graham-Bryce, 1963; Patil, et al., 1963; Schaff and Skogley, 1982; Mehta, et al., 1995), predicting effective diffusion rates based on soil type and water content is usually carried out experimentally or predicted using previously published literature. Most soil ion diffusion

literature is concerned with dilute soil solutions diffusing through nearly saturated media. Some studies reported diffusion rates using solutions as high as 1.0 M (Graham-Bryce, 1963; Palmer and Blanchar, 1980).

The process of fertilizer salt dissolution and the subsequent diffusion into relatively dry soils is a complex process that has received limited attention. Wheeting (1925) observed that in relatively dry soils dissolution was accompanied by an accumulation of water in the soil immediately surrounding the fertilizer salts and a drying out of the soil farther away from the fertilizer. A number of researchers have attributed this phenomenon to water vapor movement toward the salt due to the vapor pressure gradient induced by the salt (Lawton and Vomocil, 1954; Kolaian and Ohlrogge, 1959; Scotter and Raats, 1970). Parlange (1973) presented a theory to describe this process that was subsequently shown to have limited success in predicting the water redistribution in the wetter region adjacent to the salt (Scotter, 1974a). Scotter (1974b) found that the dissolution of salt into a relatively dry soil depended very strongly on the solubility and saturated solution vapor pressure of the salt used, and the initial soil water content.

The foundations of the conceptual model for ion diffusion processes are Fick's first and second laws of diffusion (Tyrrell and Harris, 1984). Fick's first law describes the observed instantaneous and irreversible flow or flux of ions from regions of high ion concentration to areas of low ion concentration. Mathematically, Fick's first law in one dimension states that ion flux (J, mass/length^2/time) across a plane perpendicular to the direction of flow in the x direction, is directly proportional to the mobile phase concentration (C, mass/length^3) gradient.

$$J = - D \frac{\partial C}{\partial x} \qquad [93]$$

The proportionality constant (D, length^2/time) is called the diffusion coefficient.

Because fertilizer ions diffuse more slowly through a wet porous media than in pure aqueous solutions, the diffusion coefficient is modified by factors, which account for porosity, pore geometry, physical properties, and chemical interactions with the porous media. This modified coefficient is called the effective diffusion coefficient, D_e. In this study, D_e is defined as being equal to $D\tau_a$, where τ_a is the apparent tortuosity, which includes all factors tending to reduce the rate of diffusion in the media except for the volumetric water content, θ, since θ is measured easily and independently from other factors. Thus, Fick's first law as modified for porous media can be stated as:

$$J = - D_e q \frac{\partial C}{\partial x} \qquad [94]$$

where C is defined as the concentration of the solute in the liquid phase.

Fick's first law is useful for analysis of steady fluxes, but for solving time-dependent problems, Fick's second law (derived from the first law and conservation of mass principles) is more useful. Fick's second law as modified for porous media in one dimension is:

$$\frac{\partial C}{\partial t} = D_e \frac{\partial^2 C}{\partial x^2} \qquad [95]$$

where t is time. Important assumptions made in the derivation of Eq. [95] are: (1) there is no interaction of the media with the ions; (2) θ is constant at all points in space and time;

(3) the media is sufficiently homogeneous that D_e is constant throughout the column at all points in space and time. Experiments conducted by establishing initial values and boundary conditions applicable to solutions of Fick's second law Eq. [95] form the basis of most methods to determine D_e in porous media.

A solution to Eq. [95] satisfying the specified boundary conditions, $C(0,t)=C_0$, and the initial conditions, $C(x,0)=0$, is found in Crank (1975):

$$C(x,t) = C_0 erfc \frac{x}{2\sqrt{D_e t}} \qquad [96]$$

Effective diffusion coefficients can be calculated from Eq. [96] providing the assumptions made in deriving Eq. [95] are satisfied along with additional constraints. 1. The boundary conditions are constant throughout the experiment (i.e., a sufficient supply of salt crystals is always available at the upper surface). 2. There is no convective movement of solutes and negligible water vapor movement 3. The solute never reaches the far end of the column.

The objectives of this paper are: (1) to identify the processes contributing to ion transport from concentrated salt sources in an unsaturated container medium inside a PDZ; (2) to show that the simple Fickian diffusion model has a number of constraints that severely limit its ability to predict fertilizer salt diffusion; (3) to demonstrate that initial water content and properties of the diffusing salt affect the resulting solute and water distributions in a PDZ. The experimental approach was to establish specific boundary and initial conditions using KBr and NaBr in columns filled with a standard container medium at a series of initial water contents. The resulting Br- diffusion was observed in vertical and horizontal columns.

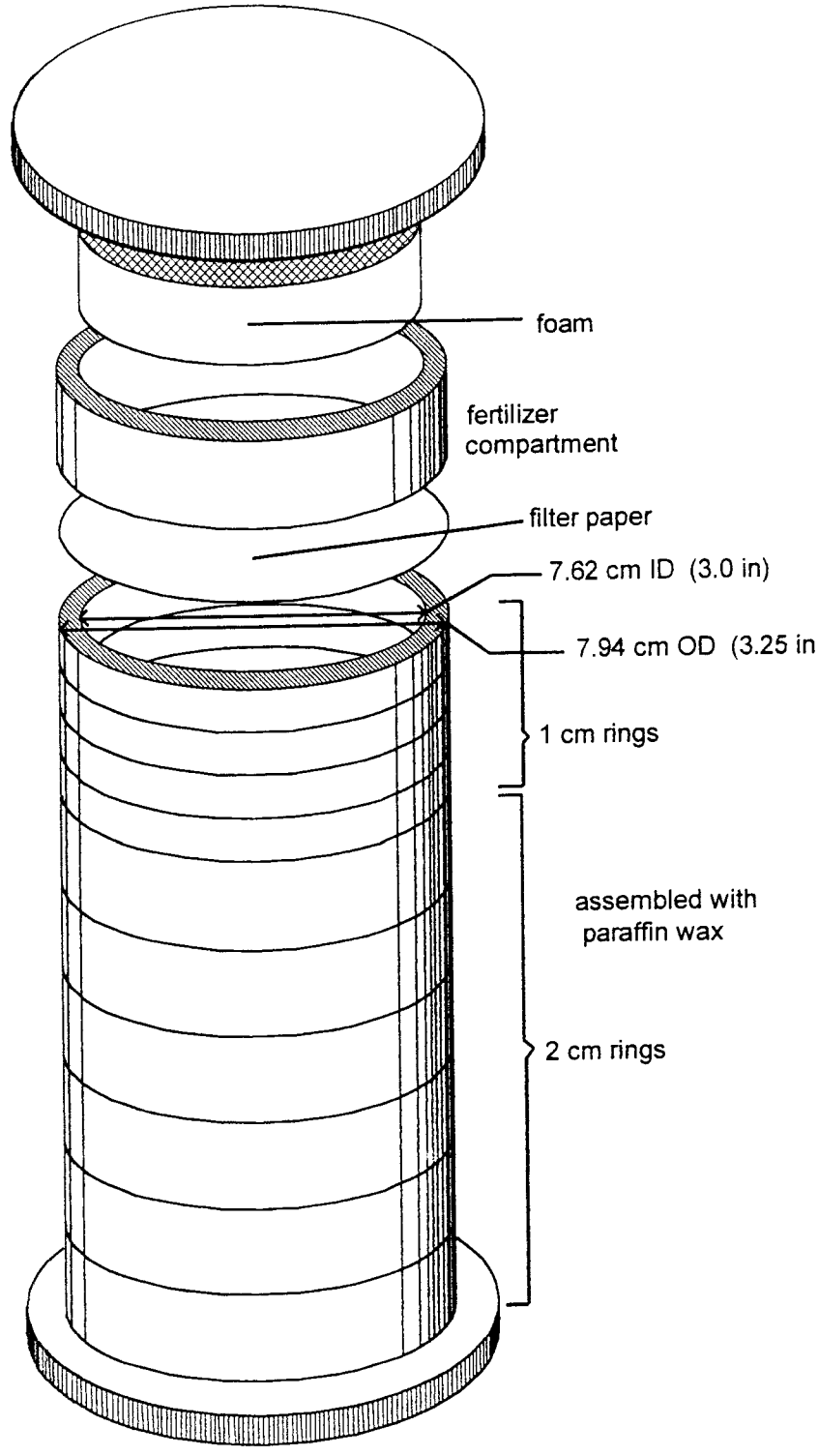

Figure 12. Construction of soil columns for diffusion experiments.

3.3 Materials and Methods

A standard 1 peat : 1 vermiculite (by volume) container medium was prepared for use in all experiments. Air dry Canadian sphagnum peat moss was sieved through a 9.42-mm screen to remove large particles. Vermiculite and the sieved peat were mixed, brought to water contents of 1.0, 2.5 and 4.0 g/g (0.17, 0.42, and 0.68 m3 of water/m3 of media) by adding the appropriate amount of tap water and allowing equilibrium in sealed containers for a minimum of one week before they were used to fill the columns.

Sixteen-cm-long columns were constructed from four 1-cm-high and six 2-cm-high rings cut from clear acrylic plastic tubing, 7.62 cm ID by 7.94 cm OD (3-inch ID x 3¼-inch OD). The column segments were assembled with hot paraffin wax as shown in Figure 12. The bottom of each column was capped with a flat acrylic base. The columns were filled with the container medium and packed by loosely filling with wet medium between increments resulting in an average dry bulk density of 0.17 g·cm-3 (SD = 0.013). The columns were filled to 4 cm above the top of the column and then leveled off to 16 cm. To form a fertilizer compartment on each column, a piece of filter paper (Whatman glass microfibre filter, 934-AH, 9 cm) was placed on top of the medium to separate the salt from the medium. An additional 2-cm ring was placed at the top of the column, and 50 grams of oven-dried salt was placed in this ring. To ensure contact was maintained between the salt-filter-medium interface, a plastic-wrapped 2-cm-thick foam disc was fitted inside the additional ring on top of the salt. A flat acrylic cap was placed on top of the column, and the entire assembly was sealed with hot paraffin wax and clamped together.

Horizontally oriented column experiments were carried out using columns filled with container medium at three water contents. Either KBr or NaBr, (solubility of Br- @ 20°C is 394 g/l for KBr and 475 g/l for NaBr, Freier, 1976) were applied to each column providing Br- concentrations equal to the respective solubility at the top boundary. The prepared columns were laid horizontally and maintained at room temperature (approx. 20°C) to be analyzed at intervals of 5, 10, 25, and 120 days. Three replicates of each salt and water content were prepared for a total of 72 columns. In vertically oriented column experiments, KBr was brought into contact with the top or the bottom of the container medium at three water contents and Br- was allowed to diffuse either upward or downward. Three replicates of each water content and diffusion direction were prepared and analyzed after 10 days for a total of 18 columns.

After the salts had diffused into the medium for the specified time, the columns were disassembled using a wide blade to retain the medium in individual sections and weighed immediately and set aside. Residual salt in the fertilizer compartment was recovered and oven-dried at 100°C to determine final salt weights (Table 1). Soluble Br- in each section was extracted by adding 15 ml of acetone (as a wetting agent) and 250 ml of distilled water to the medium in a 500-ml Erlenmeyer flask that was shaken for a minimum of 30 min. An additional 200 ml of distilled water was added to this solution and filtered (VWR Grade 415 Qualitative Filter Paper, 20.5 cm dia.) using a vacuum flask. Distilled water was added to obtain a total solution extract of 500 ml, of which 25 ml was saved for later Br- concentration determination using a bromide ion selective electrode (Orion #9435). in 2-cm increments and tamping the medium Relative Br- concentrations for each section were calculated from the concentration of Br- in the

medium solution normalized by the maximum solubility of the salt (the pure salt boundary condition). The filtered medium was oven-dried at 60°C for 24 h to determine gravimetric water content at the time each section was disassembled. After the Br- concentration in the medium was determined, the gravimetric water contents were corrected for the weight of the salt in the wet medium. Volumetric water contents were calculated from gravimetric water contents, and average bulk densities were calculated from dried medium weights.

3.4 Results and Discussion

The Fickian diffusion model was used to calculate De. To determine which treatments to include in the analysis, the model assumptions and boundary conditions were checked by inspection of the residual salt weights (Table 1), the Br- distributions (Figure 13 and Figure 14) and the water content distributions (Figure 15 and Figure 16) for each column treatment. Only days 5,10 and 25 for the column treatments with 2.5 g/g initial water content (both salts) satisfied all specified boundary conditions and most nearly the assumption of a constant water content. Effective diffusion coefficients were calculated from this subset of column treatments using a minimum residual sum of squares criterion to select the optimum value of D_e to fit Eq. [96] to the resulting Br- distributions (Figure 17). An analysis of variance of this subset showed that the differences among De were highly significant ($P<0.01$), (Table 2). Further analysis showed that De for NaBr was significantly greater than KBr after both 5 days ($P <0.05$) and 10 days ($P <0.01$) at 2.5 g/g. A comparison of Br- distributions in Figure 13 and Figure 14 showed similar differences between KBr and NaBr at other water contents.

Table 1. Residual Br^- in the fertilizer compartment for the horizontal columns after 5, 10 25 and 120 days diffusion time for KBr an2.5 and 4.0 g/g. Values are in grams of Br^- and standard deviations of three replicates are shown in parenthesis.

Salt	Day	Initial Water Content					
		1.0 g/g		2.5 g/g		4.0 g/g	
		Mean	(SD)	Mean	(SD)	Mean	(SD)
KBr	Initial	33.5	-	33.5	-	33.5	-
	5 day	28.9	(0.2)	24.9	(1.0)	12.7	(1.0)
	10 day	27.2	(0.9)	20.5	(0.3)	4.1	(2.9)
	25 day	20.6	(0.7)	11.1	(0.8)	0.1	(0.2)
	120 day	3.0	(0.8)	0.0	(0.0)	0.0	(0.0)
NaBr	Initial	39.0	-	39.0	-	39.0	-
	5 day	36.6	(0.2)	24.7	(0.4)	11.8	(1.8)
	10 day	34.9	(0.8)	16.1	(0.2)	0.0	(0.0)
	25 day	19.1	(0.2)	0.4	(0.5)	0.0	(0.1)
	120 day	0.0	(0.0)	0.0	(0.0)	0.0	(0.0)

Table 2. Effective diffusion coefficients ($cm^2\ sec^{-1}\ x\ 10^{-6}$) for Br^- in 1 peat : 1 vermiculite (by volume) medium in columns with 2.5 g/g initial water content. The sample standard error (SE) of the mean effective diffusion coefficients is $0.281\ x\ 10^{-6}\ cm^2\ sec^{-1}$.

Salt	NaBr		KBr				
	Horizontal		Horizontal			Vertical (salt at top)	Vertical (salt at bottom)
Day	5	10	5	10	25	10	10
Mean	3.62	4.65	2.74	3.38	2.79	3.33	3.26

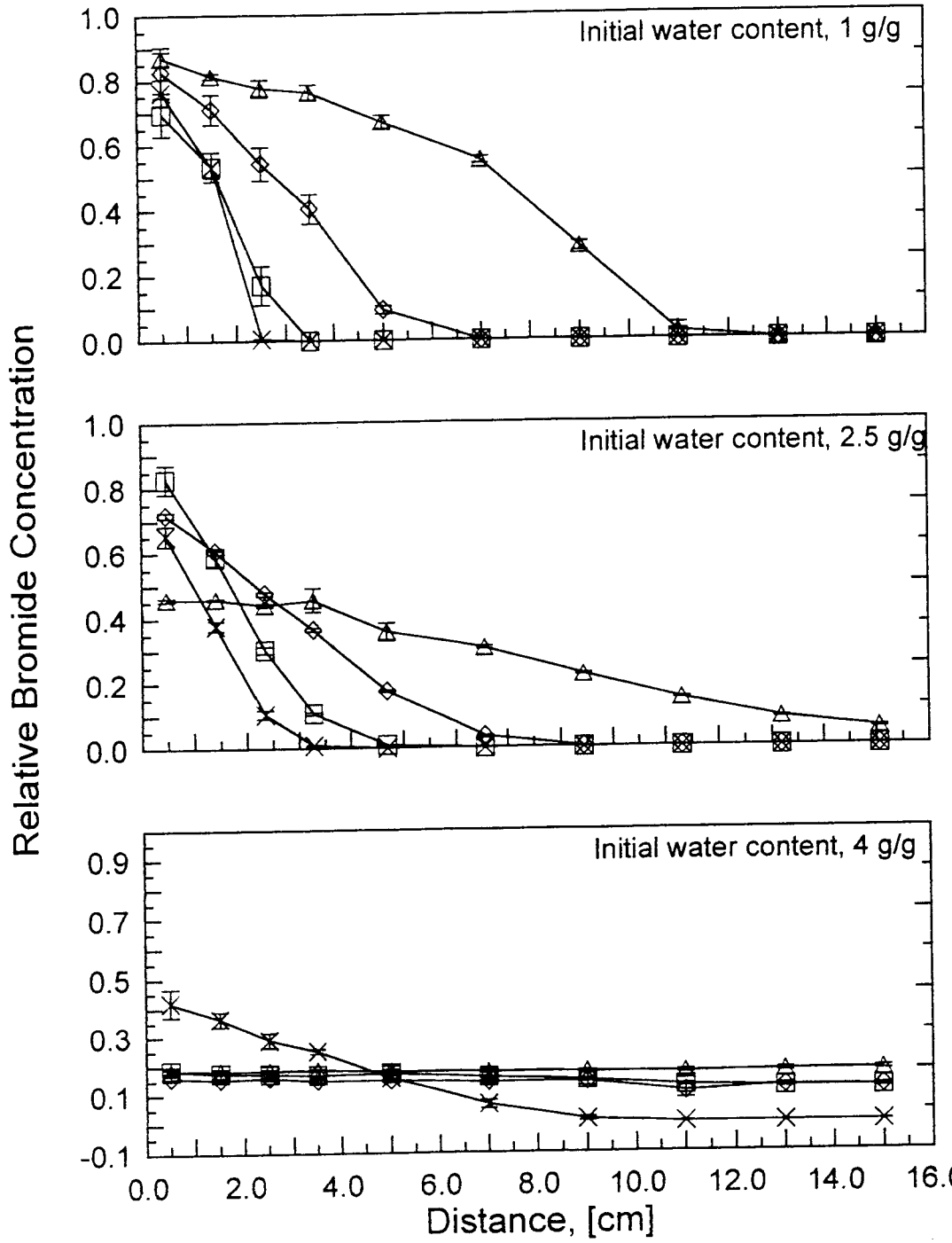

Figure 13. Average (3 replicates) relative Br^- concentrations in sections along horizontal columns with KBr as the diffusing salt after 5 (×), 10 (□), 25 (◇) and 120 days (△). Error bars represent ± 1 standard deviation.

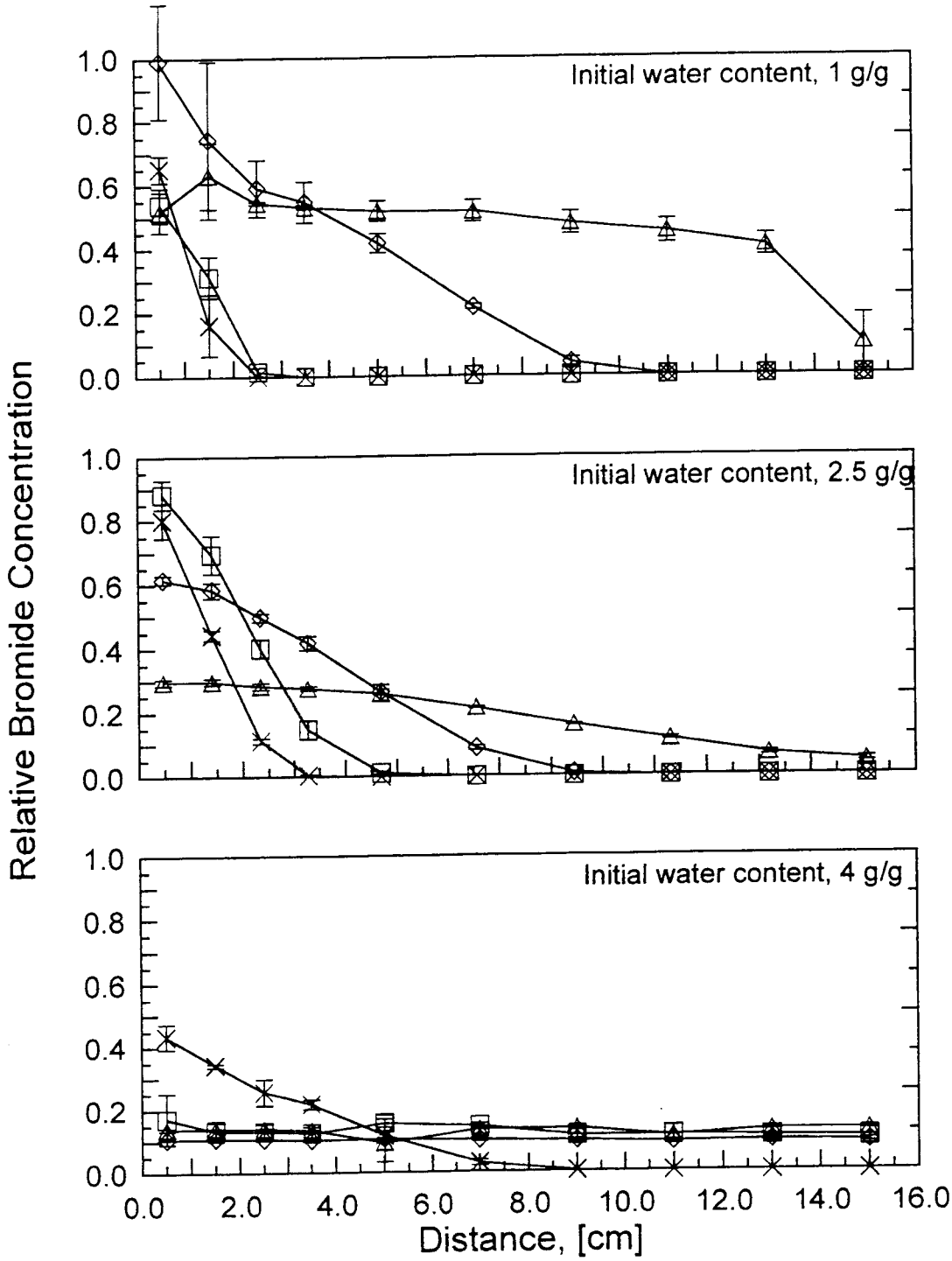

Figure 14. Average (3 replicates) relative Br^- concentrations in sections along horizontal columns with NaBr as the diffusing salt after 5 (×), 10 (□), 25 (◇) and 120 days (△). Error bars represent ± 1 standard deviation.

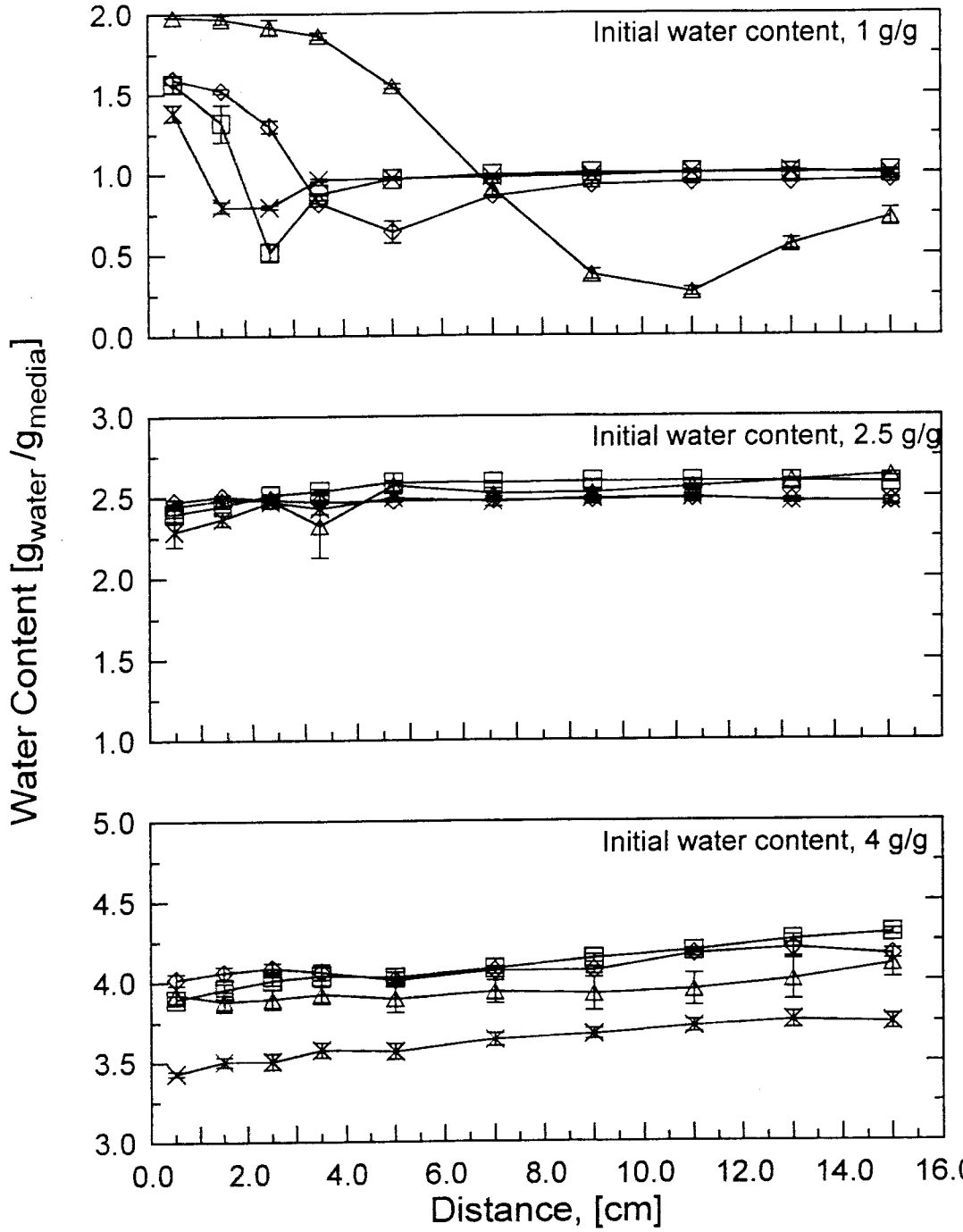

Figure 15. Final water contents in horizontal columns with KBr as the diffusing salt after 5 (×), 10 (□), 25 (◇) and 120 days (△). Error bars represent ± 1 standard deviation.

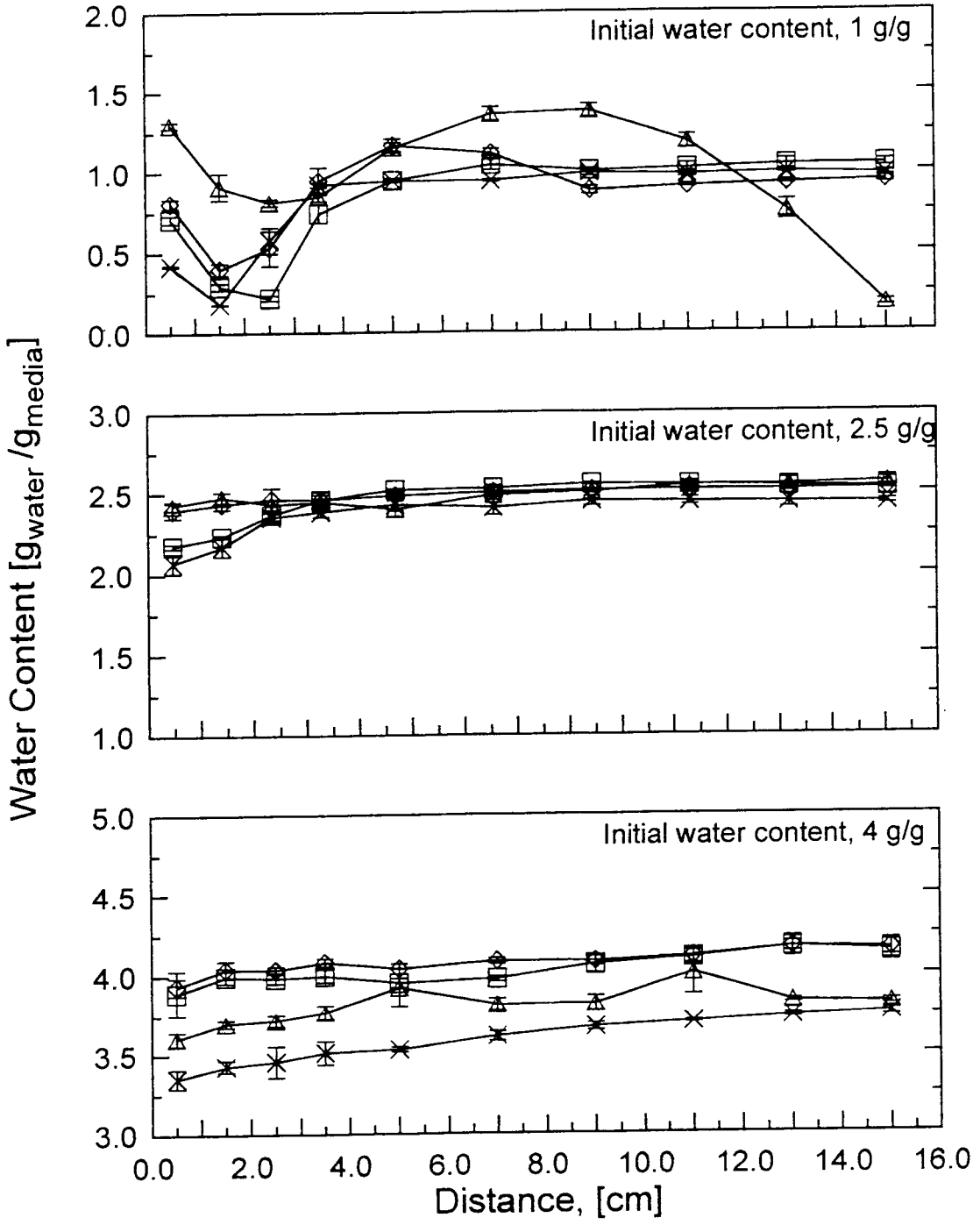

Figure 16. Final water contents in horizontal columns with NaBr as the diffusing salt after 5 (×), 10 (□), 25 (◇) and 120 days (△). Error bars represent ± 1 standard deviation.

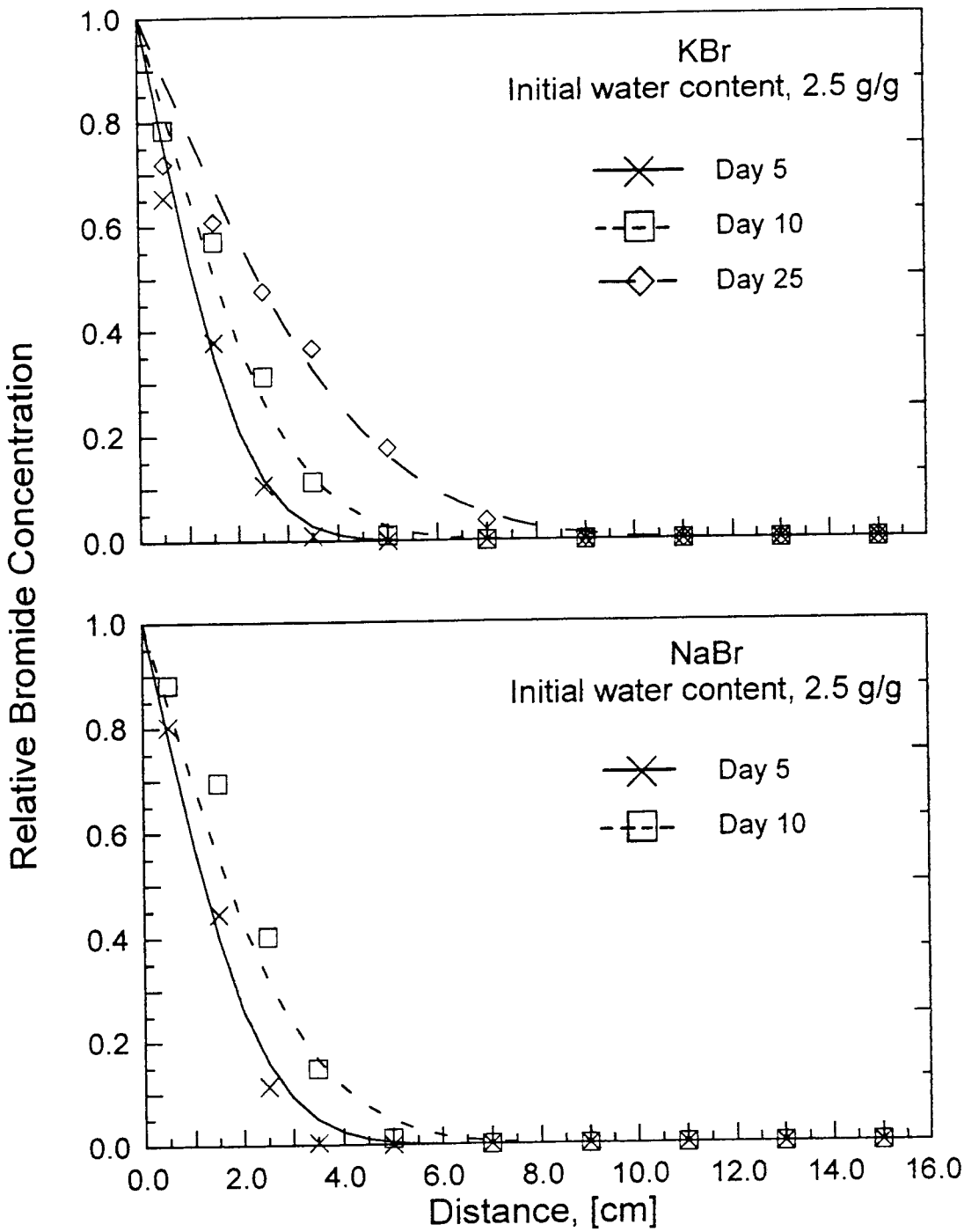

Figure 17. Relationship between the fitted effective diffusion coefficient using the Fickian diffusion model, Eq. [4], and the selected the column data.

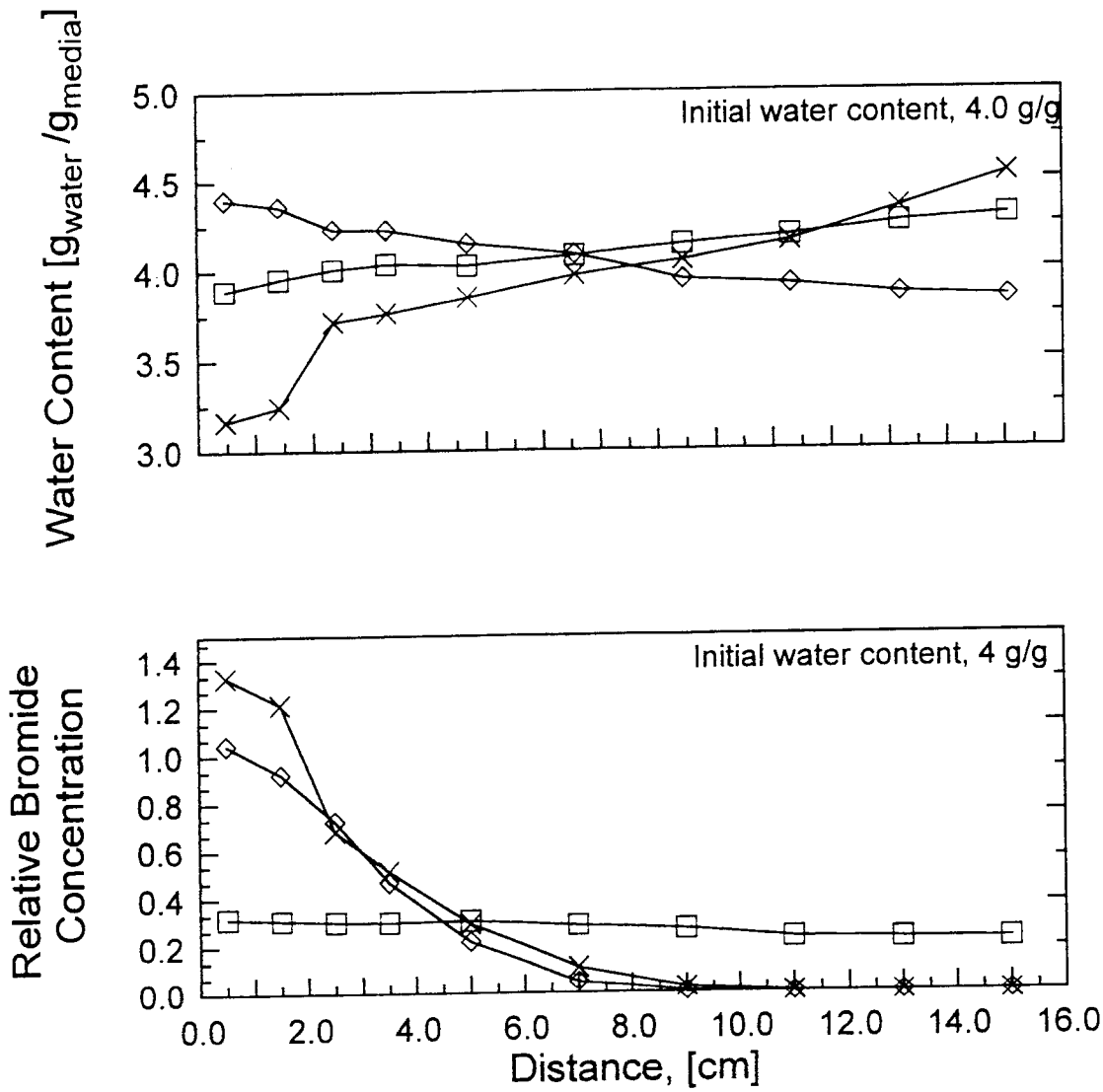

Figure 18. Average (3 replicates) relative Br^- concentrations and final water contents in vertical columns with KBr as the diffusing salt after 10 days with diffusive flux oriented up (◇), down (×) and horizontally (□).

For instance, in the column treatments at 1.0 g/g after 25 and 120 days the NaBr has moved further down the column than the KBr. Inspection of the residual Br- in the fertilizer compartment (Table 1) revealed at least 50% more Br- moving into the medium with the NaBr than the KBr in all comparable treatments except at 1.0 g/g after 5 and 10 days.

These observed differences in diffusion rates may be attributed to the greater solubility of NaBr versus KBr and the effect of the different accompanying cation of each salt. For diffusion to proceed in the columns, the cation/anion pairs must move in the same direction at the same speed to maintain electroneutrality. This type of diffusion is termed salt or mutual diffusion and the resulting diffusion coefficient consists of a harmonically averaged ion mobility for each ion (Robinson and Stokes, 1959). The diffusion coefficient at infinite dilution for KBr (2.0 x 10-5 cm2 sec-1) is greater than NaBr (1.6 x 10-5 cm2 sec-1) in an aqueous solution but, surprisingly, the calculated De for NaBr is greater than KBr in the container medium at 2.5 g/g (Table 2).

Diffusion coefficients in an aqueous solution are not constant with varying solution concentrations, but range from 1.9 - 2.4 and 1.5 - 1.7 x 10-5 cm2 sec-1 for KBr and NaBr respectively (Robinson and Stokes, 1959). The Fickian diffusion model used to calculate the effective diffusion coefficients in the columns requires that the diffusion coefficient be independent of solution concentration, or that solution concentration gradients are sufficiently small so that the diffusion coefficient can be considered to be independent of concentration. The solution concentration in the diffusion columns varies across the whole range of molalities from saturation at the salt interface to an infinitely dilute solution at the far end. This implies that De in the medium would be concentration-

dependent as well, and the simple Fickian diffusion model will not sufficiently predict the Br- movement in the columns. Using this reasoning, a complete model to predict ion movement in porous media in a PDZ would need to include a non-Fickian diffusion component with a concentration-dependent diffusion coefficient for all diffusing ions. It must be noted, however, that at all concentrations the value of De for KBr exceeds that of NaBr, thus this effect cannot explain fully the observed reversal in magnitudes of De for NaBr and KBr in the container medium.

The horizontal experiments showed slight evidence that the effective diffusion coefficient of Br- is dependent on the diffusion time. The mean effective diffusion coefficient for NaBr in medium at 2.5 g/g increased significantly ($P < 0.05$) from 5 days to 10 days (Table 2). There was no significant increase in mean De for KBr with time of diffusion. There was no difference in Br- distribution after 10 days in either the vertical columns with the salts placed on the top or bottom or the horizontal columns at water contents of 1.0 and 2.5 g/g. Plots of Br^- distribution for all orientations were similar to Figure 13 for horizontal columns after 10 days. Additionally, there was no statistical difference between D_e calculated after 10 days for KBr in medium at 2.5 g/g water content for the horizontal and vertical columns with salt placed at the top or bottom. Gravitational water distribution occurred in the columns at 4.0 g/g water contents (Figure 18). Bromide movement in vertical columns oriented with KBr at the top and bottom were similar after 10 days, whereas Br- movement was significantly greater in the horizontal column. Faster movement in the horizontal column at 4.0 g/g water content occurred in response to changes in solution density in the medium which have a negligible effect at low water contents. As KBr dissolves at the end of the column, an

unstable density gradient develops convective flows and the heavier, saturated solution on the top of the column flows down and towards the end of the column. It moves over the equally dense saturated solution on the bottom of the column and displaces the water, gradually moving toward the end of the column. A convective-diffusive flow is developed in this manner causing the salt to move down the column faster than by diffusion processes alone. This process was evident during column analysis when horizontal columns were disassembled and some of the sections were laid flat and allowed to dry, revealing higher salt concentrations in the bottom half of the section. Observations of this "drop out" effect have been reported previously in the literature (Burns and Dean, 1964), but was not observed in any of our vertical columns.

Rate of movement and distribution of Br- is dependent on the water content in the medium. As expected, diffusion rates of KBr and NaBr increased with increasing moisture contents. At 4.0 g/g initial water content over 50% of the cross-sectional area is filled with water pathways in which diffusion can occur freely; after 10 days almost all 50 g of KBr and all the NaBr moved into the medium (Table 1). At lower water contents, much less of the cross sectional area is available for diffusion of solutes and correspondingly less salt moves into the medium.

At 1.0 g/g water contents, movement of water toward the salt source at the end of the medium columns is striking (Figure 15 and Figure 16). The same movement was evident to a lesser extent in columns with 2.5 g/g water content. More water moved toward the salt compartment from the medium with the NaBr than the KBr in response to its hygroscopic properties. NaBr is characterized as "hygroscopic" and forms a hydrated molecule($NaBr \cdot 2H_2O$) whereas KBr is characterized as "slightly hygroscopic" and does

not have a hydrated form (Weast, 1987). This hygroscopic movement of water in the NaBr column created a zone of drier medium at about 2 cm from the salt compartment, forming a barrier of low water content and significantly slowing the rate of Br^- movement for NaBr in the first 10 days compared to the KBr column. The presence of concentrated solutions in the medium caused the osmotic potential of the solution to increase, resulting in a localized decrease in vapor pressure. Vapor pressure gradients cause water transport through the media as it is vaporized in areas of low solute concentration and condensed back into solution in areas of high solute concentration. At 1.0 g/g, gradients persist in the medium because the liquid phase transport in the dry medium is less than the vapor transport. This process has been reported only to occur in relatively dry soils (Wheeting, 1925; Scotter and Raats, 1970). Although not as evident at higher moisture contents, similar osmotic pressure gradients exist, and it follows that this vapor transport process would still occur in unsaturated media of higher water content as long as connected gas filled paths existed in the media. This process may be obscured at higher water contents in which liquid phase transport is sufficient to allow redistribution of the water transported through the vapor phase.

3.5 Summary

The simple Fickian diffusion model was useful for analysis of selected columns in this study, but was inadequate to predict the fertilizer ion movement in a PDZ, where it becomes necessary to model the water movement as well as the ion movement. The results of this research have important implications in predicting ion diffusion from concentrated salt sources in unsaturated porous media. 1. The initial quantity of salt

applied and the solubility and hygroscopic properties of the salt affect the movement of water near the salt and the salt diffusion rate. 2. It is necessary to recognize that there is no simple relationship between De in unsaturated media and the pure water diffusion coefficient for specific salts. 3. As expected, the ionic diffusion in the container medium increased with increasing water content. 4. At high water contents (4.0 g/g), water redistribution and solution density gradients increase gravitational flows of solution in the medium. 5. Significant water redistribution occurred in the medium in response to an osmotic potential established by the concentrated solution in the medium. These features significantly complicate the mathematical modeling of the system, rendering the simple Fickian diffusion model of limited predictive value.

Even though modeling the processes that control diffusion is a complicated task, the results of this research show that there is potential to minimize leaching losses in nursery production systems by placing fertilizer in a "protected diffusion zone". The observed ion diffusion rates in the medium were always less than the predicted maximum diffusion rates expected in pure water and significantly less than would be expected by leaching. For typical moisture contents of container media in a Conserver and CIPS, a protected diffusion zone of 15-cm length is sufficient to maintain negligible fertilizer losses, because the maximum diffusion rate of Br- salts is not expected to be greater than fertilizers providing NO3-. Although in this paper we address these issues in the context of these two particular horticultural applications, these results have broader implications for other applications such as fertilizer diffusion under plastic mulches and ion movement in saline soils with limited infiltration. Application and retention of fertilizer ions within

the plant root zone is an important step toward conserving water and fertilizer, protecting ground and surface water quality, and sustaining economic plant growth.

3.6 References

Alexander, S. V. 1993. Pollution control and prevention at containerized nursery operations. Water Sci. and Tech. 28(3-5):509-517.

Barber, S. A., J. M. Walker, and E. H. Vasey. 1963. Mechanisms for the movement of plant nutrients from the soil and fertilizer to the plant root. Agricultural and Food Chemistry. Vol 11(3):204-207.

Bhadoria P. B. S., J. Kaselowsky, N. Claassen and A. Jungk. 1991. Soil phosphate diffusion coefficients: their dependence on phosphorous concentration and buffer power. Soil Sci. Soc. Am. J. 55:56-60.

Biernbaum, J. A. 1992. Root-zone management of greenhouse container-grown crops to control water and fertilizer use. HortTechnology. 2(1):127-132.

Burns, G. R. and L. A. Dean. 1964. The movement of water and nitrate around bands of sodium nitrate in soils and glass beads. Soil Sci. Soc. Am. Proc. 28:470-474.

Cox, D. A. 1993. Reducing nitrogen leaching-losses from containerized plants: the effectiveness of controlled-released fertilizers. J of Plant Nutrition. 16(3):533-545.

Crank, J. 1975. The mathematics of diffusion. Oxford University Press, New York.

Freier, R. K. 1976. Aqueous Solutions Vol. 1. Data for inorganic and organic compounds. Walter de Gruyter. Berlin-NewYork.

Graham-Bryce, I. J. 1963. Effect of moisture content and soil type on self diffusion of ^{86}Rb in soils. J. Agric. Sci. 60:239-244.

Green, J. L. 1995. Self-contained fertilizing tube portable. Resource: Engineering and Technology for a Sustainable World. 2(8):9.

Green, J. L., B. A. Briggs, and D. L. Briggs. 1993a. Fertilizing apparatus. U.S. Patent 5,212,904. Assigned to the State of Oregon, acting by and through the State Board of Higher Education on behalf of Oregon State University. Date issued: 25 May.

Green, J. L., S. F. Kelly, B. Blackburn, J. Robbins, B. A. Briggs, and D. L. Briggs. 1993b. A protected diffusion zone (PDZ) to conserve soluble production chemicals. Combined Proc. Intl. Plant Prop. Soc. 43:40-44.

Green, J. L. and R. Schneckenburger. 1992. Pallet system for container-grown plants. U.S. Patent 5,170,581. Assigned to the State of Oregon, acting by and through the State Board of Higher Education on behalf of Oregon State University. Date issued: 2 June.

Hershey, D. R. and J. L. Paul. 1982. Leaching-losses of nitrogen from pot chrysanthemums with controlled-release fertilization. Scientia Hort. 17:145-152.

Kabashima, J. N. 1993. Innovative irrigation techniques in nursery production to reduce water usage. HortScience. 28(4):291-293.

Klute, A. and J. Letey. 1958. The dependence of ionic diffusion on the moisture content of nonadsorbing porous media. Soil Sci. Soc. Proc. 213-215.

Kolaian, J. H. and Ohlrogge, A. J. 1959. Principles of nutrient uptake from fertilizer bands IV. Accumulation of water around the bands. Agronomy J. 51:106-108.

Lawton, K. and Vomocil, J. A. 1954. The dissolution and migration of phosphorous from granular superphosphate in some Michigan soils. Soil Sci. Soc. Proc. 18:26-32.

Mehta, B. K., S. Shiozawa and M Nakano. 1995. Measurement of molecular diffusion of salts in unsaturated soil. Soil Sci. 159(2)115-121.

Nye, P. H. and P. B. Tinker. 1977. Solute movement in the soil-root system. Blackwell Scientific Publications, Oxford. 342 pages.

Olsen, S. R. and W. D. Kemper. 1968. Movement of nutrients to plant roots, p. 91-151. In: A. G. Norman (ed.) Advances in Agronomy, Am. Soc. of Agronomy. Vol. 20, edited by Academic Press.

Palmer, C. J. and R. W. Blanchar. 1980. Prediction of diffusion coefficients from the electrical conductance of soil. Soil Sci. Soc. Am. J. 44:925-929.

Parlange, J. 1973. Movement of salt and water in relatively dry soils. Soil Sci. 116(4):249-255.

Patil, A. S., K. M. King and M. H. Miller. 1963. Self-diffusion of rubidium as influenced by soil moisture tension. Can. J. of Soil. Sci. 43:44-51.

Robinson, R. A. and R. H. Stokes. 1959. Electrolyte solutions. Butterworths Scientific Publications. London.

Rost, B. 1995. The cooler king. Resource: Engineering and Technology for a Sustainable World. 2(8):8-12.

Schaff, B. E. and E. O. Skogley. 1982. Diffusion of potassium, calcium, and magnesium in Bozeman silt loam as influenced by temperature and moisture. Soil Sci. Soc. Am. J. 46:521-524.

Scotter, D. R. 1974a. Factors influencing salt and water movement near crystalline salts in relatively dry soil. Aust. J. Soil Res. 12:77-86.

Scotter, D. R. 1974b. Salt and water movement in relatively dry soil. Aust. J. Soil Res. 12:27-35.

Scotter D. R. and Raats, P. A. C. 1970. Movement of salt and water near crystalline salt in relatively dry soil. Soil Sci. 109(3):170-178.

Ticknor, R. L. and J. L. Green. 1987. Effect of irrigation methods on plant growth and water use. Proc. Int. Plant Prop. Soc. 37:45-48.

Tyrrell, H. J. V. and K. R. Harris. 1984. Diffusion in liquids: A theoretical and experimental study. Butterworth, London.

Weast, R. C. (ed.) 1987. CRC handbook of chemistry and physics. CRC Press Inc. Boca Raton Fla.

Wheeting, L. C. 1925. Certain relationships between added salts and the moisture of soils. Soil Science. 16(4):287-299.

Chapter 4. Osmotically Driven Water Vapor Flow in Unsaturated Soil

4.1 Abstract

Salts at high concentrations in unsaturated porous medium can induce significant water vapor fluxes caused by large gradients in osmotic potential. This ion-excluding redistribution of water complicates the modeling of ion diffusion in these systems. We combine existing theories of water and vapor transport in unsaturated media with aqueous electrolyte thermodynamic theory to predict soil water vapor movement using a physically based model. The model was validated using experimental data published by Wheeting, (1925). A solution is presented for a special case showing that the model explains the previously published results from soil column experiments. It is shown how gradients in water vapor driven by aqueous osmotic potentials cause significant water vapor fluxes towards regions of high ionic concentration.

4.2 Introduction

The presence of solutes in soil pore water creates an osmotic potential. Gradients in osmotic pressure can induce significant flow of water in these soils under certain conditions. This has been verified experimentally by a number of researchers (Wheeting, 1925; Letey, 1969; Raats, 1969; Scotter and Raats, 1970; Scotter, 1974a; Nassar and Horton, 1989a; Nassar et al., 1992b; Kelly et al., 1997). For osmotic water flow to occur in soils, a semi-permeable membrane is required where ions are excluded yet water can cross freely. Osmotic potentials can give rise to variations in fluid pressure in the presence of such a semi-permeable membrane. This is most commonly seen across plant

cell walls that exclude certain ions allows water to move freely across the membrane (Nobel, 1983, p. 71).

Two mechanisms are identified in the literature where an osmotic gradient due to varying solute concentrations in soil can cause water to move in either liquid or vapor phase. 1.) Liquid phase water flow can occur when anions are excluded from negatively charged soil pores which act as a semi-permeable membrane. The resulting driving force due to the osmotic pressure is quantified with an osmotic efficiency coefficient expressed as a function of concentration and water content (Kemper and Rollins, 1966). The osmotic efficiency coefficient is a function of the distribution of adsorbed ions and the thickness of the soil solution which is calculated from diffuse double-layer theory (Bresler, 1973). 2.) Vapor phase flow can occur in unsaturated soils when differing solute concentrations exist across gas filled pores separating the liquid. The gas-liquid interfaces act as semi-permeable membranes across which water vapor flows freely and ions are excluded. The resulting osmotic pressure gradient causes water vapor to flow from regions of lower solute concentration to areas of higher solute concentration. Theoretical analyses of flow have been carried out by several researchers (Letey, 1969; Parlange, 1973; Scotter, 1974b; Nassar and Horton, 1989b; Nassar et al., 1992a) which considered the complex phenomena involving coupled movement of liquid, vapor, solute and heat. This paper considers the second transport mechanism and focuses on the special case where water vapor flows exclusively in the presence of high solute concentrations.

In 1925, Wheeting conducted experiments where salts were added to columns of unsaturated soil demonstrating significant water transport towards the soil with increased salt concentration. Relationships between added salts and the moisture of soils in column

experiments were investigated using salt treated soil separated from water-treated soil. In one set of experiments soil columns were set up such that a 2-inch length soil was treated with a 1% by weight salt solution to a constant water content and 6 inches of soil was wet to the same water content but without the salt. Four treatments were tested using two soils with different textures (medium sand or clay loam) and two salts (KCl or Na_2CO_3). The two soil sections were then arranged in the column such that a 1/2 in. space existed between them. The columns were left at 18°C and determinations of water content in one inch sections were made after intervals of 5 and 15 days (Figure 19 and Figure 20). It was observed that water had moved rapidly from the unsalted soil towards the side of the column treated with (Figure 19 and Figure 20). The rate of water vapor flow was slower in the medium sand treatments as compared to the clay loam treatments of the same salt. At the end of 15 days more water flowed in both the KCl treatments as compared to the Na_2CO_3 treatments of the same soil. Wheeting concluded that water vapor flow was dependent on both soil texture and salt. This conclusion was later supported by experiments conducted by Scotter, (1974b) and Kelly et al. (1997).

The objective of this paper is to refine the existing theory of osmotically driven soil water vapor movement using a physically based model. The model was validated using the experimental data published by Wheeting (1925). Analysis of this broken column system is simpler to analyze than a continuous system where simultaneous liquid, vapor and salt are moving throughout the soil. This data provides an opportunity to verify the equations used to calculate the water vapor density and the water vapor transport mechanism necessary for a complete model of coupled water and solute transport in unsaturated soils.

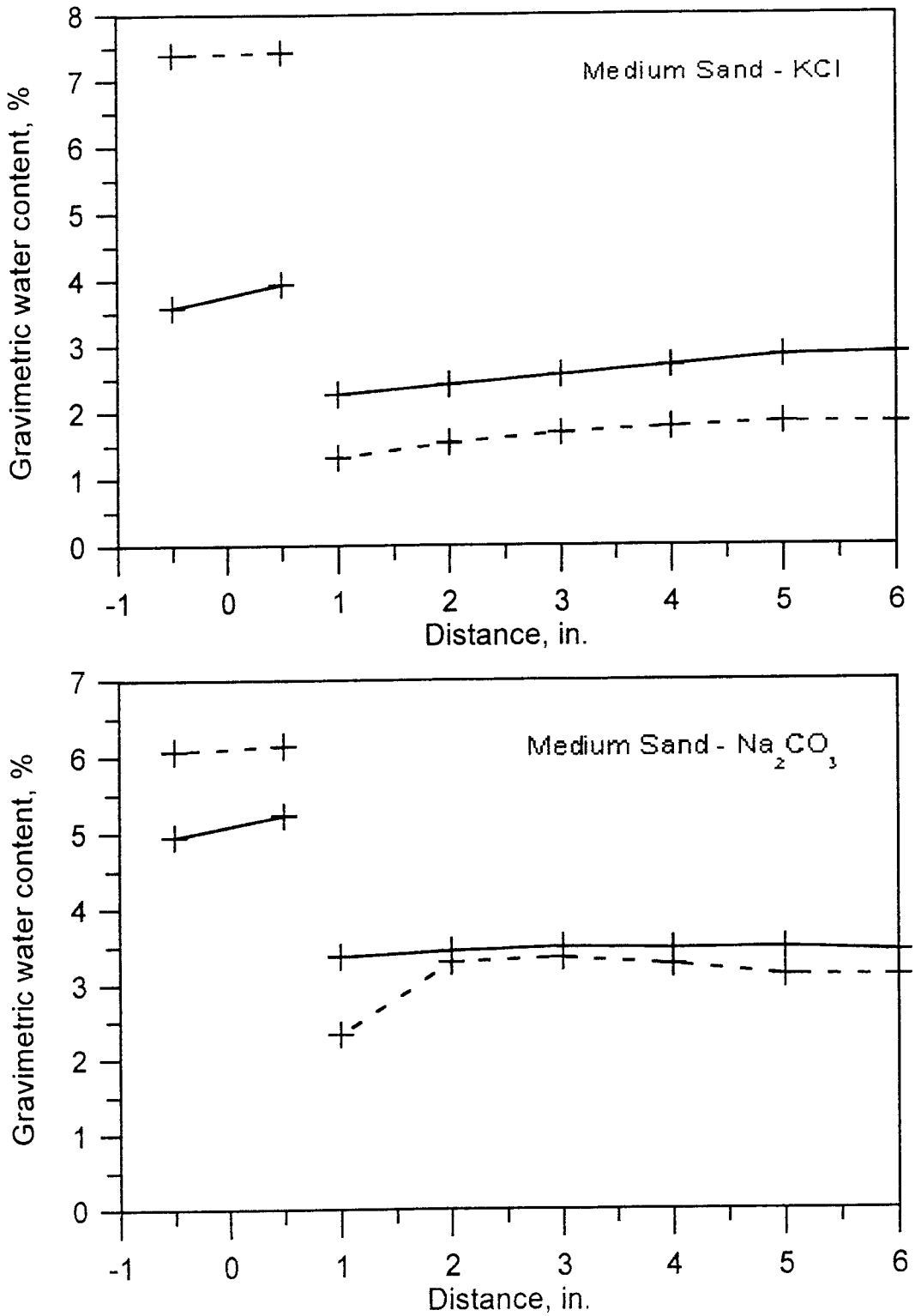

Figure 19. Gravimetric water content distributions for KCl (a) and Na_2CO_3 (b) in medium sand after 5 days (solid lines) and 15 days (dashed lines) from the broken column data of Wheeting (1925).

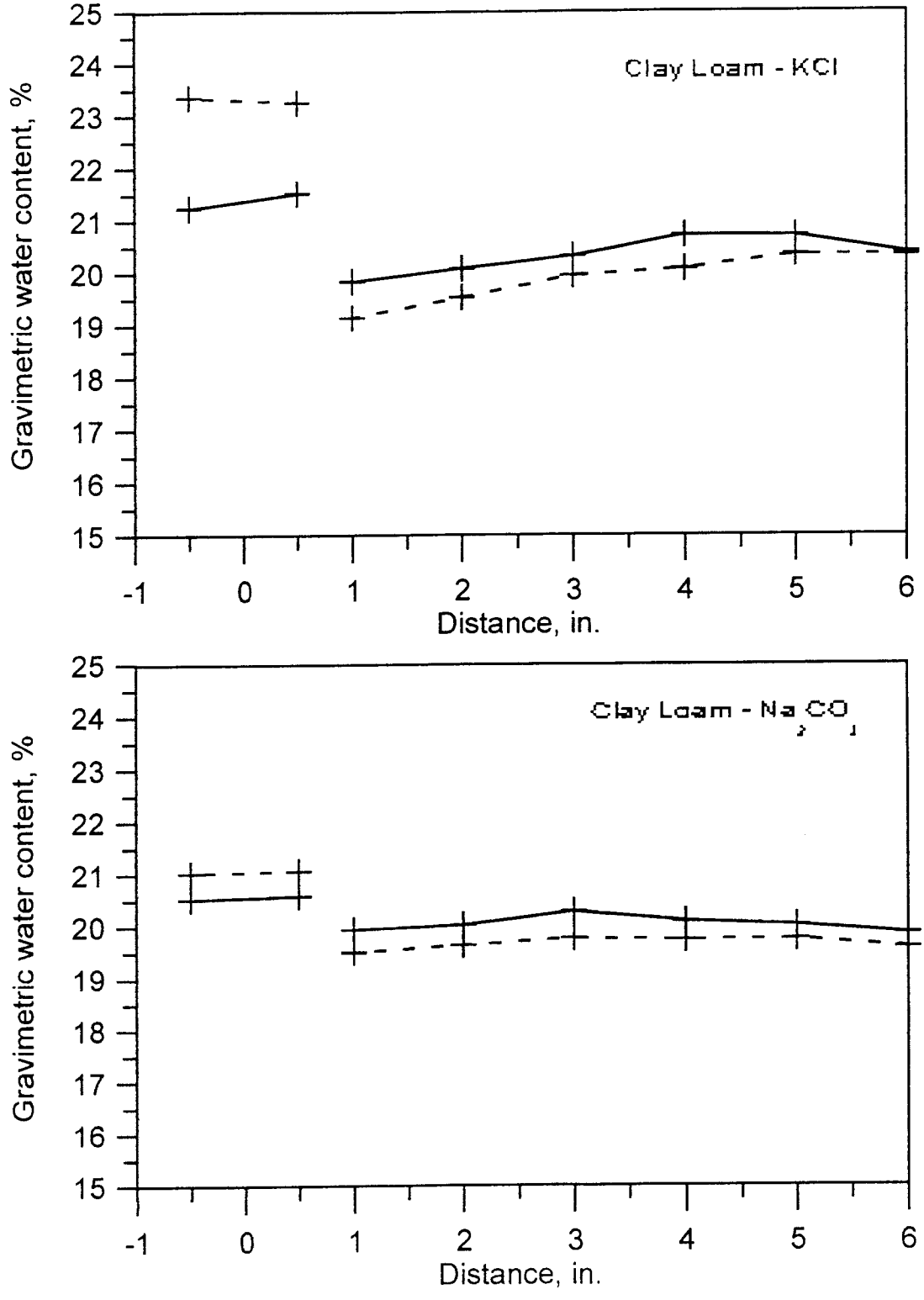

Figure 20. Gravimetric water content distributions for KCl (a) and Na_2CO_3 (b) in clay loam after 5 days (solid lines) and 15 days (dashed lines) from the broken column data of Wheeting (1925).

4.3 Model Development

In the following section we derive the set of governing differential equations describing simultaneous movement of water in the vapor and liquid phase and consequent flow of ions in unsaturated porous media. The equations are developed in one-dimension, assuming isothermal conditions. We also assume that movement of water in both the vapor and the liquid phase are first order phenomena described by Fickian diffusion (Jackson, 1964) and Darcy's law.

$$q_w^l = -K_l \frac{\mathrm{d}\Psi_l}{\mathrm{d}x} \qquad [97]$$

$$q_w^v = -D_v \frac{\mathrm{d}p_v}{\mathrm{d}x} \qquad [98]$$

$$q^{\cdot} \qquad [99]$$

where x is the spatial coordinate, q_w is the total water flux, q^l_w is the liquid water flux, and q^v_w is the water vapor flux, all with units of mass/length^2/time. K_l and D_v are first order coefficients for liquid and vapor phase flow with units of length/time. Ψ_l and p_v are the driving potentials for water in the liquid and vapor phase with units of mass/length^2.

4.3.1 Osmotic Potential, Ψ_s

The osmotic potential of a dilute solution can be calculated using Rauolt's Law, which relates the vapor pressure of a solvent above a solution to the quantity of solute dissolved in the solution (Alberty, 1987, p. 196).

$$P_i = N_i \cdot P_i^{\circ} \qquad [100]$$

where P_i is the partial pressure of the ith component of the solution, P°_i is the saturated vapor pressure of the pure component and N_i is the mole fraction of that component. For an aqueous solution,

$$N_w = \frac{P_w}{P_w^{\circ}} \qquad [101]$$

P°_w is the pressure of pure water, P_w is the vapor pressure of the solution, and N_w is the mole fraction of the water which can be calculated from

$$N_w = \frac{n_w}{n_w + \sum_{all\ j} n_j} \qquad [102]$$

where n_j is the number of moles of component j. The water potential due to the presence of solutes can than be calculated from the Van't Hoff relation (Nobel, 1983, p. 72)

$$\Psi_s = \frac{RT \ln(N_w)}{\overline{V_w}} \qquad [103]$$

where $\overline{V_w}$ is the partial molal volume of water (18.0×10^{-6} m^3/mole), T is the temperature in °K, and R is the gas constant (8.3143×10^{-6} m^3 MPa/mole/°K). It is sometimes convenient to calculate osmotic pressures in terms of the concentration of the solute, c_j. In this case Eq. [103] reduces to (Nobel, 1983, p. 74)

$$\Psi_s = RT \sum_j c_j \qquad [104]$$

which is valid for dilute ideal solutions.

Aqueous solutions with concentrations exceeding a few millimoles depart from the ideality of the Van't Hoff relation. To accurately represent the mole fraction of the water in solutions, which approaches unity as the dilution is increased, it is common to tabulate data in terms of the osmotic coefficient, ϕ. The osmotic coefficient for any aqueous solution is (Robinson and Stokes, 1959, p. 29)

$$\phi = \frac{-1000 \cdot \ln(a_w)}{18.0153 \sum_i \nu_i m_i} \qquad [105]$$

where a_w is the activity of water, ν_i is the stoichiometric number of the solute, and m_i is the molality. To calculate the osmotic coefficient in all but the most dilute solutions it is necessary to use a more complex model than Eq. [105].

One of the most widely used formula for estimation of the osmotic coefficient is Pitzer's method presented in a series of papers beginning in 1973 (Horvath, 1985, p. 217; Zemaitis et al., 1986, pp.71-75). For 1:1 electrolytes (e.g., NaCl, KBr, NaBr) Pitzer's equation is

$$\phi - 1 = -\left[A_m m_2^{1/2} / (1 + B m_2^{1/2})\right] + m_2\left[\beta_0 + \beta_1 \exp(-\alpha_1 m_2^{1/2})\right] + m_2^2 C^{\phi} \qquad [106]$$

where β_0, β_1 and C^{ϕ} are parameters specific to each electrolyte up to 6 mol/l solutions Zemaitis et al., 1986, pp. 179-190), α_1 for 1:1 and 2:1 electrolytes is 2.0 $kg^{1/2}mole^{-1/2}$, B is1.2 $kg^{1/2}mole^{-1/2}$ for all electrolytes, and m_2 is the molality of the electrolyte, mol kg^{-1} (equivalent to the ionic strength). The osmotic Debye-Huckel coefficient, A_m, is computed as

$$A_m = \frac{1}{3}\left(\frac{2\pi N_0 \rho_w}{1000}\right)^{1/2}\left(\frac{e^2}{D_0 kT}\right)^{3/2} \qquad [107]$$

where N_0 is Avogadro's number, ρ_w is the density of pure water, D_0 is the static dielectric constant of pure water, k is Boltzmann's constant, e is the absolute electronic charge, and T is the absolute temperature, °K. Once the activity of the water in solution is known it is possible to calculate the osmotic potential of the soil water solution using the Kelvin equation (Alberty, 1987,p. 310),

$$\Psi_s = \frac{RT\ln(a_w)}{\overline{V_w}} \qquad [108]$$

At low molalities most solutions act like ideal solutions and follow Raoult's law, while significant deviations often occur at higher molalities. The shape of the osmotic potential vs. solution molality is strongly dependent on the ionic species under consideration, which is accounted for in equation [106]. To account for temperature effects on the activity coefficient, Pitzer suggested corrections be made through D_0, ρ_w and T in the Debye-Huckel coefficient, A_m (Zemaitis, 1986, pp. 84-88). The activity coefficient for multicomponent mixtures of salts may also be calculated using Pitzer's method which is outlined in Zemaitis, (1986).

4.3.2 Water and liquid flow equations

For both liquid and vapor, the governing equations have similar form. We will derive these results applicable for either phase. From equations [97] or [98] we have mass movement governed by:

$$q = -K\frac{\mathrm{d}\Psi}{\mathrm{d}x} \qquad [109]$$

where K is a general first order coefficient. Applying mass conservation principles at a point one obtains

$$-\frac{\mathrm{d}q}{\mathrm{d}x} = \dot{q} + \frac{\mathrm{d}m}{\mathrm{d}t} \qquad [110]$$

where m is the mass and $\dot{q}$ is the mass source/sink term. Substituting equation [109] into equation [110] we obtain

$$\frac{\mathrm{d}m}{\mathrm{d}t} = \frac{\mathrm{d}}{\mathrm{d}x}(K\frac{\mathrm{d}\Psi}{\mathrm{d}x}) - \dot{q} \qquad [111]$$

which is a generalized mass flow equation that is modified to account for liquid, vapor and ion flow.

4.3.2.1 Liquid Flow

Equation [111] can be written for liquid mass flow.

$$\frac{\mathrm{d}m_l}{\mathrm{d}t} = \frac{\mathrm{d}}{\mathrm{d}x}(K_l\frac{\mathrm{d}\Psi_l}{\mathrm{d}x}) - \dot{m}_l \qquad [112]$$

where m_l is the mass of the liquid and $\dot{m}_l$ is a source/sink term. The source/sink term is used to couple the mass transfer of water between the gas phase and the liquid phase, which assumes that the thermodynamic equilibrium occurs much more rapidly than the transport processes. The potential term driving the liquid mass flow is composed of several individual potentials that can be calculated at any point in the flow field.

$$\Psi_l = \Psi_g + \Psi_\tau + \Psi_p \qquad [113]$$

where Ψ_g is the gravitational potential and Ψ_p represents external pressure potentials applied which is equal to zero everywhere in this system. Ψ_τ is the matric potential and can be calculated from the soil water retention function (van Genuchten, 1980).

$$\Psi_\tau = \frac{\rho_w \cdot g}{\alpha}\left[\frac{1}{\left(\frac{\theta-\theta_r}{\theta_s-\theta_r}\right)^{\frac{1}{m}}}-1\right]^{\frac{1}{n}} \qquad [114]$$

where ρ_w is the density of water, g is the gravitational constant, α is the inverse air entry pressure, θ is the soil water content, θ_r is the residual soil water content, θ_s is the saturated soil water content, n is a fitting parameter and m = 1-1/n. By substituting equation [113] into [112], the liquid water mass transport equation then becomes.

$$\frac{dm_l}{dt} = \frac{d}{dx}\left(K_l \frac{d(\Psi_\tau + \Psi_g)}{dx}\right) - \dot{m}_l \qquad [115]$$

4.3.2.2 Vapor Transport

Equation [111] can be written for vapor mass transport.

$$\frac{dm_v}{dt} = \frac{d}{dx}\left(D_v \frac{dp_v}{dx}\right) - \dot{m}_v \qquad [116]$$

where m_v is the mass of vapor, and $\dot{m}_v$ is a source/sink term for the water vapor. The potential term driving the vapor phase flow is the vapor pressure of water. The vapor pressure of water varies with temperature, osmotic potential and the matric potential. The

osmotic potential can be calculated using equations [105] through [108], or equation [104] at low molalities. The vapor pressure or water vapor density, p_v, above the solution can be calculated using

$$\frac{p_v}{p_v^0} = \exp\left(\frac{-(\Psi_s + \Psi_\tau)\overline{V}_w}{RT}\right) \qquad [117]$$

The vapor pressure above a solution can be decreased by the addition of solutes or increased matric potentials. At high molalities, there are significant differences in water vapor density between the different salt solutions at the same molality.

4.4 Methods

We wish to check the governing equations derived above using the experimental data of Wheeting (1925). To facilitate analysis given the limited data provided by Wheeting, the problem was simplified to ignore transport through the column media. The following solution considers only transport of water vapor across the 0.5 in. air space between the saline and non-saline sections assuming that redistribution in the soil is instantaneous. This assumption is supported by the data from Wheeting's experiments which show nearly uniform water content except for the Na_2CO_3:medium sand treatment at 15 days(Figure 19 and Figure 20).

Under these assumptions the rate change of moisture content of the two sections is described by the following set of equations.

$$\frac{\partial}{\partial t} m_0 = K_v \frac{A}{V_0} \cdot \frac{\Delta p_v}{\Delta x} \qquad [118]$$

$$\frac{\partial}{\partial t} m_1 = -K_v \frac{A}{V_1} \cdot \frac{\Delta p_v}{\Delta x} \qquad [119]$$

where m_0 is the mass per unit volume water content of the saline section, m_i is the mass per unit volume water content of the non-saline section and K_v is the water vapor diffusion coefficient in the airspace between the sections. The water vapor density in the saline segment, $p_v(m_0)$, and the non-saline segment, $p_v(m_1)$ is calculated using the method described in the previous section We solve these coupled non-linear differential equation numerically using a Runge-Kutta method. The model was implemented using Mathcad PLUS 6.0 (Mathsoft Inc., Cambridge, MA).

The initial water content and molalities of the saline sections used in the model were calculated from the data of Wheeting and shown in Table 3. Other than the textural classification of the soils used by Wheeting, no other soil properties were given. The soil water properties were initially estimated using other soils with similar textural classifications for which the parameters in equation [114] were known. These initial parameters were adjusted incrementally about these initial estimates in the model to subjectively achieve the best fit results shown in Figure 22 and Figure 23. The same soil parameters were used for both salt treatments in the same soil (Table 3). All other parameters are physically based depending on the particular salt and temperature.

4.5 Discussion

The modeling results shown in Figure 22 and Figure 23, confirm that significant water vapor flow occurs across the air gap and that the theory developed shows water vapor flow in the same magnitude as seen in Wheeting's original experiment. Overall, the

column treatment differences between different salts and media agree well given the limited experimental data available. The model overestimates the vapor flow for the Na_2CO_3:medium sand treatment at 15 days (Figure 22). This may be attributed to the non-instantaneous redistribution of water in the non-saline section in Wheeting's columns. Figure 19 shows a dramatic decrease in water content at the air gap at 15 days where water is not distributed evenly throughout the column. The instantaneous redistribution of water in the column is one of the assumptions made in the model development and these results might be expected.

The model could account for differences in water flow rates due to different salts. Sodium carbonate caused less water vapor transport across the interface initially than did KCl in the medium sand (Figure 22). This is due to the greater solubility of the KCl compared to that of Na_2CO_3 (Table 3). Even though the Na_2CO_3 produces a slightly larger water vapor deficit than KCl at molalities less than 1.69 mol/kg, the increased solubility of the KCl increased the vapor deficit beyond what could be achieved using Na_2CO_3 initially. As water vapor flows across the air gap and the saline section becomes more dilute the vapor flowrates become more equal (Figure 22).

Soil texture affected the flowrate due to the different matric and absorptive potentials that could be developed in the soils (Figure 22 and Figure 23). This is masked somewhat because of the different initial water contents of the medium sand and the clay loam soils. Because salt was added to the columns on a dry weight basis, more dilution occurred with the clay loam columns as compared to the columns with the medium sand. This dilution caused the vapor pressure gradient to be much lower in the clay loam treatments resulting in a slower water vapor flowrate as compared to the dryer medium

sand columns. The model explains why different salts cause different rates of water vapor movement through porous media. Using the same set of initial conditions, but changing the initial salt used in the column, different rates of water vapor movement were observed (Figure 24).

Table 3. Model parameters and Physical constants

Physical constants	
N_0, Avogadro's Number	$6.0221367 \cdot 10^{23}$
ρ_w, density of water at 20°C	0.99823 g/cm^3
D_0, static dielectric constant of water at 20°C	80.10
k, Boltzmann's constant	$1.380658 \cdot 10^{-16}$ erg/deg
e, absolute electronic charge	$4.803 \cdot 10^{-10}$ e.s.u.
T, absolute temperature	293.15 °K
K_v, diffusion coefficient of water vapor in air at 20°C	$2.42 \cdot 10^{-5}$ m^2/sec
R, gas constant	8.3143 joules

Soil water retention parameters, equation [114]

Soil texture	N	α [cm^{-1}]	θ_s [m^3/m^3]	θ_r [m^3/m^3]	ρ_b, bulk density, [gm /cm^3]
Medium sand	1.4	0.124	0.41	0.01	1.51
Clay loam	1.48	0.059	0.46	0.1	1.62

Initial conditions

Wheeting's column treatment	Water content θ_0 and θ_1, [m^3/m^3]	m_0, molality in saline-section, [mol/kg]
KCl:medium sand	0.045	3.42
Na_2CO_3:medium sand	0.058	1.69
KCl:clay loam	0.334	0.69
Na_2CO_3:clay loam	0.325	0.50

Pitzer's parameters†

Salt	β_0, $(4/3\ \beta_0)$††	β_1, $(4/3\ \beta_1)$††	C_ϕ, $(2^{5/2}/3\ C_\phi)$††	Solubility††† (20°C), [mol/kg]	Molecular Weight [g/mol]
KBr	0.0569	0.2212	-0.0018	3.31	119.01
KCl	0.04835	0.2122	-0.00084	3.42	74.56
KNO_3	-0.0816	0.0494	0.00660	2.37	101.11
NaBr	0.0973	0.2791	0.0016	4.62	102.90
NaCl	0.0765	0.2664	0.00127	4.53	58.44
Na_2CO_3	0.2530	1.128	-0.09057	1.69	105.99

† Zemaitis, 1986
†† for 2:1 electrolytes (e.g. Na_2CO_3)
††† Freier, 1976

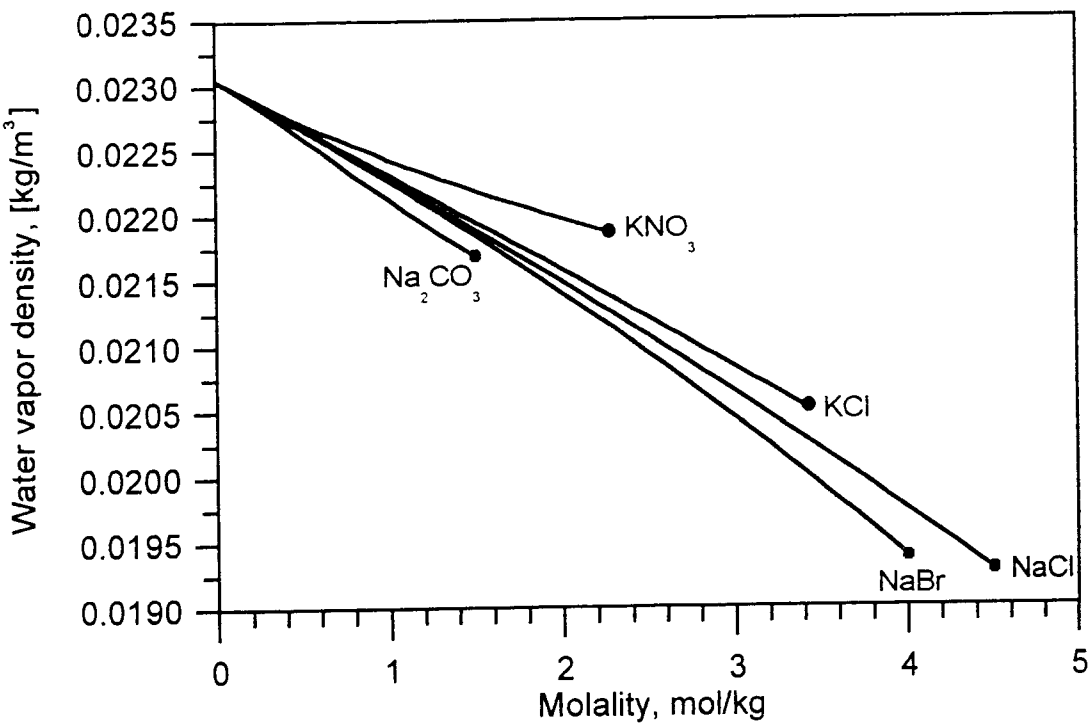

Figure 21. Water vapor density of salt solutions at 25°C calculated using equation [117]. Going from uppermost to bottommost, the lines represent aqueous solutions of KNO_3, KCl, NaCl, NaBr and Na_2CO_3 respectively. The endpoints of each line indicate the maximum solubility of the solution.

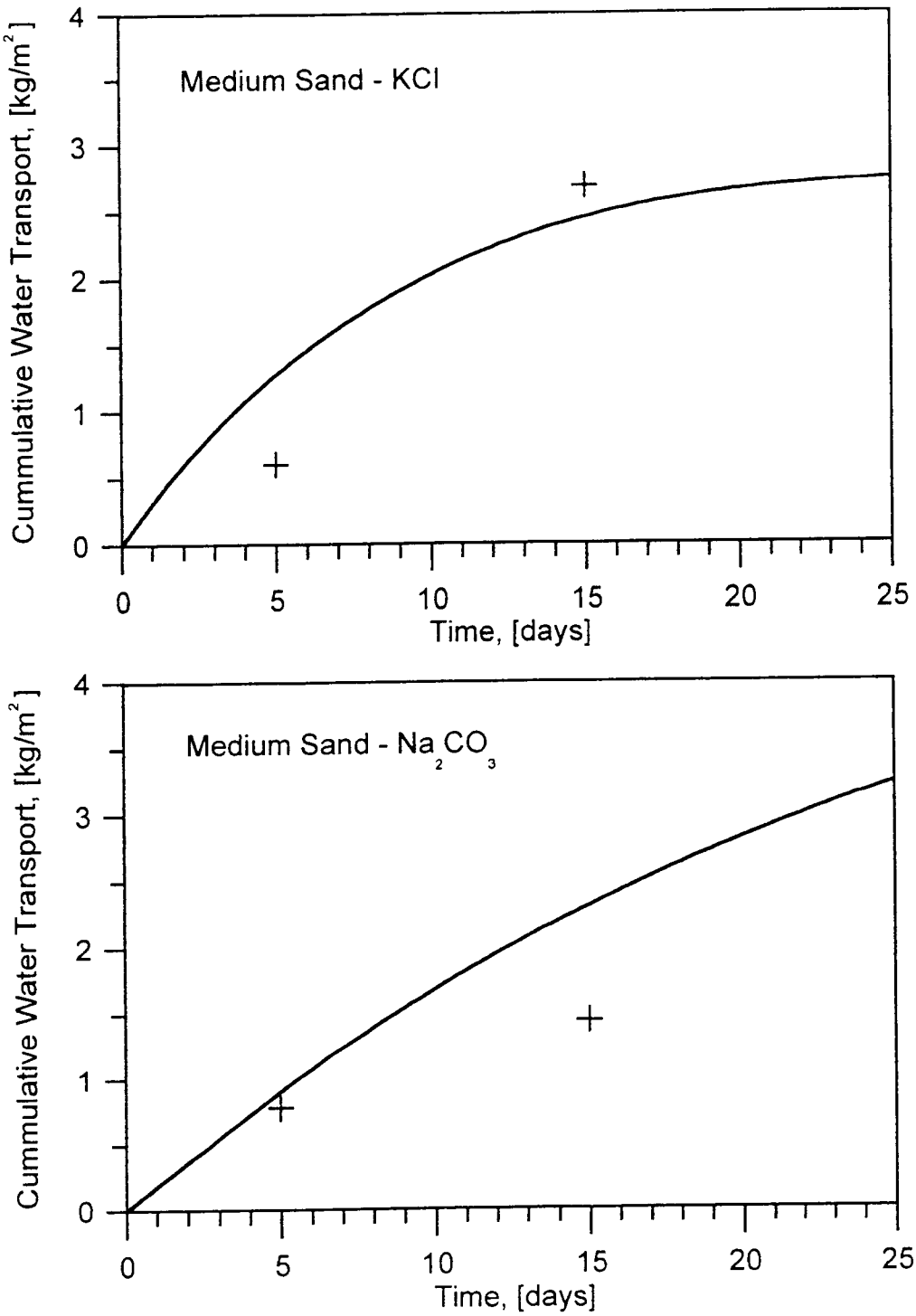

Figure 22. Cumulative water vapor flow across a 0.5 in. air gap from a non-saline section to the saline section of the broken column for KCl (a) and Na_2CO_3 (b) in medium sand. Solid line is the model result using parameters from Table 1, and points (+) are calculated from the broken column data of Wheeting (1925).

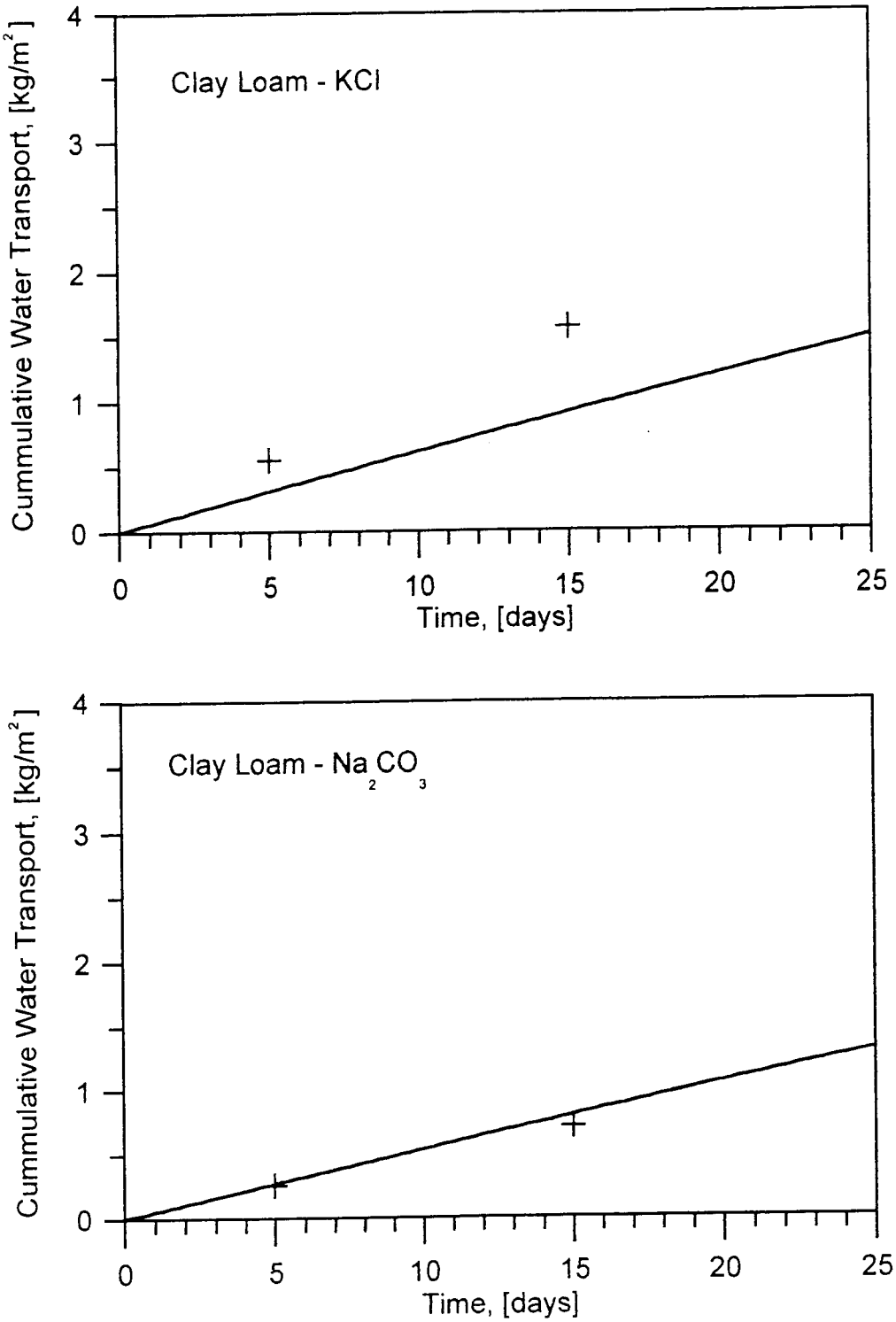

Figure 23. Cumulative water vapor flow across a 0.5 in. air gap from a non-saline section to the saline section of the broken column for KCl (a) and Na_2CO_3 (b) in clay loam. Solid line is the model result using parameters from Table 1, and points (+) are calculated from the broken column data of Wheeting (1925).

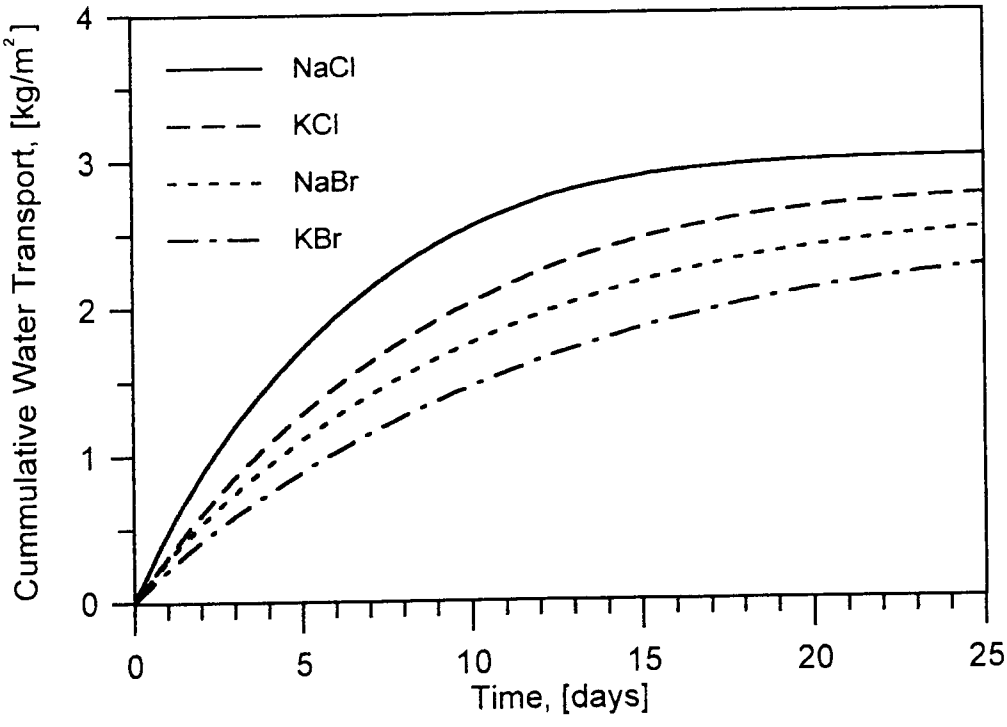

Figure 24. Cumulative water vapor flow across a 0.5 in. air gap from non-saline to saline section of a broken column in a medium sand for NaCl (solid lines), KCl (dashed line), NaBr (dotted line) , and KBr(dash-dotted line) from uppermost to bottommost curve respectively.

4.6 Summary

The objective of this paper is to refine the existing theory of osmotically driven soil water vapor movement using a physically based model. The model was validated using the experimental data published by Wheeting (1925). The model could account for differences in water transport rates due to different salts and soil textures. The results of this paper verify that significant water vapor flow can occur in the presence of salts and presents a method of solution to account for the differences observed between different salts. Further development and testing against a larger data set using a more complete soil water model, which includes coupled water flow and solute transport model is needed.

4.7 References

Alberty, R. A. 1987. Physical Chemistry. 7th ed. John Wiley and Sons, New York.

Bresler, E. 1973. Anion exclusion and coupling effects in nonsteady transport through unsaturated soils: I. Theory. Soil Sci. Soc. Am. Proc. 37:663-669.

Edlefsen, N. E. and A. B. C. Anderson. 1943. Thermodynamics of soil moisture. Hilgardia 15:31-298.

Freier, R. K. 1976. Aqueous Solutions Vol. 1. Data for inorganic and organic compounds. Walter de Gruyter, Berlin-NewYork.

Horvath, A. L. 1985. Handbook of aqueous electrolyte solutions, physical properties, estimation and correlation methods. Ellis Horwood Limited, Chichester.

Jackson, R. D. 1964. Water vapor diffusion in relatively dry soil: I. Theoretical considerations and sorption experiments. Soil Sci. Soc. Proc. 28:172-176.

Kelly, S. F., J. L. Green, J. S. Selker. 1997. Fertilizer diffusion in container medium. J. Amer. Soc. Hort. Sci. 122:122-128.

Kemper, W. D. and J. B. Rollins. 1966. Osmotic efficiency coefficients across compacted clays. Soil Sci. Soc. Am. Proc. 30:529-534.

Letey, J., W. D. Kemper and L. Noonan. 1969. The effect of osmotic pressure gradients on water movement in unsaturated soil. Soil Sci. Soc. Am. Proc., 33:15-18.

Mathsoft Inc. 1995. Mathcad User's Guide, Mathcad PLUS 6.0. Mathsoft Inc., Cambridge MA.

Nassar, I. N. and R. Horton. 1989a. Water transport in unsaturated nonisothermal salty soil: I. Experimental results. Soil Sci. Soc. Am. J. 53:1323-1329.

Nassar, I. N. and R. Horton. 1989b. Water transport in unsaturated nonisothermal salty soil: II. Theoretical development. Soil Sci. Soc. Am. J. 53:1330-1337.

Nassar, I. N., R. Horton and A. M. Globus. 1992a. Simultaneous transfer of heat, water and solute in porous media: I. Theoretical development. Soil Sci. Soc. Am. J. 56:1350-1356.

Nassar, I. N., R. Horton and A. M. Globus. 1992b. Simultaneous transfer of heat, water and solute in porous media: II. Experiment and analysis. Soil Sci. Soc. Am. J. 56:1357-1365.

Nobel, P. S. 1983. Biophysical Plant Physiology and Ecology. W. H. Freeman and Company, San Francisco.

Noborio, K., K. J. McInnes and J. L. Heilman. 1996a. Two-dimensional model for water, heat, and solute transport in furrow irrigated soil: I. Theory. Soil Sci. Soc. Am. J. 60:1001-1009.

Noborio, K., K. J. McInnes and J. L. Heilman. 1996b. Two-dimensional model for water, heat, and solute transport in furrow irrigated soil: II. Field evaluation. Soil Sci. Soc. Am. J. 60:1010-1021.

Parlange, J. 1973. Movement of salt and water in relatively dry soils. Soil Sci. 116:249-255.

Raats, P. A. C. 1969. Steady gravitational convection induced by a line source of salt in a soil. Soil Sci. Soc. Am. Proc. 33:483-487.

Robinson, R. A. and R. H. Stokes. 1959. Electrolyte solutions. 2nd ed. Butterworths Scientific Publications, London.

Scotter D. R. and Raats, P. A. C. 1970. Movement of salt and water near crystalline salt in relatively dry soil. Soil Sci. 109:170-178.

Scotter, D. R. 1974a. Salt and water movement in relatively dry soil. Aust. J. Soil Res. 12:27-35.

Scotter, D. R. 1974b. Factors influencing salt and water movement near crystalline salts in relatively dry soil. Aust. J. Soil Res. 12:77-86.

van Genuchten, M. T. 1980. A closed form solution for predicting the hydraulic conductivity of unsaturated soils. Soil Sci. Soc. Am. J. 44:892-898.

Wheeting, L. C. 1925. Certain relationships between added salts and the moisture of soils. Soil Sci. 16:287-299.

Yakirevich, A., P. Berliner and S Sorek 1997. A model for numerical simulation of evaporation from bare saline soil. Water Resour. Res. 33:1021-1033.

Zemaitis, J. F., D. M. Clark, M. Rafal, and N. C. Scrivner. 1986. Handbook of aqueous electrolyte thermodynamics. Am. Inst. of Chemical Engineers, Inc., New York.

Chapter 5. Modeling Ion Diffusion and Osmotic Water Vapor Transport in Unsaturated Porous Media

5.1 Abstract

A quantitative theory describing the diffusion of salts and the flow of liquid and vapor water in unsaturated porous media due to osmotic potential gradients was developed. The theory was implemented numerically to simulate the processes and test the predictive capabilities of the processes identified. The numerically generated predictions were compared with published data showing that the theory accounts for the coupled liquid-vapor-salt transport processes which could not be predicted using previous solute transport models. Regions of high salinity acted as sinks for water vapor generated in non-saline regions and the condensed liquid then flowed away from the saline regions.

5.2 Introduction

Development of models of the solubilization of crystalline salts, diffusion, and subsequent water flow in soils is of interest agriculturally to predict the fate of crystalline fertilizer applied directly to soils. Fertilizer may be placed in a protected diffusion zone, shielded from surface applied water to prevent leaching and minimize environmental impact (Green, 1995; Green et al., 1993a; Green et. al., 1993b). Modeling the process of diffusion under these conditions is important to incorporating and predicting the impact of these agronomic practices. In this study, existing theories of water and vapor flow in unsaturated media are combined with aqueous electrolyte thermodynamic theory to predict movement of ions in unsaturated soil systems. A model is developed to describe

the simultaneous movement of water in the vapor and liquid phase and consequent transport of ions in the liquid phase through the process of diffusion and convection.

5.3 Literature Review

In unsaturated porous media, the movement of water due at least in part to gradients in osmotic potential has been verified experimentally. Wheeting (1925) observed water transport in laboratory columns from non-saline soil to saline soil. Scotter and Raats (1972) and set up laboratory columns with crystalline salt at one end of uniformly wetted soils and observed the salt diffusion through the soil and the accumulation of water in the salinized section. Scotter (1974a) set up similar columns to determine the effect of soil texture, water content and salt type on the resulting water content and salt distribution in soil columns. Nassar and Horton (1989a) and Nassar and Horton (1992b) set up laboratory soil columns looking at the combined effect of salt, soil and temperature on the water movement. Kelly et al. (1996) used a horticultural potting media and bromide salts and concluded that redistribution of water was driven to a significant degree at low water contents by vapor phase flow, due to large gradients in osmotic potential.

Theoretical analyses and modeling of flow in the presence of osmotic potentials have been carried out by several researchers. Parlange (1973) and Scotter (1974b) presented a theoretical analysis of solute, liquid water and vapor diffusion in soils based on the observations of Scotter and Raats (1972). Nassar and Horton (1989b and 1992a) measured concentrations of salt, soil properties and temperature on water movement in unsaturated soils and found good agreement with results from their previous experiments

(Nassar and Horton, 1989a and 1992b). To simulate evaporation of water from bare saline soil, Yakirevich, et al. (1997) developed and tested a numerical model using the data of Nassar and Horton, (1989a and 1992b) and showed that osmotic pressure gradients have a significant effect on the predicted evaporation.

Analysis of the problem of a concentrated salt solution diffusing into an unsaturated porous media has not been carried out rigorously. The theoretical analysis of Parlange (1973) and Scotter (1974b) quantitatively describe parts of the transport process separately but did not consider a coupled model including liquid, vapor and solute flow simultaneously. The objective of this paper is to develop a coupled vapor-liquid-solute transport model based on the equations presented by Parlange (1973) and implement this model numerically. The theory and numerical model was tested using the previously published experimental column studies of Kelly et al. (1997) and Scotter and Raats (1972). In these experiments salt was placed at one end of a column of soil or container media at an initial constant water content and allowed to diffuse into the medium for a specified time at which water and salt distributions were determined at the end of the respective diffusion periods. Our analysis is limited to isothermal conditions, focusing on osmotic water vapor transport phenomena that occurs in the presence of high solute concentrations. The theory behind the transport equations presented here closely follows the equations presented by Parlange (1973).

5.4 Theory

5.4.1 Flow and Transport Equations

One dimensional coupled water-vapor-solute transport equations using units of mass per unit volume are used to develop the numerical model to calculate a system mass balance. The liquid flow is described by Richards equation for unsaturated flow in porous media.

$$\frac{dm_l}{dt} = \frac{d}{dx}(\rho_w K_l \frac{d\Psi_l}{dx}) + s_l \qquad [120]$$

where m_l is the mass per unit volume of the liquid [M/L^3], K_l is the hydraulic conductivity [L/T], ρ_w is the density of liquid water [M/L^3], t is time [T] s_l is a source/sink term for the liquid water [M/L^3/T] and Ψ_l is the potential term driving the liquid water [M]. The potential term driving the liquid mass flow is composed of several individual potentials that can be calculated at any point in the flow field.

$$\Psi_l = \Psi_g + \Psi_\tau \qquad [121]$$

where Ψ_g is the gravitational potential [L] and Ψ_τ is the soil matric potential [L]. The water mass conservation equation then becomes.

$$\frac{dm_l}{dt} = \frac{d}{dx}(\rho_w K_l \frac{d(\Psi_\tau + \Psi_g)}{dx}) + s_l \qquad [122]$$

The relationship between moisture content and matric potential for a given soil may be expressed using a soil moisture characteristic function such as that presented by van Genuchten (1980).

$$\Theta(\Psi_\tau) = \left[\frac{1}{1+(\alpha\Psi_\tau)^{n_{vg}}}\right]^{m_{vg}} \qquad [123]$$

where the reduced water content, or effective saturation, Θ, is defined as

$$\Theta = \frac{\theta - \theta_r}{\theta_s - \theta_r} \qquad [124]$$

Here θ_r is the residual volumetric water content at some large negative value of the matric potential (e.g. permanent wilting point, Ψ_τ=15,000 cm). θ_s is the saturated volumetric water content; θ is the volumetric water content; α, n_{vg} and m_{vg} are empirical fitting parameters where m_{vg}=1-1/n_{vg} for the Mualem conductivity model.

The hydraulic conductivity of water through a porous media can be expressed using the Mualem (1976)-vanGenuchten (1980) conductivity function using the same parameters in equation [4] with the addition of the saturated conductivity, K_{sat}. The hydraulic conductivity of the media can be determined at any matric potential (or water content).

$$K_{vg} = K_{sat}\frac{\left[1-\left(|\alpha\Psi_\tau|\right)^{n_{vg}-1}\left[1+\left(|\alpha\Psi_\tau|\right)^{n_{vg}}\right]^{\left(\frac{1}{n_{vg}}\right)-1}\right]^2}{\left[1+\left(|\alpha\Psi_\tau|\right)^{n_{vg}}\right]^{\frac{n_{vg}-1}{2n_{vg}}}} \qquad [125]$$

The vapor mass transport equation (Jackson, 1964) used in the model is

$$\frac{dm_v}{dt} = \frac{d}{dx}\left(f \cdot D_v \frac{dp_v}{dx}\right) + s_v \qquad [126]$$

where m_v is the mass per unit volume of water vapor[M/L^3], f is the air filled porosity, s_v is a source/sink term for the water vapor [M/L^3/T], p_v is the water vapor density [M/L^3] and D_v is the water vapor diffusion coefficient in air [L^2/T]. The potential term driving the vapor phase flow is the water vapor density or alternatively the vapor pressure of water. The vapor pressure of water is dependent on temperature, osmotic potential and the matric potential which can be calculated at any point in the flow field. The osmotic potential can be calculated using Pitzer's equation (Horvath, 1985, p. 217; Zemaitis et al., 1986, pp.71-75) equations following Kelly and Selker (1998)

$$\phi - 1 = -\left[A_m m_2^{1/2}/(1 + Bm_2^{1/2})\right] + m_2\left[\beta_0 + \beta_1 \exp(-\alpha_1 m_2^{1/2})\right] + m_2^2 C^{\phi} \qquad [127]$$

where β_0, β_1 and C^{ϕ} are parameters specific to each electrolyte up to 6 mol/l solutions Zemaitis et al., 1986, pp. 179-190), α_1 for 1:1 and 2:1 electrolytes is 2.0 kg$^{1/2}$mole$^{-1/2}$, B is 1.2 kg$^{1/2}$mole$^{-1/2}$ for all electrolytes, and m_2 is the molality of the electrolyte, mol kg^{-1} (equivalent to the ionic strength). The osmotic Debye-Huckel coefficient, A_m, is computed as

$$A_m = \frac{1}{3}\left(\frac{2\pi N_0 \rho_w}{1000}\right)^{1/2}\left(\frac{e^2}{D_0 kT}\right)^{3/2} \qquad [128]$$

where N_0 is Avogadro's number, ρ_w is the density of pure water, D_0 is the static dielectric constant of pure water, k is Boltzmann's constant, e is the absolute electronic charge, and T is the absolute temperature, °K. Once the activity of the water in solution is known it is possible to calculate the osmotic potential of the soil water solution using the Kelvin equation (Alberty, 1987, p. 310).

$$\Psi_s = \frac{RT\ln(a_w)}{\overline{V_w}} \qquad [129]$$

The matric potential can be calculated using equation [123]. The vapor pressure or water vapor density, p_v, above the solution can be calculated using the psychrometric equation (Alberty, 1987).

$$\frac{p_v}{p_v^0} = \exp\left(\frac{-(\Psi_s + \Psi_\tau)\overline{V_w}}{RT}\right) \qquad [130]$$

The solute transport equation for our problem is obtained by combining the conservation of mass with Fick's first law.

$$\frac{dm}{dt} = \frac{d}{dx}\left(D_e \frac{dm}{dx}\right) - \frac{m}{m_l} \cdot v_l + s_c \qquad [131]$$

where m is the mass per unit volume of solution [M/L^3], D_e is the effective ion diffusion coefficient [L^2/T], v_l is the Darcian water velocity [M/L] and s_c is the sink/source term of solute [M/L^3/T].

5.4.2 Finite Difference Equations

Expressing these mass transport equations as finite difference equations (explicit formula) yields the following equations. The liquid flow equation becomes

$$m_{l_i}^t = \frac{\Delta t \cdot \rho_w}{\Delta x^2}\left[\left(\frac{2K_{i+1}K_i}{K_{i+1}+K_i}\right)\left(\psi_{\tau_i} - \psi_{\tau_{i+1}}\right) + \left(\frac{2K_iK_{i-1}}{K_i+K_{i-1}}\right)\left(\psi_{\tau_i} - \psi_{\tau_{i-1}}\right)\right] + m_{l_i}^{t-1} \qquad [132]$$

The vapor flow equation becomes

$$m_{v_i}^{t} = \frac{\Delta t \cdot f}{\Delta x^2}\left[\left(\frac{2D_{v_{i+1}}D_{v_i}}{D_{v_{i+1}}+D_{v_i}}\right)\left(p_{v_{i+1}}-p_{v_i}\right)+\left(\frac{2D_{v_i}D_{v_{i-1}}}{D_{v_i}+D_{v_{i-1}}}\right)\left(p_{v_{i-1}}-p_{v_i}\right)\right]+m_{v_i}^{t-1} \quad [133]$$

The solute transport equation becomes

$$m_{s_i}^{t} = \frac{\Delta t}{\Delta x^2}\left[\left(\frac{2D_{e_{i+1}}D_{e_i}}{D_{e_{i+1}}+D_{e_i}}\right)\left(m_{s_{i+1}}-m_{s_i}\right)+\left(\frac{2D_{e_i}D_{e_{i-1}}}{D_{e_i}+D_{e_{i-1}}}\right)\left(m_{s_{i-1}}-m_{s_i}\right)\right]+ \frac{v_{l_i}\cdot\Delta t}{2\Delta x}\left(m_{s_{i+1}}-m_{s_{i-1}}\right)+m_{s_i}^{t-1} \quad [134]$$

The Darcian water velocity, v_l is calculated as

$$v_{l_i} = \frac{1}{\Delta x}\left[\left(\frac{2K_{i+1}K_i}{K_{i+1}+K_i}\right)\left(\psi_{\tau_{i+1}}-\psi_{\tau_i}\right)+\left(\frac{2K_iK_{i-1}}{K_i+K_{i-1}}\right)\left(\psi_{\tau_i}-\psi_{\tau_{i-1}}\right)\right] \quad [135]$$

The liquid and vapor phase flows are coupled to maintain a water balance. The procedure used was to calculate the mass of the water vapor based on the pore space in the media. If it is less than the water vapor calculated as a result of diffusion, then the difference was subtracted from the liquid water at the node (i.e. liquid water is evaporated into vapor phase). Otherwise, the difference is added to the liquid water at the node (i.e. vapor is condensed into the liquid). The resulting water content is then checked to make sure it remains within the range of saturated water content and residual water content. The coupled liquid–vapor water balance equations can be calculated using the following equations. We can define the adjusted liquid water content mass as m'_l and the adjusted water vapor mass as m'_v. Then m'_v vapor based on the liquid water content is calculated as

$$m'_v = p_v\left(\theta_s - \frac{m_l}{\rho_w}\right) \qquad [136]$$

If $m'_v > m_v$ then water is added to the liquid phase from the vapor phase (evaporation) and the following equation may be derived to adjust the liquid water content to maintain the mass balance.

$$m_l - m'_l = m'_v - m_v \qquad [137]$$

Which states that any changes in liquid mass must equal any changes in water vapor. We substitute equation [136] to obtain

$$m'_l = \left(p_v\theta_s - m_l - m_v\right)\frac{\rho_w}{p_v - \rho_w} \qquad [138]$$

If $m'_v < m_v$ then water is added to the vapor phase from the liquid phase (condensation) and the mass balance equation becomes

$$m'_l - m_l = m_v - m'_v \qquad [139]$$

and again substitute equation [136] to obtain

$$m'_l = \left(m_l + m_v - p_v\theta_s\right)\frac{\rho_w}{\rho_w - p_v} \qquad [140]$$

After the adjusted liquid water content mass is calculated using either equation [138] or [140] the water vapor mass is recalculated as

$$m'_v = p_v\left(\theta_s - \frac{m_l}{\rho_w}\right) \qquad [141]$$

5.5 Methodology

The finite difference equations were implemented using Mathcad7, (Mathsoft. Cambridge, MA) in a program we named CFLOW (Appendix 3). CFLOW is implemented using a finite difference grid with equal spacing between nodes and was limited to using a constant time step between each iteration. For this problem zero flux boundaries for liquid water and vapor transport is obtained by setting the liquid conductivity and vapor diffusion coefficient equal to zero for all time steps at the first and last node in the finite difference grid. The solute concentration at the boundary where the salt diffused from is set to the maximum solubility of the particular salt at the specified temperature. The sequence of calculations for each node at each time step proceeds as follows; 1) Calculate liquid transport using equation [132]; 2) Calculate water vapor transport using equation [133]; 3) Calculate the Darcian liquid water velocity using equation [135]; 4) Adjust the liquid and vapor mass using equations [136] - [141]; 5) Calculate the solute transport using equation [134]. The solution proceeds by repeating these steps until the specified maximum time specified.

5.6 Results and Discussion

CFLOW was used to simulate the experimental data from both Kelly et. al. (1997) and Scotter (1974b). The model parameters for the media and salt properties are shown in Table 4. Soil water retention parameters for the peat:vermiculite container media (1:1 by volume) were determined experimentally. The unsaturated conductivity function for container media was estimated from data found in Bunt (1974). Soil water retention parameters (Figure 25) and the unsaturated conductivity function (Figure 26) for the

Table 4. Model parameters

Physical constants	
N_0, Avogadro's Number	$6.0221367 \cdot 10^{23}$
ρ_w, density of water at 20°C	0.99823 g/cm^3
D_0, static dielectric constant of water at 20°C	80.10
K, Boltzmann's constant	$1.380658 \cdot 10^{-16}$ erg/deg
E, absolute electronic charge	$4.803 \cdot 10^{-10}$ e.s.u.
T, absolute temperature	293.15 °K
K_v, diffusion coefficient of water vapor in air at 20°C	$2.42 \cdot 10^{-5}$ m^2/sec
R, gas constant	8.3143 joules

Media properties

Media	n	α [m^{-1}]	θ_s [m^3/m^3]	θ_r [m^3/m^3]	ρ_b, bulk density, [gm /cm^3]	K_{sat}, [m/ s]
Peat:verm.	1.195	14	0.75	0.001	0.17	500
Loamy sand	1.236	6.14	0.48	0	1.38	3000

Salt properties†

Salt	β_0	β_1	C_ϕ	Water diffusion, [m^2/s]	Solubility†† (20°C), [mol/kg]	Molecular Weight [g/mol]
KBr	0.0569	0.2212	-0.0018	2.0×10^{-9}	3.31	119.01
NaCl	0.0765	0.2664	0.00127	1.7×10^{-9}	4.53	58.44

† Zemaitis, 1986
†† Freier, 1976

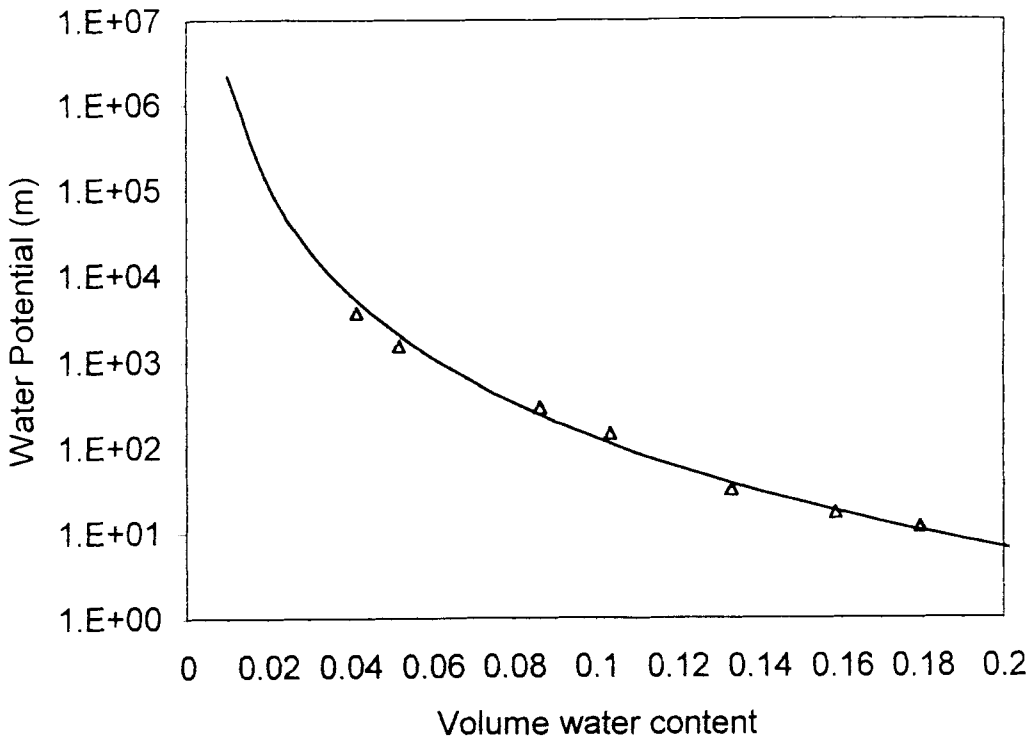

Figure 25. Soil water characteristic curve for loamy sand (Scotter, 1974a). (Δ) represent measured data. Solid line is the best fit curve using parameters in Table 4.

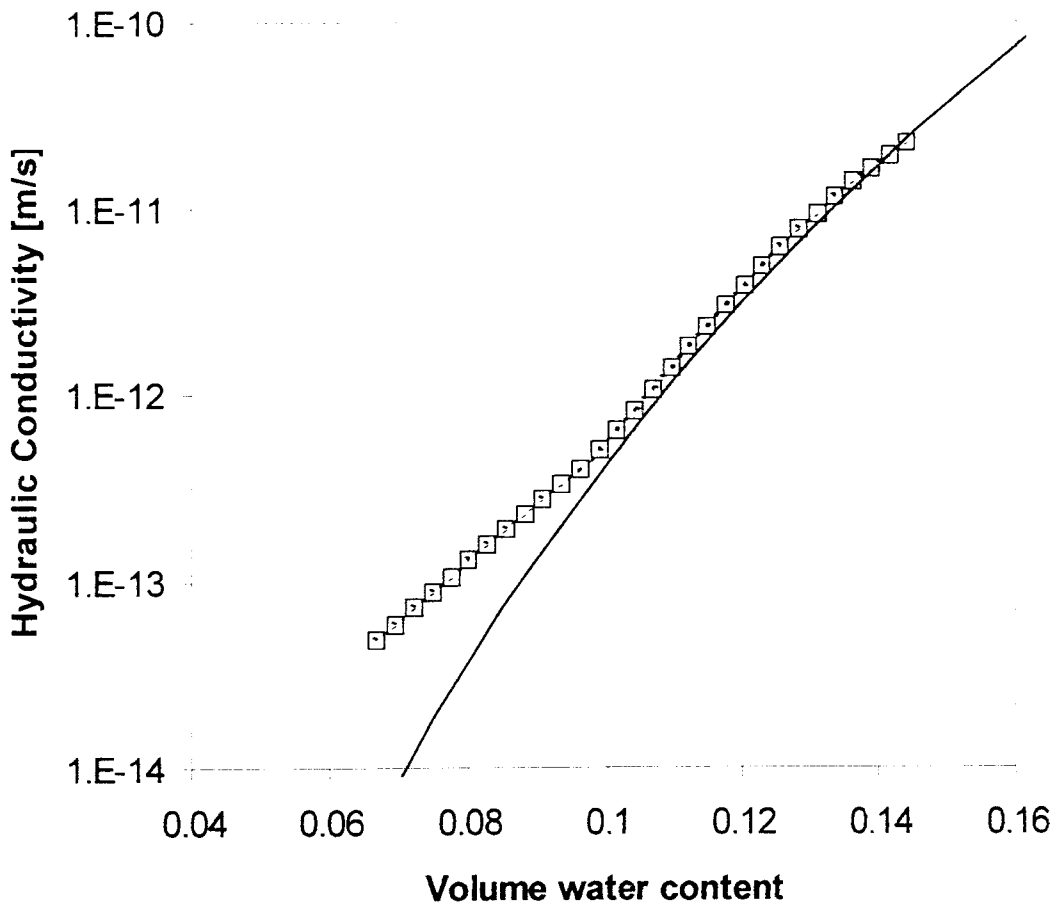

Figure 26. Unsaturated hydraulic conductivity for the loamy sand (Scotter, 1974a). (□) represent measured data. Solid line is hydraulic conductivity function using parameters from Table 4.

loamy sand used in the experiments of Scotter (1974b) were determined from graphical data presented in Scotter (1974a). The relation between water content and effective diffusion coefficient of KBr (Figure 27) for the container media was determined by fitting the analytical solution at different water contents (Kelly et. al. 1997).

The effective diffusion coefficient of NaCl in the loamy sand (Figure 27) was experimentally determined by Scotter (1974a). Scotters' diffusion coefficients were found to be significantly less than values expected using an analytical approximation assuming a constant water content (Parlange, 1973; Scotter 1974a). Using Scotters' values for diffusion coefficients in CFLOW also confirmed that they were approximately an order of magnitude less than predicted by the experimental results. This discrepancy is a result of the technique based on Porter et. al. (1960) used by Scotter (1974a) to measure the diffusion coefficients. The technique measured the counter diffusion of chloride and nitrate ions using a NaCl:$NaNO_3$ half-cell in contrast to the co-diffusion of sodium and chloride ions in Scotters' experimental columns. Therefore the relationship between water content and the effective diffusion coefficients (Figure 27) was estimated using the analytical solution based on the results of Scotter (1974b). The effective diffusion coefficients used for both the KBr in container media (Kellys' data) and the NaCl in the loamy sand (Scotter's data) was less than the respective diffusion coefficient in a pure water solution with no media present.(Robinson and Stokes, 1959).

It was found that a finite difference grid spacing of 0.04 m and time steps ranging from 225 – 900 seconds gave numerically stable solutions and minimized numerical dispersion and computation time. CFLOW model results for solute concentration and water content are overlaid on our experimental results for the container media:KBr

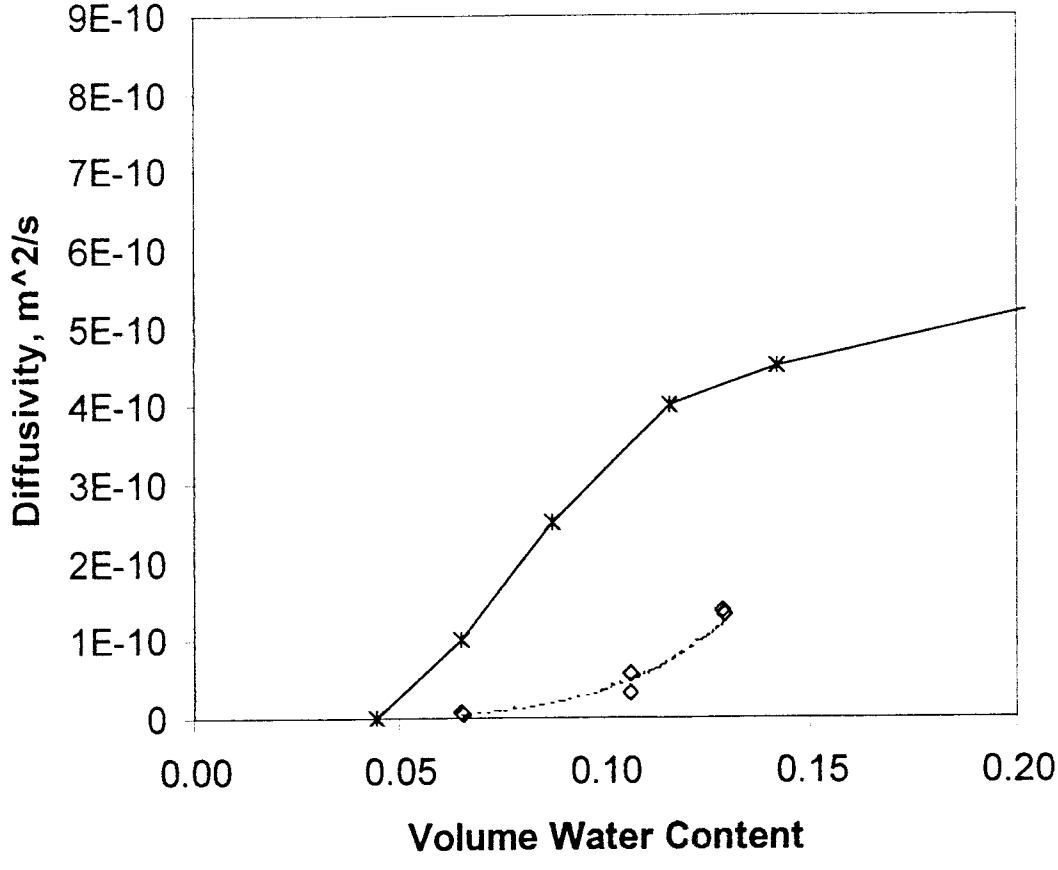

Figure 27. Relationship between effective diffusion coefficient of NaCl and water content for loamy sand (Scotter, 1974a). (◊) are experimental data reported by Scotter (1974a). (*) is the data used in the CFLOW simulations as described in the text.

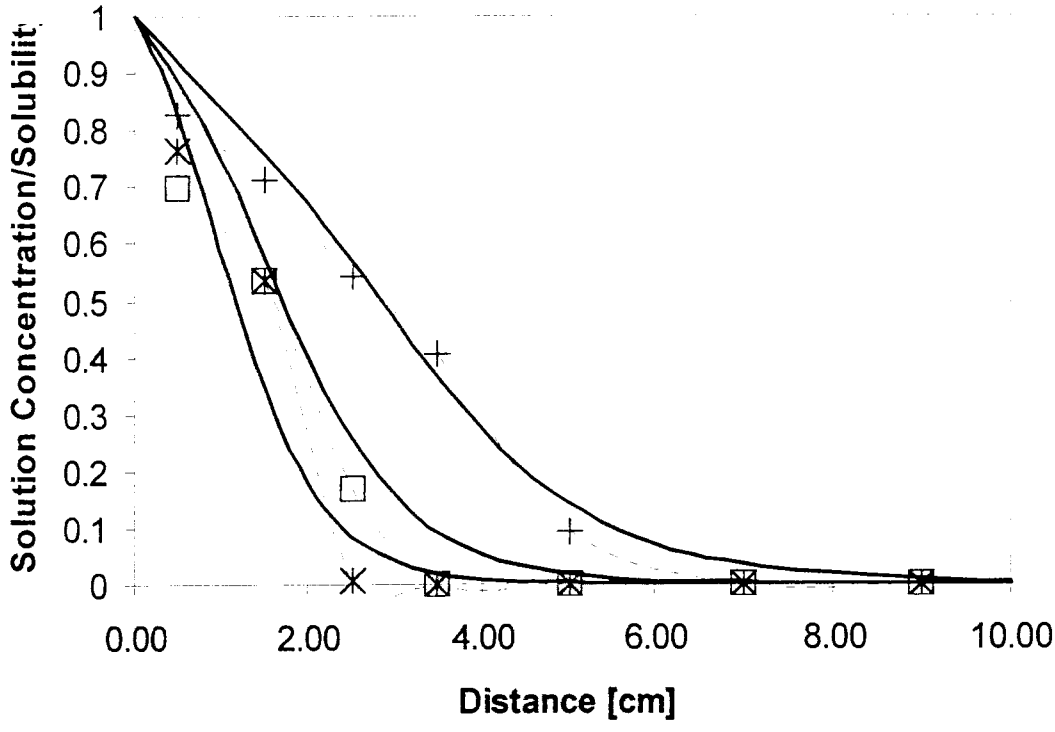

Figure 28. Solute distributions in columns of container media:KBr. Solid lines are model data at 5, 10 and 25 days from left to right. (+) 5, (□) 10 and (+) 25 day experimental data (Kelly et. al., 1997) Dashed lines connect experimental data.

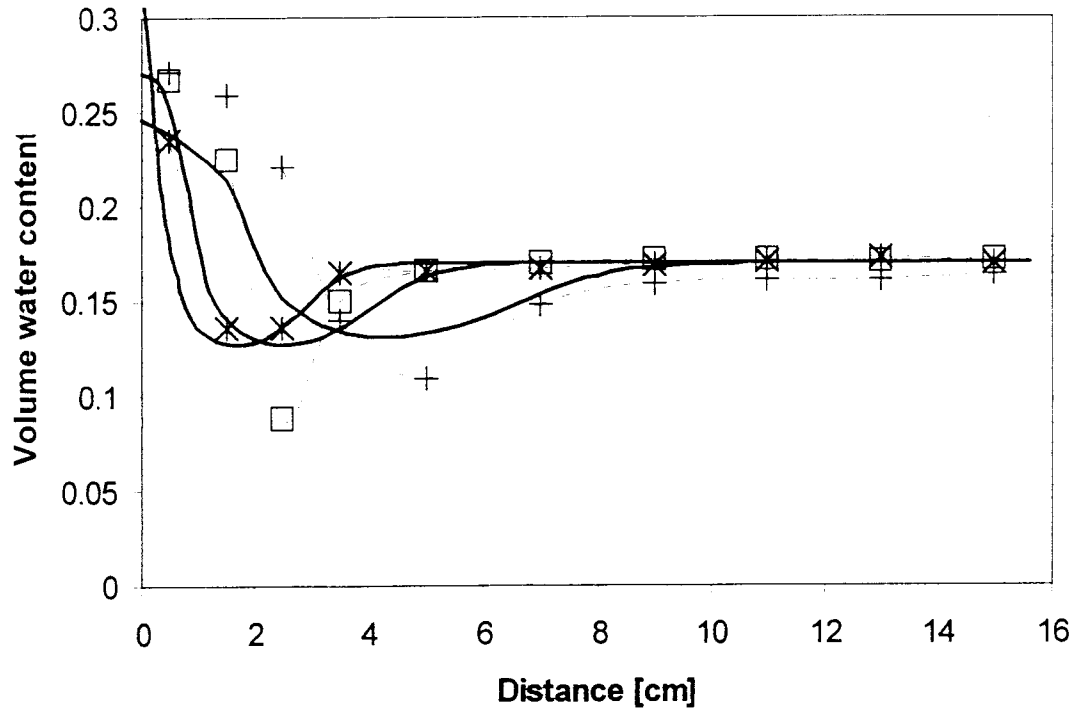

Figure 29. Water content distributions in columns. Solid lines are model data at 5, 10 and 25 days from left to right. (+) 5, (□) 10 and (+) 25 day experimental data (Kelly et. al., 1997). Dashed lines connect experimental data.

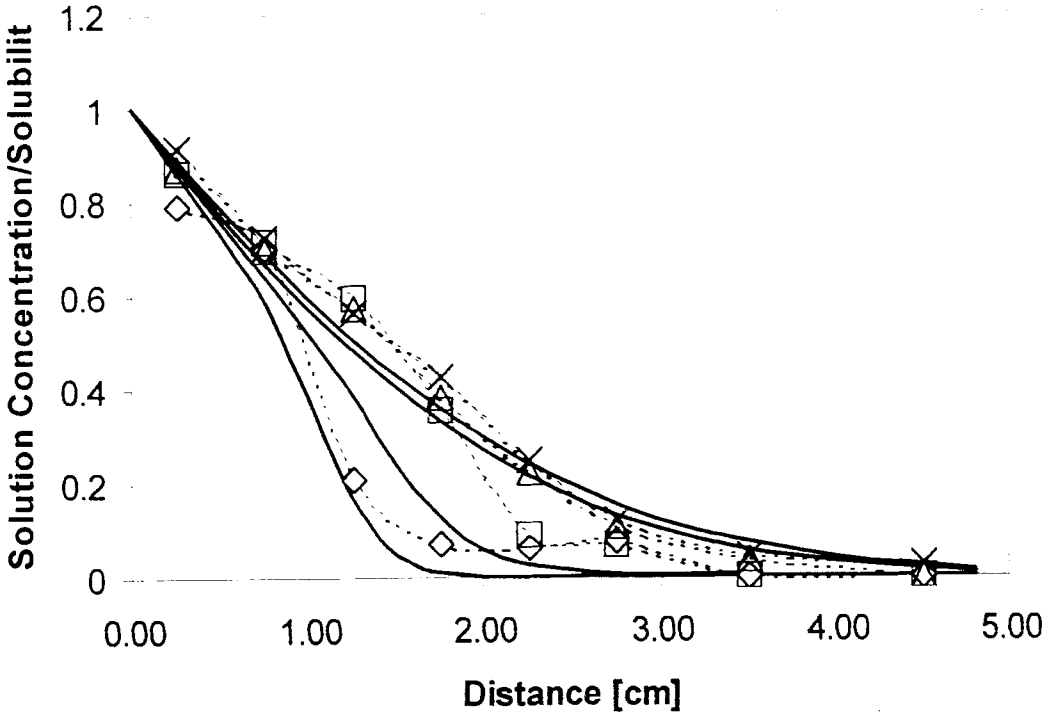

Figure 30. Solute distributions in loamy sand:NaCl columns. Solid lines are model data. (◊) 0.065, (□) 0.088, (Δ) 0.12 and ( ) 0.14 m^3/m^3 initial water content (Scotter, 1974b). Dashed lines connect experimental data.

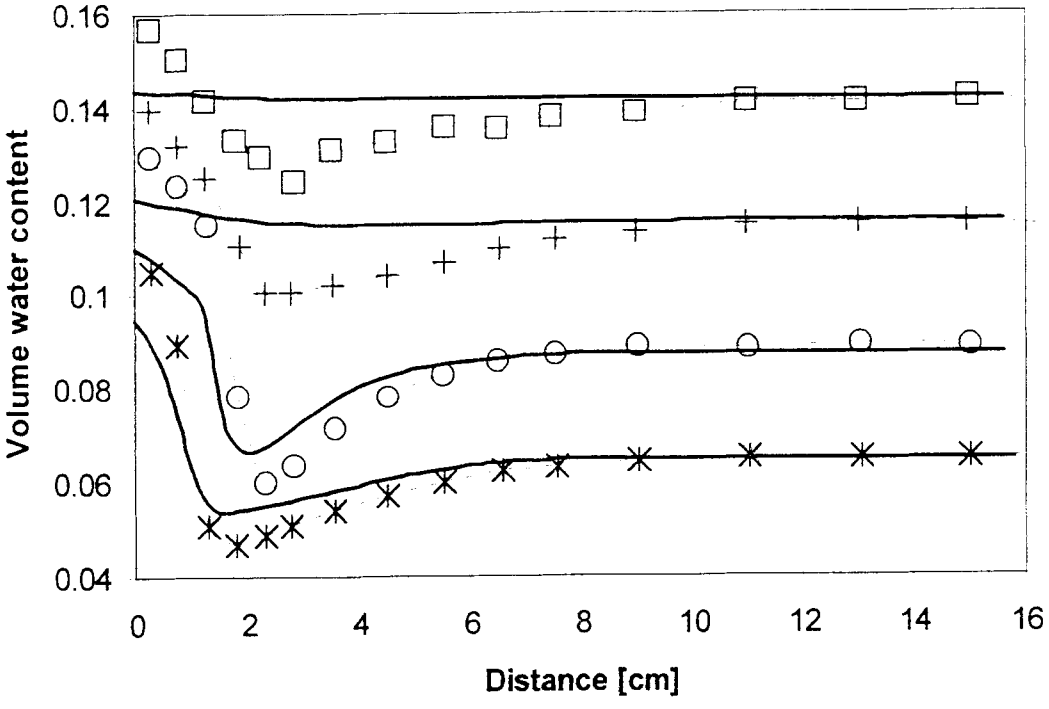

Figure 31. Water content distributions in loamy sand:NaCl columns. Solid lines are model data. (⁻·⁻) 0.065, (o) 0.088, (+) 0.12 and (□) 0.14 m^3/m^3 initial water content (Scotter, 1974b). Dashed lines connect experimental data.

columns in Figure 28 and Figure 29 and for the Scotters' results for loamy sand:NaCl columns in Figure 30 and Figure 31.

5.6.1 Characteristics of the results

The water content distributions (Figure 29 and Figure 31) at the lower initial water contents for both the model and experiments show the characteristic increase in water content at the salt-media interface and the decreased water content which occurs at the leading edge of the diffusing solute (Figure 28 and Figure 30). The increased water content at the salt-media interface (at 0 cm distance) occurs as water vapor moves towards the salt in response to the osmotic potential created by the salt in the soil. This leaves a depression in water content with low matric potential where liquid water is transported from the salt-media interface at the left and from the media at the right (Figure 27, approx. 2 cm distance). This characteristic depression occurs at a critical water content where the liquid water flow is less than the water vapor flow. For the container media, water contents of 0.17 m^3/m^3 was below this critical water content. For the loamy sand, 0.14 m^3/m^3 was below the critical water content based on the experimental results of Scotter (1974b).

The distance the salt moved down the column (Figure 28 and Figure 30) is essentially the same as would be expected using an analytical solution for solute diffusion alone and assuming a constant water content. This solution, assuming a constant water content and effective diffusion coefficient, underestimates the mass of salt entering the media. The increased water content at the salt-media interface increases the transport of salt into the media through combined effects of the increased effective diffusion

coefficient and the convective transport of solute as liquid water moves away from the interface towards the low water content trough as CFLOW illustrates. This appears in the steep increase in the curves near the salt-media interface. Although these processes don't appear to affect the distance the solute travels, it does increase the amount of solute entering the media by as much as 50%.

5.6.2 Model discussion

The results of CFLOW for the container media (Figure 28) show that the predicted distance and amount of salt diffusing into the column was similar to the experimental data. The model shows the near-source "bulge" of salt due to the increased water content and diffusion, and convection of solute by the liquid at the salt-media interface. The experimental data showed a consistent sub-saturated concentration of the salt in the solution at the influent boundary whereas the model maintained a relative solution concentration of 1. The water content distributions (Figure 29) from CFLOW showed the basic characteristics of the experimental results of high water content at the salt-media interface and the local depression of water content at the leading edge of the solute diffusion front. The location and depth of the water content depression lagged behind the experimental results at all time intervals. The depth and location of the well was sensitive to the relative rates of water vapor transport as compared to the liquid transport. Correct parameterization of the soil water characteristic and the unsaturated hydraulic conductivity function will effect these transport rates. These parameters are difficult to measure at low water contents where these transport processes occur and there probably exists a set of parameters that would fit the experimental data more closely.

The results of CFLOW for the salt distributions for the loamy sand underestimate both the distance and the quantity of salt diffused (Figure 30). The determination of the relationship between water content and the effective diffusion coefficient was difficult to determine and it appears that the procedure employed using the analytical solution underestimated the effective diffusion coefficients. The water content distributions for the loamy sand also tended to underestimate the redistribution of water transported throughout the column after 5 days at all water contents (Figure 31). This could be due to the unsaturated hydraulic conductivity function employed. The unsaturated hydraulic conductivity was determined graphically based on the water diffusivity and the soil water characteristic function measured by Scotter (1974a) (Figure 27). The measured diffusivity does not distinguish between liquid water transport and water vapor transport. Using this at low water contents, where water vapor transport approaches the magnitude of liquid transport, the unsaturated hydraulic conductivity would tend to be overestimated. It appears that decreasing the unsaturated hydraulic conductivity would increase the relative importance of the water vapor transport in the column and cause an increase in water redistribution of water at all initial water contents in Figure 31. This is apparent in the water content distributions at initial water contents of 0.12 and 0.14 m^3/m^3 where the model showed no redistribution of water due to water vapor flow.

The numerical implementation of the model using and explicit finite difference scheme worked well overall. It was fairly simple to implement and required a minimum of programming. It showed that the theory developed here was physically sound. Some of the drawbacks of the model were the high computation times due to the small time steps required to insure numerical stability, but decreasing the time steps caused increased

numerical dispersion which was apparent when the model is used to simulate out to long time intervals. Implementation of this theory using a more robust implicit numerical method would improve results by decreasing numerical dispersion and allowing for variable time steps and variable node spacing.

5.7 Conclusions

A theory describing osmotic transport of water vapor and the subsequent diffusion of salt in porous media was described. A numerical model was developed to simulate these processes. The model was tested using previously published data and showed that the theory developed describes the basic physics of these transport processes. Osmotic transport of water vapor can be a significant factor by altering the diffusion of salt through the diffusing media. The processes appear to affect the quantity of salt entering the media more than the distance the salt diffuses into the media. Knowledge of the relationship between the water content and the effective ion diffusion coefficient is important to these processes, yet difficult to measure or predict. By incorporating this theory into existing models we can gain a better understanding of the importance water vapor movement in the presence of concentrated salts.

5.8 References

Alberty, R. A. 1987. Physical Chemistry. 7th ed. John Wiley and Sons, New York.

Bunt A. C. 1988. Media mixes for container grown plants. Unwin Hyman. London.

Freier, R. K. 1976. Aqueous Solutions Vol. 1. Data for inorganic and organic compounds. Walter de Gruyter. Berlin-NewYork.

Green, J. L. 1995. Self-contained fertilizing tube portable. Resource: Engineering and Technology for a Sustainable World. 2(8):9.

Green, J. L., B. A. Briggs, and D. L. Briggs. 1993a. Fertilizing apparatus. U.S. Patent 5,212,904. Assigned to the State of Oregon, acting by and through the State Board of Higher Education on behalf of Oregon State University. Date issued: 25 May.

Green, J. L., S. F. Kelly, B. Blackburn, J. Robbins, B. A. Briggs, and D. L. Briggs. 1993b. A protected diffusion zone (PDZ) to conserve soluble production chemicals. Combined Proc. Intl. Plant Prop. Soc. 43:40-44.

Jackson, R. D. 1964. Water vapor diffusion in relatively dry soil: I. Theoretical considerations and sorption experiments. Soil Sci. Soc. Proc. 28:172-176.

Kelly, S. F., J. L. Green, J. S. Selker. 1997. Fertilizer diffusion in container medium. J. Amer. Soc. Hort. Sci. 122:122-128.

Mathsoft Inc. 1995. Mathcad User's Guide, Mathcad PLUS 6.0. Mathsoft Inc., Cambridge MA.

Nassar, I. N. and R. Horton. 1989a. Water transport in unsaturated nonisothermal salty soil: I. Experimental results. Soil Sci. Soc. Am. J. 53:1323-1329.

Nassar, I. N. and R. Horton. 1989b. Water transport in unsaturated nonisothermal salty soil: II. Theoretical development. Soil Sci. Soc. Am. J. 53:1330-1337.

Nassar, I. N., R. Horton and A. M. Globus. 1992a. Simultaneous transfer of heat, water and solute in porous media: I. Theoretical development. Soil Sci. Soc. Am. J. 56:1350-1356.

Nassar, I. N., R. Horton and A. M. Globus. 1992b. Simultaneous transfer of heat, water and solute in porous media: II. Experiment and analysis. Soil Sci. Soc. Am. J. 56:1357-1365.

Parlange, J. 1973. Movement of salt and water in relatively dry soils. Soil Sci. 116(4):249-255.

Porter, L. K., W. D. Kemper, R. D. Jackson, and B. A. Stewart. 1960 Chloride Diffusion in soils as influenced by moisture content. Soil Sci. Soc. Proc. 460-463.

Robinson, R. A. and R. H. Stokes. 1959. Electrolyte solutions. Butterworths Scientific Publications. London.

Scotter D. R. and Raats, P. A. C. 1970. Movement of salt and water near crystalline salt in relatively dry soil. Soil Sci. 109:170-178.

Scotter, D. R. 1974b. Factors influencing salt and water movement near crystalline salts in relatively dry soil. Aust. J. Soil Res. 12:77-86.

Scotter, D. R. 1974a. Salt and water movement in relatively dry soil. Aust. J. Soil Res. 12:27-35.

van Genuchten, M. T. 1980. A closed form solution for predicting the hydraulic conductivity of unsaturated soils. Soil Sci. Soc. Am. J. 44:892-898.

Yakirevich, A., P. Berliner and S Sorek 1997. A model for numerical simulation of evaporation from bare saline soil. Water Resour. Res. 33:1021-1033

Chapter 6. Summary

The initial motivation behind this study was to determine the fertilizer ion movement in a "Protected Diffusion Zone" (PDZ) (Green et al., 1993b). Two systems utilizing the concept of a PDZ are the "Closed Insulated Pallet System" (CIPS) (Green and Schneckenburger, 1992) and the "Conserver" (Green et al., 1993a; Green, 1995) are described in Chapter 1. By studying the more general problem of non-convective ion movement in unsaturated porous media, we may better understand how fertilizer moves in these systems. The research approach taken was to simplify these systems by not considering plant uptake; limiting our study to the movement of bromide as a representative ion; assuming no chemical interactions between ions and media; constant and isothermal conditions; and initially limiting the study to container media. This was achieved through complementary laboratory column experiments and modeling of the physical governing processes.

Even with all the simplifications in the approach to the problem, it was found that the physical processes affecting the rate of discharge of fertilizer from a PDZ is much more complex than initially hypothesized. An analytical solution based on the simple Fickian diffusion model was developed in Chapter 3 but limited to predicting salt distributions in media remaining at a constant water content where salt movement occurred only by molecular diffusion. In the present study, this model was found to be useful only for predicting ion diffusion of the container media at the moderate water content of 2.5 g/g. At the high water content, 4.0 g/g, salt was transported by gravity driven liquid flow caused by solute density gradients set up by the diffusing salt. At low water content, 1.0 g/g, water, the presence of the salt set up large gradients in osmotic

potential causing water vapor flow towards the salt resulting in significant water redistribution in the column. The water contents (1.0 – 4.0 g/g) used in the column experiments were chosen based on the range of water contents reported in the media from previous experiments with CIPS (Blackburn, 1992). At the moderate water content of 2.5 g/g (0.42 m^3/m^3 by volume) the soil water tension is approximately 400cm which is just above "field capacity" (≈ 340 cm). This simple diffusion model appears to work well in this range which is of horticultural interest where the goal in crop irrigation is to maintain the capillary water available for plant use. At the low water content range of 1.0 g/g (0.17 m^3/m^3) the soil water tension (≈ 15,000 cm) is close to the permanent wilting point. Under these conditions we need to consider a more complex model that accounts for water vapor flow to predict fertilizer movement such as that developed in Chapters 4 and 5. At the high water content range of 4.0 g/g (0.68 m^3/m^3) the soil water tension (4 cm) is close to saturation where we need to consider the effects of solution density and gravity driven flow (Burns and Dean, 1964). A more complete model than the analytical solution is developed in this dissertation, which is valid for the case found in systems utilizing a PDZ where low to medium water contents exist above 340 cm tension. No attempt was made to include the solution density effects expected at high water contents below 340 cm tension where gravity driven flow exists.

The objective of Chapter IV was to refine the existing theory of osmotically driven soil water vapor movement using a physically based model. The model was validated using the experimental data published by Wheeting (1925). The model could account for differences in water transport rates due to different salts and soil textures. The results verify that significant water vapor transport can occur in the presence of salts. The model

accounts for the differences observed between different salts. Further development and testing against a larger data set using a more complete soil water model, which includes coupled water and solute transport model is needed.

In Chapter V, theory was developed to predict water and salt movement in porous media. A numerical model was developed to implement this theory and tested against experimental results existing in the literature. Based on the model results the theory was shown to account for most water and salt movement. These results have implications for diffusion of salts and concentrated solutions into soils and other porous media. Salt movement is enhanced significantly through the movement of water vapor towards the salt-media interface. This increase in water content at the interface increased solubility of the salt into the media, and increased the effective diffusion rate into the soil. Different media effect the movement of water as well as different salts due to differences in solubility and ability to decrease the water vapor pressure in the vicinity of the salt.

The results of this research have important implications in predicting ion diffusion from concentrated salt sources in unsaturated porous media. 1. The initial quantity of salt applied and the solubility and hygroscopic properties of the salt affect the movement of water near the salt and the salt diffusion rate. 2. It is necessary to recognize that there is no simple relationship between the effective diffusion coefficient in unsaturated media and the pure water diffusion coefficient for specific salts. 3. The ion diffusion in the container medium increased with increasing water content. 4. At high water contents (4.0 g/g), water redistribution and solution density gradients increase gravitational flows of solution in the medium. 5.At low water contents near the permanent wilting point (15,000 cm tension) significant water redistribution occurred in the medium in response to an

osmotic potential established by the concentrated solution in the medium. These features significantly complicate the mathematical modeling of the system, rendering the simple Fickian diffusion model of limited predictive value.

Ion movement in porous media is of broad interest in many fields, such as engineering and science in addition agriculture. Beyond the agricultural aspect discussed here, ion movement in porous media is of broad interest in many other fields in engineering and science. This research has implications on the finger flow development of concentrated plumes of dissolved salts from waste storage tanks. Water vapor flow towards the developing finger may increase the extent of finger infiltration in dry soils. This theory could be developed to predict the rate of water vapor movement into concrete structures and roadways located near salt water for design and maintenance of these structures. Water vapor flow may occur through clay liners protecting landfills from leaching. Better understanding of this process can lead to increased agricultural production, improved public safety, and enhanced environmental protection.

Bibliography

Alberty, R. A. 1987. Physical Chemistry. 7th ed. John Wiley and Sons, New York.

Alexander, S. V. 1993. Pollution control and prevention at containerized nursery operations. Water Sci. and Tech. 28(3-5):509-517.

Annan, A. P. 1977. Time-domain reflectometry -- Air-gap problem for parallel wire transmission lines. Report of Activities, Part B; Geol. Surv. Can., Paper 77-1B. pps 59-62.

Arcone, S. 1986. Conductivity limitations in single-reflection time-domain reflectometry. J. Phys. E:Sci. Instrum. 19:1067-1069.

Arcone, S. A., and R. Wills. 1986. A numerical study of dielectric measurements using single-reflection time-domain reflectometry. J. Phys. E:Sci. Instrum. 19:448-454.

Baker, J. M. and Lascano, R. J. The spatial sensitivity of time-domain reflectometry. In press. Soil Science.

Baker, J. M. and R. R. Allmaras. 1990. System for automating and multiplexing soil moisture measurment by time domain reflectometry. Soil Sci. Soc. Am. J. 54(1):1-6.

Barber, S. A. 1974. Influence of the plant root on ion movement in soil. pps 523-564. in The plant root and its environment. ed. by E. W. Carson. University Press of Virginia, Charlottesville. 691 pages.

Barber, S. A. 1984. Soil Nutrient Bioavailability. John Wiley & Sons. 398 pages.

Barber, S. A., J. M. Walker, and E. H. Vasey. 1963. Mechanisms for the movement of plant nutrients from the soil and fertilizer to the plant root. Agricultural and Food Chemistry. Vol 11(3):204-207.

Barber, S. A., J. M. Walker, and E. H. Vasey. 1963. Mechanisms for the movement of plant nutrients from the soil and fertilizer to the plant root. Agricultural and Food Chemistry. Vol 11(3):204-207.

Bertolini, D., M. Cassettari, G. Salvetti, E. Tombari, and S. Veronesi. 1990. Time domain reflectometry to study the dielectric properties of liquids: Some problems and solutions. Rev. Sci. Instrum. 61(12):450-456.

Bhadoria P. B. S., J. Kaselowsky, N. Claassen and A. Jungk. 1991. Soil phosphate diffusion coefficients: their dependence on phosphorous concentration and buffer power. Soil Sci. Soc. Am. J. 55:56-60.

Biernbaum, J. A. 1992. Root-zone management of greenhouse container-grown crops to control water and fertilizer use. HortTechnology. 2(1):127-132.

Bresler, E. 1973. Anion exclusion and coupling effects in nonsteady transport through unsaturated soils: I. Theory. Soil Sci. Soc. Am. Proc. 37:663-669.

Brown, D. A., B. E. Fulton and R. E. Phillips. 1964. Ion Diffusion: I. A quick-freeze method for the measurement of ion diffusion in soil and clay systems. Soil Sci. Soc. Am. Proc. 628-632.

Bunt A. C. 1988. Media mixes for container grown plants. Unwin Hyman. London.

Burns, G. R. and L. A. Dean. 1964. The movement of water and nitrate around bands of sodium nitrate in soils and glass beads. Soil Sci. Soc. Am. Proc. 28:470-474.

Campbell, J. E. 1990. Dielectric properties and influence of conductivity in soils at one to fifty megahertz. Soil Sci. Soc. Am. J. 54:332-341.

Carter, R. G. 1990. Electromagnetic waves: microwave components and devices. 331 pp. Chapman and Hall, London.

Catriona, M., K. Gardner, J. P. Bell, J. D. Cooper,T. J. Dean, M. G. Hodnett and N. Gardner. 1991. Soil water content in Soil Analysis: Physical Methods ed. by K. A. Smith and C. E. Mullins. Marcel Dekker,Inc. New York. p.1-73.

Clarkson, T. S., L. Glasser, R. W. Tuxworth, and G. Williams. 1977. An appreciation of experimental factors in time-domain spectroscopy. Advances in Molecular Relaxation and Interaction Processes. 10:173-202.

Conca, J. L. and Judith Wright. 1990. Diffusion coefficients in gravel under unsaturated conditions. Water Resources Research Vol. 26, No. 5, 1055-1066, May 1990.

Conkling, B. L. and R. W. Blanchar. 1986. Estimation of calcium diffusion coefficients from electrical conductance. Soil Sci. Soc. Am. J. 50:1455-1459.

Conkling, D. L. and R. W. Blanchar. 1989. Calcium, magnesium, and potassium diffusion coefficients in soil estimated from electrical conductance. Soil Sci. Soc. Am. J. 53:1685-1690.

Cox, D. A. 1993. Reducing nitrogen leaching-losses from containerized plants: the effectiveness of controlled-released fertilizers. J of Plant Nutrition. 16(3):533-545.

Crank, J. 1975. The mathematics of diffusion. Oxford University Press, New York. p. 20-21.

Cutmore, N., D. Abernathy, and T. Evans. 1989. Microwave technique for the on-line determination of moisture in coal. Journal of Micowave Power and Electromagnetic Energy. 24(2):79-90.

Dalton, F. N. and M. Th. van Genuchten. 1986. The time-domain reflectometry method for measuring soil water content and salinity. Geoderma. 38:237-250.

Dalton, F. N., W. N. Herkelrath, D. S. Rawlins and J. D. Rhoades. 1984. Time-domain reflectometry: simultaneous measurement of soil water content and electrical conductivity with a single probe. Science 224:989-990.

Daniel, V. V. 1967. Dielectric relaxation. 281 pp. Academic Press, London.

Dasberg, S. and F. N. Dalton. 1985. Time domain reflectometry field measurements of soil water content and electrical conductivity. Soil Sci. Soc. Am. J. 49:293-297.

Delecki Z. and M. Hamid. 1988. A simple method for determination of the complex dielectric constant. Journal of Micowave Power and Electromagnetic Energy. 23(1):53-58.

Dunlop, J. and D. G. Smith. 1989. Telecommunications Engineering. 508 pp. Van Nostrand Reinhold, London.

Edlefsen, N. E. and A. B. C. Anderson. 1943. Thermodynamics of soil moisture. Hilgardia 15:31-298.

Fellner-Feldegg, H. 1969. The measurement of dielectrics in the time domain. The Journal of Physical Chemistry. 73(3):616-623.

Freier, R. K. 1976. Aqueous Solutions Vol. 1 Data for inorganic and organic compounds. Walter de Gruyter. Berlin-NewYork.

Gardiol F. E. 1984. Introduction to microwaves. 495 pp. Artech House, Inc. Dedham, MA.

Geraldson, C. M. 1990. Conceptual evaluation of intensive production systems for tomatoes, pp 539-544. In: Plant Nutrition - Physiology and Applications, 819 pp. Kluwer Academic Publishers.

Giese, K. and R. Tiemann. 1975. Determination of the complex permittivity from thin-sample time domain reflectometry improved analysis of the step response waveform. Advances in Molecular Relaxation Processes. 7:45-59.

Graham-Bryce, I. J. 1963. Effect of moisture content and soil type on self diffusion of ^{86}Rb in soils. J. Agric. Sci. 60:239-244.

Green, J. L. 1995. Self-contained fertilizing tube portable. Resource: Engineering and Technology for a Sustainable World. 2(8):9.

Green, J. L. and R. Schneckenburger. 1992. Pallet system for container-grown plants. U.S. Patent 5,170,581. Assigned to the State of Oregon, acting by and through the State Board of Higher Education on behalf of Oregon State University. Date issued: 2 June.

Green, J. L., B. A. Briggs, and D. L. Briggs. 1993a. Fertilizing apparatus. U.S. Patent 5,212,904. Assigned to the State of Oregon, acting by and through the State Board of Higher Education on behalf of Oregon State University. Date issued: 25 May.

Green, J. L., S. F. Kelly, B. Blackburn, J. Robbins, B. A. Briggs, and D. L. Briggs. 1993b. A protected diffusion zone (PDZ) to conserve soluble production chemicals. Combined Proc. Intl. Plant Prop. Soc. 43:40-44.

Heimovaara T. J. and W. Bouten. 1990. A computer-controlled 36-channel time domain reflectometry system for monitoring soil water contents. Water Resources Research. 26(10):2311-2316.

Hershey, D. R. and J. L. Paul. 1982. Leaching-losses of nitrogen from pot chrysanthemums with controlled-release fertilization. Scientia Hort. 17:145-152.

Hipp, J. E. 1974. Soil electromagnetic parameters as functions of frequency, soil density, and soil moisture. Proceedings of the IEEE. 62(1):98-103

Hoekstra, P. and A. Delany. 1974. Dielectric properties of soils at UHF and microwave frequencies. Journal of Geophysical Research. 79(11):1699-1708.

Horvath, A. L. 1985. Handbook of aqueous electrolyte solutions, physical properties, estimation and correlation methods. Ellis Horwood Limited, Chichester.

Jackson, R. D. 1964. Water vapor diffusion in relatively dry soil: I. Theoretical considerations and sorption experiments. Soil Sci. Soc. Proc. 28:172-176.

Jury, W. A. and K. Roth. 1990. Transfer functions and solute movement through soil: Theory and applications. 226 pages. Birkhauser Verlag Basel. Berlin, Germany.

Kabashima, J. N. 1993. Innovative irrigation techniques in nursery production to reduce water usage. HortScience. 28(4):291-293.

Kachanoski, R. G., I. J. Van Wesenbeeck, P. Von Bertoldi, A. Ward, and C. Hamlen. 1990. Measurement of soil water content during three-dimensional axial-symmetric water flow. Soil Sci. Soc. Am. J. 54:645-649.

Kelly, S. F., J. L. Green, J. S. Selker. 1997. Fertilizer diffusion in container medium. J. Amer. Soc. Hort. Sci. 122:122-128.

Kemper, W. D. and J. B. Rollins. 1966. Osmotic efficiency coefficients across compacted clays. Soil Sci. Soc. Am. Proc. 30:529-534.

Keng. J. C. W. and G. C. Topp. 1983. Measuring water content of soil columns in the laboratory: A comparison of gamma ray attenuation and TDR techniques. Can. J. Soil Sci. 63: 37-43.

Khalid K. 1988. The application of microstrip sensors for determination of moisture content in hevea rubber latex. Journal of Micowave Power and Electromagnetic Energy. 23(1):45-51.

Klute, A. and J. Letey. 1958. The dependence of ionic diffusion on the moisture content of nonadsorbing porous media. Soil Sci. Soc. Proc. 213-215.

Knight, J. H. 1992. Sensitivity of time domain reflectometry measurements to lateral variations in soil water content. Water Resources Research 28(9):2345-2352.

Kolaian, J. H. and Ohlrogge, A. J. 1959. Principles of nutrient uptake from fertilizer bands IV. Accumulation of water around the bands. Agronomy J. 51:106-108.

Korn, G. A. and T. M. Korn. Mathematical handbook for scientists and engineers. McGraw-Hill Book Co. New York. p. 299.

Kruger, W., H. Benkenstein and H. Pagel. 1981. Untersuchungen zur Nitratdiffusion in Boden. Arch. Acker-u. Pflanzenbau u. Bodenkd., Berlin 25(1):653-661.

Lawton, K. and Vomocil, J. A. 1954. The dissolution and migration of phosphorous from granular superphosphate in some Michigan soils. Soil Sci. Soc. Proc. 18:26-32.

Letey, J., W. D. Kemper and L. Noonan. 1969. The effect of osmotic pressure gradients on water movement in unsaturated soil. Soil Sci. Soc. Am. Proc., 33:15-18.

Massee, T. W., R. A. Olsen and E. O. Skogley. 1977. Characterizing soil fertility by ion diffusive flux measurements. Plant and Soil. 47:663-679.

Mathsoft Inc. 1995. Mathcad User's Guide, Mathcad PLUS 6.0. Mathsoft Inc., Cambridge MA.

Mehta, B. K., S. Shiozawa and M Nakano. 1995. Measurement of molecular diffusion of salts in unsaturated soil. Soil Sci. 159(2)115-121.

Merabet, M. and T. K. Bose. 1988. Dielectric measurements of water in the radio and microwave frequencies by time domain reflectometry. J. Phys. Chem. 92:6149-6150.

Metaxas A. C., and R. J. Meredith. 1983. Industrial microwave heating. 357 pp. IEE Power Engineering Series 4. Peter Peregrinus Ltd. London, UK.

Miyazaki, T., T. Kasubuchi, and S. Hasegawa. 1991. A statistical approach for predicting accuracies of soil properties measured by single, double and dual gamma beams. J. of Soil Sci. 42:127-137.

Mochoge, B. O. 1984. Simulation of nitrate movement in undisturbed soil columns. Agriculture, Ecosystems and Environment. 11:105-115.

Mott, C. J. B. and P. H. Nye. 1968. Contribution of adsorbed strontium to its self diffusion in a moisture-saturated soil. Soil Science. 105:1:18-23.

Nadler, A., S. Dasberg, and I. Lapid. 1991. Time domain reflectometry measurements of water content and electrical conductivity of layered soil columns. Soil Sci. Soc. Am. J. 55:938-943.

Nadler, A., S. Dasberg, I. Lapid. 1991. Time domain reflectometry measurements of water content and electrical conductivity of layered soil columns. Soil Sci. Soc. Am. J. 55(4):938-943.

Nassar, I. N. and R. Horton. 1989a. Water transport in unsaturated nonisothermal salty soil: I. Experimental results. Soil Sci. Soc. Am. J. 53:1323-1329.

Nassar, I. N. and R. Horton. 1989b. Water transport in unsaturated nonisothermal salty soil: II. Theoretical development. Soil Sci. Soc. Am. J. 53:1330-1337.

Nassar, I. N., R. Horton and A. M. Globus. 1992a. Simultaneous transfer of heat, water and solute in porous media: I. Theoretical development. Soil Sci. Soc. Am. J. 56:1350-1356.

Nassar, I. N., R. Horton and A. M. Globus. 1992b. Simultaneous transfer of heat, water and solute in porous media: II. Experiment and analysis. Soil Sci. Soc. Am. J. 56:1357-1365.

Nelson, S. O. 1985. RF and microwave energy applications for potential agricultural applications. J. Microwave Power. pp 65-70.

Nervin, S. V. 1970. Physics of the soil: Chapter XII. Dielectric properties of soils. Keter Press, Jerusalem. pp 313-343.

Nobel, P. S. 1983. Biophysical Plant Physiology and Ecology. W. H. Freeman and Company, 608 pages. San Francisco.

Noborio, K., K. J. McInnes and J. L. Heilman. 1996a. Two-dimensional model for water, heat, and solute transport in furrow irrigated soil: I. Theory. Soil Sci. Soc. Am. J. 60:1001-1009.

Noborio, K., K. J. McInnes and J. L. Heilman. 1996b. Two-dimensional model for water, heat, and solute transport in furrow irrigated soil: II. Field evaluation. Soil Sci. Soc. Am. J. 60:1010-1021.

Nye, P. H. 1966. The measurement and mechanism of ion diffusion in soil. I. The relation between self-diffusion and bulk diffusion. Journal of Soil Science, 17(1):17-23.

Nye, P. H. and M. Ramzan. 1979. Measurement and mechanism of ion diffusion in soil. X. Prediction of soil acidity gradients in acid-base transfers. J. of Soil Sci. 30:43-51.

Nye, P. H. and P. B. Tinker. 1977. Solute movement in the soil-root system. Blackwell Scientific Publications, Oxford. 342 pages.

Olsen, S. R. and W. D. Kemper. 1968. Movement of nutrients to plant roots. p 91-151. In: Advances in Agronomy, American Society of Agronomy. Vol. 20, edited by A. G. Norman. Academic Press.

Olsen, S. R., W. D. Kemper, and J. C. Van Schaik. 1965. Self-diffusion coefficients of phosphorous in soil measured by transient and steady state methods. Soil Sci. Soc. Proc. 154-158.

Palmer, C. J. and R. W. Blanchar. 1980. Prediction of diffusion coefficients from the electrical conductance of soil. Soil Sci. Soc. Am. J. 44:925-929.

Parlange, J. 1973. Movement of salt and water in relatively dry soils. Soil Sci. 116(4):249-255.

Patil, A. S., K. M. King and M. H. Miller. 1963. Self-diffusion of rubidium as influenced by soil moisture tension. Can. J. of Soil. Sci. 43:44-51.

Patterson D. E. and N. Smith. 1980. The use of time domain reflectometry for the measurement of unfrozen water content in frozen soils. Cold Regions Science and Technology. 3:205-210.

Phillips, R. E. and D. A. Brown. 1964. Ion diffusion: II. Comparison of apparent self and counter diffusion coefficients. Soil Sci. Soc. Am. Proc. 758-763.

Porter, L. K., W. D. Kemper, R. D. Jackson, and B. A. Stewart. 1960 Chloride Diffusion in soils as influenced by moisture content. Soil Sci. Soc. Proc. 460-463.

Raats, P. A. C. 1969. Steady gravitational convection induced by a line source of salt in a soil. Soil Sci. Soc. Am. Proc. 33:483-487.

Rhoades, J. D., and J. D. Oster. 1986. Solute Content. in Methods of Soil Analysis, Part 1. Physical and Mineralogical Methods-Agronomy Monograph no. 9 (2nd edition) ed. by A. Klute. Soil Sci. Soc. Am. p. 985-1006.

Robinson, R. A. and R. H. Stokes. 1959. Electrolyte solutions. 2nd ed. Butterworths Scientific Publications, London.

Rost, B. 1995. The cooler king. Resource: Engineering and Technology for a Sustainable World. 2(8):8-12.

Roth, K. R., Schulin, H. Flucher, and W. Attinger. 1990. Calibration of time domain reflectometry for water content measurement using a composite dielectric approach. Water Resources Research. 26(10):2267-2273.

Saxena, S. K., L. Boersma, F. T. Lindstrom and J. L. Young. 1974. Effect of pore size on diffusion coefficients in porous media. Soil Science. 117(2):80-86.

Schaff, B. E. and E. O. Skogley. 1982. Diffusion of potassium, calcium, and magnesium in Bozeman silt loam as influenced by temperature and moisture. Soil Sci. Soc. Am. J. 46:521-524.

Schofield, R. K. and I. D. Graham-Bryce. 1960. Diffusion of ions in soils. Nature 188:1048-1049.

Scotter D. R. and Raats, P. A. C. 1970. Movement of salt and water near crystalline salt in relatively dry soil. Soil Sci. 109:170-178.

Scotter, D. R. 1974a. Factors influencing salt and water movement near crystalline salts in relatively dry soil. Aust. J. Soil Res. 12:77-86.

Scotter, D. R. 1974b. Salt and water movement in relatively dry soil. Aust. J. Soil Res. 12:27-35.

Skogley, E. O. and B. E. Schaff. 1985. Ion diffusion in soils as related to soil physical and chemical properties. Soil Sci. Am. J. 49:847-850.

Sonneveld, C. and W. Voogt. 1990. Response of tomatoes (Lycopersicon esculentum) to an unequal distribution of nutrients in the root environment, pp. 509-514. In: Plant Nutrition - Physiology and Applications, 819 pp. Kluwer Academic Publishers.

Sphicopoulos, T., V. Teodoridis, and F. Gardiol. 1985. Simple nondestructive method for the measurement of material permittivity. J. Microwave Power. pp 165-172.

Stein, J. and D. S. Kane. 1983. Monitoring the unfrozen water content of soil and snow using time domain reflectometry. Water Resources Research. 19(6):1573-1584.

Tektronix Corp., Beaverton OR. Digital IC Characterization Seminar. Presentation Handouts.

Thomas, A. M. 1965. *In situ* measurement of moisture in soil and similiar substances by 'fringe' capacitance. 21-27.

Ticknor, R. L. and J. L. Green. 1987. Effect of irrigation methods on plant growth and water use. Proc. Int. Plant Prop. Soc. 37:45-48.

Topp G. C., and J. L. Davis. 1982. Measurement of soil water content using time domain reflectometry. Canadian Hydrology Symposium: 82. Associate Committee of

Hydrology. National Research Council of Canada. June 14-15 1982. Fredericton, New Brunswick. 269-287.

Topp, G. C. and J. L. Davis. 1981. Detecting infiltration of water through soil cracks by time-domain reflectometry. Geoderma 26:13-23.

Topp, G. C. and J. L. Davis. 1985. Measurement of soil water content using time-domain reflectometry (TDR): A field evaluation. Soil Sci. Soc. Am. J. 49:19-24.

Topp, G. C. The application of time-domain reflectometry (TDR) to soil water content measurement. Land Resource Research Centre, Agriculture Canada, Ottawa, Canada, K1A OC6.

Topp, G. C., J. L. Davis, and A. P. Annan. 1980. Electromagnetic determination of soil water content: measurements in coaxial transmission lines. Water Resources Research. 16(3):574-582.

Topp, G. C., J. L. Davis, and A. P. Annan. 1982. Electromagnetic determination of soil water content using TDR: I. Applications to wetting fronts and steep gradients. Soil Sci. Soc. Am. J. 46:672-678.

Topp, G. C., J. L. Davis, and A. P. Annan. 1982. Electromagnetic determination of soil water content using TDR: II. Evaluation of installation and configuration of parallel transmission lines. Soil Sci. Soc. Am. J. 46:678-684.

Topp, G. C., M. Yanuka, W. D. Zebchuk and S. Zegelin. 1988. Determination of electrical conductivity using time domain reflectometry: Soil and water experiments in coaxial lines. Water Resources Research, 24(7):945-952.

Topp, G. C., W. D. Zebchuk, and J. Dumanski. 1980. The variation of in situ measures soil water properties within soil map units. Can. J. Soil Sci. 60:497-509.

Tracy, J. C. and M. A. Marino. 1989. Solute movement through root soil environment. Journal of Irrigation and Drainage Engineering. 115:4:608-625.

Tyrrell, H. J. V. and K. R. Harris. 1984. Diffusion in liquids: A theoretical and experimental study. Butterworth, London.

Vaidyanathan, L. V. and P. H. Nye. 1966. The measurement and mechanism of ion diffusion in soils. II. An exchange resin paper method for measurement of the diffusive flux and diffusion coefficient of nutrient ions in soils. Journal of Soil Science. 17(2):175-183.

van Genuchten, M. T. 1980. A closed form solution for predicting the hydraulic conductivity of unsaturated soils. Soil Sci. Soc. Am. J. 44:892-898.

Van Loon, W. K. P., E. Perfect, P. H. Groenevelt. and B. D. Kay. 1990. A new method to measure bulk electrical conductivity in soils with time domain reflectometry. Can. J. Soil Sci. 70:403:410.

Von Hippel A. R. 1954. Dielectric materials and applications. Papers by twenty two contributors. 438 pp. Edited by A. R. Von Hippel. MIT Press.

Wagenet, R. J. 1983. Principles of salt movement in soils. in Chemical mobility and reactivity in soil systems. Soil Sci. Soc. of Am. Special publication number 11. ed. D. W. Nelson. pps 123-141.

Weast, R. C. (ed.) 1987. CRC handbook of chemistry and physics. CRC Press Inc. Boca Raton Fla.

Wheeting, L. C. 1925. Certain relationships between added salts and the moisture of soils. Soil Science. 16(4):287-299.

Wobschall, D. 1977. A theory of the complex dielectric permittivity of soil containing water: The semidisperse model. IEEE Transactions on Geoscience Electronics. GE-15(1):49-58.

Yakirevich, A., P. Berliner and S Sorek 1997. A model for numerical simulation of evaporation from bare saline soil. Water Resour. Res. 33:1021-1033.

Yanuka M., G. C. Topp, S. Zegelin, and W. D. Zebchuk. 1988. Multiple reflection and attenuation of time domain reflectometry pulses: Theoretical considerations for applications to soil and water. Water Resources Research. 24(7):939-944.

Zegelin S. J., I. White, and D. R. Jenkins. 1989. Improved fields probes for soil water content and electrical conductivity measurement using time domain reflectometry. Water Resources Research. 25(11):2367-2376.

Appendices

Appendix A. Diffusion Column Data

Table 5. Diffusion column data

Column #	Orientation	Diffusion Time, [d]	Diffusing Salt	Salt Solubility @ 20C [g/l]	Initial Salt Wt. [g]	Final Salt Wt. [g]	Initial Water Content [g/g]	Empty Column Weight [g]	Date Column Packed
COL	ORIENT	DAY	SALT	SOL	START	END	IGWC	ECW	DP
2	Horz	5	NaBr	475	50	47.2	0.9	209.77	08/27/92
3	Horz	5	NaBr	475	50	46.69	0.9	207.56	08/27/92
4	Horz	5	NaBr	475	50	47.07	0.9	206.61	08/27/92
5	Horz	5	KBr	394	50	43.34	0.9	205.15	08/27/92
6	Horz	5	KBr	394	50	43.06	0.9	207.11	08/27/92
7	Horz	5	KBr	394	50	42.84	0.9	206.52	08/27/92
8	Horz	5	NaBr	475	50	32.09	2.4	206.25	08/27/92
9	Horz	5	NaBr	475	50	31.11	2.4	206.47	08/27/92
10	Horz	5	NaBr	475	50	31.61	2.4	206.95	08/27/92
11	Horz	5	KBr	394	50	38.83	2.4	210.82	08/27/92
12	Horz	5	KBr	394	50	36.5	2.4	209.47	08/27/92
13	Horz	5	KBr	394	50	36.08	2.4	208.75	08/27/92
14	Horz	5	NaBr	475	50	17.78	3.6	209.67	08/27/92
15	Horz	5	NaBr	475	50	13.24	3.6	208.29	08/27/92
16	Horz	5	NaBr	475	50	14.36	3.6	207.91	08/27/92
17	Horz	5	KBr	394	50	19.52	3.6	208.4	08/27/92
18	Horz	5	KBr	394	50	20.16	3.6	208.43	08/27/92
19	Horz	5	KBr	394	50	17.34	3.6	215.7	08/27/92
20	Horz	120	NaBr	475	50	0	0.9	203.57	08/28/92
21	Horz	120	NaBr	475	50	0	0.9	210.02	08/28/92
22	Horz	120	NaBr	475	50	0	0.9	209.95	08/28/92
23	Horz	120	KBr	394	50	3.22	0.9	210.01	08/28/92
24	Horz	120	KBr	394	50	4.93	0.9	215.47	08/28/92
25	Horz	120	KBr	394	50	5.37	0.9	205.85	08/28/92
26	Horz	120	NaBr	475	50	0	2.4	206.89	08/28/92
27	Horz	120	NaBr	475	50	0	2.4	211.37	08/28/92
28	Horz	120	NaBr	475	50	0	2.4	212.11	08/28/92
29	Horz	120	KBr	394	50	0	2.4	209.88	08/28/92
30	Horz	120	KBr	394	50	0	2.4	211.36	08/28/92
31	Horz	120	KBr	394	50	0	2.4	207.05	08/28/92
32	Horz	120	NaBr	475	50	0	3.6	203.51	08/28/92
33	Horz	120	NaBr	475	50	0	3.6	211.11	08/28/92
34	Horz	120	NaBr	475	50	0	3.6	209.56	08/28/92
35	Horz	120	KBr	394	50	0	3.6	209.17	08/28/92
36	Horz	120	KBr	394	50	0	3.6	210.32	08/28/92
37	Horz	120	KBr	394	50	0	3.6	206.28	08/28/92
38	Horz	10	NaBr	475	50	45.44	0.961	211.35	10/26/92
39	Horz	10	NaBr	475	50	45.18	0.961	212.56	10/26/92
40	Horz	10	NaBr	475	50	43.45	0.961	214.24	10/26/92

Table 5. (continued)

Column #	Orientation	Diffusion Time, [d]	Diffusing Salt	Salt Solubility @ 20C [g/l]	Initial Salt Wt. [g]	Final Salt Wt. [g]	Initial Water Content [g/g]	Empty Column Weight [g]	Date Column Packed
COL	ORIENT	DAY	SALT	SOL	START	END	IGWC	ECW	DP
41	Horz	10	KBr	394	50	39.98	0.961	213.63	10/26/92
42	Horz	10	KBr	394	50	39.44	0.961	219.52	10/26/92
43	Horz	10	KBr	394	50	38.38	0.961	214.31	10/26/92
44	Horz	10	KBr	394	50	30.95	2.4833	213.07	10/26/92
45	Horz	10	KBr	394	50	31.17	2.4833	211	10/26/92
46	Horz	10	KBr	394	50	30.31	2.4833	213.31	10/26/92
47	Horz	10	NaBr	475	50	20.46	2.4833	219.49	10/26/92
48	Horz	10	NaBr	475	50	20.66	2.4833	216.49	10/26/92
49	Horz	10	NaBr	475	50	20.88	2.4833	211.25	10/26/92
50	Horz	10	NaBr	475	50	0	4.0084	217.22	10/27/92
51	Horz	10	NaBr	475	50	0	4.0084	214.76	10/27/92
52	Horz	10	NaBr	475	50	0	4.0084	214.55	10/27/92
53	Horz	10	KBr	394	50	1.08	4.0084	218.67	10/27/92
54	Horz	10	KBr	394	50	1.4	4.0084	210.93	10/27/92
55	Horz	10	KBr	394	50	2.18	4.0084	213.38	10/27/92
56	Horz	25	KBr	394	50	17.49	2.4833	206.83	02/22/93
57	Horz	25	KBr	394	50	15.24	2.4833	200.78	02/22/93
58	Horz	25	KBr	394	50	16.94	2.4833	199.71	02/22/93
59	Horz	25	NaBr	475	50	0.22	2.4833	201.27	02/22/93
60	Horz	25	NaBr	475	50	1.2	2.4833	202.74	02/22/93
61	Horz	25	NaBr	475	50	0.14	2.4833	200.51	02/22/93
62	Horz	25	KBr	394	50	30.13	0.961	201.86	02/22/93
63	Horz	25	KBr	394	50	31.92	0.961	201.89	02/22/93
64	Horz	25	KBr	394	50	30.29	0.961	201.1	02/22/93
65	Horz	25	NaBr	475	50	24.09	0.961	202.03	02/22/93
66	Horz	25	NaBr	475	50	24.67	0.961	203.82	02/22/93
67	Horz	25	NaBr	475	50	24.54	0.961	202.25	02/22/93
68	Horz	25	KBr	394	50	0	4.0084	204.29	02/22/93
69	Horz	25	KBr	394	50	0.47	4.0084	196.71	02/22/93
70	Horz	25	KBr	394	50	0	4.0084	208.65	02/22/93
71	Horz	25	NaBr	475	50	0	4.0084	204.82	02/22/93
72	Horz	25	NaBr	475	50	0	4.0084	206.24	02/22/93
73	Horz	25	NaBr	475	50	0.18	4.0084	208.67	02/22/93
74	Down	10	KBr	394	50	42.62	1.0055	216.9	02/22/93
75	Down	10	KBr	394	50	40.89	1.0055	200.82	02/22/93
76	Down	10	KBr	394	50	41.6	1.0055	208.12	02/22/93
77	Up	10	KBr	394	50	40.04	1.0055	205.52	02/22/93
78	Up	10	KBr	394	50	39.72	1.0055	203.33	02/22/93
79	Up	10	KBr	394	50	42.33	1.0055	208.55	02/22/93
80	Down	10	KBr	394	50	30.18	2.5002	215.72	02/22/93
81	Down	10	KBr	394	50	31.24	2.5002	208.65	02/22/93
82	Down	10	KBr	394	50	30	2.5002	206.67	02/22/93
83	Up	10	KBr	394	50	30.27	2.5002	205.48	02/22/93
84	Up	10	KBr	394	50	30.6	2.5002	219.43	02/22/93
85	Up	10	KBr	394	50	30.26	2.5002	212.14	02/22/93
86	Down	10	KBr	394	50	12.2	4.0763	212.87	02/22/93
87	Down	10	KBr	394	50	11.32	4.0763	207.05	02/22/93
88	Down	10	KBr	394	50	10.7	4.0763	207.38	02/22/93
89	Up	10	KBr	394	50	4.22	4.0763	209.47	02/22/93
90	Up	10	KBr	394	50	6.76	4.0763	208.24	02/22/93
91	Up	10	KBr	394	50	5.78	4.0763	206.03	02/22/93

Table 5. (continued)

Column #	Packed Column Weight [g]	Date Column Sealed	Time Column Sealed	Sealed Column Weight [g]	Date Column Opened	Time Column Opened	Opened Column Weight [g]	Molecular Weight of Salt
COL	PCW	DS	TS	SCW	DO	TO	OCW	MWS
2	438.13	08/31/92	03:15 PM	743.43	09/05/92	04:00 PM	743.45	102.9
3	446.34	08/31/92	03:45 PM	758.21	09/05/92	04:45 PM	758.21	102.9
4	442.68	08/31/92	03:50 PM	753.91	09/05/92	05:13 PM	753.94	102.9
5	443.14	08/31/92	03:29 PM	754.23	09/05/92	06:34 PM	754.23	119
6	442.83	08/31/92	03:25 PM	751.41	09/05/92	07:09 PM	751.39	119
7	449	08/31/92	03:30 PM	757.56	09/05/92	07:30 PM	757.58	119
8	623.71	08/31/92	04:25 PM	934.42	09/05/92	08:07 PM	934.45	102.9
9	635.45	08/31/92	04:30 PM	949.32	09/05/92	08:37 PM	949.27	102.9
10	631.71	08/31/92	04:35 PM	944.23	09/05/92	08:50 PM	944.25	102.9
11	645.04	08/31/92	04:40 PM	952.29	09/05/92	09:13 PM	952.34	119
12	630.19	08/31/92	04:45 PM	941.05	09/05/92	09:58 PM	941.02	119
13	627.59	08/31/92	04:50 PM	938.24	09/05/92	10:41 PM	938.23	119
14	736.87	08/31/92	04:45 PM	1047.56	09/05/92	11:00 PM	1047.48	102.9
15	734.99	08/31/92	05:00 PM	1047.06	09/05/92	11:20 PM	1046.98	102.9
16	741.46	08/31/92	05:10 PM	1056.94	09/05/92	11:45 PM	1056.89	102.9
17	745.51	08/31/92	05:20 PM	1056.25	09/06/92	12:10 AM	1055.21	119
18	751.05	08/31/92	05:25 PM	1063.89	09/06/92	12:30 AM	1062.61	119
19	765.39	08/31/92	05:30 PM	1085.78	09/06/92	01:00 AM	1085.78	119
20	434.22	08/31/92	05:35 PM	743.93	02/03/93	08:00 PM	741.85	102.9
21	447.33	08/31/92	05:50 PM	757.75	02/03/93	08:15 PM	753.36	102.9
22	443.81	08/31/92	05:50 PM	756.51	02/03/93	08:30 PM	755.39	102.9
23	445.06	08/31/92	06:00 PM	756.45	02/03/93	08:45 PM	752.62	119
24	450.04	08/31/92	06:05 PM	762.56	02/03/93	09:00 PM	761.96	119
25	437.67	08/31/92	06:10 PM	752.18	02/03/93	09:15 PM	750.66	119
26	635.76	08/31/92	06:15 PM	943.85	02/03/93	09:30 PM	939.49	102.9
27	640.97	08/31/92	06:25 PM	945.57	02/03/93	09:45 PM	944.63	102.9
28	639.65	08/31/92	06:35 PM	947.43	02/03/93	10:00 PM	940.12	102.9
29	625.45	08/31/92	06:40 PM	928.07	02/03/93	10:30 PM	929.74	119
30	631.6	08/31/92	06:45 PM	933.72	02/03/93	10:45 PM	931.31	119
31	628.83	08/31/92	06:50 PM	934.66	02/03/93	11:00 PM	931.77	119
32	752.57	08/31/92	07:00 PM	1058.28	02/03/93	11:15 PM	1048.72	102.9
33	765.26	08/31/92	07:05 PM	1065.28	02/03/93	11:30 PM	1060.95	102.9
34	757.5	08/31/92	07:10 PM	1060.45	02/03/93	11:45 PM	1057.43	102.9
35	752.33	08/31/92	07:15 PM	1054.66	02/04/93	12:00 AM	1057.15	119
36	767.73	08/31/92	07:20 PM	1060.79	02/04/93	12:15 AM	1063.01	119
37	750.04	08/31/92	07:25 PM	1049.59	02/04/93	12:30 AM	1050.69	119
38	459.34	10/27/92	03:30 PM	775.7	11/06/92	02:40 PM	775.61	102.9
39	463.76	10/27/92	03:31 PM	785.02	11/06/92	03:00 PM	785.02	102.9
40	481.97	10/27/92	03:42 PM	798.7	11/06/92	03:30 PM	798.7	102.9

Table 5. (continued)

Column #	Packed Column Weight [g]	Date Column Sealed	Time Column Sealed	Sealed Column Weight [g]	Date Column Opened	Time Column Opened	Opened Column Weight [g]	Molecular Weight of Salt
COL	PCW	DS	TS	SCW	DO	TO	OCW	MWS
41	474.1	10/27/92	03:47 PM	792.79	11/06/92	03:50 PM	792.8	119
42	475.96	10/27/92	03:53 PM	789.85	11/06/92	04:06 PM	788.81	119
43	478.14	10/27/92	03:58 PM	796.1	11/06/92	04:35 PM	796.04	119
44	588.49	10/27/92	04:06 PM	906.99	11/06/92	04:50 PM	907.01	119
45	617.09	10/27/92	04:10 PM	932.51	11/06/92	08:00 PM	932.56	119
46	622.08	10/27/92	04:15 PM	940.48	11/06/92	08:30 PM	940.49	119
47	641.88	10/27/92	04:19 PM	973.58	11/06/92	09:20 PM	973.55	102.9
48	610.89	10/27/92	04:24 PM	927.83	11/06/92	09:50 PM	927.81	102.9
49	618.97	10/27/92	04:40 PM	937.22	11/06/92	10:10 PM	937.21	102.9
50	835.62	10/27/92	04:45 PM	1154.99	11/06/92	10:45 PM	1154.98	102.9
51	821.78	10/27/92	04:45 PM	1138.55	11/06/92	11:12 PM	1138.59	102.9
52	846.67	10/27/92	04:56 PM	1168.44	11/06/92	11:30 PM	1168.46	102.9
53	849.16	10/27/92	04:59 PM	1162.02	11/07/92	12:10 AM	1161.99	119
54	832.2	10/27/92	05:02 PM	1151.32	11/07/92	12:26 AM	1151.1	119
55	858.38	10/27/92	05:06 PM	1181.58	11/07/92	12:44 AM	1181.59	119
56	623.22	02/22/93	10:00 PM	929.75	03/24/93	09:30 AM	929.58	119
57	632.32	02/22/93	10:00 PM	943.55	03/24/93	09:30 AM	943.84	119
58	622.46	02/22/93	10:00 PM	933.08	03/24/93	09:30 AM	934.71	119
59	627.75	02/22/93	10:00 PM	933.7	03/24/93	09:30 AM	933.38	102.9
60	613.34	02/22/93	10:00 PM	924.4	03/24/93	09:30 AM	925.91	102.9
61	614.01	02/22/93	10:00 PM	927.06	03/24/93	09:30 AM	925.64	102.9
62	468.54	02/22/93	10:00 PM	778.11	03/24/93	09:30 AM	780.5	119
63	468.01	02/22/93	10:00 PM	781.92	03/24/93	09:30 AM	783.3	119
64	468.6	02/22/93	10:00 PM	768.39	03/24/93	09:30 AM	767.82	119
65	469.31	02/22/93	10:00 PM	776.74	03/24/93	09:30 AM	776.52	102.9
66	467.36	02/22/93	10:00 PM	782.94	03/24/93	09:30 AM	782.72	102.9
67	466.38	02/22/93	10:00 PM	772.32	03/24/93	09:30 AM	770.64	102.9
68	829.06	02/22/93	10:00 PM	1138.47	03/24/93	09:30 AM	1140.77	119
69	832.38	02/22/93	10:00 PM	1148.28	03/24/93	09:30 AM	1150.78	119
70	855.92	02/22/93	10:00 PM	1162.11	03/24/93	09:30 AM	1163.63	119
71	833.36	02/22/93	10:00 PM	1147.58	03/24/93	09:30 AM	1146.97	102.9
72	831.04	02/22/93	10:00 PM	1141.05	03/24/93	09:30 AM	1133.26	102.9
73	844.7	02/22/93	10:00 PM	1157.7	03/24/93	09:30 AM	1155.66	102.9
74	476.55	02/27/93	10:00 PM	777.48	03/09/93	10:30 PM	776.01	119
75	457.16	02/27/93	10:00 PM	780.68	03/09/93	10:45 PM	780.24	119
76	460.73	02/27/93	10:00 PM	769.99	03/09/93	11:00 PM	769.42	119
77	458.66	02/27/93	10:00 PM	770.53	03/09/93	11:15 PM	770.52	119
78	458.42	02/27/93	10:00 PM	769	03/09/93	11:30 PM	768.95	119
79	457.61	02/27/93	10:00 PM	770.96	03/09/93	11:45 PM	770.86	119
80	618.64	02/27/93	11:00 PM	926.33	03/09/93	12:00 AM	926.17	119
81	609.7	02/27/93	11:00 PM	917.32	03/10/93	12:15 AM	917.32	119
82	604.77	02/27/93	11:00 PM	914.54	03/10/93	12:30 AM	914.47	119
83	609	02/27/93	11:00 PM	919.56	03/10/93	12:45 AM	919.39	119
84	629.63	02/27/93	11:00 PM	943.81	03/10/93	01:00 AM	943.85	119
85	623.85	02/27/93	11:00 PM	933.12	03/10/93	01:15 AM	932.94	119
86	809.13	02/27/93	11:30 PM	1120	03/10/93	01:30 AM	1120.01	119
87	798.54	02/27/93	11:30 PM	1110.58	03/10/93	01:45 AM	1110.57	119
88	793.28	02/27/93	11:30 PM	1071.48	03/10/93	02:00 AM	1071.41	119
89	798.12	02/27/93	11:30 PM	1112.05	03/10/93	02:15 AM	1110.81	119
90	823.16	02/27/93	11:30 PM	1137.77	03/10/93	02:30 AM	1137.6	119
91	815.85	02/27/93	11:30 PM	1088.5	03/10/93	02:45 AM	1088.34	119

Table 6. Bromide concentrations from 500 ml extracts.

Column #	Bromide Concentrations Molar concentration from 500 ml media extracts Sections #1-#4 are 1cm sections, #5-#10 are 2 cm sections									
COL	#1 MOL1	#2 MOL2	#3 MOL3	#4 MOL4	#5 MOL5	#6 MOL6	#7 MOL7	#8 MOL8	#9 MOL9	#10 MOL10
2	0.01644	0.00793	0	0	0	0	0	0	0	0
3	0.02442	0.00247	0	0	0	0	0	0	0	0
4	0.01676	0.00419	0	0	0	0	0	0	0	0.00001
5	0.06341	0.03398	0.00054	0.00001	0	0	0	0	0	0.00003
6	0.0615	0.03385	0.00034	0	0	0	0.00001	0	0	0.0003
7	0.0639	0.0451	0.00045	0.00001	0.00001	0	0	0	0	0.00001
8	0.16044	0.14748	0.03696	0.00235	0.00004	0	0	0	0	0.00001
9	0.19671	0.13351	0.0422	0.00233	0.00006	0.00001	0	0	0	0.00001
10	0.18983	0.13404	0.03408	0.00006	0.00001	0	0	0	0	0
11	0.10672	0.07849	0.01997	0.00097	0.00004	0	0.00001	0	0	0.00001
12	0.0962	0.083	0.02516	0.00239	0.00008	0.00001	0	0	0	0.00001
13	0.09266	0.0768	0.02377	0.00266	0.0001	0	0	0	0	0
14	0.09266	0.15385	0.08965	0.08965	0.08197	0.0149	0.00024	0.00001	0.00001	0.00006
15	0.13378	0.15758	0.11963	0.09798	0.11225	0.0339	0.00271	0.00004	0.00002	0.00002
16	0.15715	0.14332	0.12358	0.11003	0.12408	0.03129	0.00187	0.00002	0.00002	0.00001
17	0.09337	0.11136	0.10742	0.07168	0.09045	0.0318	0.00318	0.00002	0.00001	0.00003
18	0.0946	0.09018	0.08597	0.06686	0.08383	0.02925	0.00359	0.00004	0.00003	0.00002
19	0.07658	0.11096	0.07476	0.07627	0.09716	0.05299	0.0145	0.00117	0.00002	0.00005
20	0.04059	0.07762	0.0597	0.05692	0.15259	0.1869	0.18322	0.16921	0.10585	0.01021
21	0.0558	0.06944	0.06542	0.05783	0.17147	0.19294	0.17961	0.1387	0.08141	0.00209
22	0.05602	0.07027	0.07027	0.06163	0.15301	0.17644	0.16693	0.13374	0.0678	0.00114
23	0.10588	0.14361	0.13111	0.11597	0.19023	0.0825	0.01956	0.00003	0.00003	0.00003
24	0.09915	0.14192	0.12404	0.12728	0.1843	0.07943	0.02051	0.00368	0.00001	0.00005
25	0.08701	0.12804	0.1221	0.12161	0.1696	0.09568	0.01375	0.00002	0.00001	0.00002
26	0.06909	0.081	0.1212	0.09609	0.1825	0.15692	0.10801	0.0794	0.04228	0.03047
27	0.08036	0.09162	0.10571	0.0891	0.19839	0.14843	0.12072	0.08462	0.05444	0.03398
28	0.08597	0.11602	0.10487	0.10281	0.16524	0.1404	0.10404	0.07363	0.0441	0.02335
29	0.0794	0.10119	0.0992	0.08395	0.15817	0.12813	0.09346	0.06617	0.03818	0.02117
30	0.08993	0.10054	0.10216	0.09137	0.17143	0.1297	0.09433	0.06159	0.0354	0.01963
31	0.08607	0.097	0.09101	0.11019	0.14159	0.13022	0.09547	0.06409	0.03926	0.02424
32	0.03348	0.06886	0.06723	0.06538	0.01287	0.1366	0.15031	0.07822	0.13231	0.11152
33	0.05367	0.06606	0.06148	0.07388	0.12592	0.14138	0.13859	0.13477	0.12693	0.1186
34	0.04378	0.06931	0.06903	0.07184	0.12795	0.13263	0.12592	0.12294	0.12343	0.11579
35	0.04955	0.0658	0.05907	0.06197	0.10797	0.11625	0.10754	0.11812	0.11395	0.10458
36	0.0424	0.05519	0.05884	0.04819	0.12294	0.11487	0.11395	0.11215	0.11487	0.10251
37	0.04721	0.06647	0.05923	0.05737	0.10835	0.1033	0.10133	0.10255	0.09699	0.09661
38	0.01967	0.01898	0.00005	0.00001	0.00001	0.00001	0	0	0	0
39	0.02384	0.01292	0.00135	0	0	0	0	0	0	0
40	0.02329	0.01091	0.00066	0	0	0	0	0	0	0.00001
41	0.06245	0.0665	0.01322	0.00003	0	0	0	0	0	0.00001
42	0.0808	0.05825	0.00251	0.00001	0.00001	0	0	0	0	0.00001
43	0.06899	0.09086	0.01112	0.00002	0	0	0	0.00001	0.00001	0.00001
44	0.10092	0.13695	0.06352	0.02375	0.00383	0.0002	0	0	0	0.00001
45	0.13115	0.11073	0.06018	0.02317	0.00341	0.00003	0.00001	0	0	0.00002
46	0.12461	0.12027	0.05645	0.01998	0.00387	0.00003	0	0	0	0.00002
47	0.22838	0.18908	0.1217	0.03735	0.00417	0.00002	0.00001	0	0	0.00002
48	0.16938	0.22286	0.12975	0.05577	0.01087	0.00003	0.00001	0.00001	0	0.00001
49	0.18319	0.21683	0.13335	0.05037	0.0085	0.00004	0.00001	0	0.00001	0.00001
50	0.04237	0.05339	0.05134	0.05692	0.15105	0.14944	0.12665	0.15485	0.15051	0.14944
51	0.13337	0.08752	0.07646	0.0821	0.16805	0.16805	0.1009	0.08567	0.08008	0.06446
52	0.06775	0.07565	0.07274	0.07431	0.18238	0.16865	0.16392	0.15051	0.14269	0.13576
53	0.06355	0.06897	0.06355	0.06679	0.14944	0.14525	0.1382	0.09566	0.09772	0.0869
54	0.05987	0.05356	0.0542	0.05708	0.10987	0.10643	0.09093	0.08808	0.08738	0.07754
55	0.06132	0.05229	0.05662	0.05618	0.10433	0.09964	0.09424	0.09056	0.08397	0.08297
56	0.1349	0.12753	0.09746	0.0855	0.07108	0.01603	0.00131	0.00013	0.00007	0.00006
57	0.15095	0.1296	0.10064	0.0805	0.07459	0.01649	0.00139	0.00011	0.00002	0.00007
58	0.12008	0.12807	0.10227	0.08018	0.07489	0.0148	0.00137	0.00011	0.00003	0.00006
59	0.15588	0.19439	0.16626	0.15035	0.189	0.0541	0.00576	0.00035	0.00011	0.00011
60	0.15943	0.17681	0.16527	0.13257	0.17681	0.06149	0.00452	0.00021	0.00004	0.00004
61	0.15991	0.21188	0.16583	0.14604	0.17751	0.06441	0.00553	0.000037	0.00003	0.00005
62	0.08395	0.08865	0.05479	0.02774	0.01715	0.00043	0.00001	0.00001	0	0.00001
63	0.08755	0.10522	0.06833	0.03533	0.01082	0.00003	0.00002	0.00002	0.00001	0.00001
64	0.08825	0.10564	0.07429	0.03133	0.00799	0.000003	0.000001	0.00001	0.00001	0.00001
65	0.06138	0.02251	0.05734	0.08059	0.14939	0.07281	0.00568	0.00002	0.00001	0.00001
66	0.07859	0.07612	0.04825	0.07763	0.14545	0.074	0.01036	0.00004	0.00004	0.00005
67	0.05965	0.04315	0.0349	0.07195	0.14957	0.07763	0.017	0.00004	0.00001	0.00004
68	0.05482	0.0525	0.05658	0.05162	0.10886	0.10929	0.10383	0.09222	0.09406	0.0849
69	0.05228	0.05459	0.05746	0.04536	0.10383	0.10011	0.10465	0.04774	0.08034	0.07454

Table 6. (continued)

Column #	Bromide Concentrations Molar concentration from 500 ml media extracts Sections #1-#4 are 1cm sections, #5-#10 are 2 cm sections									
	#1	#2	#3	#4	#5	#6	#7	#8	#9	#10
COL	MOL1	MOL2	MOL3	MOL4	MOL5	MOL6	MOL7	MOL8	MOL9	MOL10
70	0.04718	0.05656	0.05228	0.05166	0.10886	0.10221	0.10383	0.09748	0.09787	0.08661
71	0.05838	0.05634	0.05861	0.05838	0.12948	0.10383	0.11313	0.11224	0.11733	0.10261
72	0.0459	0.05729	0.05916	0.05706	0.1229	0.12142	0.11247	0.10376	0.11293	0.09612
73	0.05264	0.06812	0.06037	0.0594	0.11616	0.116663	0.1076	0.10376	0.10129	0.09158
74	0.0678	0.03489	0.00016	0.00002	0.00002	0.00002	0.00002	0.00001	0.00001	0.00003
75	0.06066	0.06018	0.00804	0.00001	0.00001	0.00001	0.00002	0.00004	0.00003	0.00006
76	0.06312	0.05092	0.00363	0.00002	0.00002	0.00001	0.00003	0.00001	0.00002	0.00002
77	0.06312	0.07226	0.00757	0.00003	0.00003	0.00002	0.00001	0.00001	0.00001	0.00003
78	0.07655	0.07655	0.00421	0.00001	0.00002	0.00003	0.00002	0.00003	0.00002	0.00004
79	0.06462	0.03903	0.00015	0.00001	0.00003	0.00001	0.00001	0.00001	0.00001	0.00005
80	0.11778	0.10064	0.05634	0.01896	0.00337	0.00005	0.00003	0.00003	0.00002	0.00033
81	0.11613	0.10996	0.0639	0.02176	0.00377	0.00006	0.00002	0.00001	0.00001	0.00004
82	0.10306	0.11996	0.07825	0.02889	0.00551	0.00006	0.00004	0.00003	0.00003	0.00003
83	0.09857	0.11803	0.07484	0.02936	0.00678	0.00008	0.00003	0.00003	0.00002	0.00003
84	0.12444	0.1155	0.06011	0.02001	0.0037	0.00007	0.00002	0.00002	0.00002	0.00005
85	0.12324	0.0998	0.05442	0.02152	0.00412	0.00007	0.00002	0.00001	0.00002	0.00004
86	0.17706	0.16879	0.13711	0.09514	0.12129	0.04302	0.00758	0.00042	0.00006	0.00006
87	0.3243	0.3243	0.12825	0.1018	0.13452	0.05442	0.01642	0.00111	0.00011	0.00009
88	0.18486	0.16069	0.11806	0.07785	0.08263	0.02068	0.00151	0.00013	0.00003	0.00007
89	0.19787	0.15562	0.14024	0.07536	0.07357	0.01581	0.00168	0.00013	0.00005	0.00004
90	0.19787	0.16658	0.11901	0.08263	0.07812	0.01748	0.00206	0.00018	0.00008	0.00012
91	0.17689	0.17831	0.17132	0.09023	0.086	0.02019	0.0026	0.00024	0.00007	0.00006

Table 7. Wet media weights.

Column #	Media Weights Wet [g] by sections [g]									
COL	#1 WET1	#2 WET2	#3 WET3	#4 WET4	#5 WET5	#6 WET6	#7 WET7	#8 WET8	#9 WET9	#10 WET10
2	5.3	10.18	11.76	14.46	29.51	29.21	26.77	29.81	29.17	27.12
3	7.66	13.26	10.36	15.04	28.83	29.49	31.06	30.5	31.65	26.32
4	6.07	11.97	9.79	14.7	30	30.23	28.75	30.1	30.47	28.48
5	14.68	15.53	14.39	15.5	28.68	30.99	29.39	30.01	30.58	28.54
6	15.5	14.73	13.95	15.51	28.01	30.09	30.83	30.67	30.89	26.59
7	15.91	17.15	12.99	15.2	30.86	30.96	31.17	29.52	32.43	28.65
8	24.18	32.33	27.72	27.37	54.06	51.87	51.45	52.85	52.97	47.2
9	27.15	29.65	29.52	26.56	54.3	55.18	54.37	54.43	55.41	47.83
10	27.78	31.88	27.66	26.92	53.51	53.38	53.45	52.32	54.12	49.51
11	25.09	30.64	31.79	24.75	54.5	55.66	55.52	54.5	58.36	51.31
12	22.19	29.54	27.28	27.22	55.05	54.68	54.35	55.99	52.18	49.86
13	23.27	30.3	27.3	27.97	51.93	53.19	54.9	53.14	53.74	51.86
14	21.09	39.65	35.975	35.975	63.93	63.94	67.41	78.63	76.72	65.38
15	25.53	39.36	35.54	36.35	71.59	70.88	69.31	69.99	72.22	63
16	33.72	36.42	36.89	38.95	74.5	68.03	68.12	69.62	69.39	64.18
17	25.39	36.11	41.85	34.48	72.67	70.45	73.23	71.5	69.41	64.54
18	33.71	34.57	40.26	33.82	69.72	67.44	72.23	70.03	73.62	67.12
19	26.11	41.7	35.99	39.61	68.71	68.68	69.84	74.69	79.54	68.87
20	8.95	18.46	16.49	15.69	36.14	42.15	42.85	41.5	33.82	16.74
21	12.19	17.1	18.11	16.18	40.91	42.94	43.42	39.52	29.74	16.55
22	15.1	14.88	18.49	16.14	39.5	43.16	43.5	38.47	28.46	16.94
23	21.35	30.04	28.17	26.2	48.44	32.03	21.14	19.79	21.1	23.8
24	18.88	28.93	26.27	27.14	47.4	31.36	22.14	20.63	24.06	26.01
25	17.09	26.73	27.59	27.69	46.69	35.42	20.36	19.46	23.77	23.33
26	21.88	25.35	40.64	31.9	65.07	64.96	58.84	55.68	54.1	50.42
27	24.77	28.36	33.31	29.66	62.29	61.35	63.27	60.69	58.92	50.75
28	25.74	34.21	32.82	32.79	62.9	56.75	55.76	56.41	56.41	49.76
29	25.49	31.75	32.12	28.35	60.31	58.22	56.68	57.44	56.6	48.88
30	28.03	31.49	32.88	30.84	61.92	58.46	57.73	55.94	54.48	49.22
31	27.29	30.93	30.47	33.34	61.75	57.68	56.28	55.79	53.98	52.8
32	18.13	37.25	36.87	37.24	70.79	78.68	79.35	78.12	78.18	67.06
33	29.98	36.63	33.98	42.24	71.99	79.45	77.83	77	75.34	67.75
34	25.37	38.65	38.38	40.36	72.69	75.17	74.47	72.42	71.24	67.42
35	30.84	41.53	36.91	39.1	68.82	75.18	71.1	78.11	73.9	67.8
36	27.95	36.6	39.4	31.46	82.31	77.89	76.52	78.59	78.78	68.31
37	31.77	45.36	40.05	37.87	75.08	73.33	71.53	73.46	68.55	67.7
38	5.01	11.84	12.95	11.15	31.46	31.85	32.04	32.41	30.95	28.55
39	7.36	11.22	12.58	13.84	32.06	31.96	30.97	30.94	31.2	29.46
40	7.49	12.51	12.49	14.74	32.98	34.65	34.37	33.81	34.61	30.97
41	17.96	24.53	14.79	14.75	33.47	32.91	33.2	33.4	33.72	29.42
42	18.79	20.78	11.91	15.92	31.15	32.25	32.86	32.07	32.82	31.25
43	16.92	27.17	13.19	15.96	31.86	33.63	33.91	33.51	32.52	32.38
44	18.5	33.19	27.56	26.97	49.15	47.69	48.48	47.56	46.98	44.1
45	25.82	29.35	27.35	28.15	53.7	53.23	53.63	51.68	50.97	46.55
46	25.57	31.73	26.98	25.59	51.88	53.18	52.11	54.83	54.31	47.84
47	31.9	32.27	31.69	28.79	51.66	54.24	53.09	52.94	54.48	48.95
48	22.4	32.92	30.15	26.95	52.23	49.41	48.41	50.89	50.97	47.69
49	23.71	34.14	30.78	28	51.02	52.7	51.8	51.73	53.3	48.22
50	33.13	42.14	38.36	41.55	82.85	82.69	86.31	85.26	85.56	86.02
51	40.06	41.4	37.47	42.97	77.64	84.99	83.12	79.66	81.17	74.54
52	35.81	40.29	40.41	43.42	88.31	87.85	88.12	86.25	85.01	82.1
53	36.81	41.4	40.27	42.31	84.24	87.46	89.24	84.01	89.34	78.95
54	40.62	38.91	38.26	41.57	82.84	88.73	82.1	83.44	88.07	79.45
55	43.48	37.8	43.4	43.39	85.29	87.72	87.81	88.92	84.26	85.86
56	29.07	31.63	30.07	32.52	53.26	56.82	51.32	53.71	54.7	50.24
57	32.36	32.76	31.16	31.22	56.28	56.9	57.81	55.18	55.88	51.06
58	26.35	31.1	30.64	31.41	58.71	51.46	55.85	56.19	55.9	52.76
59	26.88	34.99	33.13	33.3	63.63	56.51	55.88	56.26	57.17	53.01
60	26.8	31.91	33.54	32.11	62.37	56.91	50.82	53.42	54.57	51.07
61	27.18	36.14	32.72	33.34	58.61	56.27	51.95	53.8	56.83	49.65
62	20.56	24.61	21.54	17.59	32.25	31.67	33.23	34.14	32.96	31.52
63	17.16	24.53	20.66	17.05	28.02	32.45	34.25	35.32	34.55	32.11
64	19.37	25.86	23.81	16.02	27.35	32.87	33.72	34.36	34.98	30.92
65	11.83	12.28	16.88	20.78	45.94	39.7	32.97	33.25	33.9	32.19
66	11.26	16.39	14.12	18.5	42.73	38.84	33.63	32.85	34.26	31.06
67	10.62	12.75	14.45	19.48	41.43	42.18	33.76	33.49	35.05	29.6
68	37.48	37.22	40.59	38.87	83.36	86.31	86.64	87.14	87.59	81.41
69	39.26	44.25	41.44	35.76	84	88.17	87.68	88.97	82.58	76.94

Table 7. (continued)

Column #	Media Weights Wet [g] by sections [g]									
COL	#1 WET1	#2 WET2	#3 WET3	#4 WET4	#5 WET5	#6 WET6	#7 WET7	#8 WET8	#9 WET9	#10 WET10
70	37.38	45.13	41.72	43.16	89.4	86.87	88.32	87.95	89.36	80.42
71	41.18	40.16	42.64	40.97	88.82	80.68	87.31	88.47	84.57	76.54
72	32.32	41.76	41.07	41.94	87.23	85.33	81.88	81.99	87.32	77.36
73	36.72	42.82	41.05	43.04	82.56	86.94	85.38	87.7	84.59	78.74
74	16.26	15.51	11.71	15.17	32.37	33.4	32.6	34.34	34.8	30.73
75	14.15	19.29	12.79	14.84	33.46	32.94	31.88	32.39	33.53	31.06
76	14.89	19.11	11.88	13.95	30.46	32.34	32.11	33.65	32.8	30.89
77	15.46	22.06	11.25	13.56	31.21	33.08	32.56	33.68	32.88	30.18
78	17.23	23.39	11.27	14.39	31.76	33.2	31.91	32.13	31.93	30.47
79	15.51	16.3	10.37	14.61	31.6	32.89	32.33	32.07	31.07	29.1
80	27.18	30.83	27.46	25.81	53.81	50.78	51.97	50.79	49.4	49.29
81	24.24	27.87	27.31	26.01	50.77	50.95	53.91	52.08	52.7	48.92
82	19.8	30.09	29.87	28.45	51.47	49.79	52.04	51.82	52.77	46.97
83	19.49	30.34	29.59	26.9	52.86	53.27	50.85	51.55	52.96	49.94
84	25.58	29.81	29.16	26.24	52.15	54.37	52.13	53.68	53.95	47.34
85	26.79	28.22	27.04	27.72	53.42	54.26	53.16	54.81	52.15	47.61
86	36.68	40.18	43.6	37.29	78.75	76.97	77.46	74.22	79.06	81.76
87	37.63	37.63	38.08	38.13	81.34	73.03	80.3	77.72	80.54	78.21
88	38.73	40.76	39.98	37.74	75.86	75.17	72.72	77.35	76.22	82.69
89	48.59	43.34	50.39	36.49	73.36	72.85	74.64	72.62	72.91	63.63
90	48.54	46.65	42.56	42.01	80.14	77.79	75.21	76.66	74.9	69.98
91	43.93	46.34	48.6	42.69	79.28	77.97	75.04	72.34	77.01	68.85

Table 8. Dry filter paper weights.

Column #	Dry Filter Weights by Section All weights in grams									
COL	#1 FLTR1	#2 FLTR2	#3 FLTR3	#4 FLTR4	#5 FLTR5	#6 FLTR6	#7 FLTR7	#8 FLTR8	#9 FLTR9	#10 FLTR10
2	2.48	2.45	2.43	2.35	2.42	2.48	2.4	2.41	2.37	2.43
3	2.46	2.42	2.34	2.36	2.39	2.35	2.36	2.4	2.4	2.39
4	2.26	2.39	2.41	2.51	2.39	2.3	2.4	2.37	2.47	2.43
5	2.29	2.39	2.32	2.42	2.39	2.33	2.41	2.4	2.42	2.38
6	2.41	2.41	2.48	2.42	2.38	2.36	2.47	2.46	2.47	2.35
7	2.48	2.39	2.44	2.52	2.39	2.45	2.4	2.42	2.47	2.31
8	2.4	2.39	2.4	2.33	2.41	2.38	2.42	2.35	2.36	2.19
9	2.31	2.21	2.4	2.34	2.26	2.23	2.33	2.4	2.23	2.44
10	2.36	2.1	2.34	2.35	2.44	2.1	2.4	2.37	2.43	2.44
11	2.06	2.3	2.34	2.13	2.42	2.25	2.24	2.38	2.43	2.31
12	2.08	2.26	2.32	2.4	2.39	2.41	2.35	2.36	2.43	2.44
13	2.49	2.01	2.4	2.32	2.36	2.36	2.37	2.3	2.41	2.31
14	2.32	2.31	1.15	1.15	2.32	2.33	2.31	2.31	2.34	2.39
15	2.36	2.32	2.42	2.4	2.3	2.34	2.4	2.41	2.37	2.4
16	2.35	2.43	2.37	2.35	2.32	2.35	2.33	2.36	2.33	2.35
17	2.39	2.32	2.42	2.43	2.4	2.38	2.35	2.37	2.33	2.35
18	2.36	2.37	2.32	2.41	2.37	2.32	2.36	2.36	2.4	2.34
19	2.38	2.35	2.34	2.43	2.4	2.33	2.31	2.38	2.41	2.38
20	2.33	2.43	2.42	2.35	2.31	2.35	2.37	2.43	2.35	2.35
21	2.3	2.4	2.38	2.37	2.37	2.32	2.41	2.39	2.34	2.34
22	2.37	2.44	2.42	2.33	2.31	2.35	2.38	2.39	2.26	2.32
23	2.39	2.36	2.38	2.33	2.35	2.41	2.44	2.42	2.33	2.34
24	2.39	2.4	2.4	2.34	2.34	2.36	2.41	2.41	2.29	2.39
25	2.37	2.31	2.34	2.31	2.43	2.39	2.34	2.33	2.35	2.39
26	2.4	2.37	2.29	2.41	2.38	2.36	2.33	2.24	2.37	2.39
27	2.36	2.34	2.34	2.38	2.42	2.43	2.34	2.26	2.39	2.39
28	2.38	2.33	2.33	2.36	2.41	2.42	2.33	2.31	2.35	2.34
29	2.37	2.34	2.3	2.37	2.37	2.4	2.3	2.29	2.34	2.4
30	2.43	2.27	2.28	2.35	2.4	2.42	2.3	2.36	2.37	2.42
31	2.43	2.28	2.29	2.35	2.42	2.42	2.27	2.34	2.36	2.45
32	2.38	2.35	2.35	2.41	2.46	2.43	2.33	2.32	2.42	2.43
33	2.42	2.34	2.31	2.4	2.38	2.35	2.38	2.27	2.34	2.41
34	2.41	2.31	2.32	2.39	2.44	2.43	2.36	2.33	2.39	2.46
35	2.45	2.41	2.35	2.46	2.42	2.33	2.35	2.3	2.39	2.41
36	2.33	2.32	2.29	2.39	2.45	2.34	2.37	2.37	2.41	2.44
37	2.37	2.42	2.35	2.42	2.45	2.38	2.33	2.35	2.29	2.33
38	2.38	2.36	2.41	2.33	2.35	2.4	2.4	2.4	2.38	2.36
39	2.36	2.35	2.4	2.36	2.32	2.35	2.33	2.4	2.4	2.35
40	2.3	2.37	2.37	2.38	2.38	2.37	2.35	2.38	2.34	2.41
41	2.37	2.29	2.32	2.36	2.38	2.37	2.33	2.25	2.4	2.41
42	2.42	2.33	2.44	2.37	2.31	2.45	2.43	2.33	2.35	2.36
43	2.43	2.43	2.35	2.36	2.34	2.42	2.41	2.41	2.43	2.36
44	2.4	2.44	2.39	2.38	2.37	2.41	2.4	2.43	2.38	2.35
45	2.4	2.41	2.36	2.37	2.36	2.39	2.45	2.38	2.39	2.34
46	2.38	2.35	2.3	2.38	2.33	2.42	2.41	2.38	2.35	2.34
47	2.39	2.41	2.37	2.36	2.36	2.37	2.39	2.33	2.33	2.41
48	2.39	2.24	2.4	2.36	2.35	2.37	2.4	2.36	2.41	2.37
49	2.31	2.39	2.35	2.35	2.31	2.32	2.41	2.36	2.35	2.33
50	2.38	2.4	2.38	2.34	2.33	2.36	2.4	2.4	2.34	2.32
51	2.36	2.39	2.38	2.32	2.35	2.3	2.36	2.45	2.33	2.32
52	2.26	2.39	2.43	2.31	2.37	2.28	2.37	2.4	2.29	2.35
53	2.28	2.33	2.41	2.34	2.33	2.31	2.31	2.39	2.27	2.34
54	2.28	2.34	2.39	2.32	2.33	2.27	2.33	2.34	2.36	2.35
55	2.32	2.33	2.36	2.29	2.31	2.26	2.31	2.31	2.32	2.36
56	2.45	2.47	2.39	2.39	2.35	2.3	2.3	2.4	2.46	2.4
57	2.33	2.35	2.41	2.42	2.37	2.33	2.32	2.4	2.38	2.38
58	2.34	2.32	2.42	2.39	2.37	2.36	2.3	2.42	2.42	2.39
59	2.28	2.33	2.33	2.37	2.4	2.28	2.36	2.43	2.39	2.36
60	2.28	2.36	2.36	2.41	2.36	2.27	2.36	2.39	2.35	2.39
61	2.34	2.37	2.41	2.41	2.41	2.34	2.35	2.37	2.4	2.38
62	2.4	2.35	2.36	2.37	2.35	2.37	2.35	2.31	2.39	2.38
63	2.3	2.35	2.33	2.44	2.41	2.34	2.36	2.32	2.43	2.48
64	2.37	2.34	2.32	2.45	2.4	2.35	2.33	2.43	2.44	2.41
65	2.36	2.34	2.36	2.44	2.38	2.4	2.26	2.37	2.41	2.45
66	2.36	2.29	2.33	2.46	2.37	2.37	2.4	2.32	2.43	2.45
67	2.38	2.35	2.29	2.43	2.42	2.42	2.36	2.37	2.42	2.43
68	2.38	2.39	2.31	2.4	2.37	2.43	2.34	2.31	2.42	2.44
69	2.37	2.28	2.33	2.42	2.33	2.34	2.24	2.32	2.39	2.4

Table 8. (continued)

Column #

Dry Filter Weights by Section
All weights in grams

COL	#1 FLTR1	#2 FLTR2	#3 FLTR3	#4 FLTR4	#5 FLTR5	#6 FLTR6	#7 FLTR7	#8 FLTR8	#9 FLTR9	#10 FLTR10
70	2.31	2.28	2.38	2.38	2.42	2.41	2.36	2.4	2.43	2.37
71	2.41	2.38	2.39	2.42	2.38	2.36	2.36	2.35	2.31	2.39
72	2.29	2.32	2.32	2.3	2.38	2.34	2.38	2.32	2.31	2.4
73	2.35	2.33	2.36	2.36	2.36	2.34	2.33	2.32	2.47	2.36
74	2.34	2.37	2.32	2.29	2.46	2.31	2.39	2.32	2.35	2.38
75	2.35	2.32	2.32	2.34	2.42	2.33	2.33	2.29	2.33	2.39
76	2.38	2.39	2.35	2.41	2.4	2.34	2.3	2.32	2.41	2.42
77	2.37	2.35	2.32	2.38	2.39	2.38	2.37	2.4	2.44	2.45
78	2.35	2.35	2.35	2.38	2.44	2.43	2.35	2.32	2.39	2.39
79	2.37	2.33	2.34	2.4	2.4	2.45	2.32	2.33	2.34	2.41
80	2.43	2.31	2.36	2.33	2.38	2.42	2.31	2.29	2.34	2.41
81	2.44	2.31	2.31	2.39	2.41	2.39	2.33	2.25	2.34	2.4
82	2.4	2.34	2.24	2.35	2.34	2.36	2.35	2.36	2.4	2.4
83	2.38	2.34	2.29	2.31	2.41	2.39	2.31	2.32	2.35	2.42
84	2.44	2.3	2.32	2.33	2.37	2.39	2.35	2.37	2.39	2.38
85	2.39	2.26	2.34	2.37	2.42	2.42	2.34	2.3	2.34	2.43
86	2.42	2.35	2.35	2.37	2.4	2.4	2.31	2.31	2.39	2.39
87	1.22	1.23	2.33	2.35	2.4	2.41	2.4	2.32	2.36	2.39
88	2.47	2.42	2.42	2.39	2.32	2.32	2.46	2.47	2.43	2.34
89	2.34	2.44	2.4	2.34	2.34	2.39	2.36	2.43	2.38	2.33
90	2.36	2.46	2.44	2.45	2.37	2.35	2.42	2.45	2.42	2.35
91	2.35	2.45	2.43	2.37	2.36	2.28	2.43	2.41	2.35	2.35

Table 9. Media and filter paper oven dry weights.

Column #	Media & Filter Paper Weights Oven Dry [g] by Section									
	#1	#2	#3	#4	#5	#6	#7	#8	#9	#10
COL	MDFLTR1	MDFLTR2	MDFLTR3	MDFLTR4	MDFLTR5	MDFLTR6	MDFLTR7	MDFLTR8	MDFLTR9	MDFLTR10
2	5.75	10.75	10.51	9.75	17.63	17.49	16.1	17.73	17.16	16.3
3	7.12	13.54	8.31	10.22	17.16	17.62	17.66	17.64	18.17	15.54
4	6.07	12.4	8.75	10.21	17.8	17.74	16.84	17.45	17.7	16.77
5	7.59	10.56	10.27	10.26	16.8	17.97	17.3	17.36	17.45	16.54
6	7.7	9.68	10.34	10.37	16.68	17.63	17.94	17.85	17.91	15.92
7	8.05	10.8	9.57	10.21	17.96	17.9	17.92	17.02	18.57	16.47
8	7.98	10.43	10.14	10.25	17.83	17.2	17.09	17.51	17.46	15.82
9	8.8	9.95	10.62	10.29	18.32	18.57	18.22	18.36	18.61	16.43
10	8.96	10.68	10.32	10.28	18.17	18.04	18.06	17.62	18.24	16.92
11	8.56	10.32	11.2	9.48	18.2	18.51	18.4	18.19	19.37	17.3
12	7.83	9.98	9.9	10.24	18.13	18.13	17.94	18.43	17.45	16.75
13	8.12	10.31	10.02	10.34	17	17.46	17.79	17.2	17.75	17.14
14	6.3	9.76	8.115	8.115	15.69	16.15	16.87	19.04	18.59	16.25
15	6.9	9.88	9.43	9.61	17.02	17.21	17.08	17.26	17.63	15.52
16	8.82	9.37	9.74	10.21	17.76	16.91	16.89	17.2	16.9	15.81
17	7.3	9.44	10.89	9.48	17.81	17.47	18.19	17.73	17.14	16.18
18	9.07	9.22	10.32	9.14	16.87	16.67	17.77	17.17	17.93	16.48
19	7.59	10.54	9.7	10.34	16.35	16.43	16.94	17.96	18.79	16.65
20	5.49	10.1	10.26	9.62	16.7	17.56	17.7	18	18.09	16.04
21	6.7	9.6	11.04	10.06	18	17.14	17.76	18.56	18.02	16.76
22	7.91	9.35	10.87	9.53	17.55	17.23	17.38	17.27	17.43	16.51
23	8.14	10.7	10.33	9.75	18.45	17.35	17.03	18.4	16.37	16.97
24	7.39	10.19	9.86	10.14	17.85	17.96	17.37	17.92	17.1	16.75
25	6.94	9.51	9.89	10.29	18.18	18.2	17.41	17.9	17.55	15.74
26	7.93	8.78	12.66	10.44	18.9	19.21	17.82	17.01	17.07	16.2
27	8.6	9.31	10.71	10.01	18.78	18.24	19.03	18.32	18.16	16.03
28	8.99	10.91	10.82	10.72	19.02	17.15	17.12	17.57	18.05	16.29
29	8.79	10.17	10.33	9.45	17.73	17.23	17.15	17.63	17.69	15.58
30	9.5	10.15	10.49	10.11	18.2	17.55	17.57	17.34	17.03	15.72
31	9.42	10.16	10.09	12.2	17.46	17.56	17.32	17.35	16.96	16.8
32	6.02	9.67	9.69	9.72	16.16	17.8	17.69	16.56	17.45	15.43
33	8.37	9.52	8.9	10.49	16	17.46	17.1	16.79	16.94	15.53
34	7.63	10.02	9.87	10.33	16.73	16.98	16.89	16.32	16.1	15.4
35	8.39	10.5	9.53	9.99	15.78	16.79	16.18	17.52	16.58	15.23
36	7.54	9.19	9.68	8.25	17.72	16.77	16.4	16.78	16.51	14.63
37	8.5	11.25	10.1	9.72	17.19	16.62	16.35	16.55	15.53	14.88
38	4.78	10.74	13.29	9.17	18.7	17.51	18.58	18.7	17.83	16.56
39	6.16	10.55	12.59	10.09	18.66	18.15	17.73	17.89	17.89	16.76
40	6.18	12	12.37	10.54	19.18	19.7	19.31	18.67	18.79	17.3
41	8.18	11.13	11.2	10.25	19.27	18.83	18.97	19.02	19.26	17.07
42	8.68	11.13	10.73	10.77	18.21	18.62	18.68	18.16	18.76	17.9
43	7.97	12.26	10.69	10.87	18.43	19.21	19.28	19.04	18.59	18.35
44	6.76	10.49	9.48	9.78	15.94	15.64	15.87	15.65	15.38	14.65
45	8.39	9.61	9.5	10.03	17.31	17.25	17.37	16.76	16.56	15.28
46	8.35	10.17	9.32	9.35	16.73	17.25	16.86	17.58	17.52	15.72
47	9.49	10	10.2	10.22	16.96	17.72	17.27	17.1	17.81	16.36
48	7.32	9.69	9.87	9.4	17.02	16.27	16.06	16.72	16.83	15.88
49	7.5	10.27	9.98	9.98	16.76	17.38	16.99	17.07	17.35	15.95
50	8.57	10.29	9.6	10.07	17.75	17.69	18.08	17.67	17.47	17.67
51	9.88	10.07	9.38	10.32	16.84	18.02	18.17	17.68	17.79	16.69
52	8.9	9.87	9.91	10.47	18.63	18.67	18.64	18.02	17.54	17.06
53	9.34	10.17	10	10.37	18.08	18.43	18.72	17.85	18.62	16.67
54	10.1	9.82	9.61	10.13	17.9	18.89	17.48	17.8	18.48	16.66
55	10.62	9.43	10.49	10.28	18.28	18.68	18.63	18.68	17.56	17.95
56	9.26	9.98	9.89	10.82	16.86	18.49	17.13	17.84	18.24	17.03
57	9.96	10.23	10.22	10.49	17.67	18.48	18.83	18.29	18.47	17.08
58	8.5	9.77	10.01	10.45	18.35	16.93	18.22	18.34	18.44	17.45
59	8.2	10.16	9.78	10.22	18.43	17.74	18.23	18.42	18.58	17.37
60	8.32	9.53	10.02	9.99	18.16	17.84	16.71	17.66	17.92	16.94
61	8.59	10.58	10.25	10.56	17.27	17.69	17.08	17.56	18.57	16.48
62	8.94	10.79	10.96	11.21	20.11	19.3	19.17	19.61	19.4	18.79
63	7.65	10.33	10.24	11.11	19.88	19.75	20.24	20.55	20.14	18.62
64	8.46	10.9	11.08	10.64	19.58	19.93	19.99	20.21	20.31	18.06
65	7.67	10.85	10.74	10.77	20.14	19.9	19.91	19.62	19.82	18.83
66	6.87	11.4	10.67	10.9	19.73	19.72	20.25	19.59	20.31	18.41
67	6.8	10.21	11.7	11.1	19.07	20.43	19.52	20.05	20.73	17.97
68	9.33	9.23	9.77	9.55	18.09	18.47	18.49	18.57	18.58	17.51
69	9.88	10.63	10.13	9.13	18.18	19	18.82	19.1	17.89	16.89

Table 9. (continued)

Column #	Media & Filter Paper Weights Oven Dry [g] by Section									
	#1	#2	#3	#4	#5	#6	#7	#8	#9	#10
COL	MDFLTR1	MDFLTR2	MDFLTR3	MDFLTR4	MDFLTR5	MDFLTR6	MDFLTR7	MDFLTR8	MDFLTR9	MDFLTR10
70	9.37	10.84	10.15	10.63	19.51	18.82	18.98	18.59	18.55	17.14
71	10.22	9.87	10.39	9.99	19.05	17.48	18.48	18.5	17.69	16.17
72	8.6	10.31	10.07	10.18	18.83	18.05	17.68	17.79	18.53	16.81
73	9.27	10.16	9.97	10.31	17.63	18.55	18.35	18.68	17.95	17.03
74	8.21	10.76	10.36	10.34	19.24	19.75	19.23	20.1	20.37	18.23
75	7.26	10.55	11.1	10.67	20.02	19.53	18.83	19.01	19.8	18.56
76	7.61	11.28	10.64	9.92	18.33	19.09	18.85	19.72	19.16	18.2
77	7.43	11.21	10.16	10.02	18.8	19.48	19.07	19.65	19.5	18.14
78	8.15	11.83	10.58	10.43	19.07	19.55	18.58	18.9	19.07	18.41
79	7.69	10.78	10.02	10.44	19.01	19.49	19.01	18.99	18.56	18.29
80	9.01	10.15	9.65	9.65	18.08	17.18	17.41	17.21	16.76	16.69
81	8.22	9.3	9.53	9.63	17.13	17.25	17.94	17.29	17.52	16.44
82	7.09	9.78	10.07	10.26	17.15	16.76	17.41	17.26	17.59	15.9
83	7.04	9.74	10.03	9.97	17.61	17.58	17.11	17.32	17.87	17.14
84	8.49	9.74	10.07	9.64	17.38	18.28	17.51	18.02	18	16.35
85	8.71	9.22	9.44	10.07	17.96	18.33	17.84	18.32	17.58	16.49
86	9.11	9.7	10.36	9.34	17.61	17.44	17.52	16.66	17.06	17.03
87	8.2	8.21	9.45	9.59	18.2	16.58	18.08	17.38	17.42	16.55
88	9.37	9.8	9.81	9.62	17.16	17.44	16.96	17.51	16.81	17.4
89	10.02	9.41	11.04	8.84	16.17	16.78	17.5	17.24	17.43	15.68
90	9.88	9.96	9.61	9.84	17.39	17.59	17.58	17.96	17.81	16.87
91	9.05	9.67	10.39	9.74	16.84	17.15	17.54	17.14	18.13	16.28

Table 10. Bromide concentrations grams bromide per gram dry media.

Column #	Bromide Concentrations by Section Grams Br-/ Gram Dry Media									
COL	#1 CONC1	#2 CONC2	#3 CONC3	#4 CONC4	#5 CONC5	#6 CONC6	#7 CONC7	#8 CONC8	#9 CONC9	#10 CONC10
2	0.201	0.038	0.000	0.000	0.000	0.000	0.000	0.000	0.000	0.000
3	0.209	0.009	0.000	0.000	0.000	0.000	0.000	0.000	0.000	0.000
4	0.176	0.017	0.000	0.000	0.000	0.000	0.000	0.000	0.000	0.000
5	0.478	0.166	0.003	0.000	0.000	0.000	0.000	0.000	0.000	0.000
6	0.464	0.186	0.002	0.000	0.000	0.000	0.000	0.000	0.000	0.001
7	0.458	0.214	0.003	0.000	0.000	0.000	0.000	0.000	0.000	0.000
8	1.149	0.733	0.191	0.012	0.000	0.000	0.000	0.000	0.000	0.000
9	1.211	0.689	0.205	0.012	0.000	0.000	0.000	0.000	0.000	0.000
10	1.149	0.624	0.171	0.000	0.000	0.000	0.000	0.000	0.000	0.000
11	0.656	0.391	0.090	0.005	0.000	0.000	0.000	0.000	0.000	0.000
12	0.668	0.430	0.133	0.012	0.000	0.000	0.000	0.000	0.000	0.000
13	0.658	0.370	0.125	0.013	0.000	0.000	0.000	0.000	0.000	0.000
14	0.930	0.825	0.514	0.514	0.245	0.043	0.001	0.000	0.000	0.000
15	1.177	0.833	0.682	0.543	0.305	0.091	0.007	0.000	0.000	0.000
16	0.970	0.825	0.670	0.559	0.321	0.086	0.005	0.000	0.000	0.000
17	0.760	0.625	0.507	0.406	0.235	0.084	0.008	0.000	0.000	0.000
18	0.563	0.526	0.429	0.397	0.231	0.081	0.009	0.000	0.000	0.000
19	0.587	0.541	0.406	0.385	0.278	0.150	0.040	0.003	0.000	0.000
20	0.513	0.404	0.304	0.313	0.424	0.491	0.477	0.434	0.269	0.030
21	0.507	0.385	0.302	0.300	0.438	0.520	0.467	0.343	0.207	0.006
22	0.404	0.406	0.332	0.342	0.401	0.474	0.445	0.359	0.179	0.003
23	0.736	0.688	0.659	0.624	0.472	0.221	0.054	0.000	0.000	0.000
24	0.792	0.728	0.664	0.652	0.475	0.203	0.055	0.009	0.000	0.000
25	0.761	0.710	0.646	0.609	0.430	0.242	0.036	0.000	0.000	0.000
26	0.499	0.505	0.467	0.478	0.441	0.372	0.279	0.215	0.115	0.088
27	0.515	0.525	0.505	0.467	0.484	0.375	0.289	0.211	0.138	0.100
28	0.520	0.540	0.493	0.491	0.397	0.381	0.281	0.193	0.112	0.067
29	0.494	0.516	0.494	0.474	0.411	0.345	0.251	0.172	0.099	0.064
30	0.508	0.510	0.497	0.470	0.433	0.342	0.247	0.164	0.096	0.059
31	0.492	0.492	0.466	0.447	0.376	0.344	0.253	0.171	0.107	0.067
32	0.367	0.376	0.366	0.357	0.038	0.355	0.391	0.220	0.352	0.343
33	0.360	0.368	0.373	0.365	0.369	0.374	0.376	0.371	0.347	0.361
34	0.335	0.359	0.365	0.361	0.358	0.364	0.346	0.351	0.360	0.357
35	0.333	0.325	0.329	0.329	0.323	0.321	0.311	0.310	0.321	0.326
36	0.325	0.321	0.318	0.329	0.322	0.318	0.324	0.311	0.325	0.336
37	0.308	0.301	0.305	0.314	0.294	0.290	0.289	0.289	0.293	0.308
38	0.327	0.090	0.000	0.000	0.000	0.000	0.000	0.000	0.000	0.000
39	0.251	0.063	0.005	0.000	0.000	0.000	0.000	0.000	0.000	0.000
40	0.240	0.045	0.003	0.000	0.000	0.000	0.000	0.000	0.000	0.000
41	0.429	0.301	0.059	0.000	0.000	0.000	0.000	0.000	0.000	0.000
42	0.516	0.264	0.012	0.000	0.000	0.000	0.000	0.000	0.000	0.000
43	0.498	0.369	0.053	0.000	0.000	0.000	0.000	0.000	0.000	0.000
44	0.925	0.680	0.358	0.128	0.011	0.001	0.000	0.000	0.000	0.000
45	0.875	0.614	0.337	0.121	0.009	0.000	0.000	0.000	0.000	0.000
46	0.834	0.614	0.321	0.115	0.011	0.000	0.000	0.000	0.000	0.000
47	1.285	0.995	0.621	0.190	0.011	0.000	0.000	0.000	0.000	0.000
48	1.373	1.195	0.694	0.316	0.030	0.000	0.000	0.000	0.000	0.000
49	1.410	1.099	0.698	0.264	0.024	0.000	0.000	0.000	0.000	0.000
50	0.273	0.270	0.284	0.294	0.391	0.389	0.323	0.405	0.397	0.389
51	0.709	0.455	0.436	0.410	0.463	0.427	0.255	0.225	0.207	0.179
52	0.408	0.404	0.389	0.364	0.448	0.411	0.403	0.385	0.374	0.369
53	0.360	0.351	0.335	0.332	0.379	0.360	0.336	0.247	0.239	0.242
54	0.306	0.286	0.300	0.292	0.282	0.256	0.240	0.228	0.217	0.216
55	0.295	0.294	0.278	0.281	0.261	0.242	0.231	0.221	0.220	0.213
56	0.791	0.678	0.519	0.405	0.196	0.040	0.004	0.000	0.000	0.000
57	0.790	0.657	0.515	0.399	0.195	0.041	0.003	0.000	0.000	0.000
58	0.779	0.687	0.538	0.397	0.187	0.041	0.003	0.000	0.000	0.000
59	1.052	0.992	0.892	0.765	0.471	0.140	0.015	0.001	0.000	0.000
60	1.055	0.985	0.862	0.699	0.447	0.158	0.013	0.001	0.000	0.000
61	1.022	1.031	0.845	0.716	0.477	0.168	0.015	0.000	0.000	0.000
62	0.513	0.420	0.255	0.125	0.039	0.001	0.000	0.000	0.000	0.000
63	0.654	0.527	0.345	0.163	0.025	0.000	0.000	0.000	0.000	0.000
64	0.579	0.493	0.339	0.153	0.019	0.000	0.000	0.000	0.000	0.000
65	0.462	0.106	0.273	0.387	0.336	0.166	0.013	0.000	0.000	0.000
66	0.696	0.334	0.231	0.367	0.335	0.170	0.023	0.000	0.000	0.000
67	0.539	0.219	0.148	0.332	0.359	0.172	0.040	0.000	0.000	0.000
68	0.315	0.307	0.303	0.288	0.277	0.272	0.257	0.227	0.233	0.225
69	0.278	0.261	0.294	0.270	0.262	0.240	0.252	0.114	0.207	0.206

Table 10. (continued)

Bromide Concentrations by Section
Grams Br-/ Gram Dry Media

Column #	#1	#2	#3	#4	#5	#6	#7	#8	#9	#10
COL	CONC1	CONC2	CONC3	CONC4	CONC5	CONC6	CONC7	CONC8	CONC9	CONC10
70	0.267	0.264	0.269	0.250	0.254	0.249	0.250	0.241	0.243	0.234
71	0.299	0.301	0.293	0.308	0.310	0.274	0.280	0.278	0.305	0.297
72	0.291	0.286	0.305	0.289	0.298	0.309	0.294	0.268	0.278	0.266
73	0.304	0.348	0.317	0.299	0.304	0.288	0.268	0.253	0.261	0.249
74	0.461	0.166	0.001	0.000	0.000	0.000	0.000	0.000	0.000	0.000
75	0.494	0.292	0.037	0.000	0.000	0.000	0.000	0.000	0.000	0.000
76	0.482	0.229	0.017	0.000	0.000	0.000	0.000	0.000	0.000	0.000
77	0.498	0.326	0.039	0.000	0.000	0.000	0.000	0.000	0.000	0.000
78	0.527	0.323	0.020	0.000	0.000	0.000	0.000	0.000	0.000	0.000
79	0.485	0.185	0.001	0.000	0.000	0.000	0.000	0.000	0.000	0.000
80	0.715	0.513	0.309	0.103	0.009	0.000	0.000	0.000	0.000	0.001
81	0.803	0.628	0.354	0.120	0.010	0.000	0.000	0.000	0.000	0.000
82	0.878	0.644	0.399	0.146	0.015	0.000	0.000	0.000	0.000	0.000
83	0.845	0.637	0.386	0.153	0.018	0.000	0.000	0.000	0.000	0.000
84	0.822	0.620	0.310	0.109	0.010	0.000	0.000	0.000	0.000	0.000
85	0.779	0.573	0.306	0.112	0.011	0.000	0.000	0.000	0.000	0.000
86	1.057	0.917	0.684	0.545	0.319	0.114	0.020	0.001	0.000	0.000
87	1.856	1.856	0.720	0.562	0.340	0.153	0.042	0.003	0.000	0.000
88	1.070	0.870	0.638	0.430	0.222	0.055	0.004	0.000	0.000	0.000
89	1.029	0.892	0.648	0.463	0.213	0.044	0.004	0.000	0.000	0.000
90	1.051	0.887	0.663	0.447	0.208	0.046	0.005	0.000	0.000	0.000
91	1.055	0.987	0.860	0.489	0.237	0.054	0.007	0.001	0.000	0.000

Table 11. Gravimetric water contents.

Column #	Gravimetric Water Content by Section Grams Water / Gram Dry Media									
COL	#1 GWC1	#2 GWC2	#3 GWC3	#4 GWC4	#5 GWC5	#6 GWC6	#7 GWC7	#8 GWC8	#9 GWC9	#10 GWC10
2	0.42	0.19	0.46	0.95	0.94	0.95	0.95	0.95	0.97	0.96
3	0.43	0.18	0.74	0.91	0.95	0.93	1.03	1.00	1.01	1.00
4	0.42	0.18	0.54	0.91	0.95	0.96	0.99	1.00	1.00	0.99
5	1.29	0.73	0.81	0.98	0.99	0.98	0.97	1.01	1.03	1.02
6	1.47	0.84	0.77	0.95	0.96	0.97	0.99	0.99	1.00	0.96
7	1.40	0.83	0.82	0.98	0.98	1.00	1.01	1.02	1.01	1.02
8	2.18	2.29	2.39	2.44	2.51	2.50	2.51	2.49	2.51	2.46
9	1.97	2.14	2.39	2.33	2.38	2.38	2.42	2.41	2.38	2.42
10	2.06	2.09	2.30	2.39	2.40	2.35	2.41	2.43	2.42	2.42
11	2.20	2.43	2.50	2.36	2.45	2.42	2.44	2.45	2.45	2.42
12	2.19	2.40	2.47	2.46	2.50	2.48	2.49	2.48	2.47	2.48
13	2.48	2.28	2.46	2.47	2.55	2.52	2.56	2.57	2.50	2.50
14	3.37	3.50	3.65	3.65	3.54	3.58	3.63	3.70	3.72	3.72
15	3.45	3.37	3.39	3.50	3.56	3.68	3.71	3.71	3.73	3.80
16	3.24	3.42	3.34	3.40	3.50	3.59	3.67	3.69	3.76	3.77
17	3.41	3.45	3.43	3.48	3.48	3.58	3.62	3.65	3.69	3.67
18	3.46	3.52	3.60	3.63	3.58	3.62	3.68	3.73	3.74	3.75
19	3.42	3.55	3.48	3.62	3.65	3.72	3.73	3.79	3.86	3.83
20	1.32	1.00	0.80	0.85	1.09	1.28	1.32	1.23	0.88	0.19
21	1.26	0.99	0.79	0.80	1.18	1.38	1.36	1.10	0.69	0.14
22	1.32	0.75	0.86	0.90	1.19	1.43	1.46	1.23	0.70	0.19
23	1.98	1.91	1.88	1.91	1.54	0.92	0.40	0.24	0.50	0.63
24	1.98	1.99	1.86	1.83	1.58	0.81	0.43	0.32	0.62	0.81
25	1.98	2.00	2.01	1.86	1.53	1.00	0.31	0.25	0.56	0.75
26	2.46	2.45	2.45	2.49	2.50	2.48	2.52	2.56	2.57	2.56
27	2.46	2.54	2.48	2.42	2.32	2.51	2.50	2.57	2.60	2.62
28	2.37	2.45	2.37	2.43	2.39	2.47	2.49	2.50	2.48	2.50
29	2.48	2.54	2.51	2.53	2.52	2.58	2.57	2.57	2.59	2.64
30	2.46	2.49	2.51	2.50	2.49	2.52	2.53	2.57	2.62	2.64
31	2.41	2.43	2.44	1.94	2.73	2.47	2.49	2.55	2.59	2.61
32	3.61	3.71	3.66	3.74	4.13	3.76	3.78	4.27	3.85	3.82
33	3.68	3.73	3.78	3.86	3.92	3.88	3.91	3.93	3.81	3.80
34	3.53	3.65	3.72	3.72	3.73	3.80	3.78	3.83	3.84	3.85
35	3.86	3.81	3.81	3.86	3.83	3.88	3.83	3.82	3.89	3.96
36	4.04	4.01	4.01	4.04	4.07	4.08	4.13	4.14	4.26	4.27
37	3.88	3.84	3.86	3.87	3.80	3.86	3.81	3.88	3.88	4.09
38	0.76	0.32	0.19	0.63	0.92	1.11	0.98	0.99	1.00	1.01
39	0.69	0.31	0.23	0.79	0.96	1.02	1.01	1.00	1.01	1.04
40	0.69	0.25	0.25	0.81	0.96	1.00	1.03	1.08	1.10	1.08
41	1.66	1.47	0.61	0.87	0.98	1.00	1.00	0.99	1.00	1.01
42	1.49	1.10	0.42	0.90	0.96	0.99	1.02	1.03	1.00	1.01
43	1.56	1.39	0.53	0.88	0.98	1.00	1.01	1.02	1.01	1.02
44	2.32	2.44	2.53	2.52	2.61	2.60	2.60	2.60	2.61	2.59
45	2.44	2.46	2.49	2.55	2.58	2.58	2.59	2.59	2.60	2.60
46	2.45	2.44	2.52	2.56	2.59	2.59	2.61	2.61	2.58	2.58
47	2.21	2.26	2.43	2.47	2.53	2.53	2.57	2.58	2.52	2.51
48	2.17	2.22	2.34	2.51	2.53	2.55	2.54	2.54	2.53	2.53
49	2.16	2.23	2.34	2.41	2.51	2.50	2.55	2.52	2.55	2.54
50	4.08	4.07	4.03	4.08	3.98	4.00	4.18	4.18	4.26	4.21
51	3.62	3.94	3.92	3.96	3.89	3.98	4.00	4.01	4.04	4.01
52	3.99	3.98	4.01	3.96	3.98	3.95	4.01	4.14	4.20	4.21
53	3.85	3.93	3.97	3.94	3.97	4.07	4.10	4.19	4.23	4.27
54	3.89	3.92	4.00	4.03	4.04	4.08	4.18	4.17	4.25	4.34
55	3.94	4.03	4.06	4.15	4.08	4.10	4.15	4.21	4.31	4.29
56	2.48	2.53	2.49	2.45	2.47	2.47	2.46	2.48	2.47	2.43
57	2.45	2.50	2.47	2.47	2.48	2.48	2.50	2.47	2.47	2.47
58	2.50	2.49	2.50	2.50	2.49	2.49	2.50	2.53	2.49	2.50
59	2.49	2.48	2.56	2.48	2.50	2.52	2.51	2.52	2.53	2.53
60	2.38	2.47	2.52	2.54	2.50	2.50	2.53	2.50	2.50	2.51
61	2.33	2.37	2.33	2.37	2.47	2.50	2.51	2.54	2.51	2.52
62	1.63	1.50	1.25	0.86	0.78	0.87	0.98	0.97	0.94	0.92
63	1.55	1.55	1.27	0.80	0.58	0.86	0.92	0.94	0.95	0.99
64	1.60	1.53	1.38	0.80	0.57	0.87	0.91	0.93	0.96	0.98
65	0.77	0.34	0.74	1.11	1.25	1.10	0.86	0.93	0.95	0.97
66	0.80	0.47	0.46	0.82	1.13	1.07	0.86	0.90	0.92	0.95
67	0.86	0.40	0.39	0.92	1.13	1.17	0.93	0.89	0.91	0.90
68	4.08	4.13	4.14	4.15	4.03	4.11	4.11	4.13	4.19	4.18
69	3.95	4.04	4.02	4.06	4.04	4.05	4.04	4.19	4.12	4.10

Table 11. (continued)

Column #	Gravimetric Water Content by Section Grams Water / Gram Dry Media									
	#1	#2	#3	#4	#5	#6	#7	#8	#9	#10
COL	GWC1	GWC2	GWC3	GWC4	GWC5	GWC6	GWC7	GWC8	GWC9	GWC10
70	4.03	4.01	4.10	3.98	3.98	4.04	4.06	4.19	4.30	4.21
71	3.97	4.06	4.04	4.10	4.02	4.06	4.14	4.20	4.19	4.26
72	3.83	3.94	3.99	4.03	4.00	4.12	4.06	4.03	4.11	4.10
73	4.00	4.12	4.08	4.12	4.10	4.08	4.06	4.11	4.20	4.12
74	1.31	0.68	0.46	0.88	0.93	0.92	0.94	0.93	0.93	0.94
75	1.39	1.05	0.42	0.78	0.90	0.92	0.93	0.94	0.92	0.92
76	1.36	0.92	0.42	0.86	0.91	0.93	0.94	0.93	0.96	0.96
77	1.56	1.16	0.40	0.77	0.90	0.93	0.95	0.95	0.93	0.92
78	1.44	1.14	0.35	0.79	0.91	0.94	0.97	0.94	0.91	0.90
79	1.43	0.74	0.35	0.82	0.90	0.93	0.94	0.92	0.92	0.83
80	2.42	2.42	2.46	2.42	2.42	2.44	2.44	2.40	2.43	2.45
81	2.39	2.36	2.43	2.47	2.44	2.43	2.45	2.46	2.47	2.48
82	2.34	2.40	2.42	2.45	2.46	2.46	2.46	2.48	2.47	2.48
83	2.34	2.46	2.44	2.36	2.46	2.51	2.44	2.44	2.41	2.39
84	2.41	2.39	2.45	2.48	2.46	2.42	2.44	2.43	2.46	2.39
85	2.46	2.48	2.50	2.49	2.43	2.41	2.43	2.42	2.42	2.39
86	3.43	3.55	3.76	3.80	3.86	4.00	4.07	4.17	4.39	4.58
87	2.53	2.53	3.63	3.70	3.81	4.00	4.08	4.16	4.35	4.52
88	3.54	3.65	3.77	3.79	3.89	3.92	4.01	4.14	4.30	4.49
89	4.30	4.33	4.18	4.15	4.09	4.02	3.93	3.90	3.84	3.77
90	4.40	4.33	4.27	4.24	4.13	4.06	3.96	3.94	3.87	3.82
91	4.50	4.43	4.25	4.30	4.24	4.19	3.96	3.91	3.88	3.94

Table 12. Oven dry media weights.

Column #	Dry Media Weight by Section Grams									
COL	#1 DRYMD1	#2 DRYMD2	#3 DRYMD3	#4 DRYMD4	#5 DRYMD5	#6 DRYMD6	#7 DRYMD7	#8 DRYMD8	#9 DRYMD9	#10 DRYMD10
2	3.27	8.30	8.08	7.40	15.21	15.01	13.70	15.32	14.79	13.87
3	4.66	11.12	5.97	7.86	14.77	15.27	15.30	15.24	15.77	13.15
4	3.81	10.01	6.34	7.70	15.41	15.44	14.44	15.08	15.23	14.34
5	5.30	8.17	7.95	7.84	14.41	15.64	14.89	14.96	15.03	14.16
6	5.29	7.27	7.86	7.95	14.30	15.27	15.47	15.39	15.44	13.57
7	5.57	8.41	7.13	7.69	15.57	15.45	15.52	14.60	16.10	14.16
8	5.58	8.04	7.74	7.92	15.42	14.82	14.67	15.16	15.10	13.63
9	6.49	7.74	8.22	7.95	16.06	16.34	15.89	15.96	16.38	13.99
10	6.60	8.58	7.98	7.93	15.73	15.94	15.66	15.25	15.81	14.48
11	6.50	8.02	8.86	7.35	15.78	16.26	16.16	15.81	16.94	14.99
12	5.75	7.72	7.58	7.84	15.74	15.72	15.59	16.07	15.02	14.31
13	5.63	8.30	7.62	8.02	14.64	15.10	15.42	14.90	15.34	14.83
14	3.98	7.45	6.97	6.97	13.37	13.82	14.56	16.73	16.25	13.86
15	4.54	7.56	7.01	7.21	14.72	14.87	14.68	14.85	15.26	13.12
16	6.47	6.94	7.37	7.86	15.44	14.56	14.56	14.84	14.57	13.46
17	4.91	7.12	8.47	7.05	15.41	15.09	15.84	15.36	14.81	13.83
18	6.71	6.85	8.00	6.73	14.50	14.35	15.41	14.81	15.53	14.14
19	5.21	8.19	7.36	7.91	13.95	14.10	14.63	15.58	16.38	14.27
20	3.16	7.67	7.84	7.27	14.39	15.21	15.33	15.57	15.74	13.69
21	4.40	7.20	8.66	7.69	15.63	14.82	15.35	16.17	15.68	14.42
22	5.54	6.91	8.45	7.20	15.24	14.88	15.00	14.88	15.17	14.19
23	5.75	8.34	7.95	7.42	16.10	14.94	14.59	15.98	14.04	14.63
24	5.00	7.79	7.46	7.80	15.51	15.60	14.96	15.51	14.81	14.36
25	4.57	7.20	7.55	7.98	15.75	15.81	15.07	15.57	15.20	13.35
26	5.53	6.41	10.37	8.03	16.52	16.85	15.49	14.77	14.70	13.81
27	6.24	6.97	8.37	7.63	16.36	15.81	16.69	16.06	15.77	13.64
28	6.61	8.58	8.49	8.36	16.61	14.73	14.79	15.26	15.70	13.95
29	6.42	7.83	8.03	7.08	15.36	14.83	14.85	15.34	15.35	13.18
30	7.07	7.88	8.21	7.76	15.80	15.13	15.27	14.98	14.66	13.30
31	6.99	7.88	7.80	9.85	15.04	15.14	15.05	15.01	14.60	14.35
32	3.64	7.32	7.34	7.31	13.70	15.37	15.36	14.24	15.03	13.00
33	5.95	7.18	6.59	8.09	13.62	15.11	14.72	14.52	14.60	13.12
34	5.22	7.71	7.55	7.94	14.29	14.55	14.53	13.99	13.71	12.94
35	5.94	8.09	7.18	7.53	13.36	14.46	13.83	15.22	14.19	12.82
36	5.21	6.87	7.39	5.86	15.27	14.43	14.03	14.41	14.10	12.19
37	6.13	8.83	7.75	7.30	14.74	14.24	14.02	14.20	13.24	12.55
38	2.40	8.38	10.88	6.84	16.35	15.11	16.18	16.30	15.45	14.20
39	3.80	8.20	10.19	7.73	16.34	15.80	15.40	15.49	15.49	14.41
40	3.88	9.63	10.00	8.16	16.80	17.33	16.96	16.29	16.45	14.89
41	5.81	8.84	8.88	7.89	16.89	16.46	16.64	16.77	16.86	14.66
42	6.26	8.80	8.29	8.40	15.90	16.17	16.25	15.83	16.41	15.54
43	5.54	9.83	8.34	8.51	16.09	16.79	16.87	16.63	16.16	15.99
44	4.36	8.05	7.09	7.40	13.57	13.23	13.47	13.22	13.00	12.30
45	5.99	7.20	7.14	7.66	14.95	14.86	14.92	14.38	14.17	12.94
46	5.97	7.82	7.02	6.97	14.40	14.83	14.45	15.20	15.17	13.38
47	7.10	7.59	7.83	7.86	14.60	15.35	14.88	14.77	15.48	13.95
48	4.93	7.45	7.47	7.04	14.67	13.90	13.66	14.36	14.42	13.51
49	5.19	7.88	7.63	7.63	14.45	15.06	14.58	14.71	15.00	13.62
50	6.19	7.89	7.22	7.73	15.42	15.33	15.68	15.27	15.13	15.35
51	7.52	7.68	7.00	8.00	14.49	15.72	15.81	15.23	15.46	14.37
52	6.64	7.48	7.48	8.16	16.26	16.39	16.27	15.62	15.25	14.71
53	7.06	7.84	7.59	8.03	15.75	16.12	16.41	15.46	16.35	14.33
54	7.82	7.48	7.22	7.81	15.57	16.62	15.15	15.46	16.12	14.31
55	8.30	7.10	8.13	7.99	15.97	16.42	16.32	16.37	15.24	15.59
56	6.81	7.51	7.50	8.43	14.51	16.19	14.83	15.44	15.78	14.63
57	7.63	7.88	7.81	8.07	15.30	16.15	16.51	15.89	16.09	14.70
58	6.16	7.45	7.59	8.06	15.98	14.57	15.92	15.92	16.02	15.06
59	5.92	7.83	7.45	7.85	16.03	15.46	15.87	15.99	16.19	15.01
60	6.04	7.17	7.66	7.58	15.80	15.57	14.35	15.27	15.57	14.55
61	6.25	8.21	7.84	8.15	14.86	15.35	14.73	15.19	16.17	14.10
62	6.54	8.44	8.60	8.84	17.76	16.93	16.82	17.30	17.01	16.41
63	5.35	7.98	7.91	8.67	17.47	17.41	17.88	18.23	17.71	16.14
64	6.09	8.56	8.76	8.19	17.18	17.58	17.66	17.78	17.87	15.65
65	5.31	8.51	8.38	8.33	17.76	17.50	17.65	17.25	17.41	16.38
66	4.51	9.11	8.34	8.44	17.36	17.35	17.85	17.27	17.88	15.96
67	4.42	7.86	9.41	8.67	16.65	18.01	17.16	17.68	18.31	15.54
68	6.95	6.84	7.46	7.15	15.72	16.04	16.15	16.26	16.16	15.07
69	7.51	8.35	7.80	6.71	15.85	16.66	16.58	16.78	15.50	14.49

Table 12. (continued)

Dry Media Weight by Section
Grams

Column #										
	#1	#2	#3	#4	#5	#6	#7	#8	#9	#10
COL	DRYMD1	DRYMD2	DRYMD3	DRYMD4	DRYMD5	DRYMD6	DRYMD7	DRYMD8	DRYMD9	DRYMD10
70	7.06	8.56	7.77	8.25	17.09	16.41	16.62	16.19	16.12	14.77
71	7.81	7.49	8.00	7.57	16.67	15.12	16.12	16.15	15.38	13.78
72	6.31	7.99	7.75	7.88	16.45	15.71	15.30	15.47	16.22	14.41
73	6.92	7.83	7.61	7.95	15.27	16.21	16.02	16.36	15.48	14.67
74	5.87	8.39	8.04	8.05	16.78	17.44	16.84	17.78	18.02	15.85
75	4.91	8.23	8.78	8.33	17.60	17.20	16.50	16.72	17.47	16.17
76	5.23	8.89	8.29	7.51	15.93	16.75	16.55	17.40	16.75	15.78
77	5.06	8.86	7.84	7.64	16.41	17.10	16.70	17.25	17.06	15.69
78	5.80	9.48	8.23	8.05	16.63	17.12	16.23	16.58	16.68	16.02
79	5.32	8.45	7.68	8.04	16.61	17.04	16.69	16.66	16.22	15.88
80	6.58	7.84	7.29	7.32	15.70	14.76	15.10	14.92	14.42	14.28
81	5.78	6.99	7.22	7.24	14.72	14.86	15.61	15.04	15.18	14.04
82	4.69	7.44	7.83	7.91	14.81	14.40	15.06	14.90	15.19	13.50
83	4.66	7.40	7.74	7.66	15.20	15.19	14.80	15.00	15.52	14.72
84	6.05	7.44	7.75	7.31	15.01	15.89	15.16	15.65	15.61	13.97
85	6.32	6.96	7.10	7.70	15.54	15.91	15.50	16.02	15.24	14.06
86	6.69	7.35	8.01	6.97	15.21	15.04	15.21	14.35	14.67	14.64
87	6.98	6.98	7.12	7.24	15.80	14.17	15.68	15.06	15.06	14.16
88	6.90	7.38	7.39	7.23	14.84	15.12	14.50	15.04	14.38	15.06
89	7.68	6.97	8.64	6.50	13.83	14.39	15.14	14.81	15.05	13.35
90	7.52	7.50	7.17	7.39	15.02	15.24	15.16	15.51	15.39	14.52
91	6.70	7.22	7.96	7.37	14.48	14.87	15.11	14.73	15.78	13.93

Table 13. Relative bromide concentrations

Column #	Relative Bromide Concentrations by Section Grams Br-/ Maximum Solubility									
	#1	#2	#3	#4	#5	#6	#7	#8	#9	#10
COL	CONCL1	CONCL2	CONCL3	CONCL4	CONCL5	CONCL6	CONCL7	CONCL8	CONCL9	CONCL10
2	1.01	0.43	0.00	0.00	0.00	0.00	0.00	0.00	0.00	0.00
3	1.01	0.10	0.00	0.00	0.00	0.00	0.00	0.00	0.00	0.00
4	0.89	0.20	0.00	0.00	0.00	0.00	0.00	0.00	0.00	0.00
5	0.94	0.57	0.01	0.00	0.00	0.00	0.00	0.00	0.00	0.00
6	0.80	0.56	0.01	0.00	0.00	0.00	0.00	0.00	0.00	0.00
7	0.83	0.66	0.01	0.00	0.00	0.00	0.00	0.00	0.00	0.00
8	1.11	0.67	0.17	0.01	0.00	0.00	0.00	0.00	0.00	0.00
9	1.29	0.68	0.18	0.01	0.00	0.00	0.00	0.00	0.00	0.00
10	1.17	0.63	0.16	0.00	0.00	0.00	0.00	0.00	0.00	0.00
11	0.76	0.41	0.09	0.01	0.00	0.00	0.00	0.00	0.00	0.00
12	0.77	0.45	0.14	0.01	0.00	0.00	0.00	0.00	0.00	0.00
13	0.67	0.41	0.13	0.01	0.00	0.00	0.00	0.00	0.00	0.00
14	0.58	0.50	0.30	0.30	0.15	0.03	0.00	0.00	0.00	0.00
15	0.72	0.52	0.42	0.33	0.18	0.05	0.00	0.00	0.00	0.00
16	0.63	0.51	0.42	0.35	0.19	0.05	0.00	0.00	0.00	0.00
17	0.57	0.46	0.37	0.30	0.17	0.06	0.01	0.00	0.00	0.00
18	0.41	0.38	0.30	0.28	0.16	0.06	0.01	0.00	0.00	0.00
19	0.44	0.39	0.30	0.27	0.19	0.10	0.03	0.00	0.00	0.00
20	0.82	0.85	0.80	0.78	0.82	0.81	0.76	0.74	0.64	0.33
21	0.84	0.82	0.80	0.79	0.78	0.80	0.72	0.66	0.63	0.09
22	0.64	1.14	0.82	0.80	0.71	0.70	0.64	0.62	0.54	0.04
23	0.94	0.91	0.89	0.83	0.78	0.61	0.34	0.00	0.00	0.00
24	1.01	0.93	0.91	0.91	0.76	0.64	0.33	0.08	0.00	0.00
25	0.98	0.90	0.82	0.83	0.71	0.61	0.29	0.00	0.00	0.00
26	0.43	0.43	0.40	0.40	0.37	0.32	0.23	0.18	0.09	0.07
27	0.44	0.43	0.43	0.41	0.44	0.32	0.24	0.17	0.11	0.08
28	0.46	0.46	0.44	0.43	0.35	0.32	0.24	0.16	0.10	0.06
29	0.51	0.52	0.50	0.48	0.42	0.34	0.25	0.17	0.10	0.06
30	0.53	0.52	0.50	0.48	0.44	0.34	0.25	0.16	0.09	0.06
31	0.52	0.51	0.48	0.59	0.35	0.35	0.26	0.17	0.11	0.07
32	0.21	0.21	0.21	0.20	0.02	0.20	0.22	0.11	0.19	0.19
33	0.21	0.21	0.21	0.20	0.20	0.20	0.20	0.20	0.19	0.20
34	0.20	0.21	0.21	0.20	0.20	0.20	0.19	0.19	0.20	0.20
35	0.22	0.22	0.22	0.22	0.21	0.21	0.21	0.21	0.21	0.21
36	0.20	0.20	0.20	0.21	0.20	0.20	0.20	0.19	0.19	0.20
37	0.20	0.20	0.20	0.21	0.20	0.19	0.19	0.19	0.19	0.19
38	0.91	0.59	0.00	0.00	0.00	0.00	0.00	0.00	0.00	0.00
39	0.77	0.43	0.05	0.00	0.00	0.00	0.00	0.00	0.00	0.00
40	0.73	0.38	0.02	0.00	0.00	0.00	0.00	0.00	0.00	0.00
41	0.66	0.52	0.25	0.00	0.00	0.00	0.00	0.00	0.00	0.00
42	0.88	0.61	0.07	0.00	0.00	0.00	0.00	0.00	0.00	0.00
43	0.81	0.67	0.26	0.00	0.00	0.00	0.00	0.00	0.00	0.00
44	1.01	0.71	0.36	0.13	0.01	0.00	0.00	0.00	0.00	0.00
45	0.91	0.63	0.34	0.12	0.01	0.00	0.00	0.00	0.00	0.00
46	0.86	0.64	0.32	0.11	0.01	0.00	0.00	0.00	0.00	0.00
47	1.23	0.93	0.54	0.16	0.01	0.00	0.00	0.00	0.00	0.00
48	1.33	1.13	0.62	0.27	0.02	0.00	0.00	0.00	0.00	0.00
49	1.38	1.04	0.63	0.23	0.02	0.00	0.00	0.00	0.00	0.00
50	0.14	0.14	0.15	0.15	0.21	0.20	0.16	0.20	0.20	0.19
51	0.41	0.24	0.23	0.22	0.25	0.23	0.13	0.12	0.11	0.09
52	0.22	0.21	0.20	0.19	0.24	0.22	0.21	0.20	0.19	0.18
53	0.24	0.23	0.21	0.21	0.24	0.22	0.21	0.15	0.14	0.14
54	0.20	0.19	0.19	0.18	0.18	0.16	0.15	0.14	0.13	0.13
55	0.19	0.19	0.17	0.17	0.16	0.15	0.14	0.13	0.13	0.13
56	0.81	0.68	0.53	0.42	0.20	0.04	0.00	0.00	0.00	0.00
57	0.82	0.67	0.53	0.41	0.20	0.04	0.00	0.00	0.00	0.00
58	0.79	0.70	0.55	0.40	0.19	0.04	0.00	0.00	0.00	0.00
59	0.89	0.84	0.73	0.65	0.40	0.12	0.01	0.00	0.00	0.00
60	0.93	0.84	0.72	0.58	0.38	0.13	0.01	0.00	0.00	0.00
61	0.92	0.92	0.76	0.63	0.41	0.14	0.01	0.00	0.00	0.00
62	0.80	0.71	0.52	0.37	0.13	0.00	0.00	0.00	0.00	0.00
63	1.07	0.86	0.69	0.51	0.11	0.00	0.00	0.00	0.00	0.00
64	0.92	0.82	0.62	0.48	0.08	0.00	0.00	0.00	0.00	0.00
65	1.27	0.66	0.78	0.73	0.57	0.32	0.03	0.00	0.00	0.00
66	1.83	1.51	1.05	0.94	0.63	0.34	0.06	0.00	0.00	0.00
67	1.31	1.15	0.81	0.76	0.67	0.31	0.09	0.00	0.00	0.00
68	0.20	0.19	0.19	0.18	0.17	0.17	0.16	0.14	0.14	0.14
69	0.18	0.16	0.19	0.17	0.16	0.15	0.16	0.07	0.13	0.13

Table 13. (continued)

Column #	Relative Bromide Concentrations by Section Grams Br-/ Maximum Solubility									
	#1	#2	#3	#4	#5	#6	#7	#8	#9	#10
COL	CONCL1	CONCL2	CONCL3	CONCL4	CONCL5	CONCL6	CONCL7	CONCL8	CONCL9	CONCL10
70	0.17	0.17	0.17	0.16	0.16	0.16	0.16	0.15	0.14	0.14
71	0.16	0.16	0.15	0.16	0.16	0.14	0.14	0.14	0.15	0.15
72	0.16	0.15	0.16	0.15	0.16	0.16	0.15	0.14	0.14	0.14
73	0.16	0.18	0.16	0.15	0.16	0.15	0.14	0.13	0.13	0.13
74	0.90	0.62	0.00	0.00	0.00	0.00	0.00	0.00	0.00	0.00
75	0.90	0.70	0.22	0.00	0.00	0.00	0.00	0.00	0.00	0.00
76	0.90	0.63	0.11	0.00	0.00	0.00	0.00	0.00	0.00	0.00
77	0.81	0.71	0.25	0.00	0.00	0.00	0.00	0.00	0.00	0.00
78	0.93	0.72	0.15	0.00	0.00	0.00	0.00	0.00	0.00	0.00
79	0.86	0.63	0.01	0.00	0.00	0.00	0.00	0.00	0.00	0.00
80	0.75	0.54	0.32	0.11	0.01	0.00	0.00	0.00	0.00	0.00
81	0.85	0.68	0.37	0.12	0.01	0.00	0.00	0.00	0.00	0.00
82	0.95	0.68	0.42	0.15	0.02	0.00	0.00	0.00	0.00	0.00
83	0.92	0.66	0.40	0.16	0.02	0.00	0.00	0.00	0.00	0.00
84	0.87	0.66	0.32	0.11	0.01	0.00	0.00	0.00	0.00	0.00
85	0.80	0.59	0.31	0.11	0.01	0.00	0.00	0.00	0.00	0.00
86	0.78	0.66	0.46	0.36	0.21	0.07	0.01	0.00	0.00	0.00
87	1.86	1.86	0.50	0.38	0.23	0.10	0.03	0.00	0.00	0.00
88	0.77	0.60	0.43	0.29	0.15	0.04	0.00	0.00	0.00	0.00
89	0.61	0.52	0.39	0.28	0.13	0.03	0.00	0.00	0.00	0.00
90	0.61	0.52	0.39	0.27	0.13	0.03	0.00	0.00	0.00	0.00
91	0.59	0.57	0.51	0.29	0.14	0.03	0.00	0.00	0.00	0.00

Appendix B. Mathcad Program Listing – Vapor Transport

Analysis of Wheeting (1925) broken column data

In the broken columns of Wheeting, water moves from the soil with no salt to the soil with the salt solutic across the air gap. The rate at which water vapor moves across the air gap is described by the one dimensional diffusion of water vapor across the air gap from the section with no salt to the section with salt added.

Physical Constants

$\rho_g := 0.99823 \cdot \frac{gm}{cm^3}$ density of water at 20C

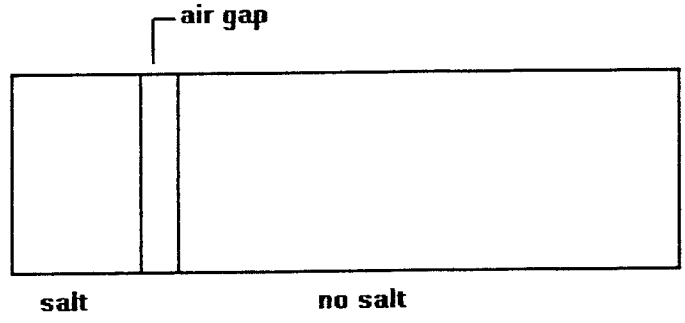

Rate Equations

$\frac{d}{dt}\theta_1 = K_v \cdot \frac{d}{dx} P_v$ $\frac{d}{dt}\theta_2 = -K_v \cdot \frac{d}{dx} P_v$ rate change in moisture content

Initial Water Contents

$V_1 := 79.19 \cdot cm^3$ $V_2 := 260.19 \cdot cm^3$ total volume of section

$\theta_1 := 0.325$ $\theta_2 := 0.325$ initial water content

$m_1 := \theta_1 \cdot V_1 \cdot \rho_g$ $m_2 := \theta_2 \cdot V_2 \cdot \rho_g$

$m_1 = \circ gm$ $m_2 = \circ gm$ total mass of water in each section

Initial Salt Concentrations

The two inch length of soil was treated with a 1% by weight salt solution to a constant water content.

$M_w := 105.989 \cdot gm$ molecular weight of the salt

$mt_{soil} := 500 \cdot gm$ total mass of the soil

$m_{soil} := 1.75 \cdot in \frac{mt_{soil}}{8 \cdot in}$ mass of soil in salt side of column

$Salt := (m_{soil} + m_l) \cdot 0.01$ 1% solution by weight

$Salt = \bullet gm$ mass of salt

$$molality(m_{H2O}, Salt) := \begin{cases} 1.69 \cdot kg^{-1} & \text{if } \frac{Salt}{m_{H2O} \cdot M_w} \geq 1.69 \cdot kg^{-1} \\ \frac{Salt}{m_{H2O} \cdot M_w} & \text{otherwise} \end{cases}$$ initial molality of the salt solution

$molality(m_l, Salt) =$

Calculation of the vapor pressure gradient

$$\frac{d}{dx} P_v = \frac{P_{v1} - P_{v2}}{dx}$$

Pitzer's Method (Pitzer, 1973)

Note: this section is unitless

Constants

$N_o := 6.0221367 \cdot 10^{23}$ Avagodro's number

$\rho_w := 0.99823$ density of water, g/cm³

$D_o := 80.10$ static dielectric constant of water, at 20 deg C

$k := 1.380658 \cdot 10^{-16}$ Boltzmann's constant, erg/deg

$e := 4.803 \cdot 10^{-10}$ absolute electronic charge, e.s.u

$T := (273.15 + 20)$ absolute temperature, deg Kelvin

Debeye-Huckel osmotic coefficient

$$A_m(T) := \frac{1}{3} \cdot \sqrt{\frac{2 \cdot \pi \cdot N_o \cdot \rho_w}{1000}} \cdot \left(\frac{e^2}{D_o \cdot k \cdot T} \right)^{\frac{3}{2}}$$

$A_m(298.15) =$

Osmotic Coefficient for 1:1 electrolytes

Pitzer's parameters (Zemaitis et al. 1986)

KBr : β_0=0.0569, β_1=0.2212, C_ϕ=-0.00180, max molarity=5.5

NaBr: β_0=0.0973, β_1=0.2791, C_ϕ=0.0016, max molarity=4

NaCl: β_0=0.0765, β_1=0.2664, C_ϕ=0.00127, max molarity=6

KCl: β_0=0.04835, β_1=0.2122, C_ϕ=-0.00084 ,max molarity=4.8

NH_4NO_3: β_0=-0.0154, β_1=0.1120, C_ϕ=-0.00003 ,max molarity=6

Na_2CO_3: $4/3\beta_0$=0.2530, $4/3\beta_1$=1.128, 2^[5/2]/3C_ϕ=-0.09057 ,max molarity=1.5

$\beta_0 := 0.2530$ $\beta_1 := 1.128$ $C_\phi := -0.09057$ parameters dependent on solute

$B := 1.2$ $\alpha_1 := 2.0$ parameters independent of solute

$$\phi(mol) := -\left[\frac{A_m(T)\cdot\sqrt{mol}}{1 + B\cdot\sqrt{mol}}\right] + mol\cdot\beta_0 + \beta_1\cdot\exp\left(-\alpha_1\sqrt{mol}\right) + mol^2\cdot C_\phi + 1$$

$\phi(molality\,m_1, Salt\cdot kg) =$ at $T =$

Osmotic Potential

$M_{H2O} := 18.0016\cdot mole^{-1}$ molecular weight of water

$V_w := 18\cdot10^{-6}\cdot\frac{m^3}{mole}$ partial molar volume of water

$R := 8.3143\cdot joule\cdot K^{-1}\cdot mole^{-1}$ gas constant

$\rho_w := 0.99823\cdot\frac{gm}{cm^3}$ density of water at 20C

$v := 2$ number of ions resulting from one molecule of electrolyte

$T := T\cdot K$ $T =$ add units to temperature

$$\Psi_s(mol) := \phi(mol)\cdot\frac{R\cdot T\cdot v\cdot mol\cdot mole\cdot M_{H2O}}{1000\cdot V_w}$$

$\Psi_s(molality\,m_1, Salt\cdot kg) =$ ·Pa osmotic potential, Pa

$$h := \frac{\Psi_s(molality\,m_1, Salt\cdot kg)}{\rho_w\cdot g}$$ $h =$ osmotic potential, m of H_2O

$molal := 0, 0.1 .. 1.69$

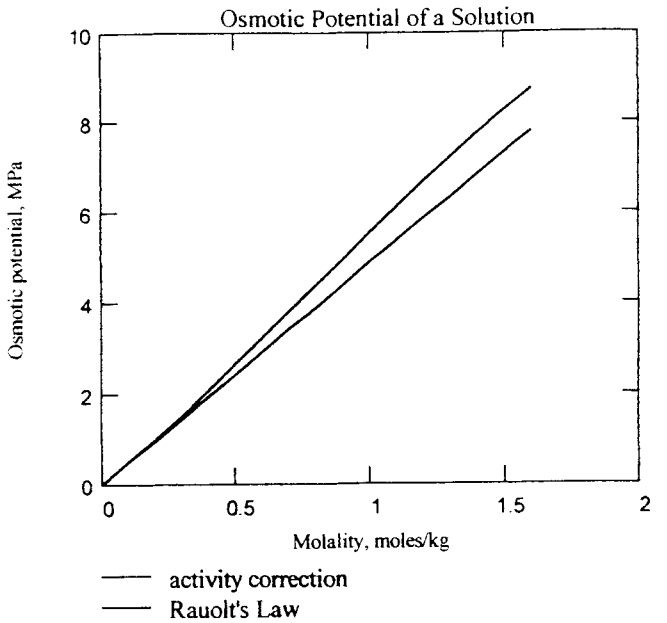

Matric Potential

$\theta_r := 0.1 \qquad \alpha := 0.059 \cdot cm^{-1}$

$\theta_s := 0.39 \qquad n_{vg} := 1.48$

soil parameters

$$m_{vg} := 1 - \frac{1}{n_{vg}}$$

$$\Psi_m(\theta) := \frac{\rho_w \cdot g}{\alpha} \cdot \left[\left(\frac{\theta - \theta_r}{\theta_s - \theta_r} \right)^{\frac{1}{m_{vg}}} - 1 \right]^{\frac{1}{n_{vg}}}$$

van Genuchten equation

$\Psi_m(\theta_1) = 1.863 \cdot 10^3 \cdot Pa$

matric potential

Calculation of the water vapor density, ρ_{wv}

$$rh(mol, \theta) := \exp\left[\frac{-\Psi_s(mol) + \Psi_m(\theta) \cdot V_w}{R \cdot T} \right]$$

relative vapor pressure (relative humidity)

$rh(molality(m_1, Salt) \cdot kg, \theta_1) = 0.98068$

$rh(molality(m_1, Salt) \cdot kg, \theta_s) = 0.98069$

$Po_{wv} := 17.30 \cdot \frac{gm}{m^3}$

saturation water vapor density (concentration) of water vapor (i.e., at 100% relative hunidity) at 20C

$p_{wv}(mol,\theta) := rh(mol,\theta)\cdot Po_{wv}$ water vapor density at molality m

$p_{wv}(molality\,m_1, Salt, kg, \theta_1) = 16.966\,\frac{gm}{m^3}$

molal := 0 .. 2

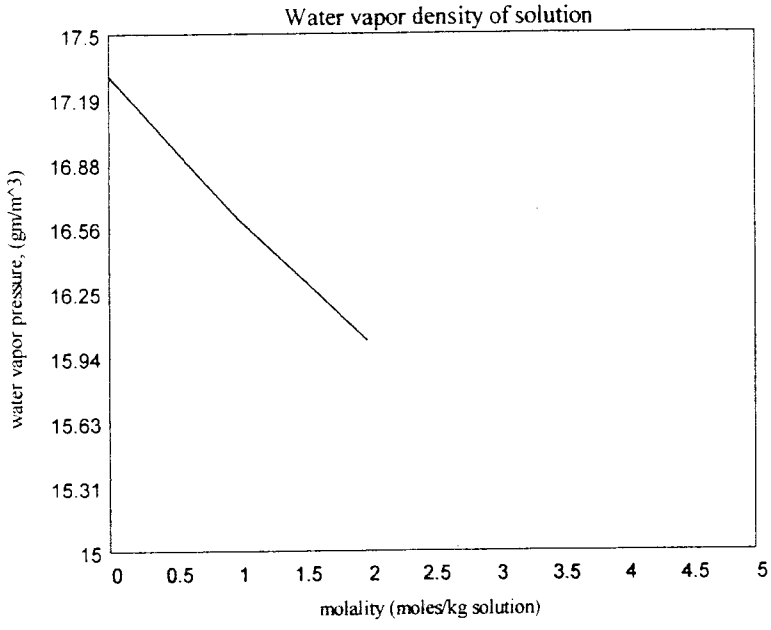

$P_v(mass, Salt, \theta) := p_{wv}(molality(mass, Salt)\cdot kg, \theta)$

$P_v(m_1, Salt, \theta_s) = 16.966\,\frac{gm}{m^3}$

$P_v(m_1, Salt, \theta_1) = 16.966\,\frac{gm}{m^3}$

$K_v := 2.42\cdot 10^{-5}\,\frac{m^2}{sec}$ diffusion coefficient of water vapor in air at 20C

dx := 0.5·in

dx = 1.27 cm

$P_{v1} := P_v(m_1, Salt, \theta_1)$

$P_{v2} := P_v(m_2, 0\cdot gm, \theta_2)$

$P_{v1} = 16.966\,\frac{gm}{m^3}$ $P_{v2} = 17.3\,\frac{gm}{m^3}$

$\theta_0 := \theta_1$ $\quad Salt_1 := Salt$ $\quad m_0 := m_1$

$\theta_1 := \theta_2$ $\quad Salt_2 := \frac{Salt}{100}$ $\quad m_1 := m_2$

$A := \pi \cdot \left(\frac{1.875}{2} \cdot in\right)^2$ $\quad A = 17.814 \cdot cm^2$ cross sectional area

$$q := \frac{-K_v \cdot A}{dx} \cdot \left(P_v\left(m_0, Salt_1, \frac{m_0}{\rho_w \cdot V_1}\right) + \frac{K_v \cdot A}{dx} \cdot P_v\left(m_1, Salt_2, \frac{m_1}{\rho_w \cdot V_2}\right)\right)$$

$q = 0.098 \cdot \frac{gm}{day}$

Create a vector of derivatives

$$dtheta(t, m) := \begin{bmatrix} -K_v \cdot A \cdot \dfrac{P_v\left(m_0, Salt_1, \frac{m_0}{\rho_w \cdot V_1}\right) - P_v\left(m_1, Salt_2, \frac{m_1}{\rho_w \cdot V_2}\right)}{dx} \\ K_v \cdot A \cdot \dfrac{P_v\left(m_0, Salt_1, \frac{m_0}{\rho_w \cdot V_1}\right) - P_v\left(m_1, Salt_2, \frac{m_1}{\rho_w \cdot V_2}\right)}{dx} \end{bmatrix}$$

Specify initial conditions

$init_0 := \frac{m_1}{kg}$ $\quad init_1 := \frac{m_2}{kg}$

Beginning and ending times:

$$dtheta(0, m) = \begin{bmatrix} 1.131 \cdot 10^{-9} \\ -1.131 \cdot 10^{-9} \end{bmatrix} \cdot kg \cdot sec^{-1}$$

$t0 := 0$ $\quad t1 := 60 \cdot 60 \cdot 24 \cdot 25$

Number of steps: $n := 100$ $\quad i := 1 .. n + 1$

Solution using **rkfixed**:

$S := rkfixed(init, t0, t1, n, dtheta)$

$T := S^{<0>}$ $\quad Theta0 := S^{<1>}$ $\quad Theta1 := S^{<2>}$

$j := 0 .. 1$

$smoisture_j :=$ $\quad nsmoisture_j :=$ $\quad time_j :=$ Column data, Wheeting 1925

0.503	0.414	5
1.046	1.484	15

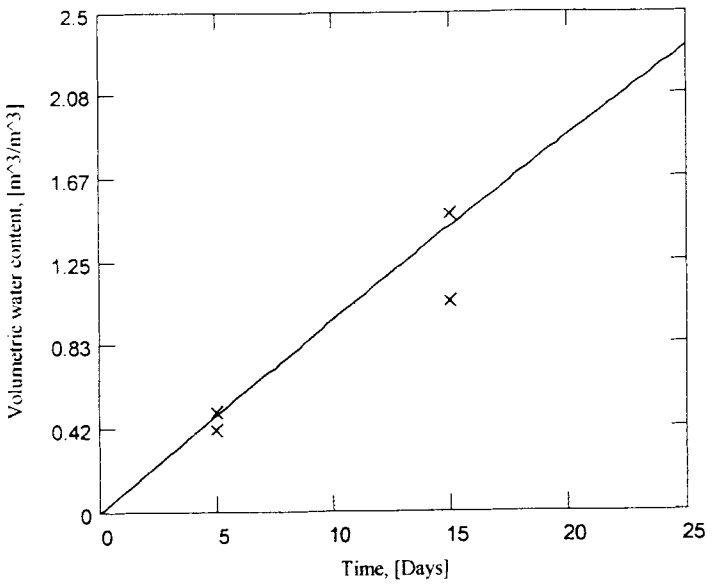

$$\frac{\left(\frac{Theta0}{gm}\right)_{i-1} + \left(\frac{Theta1}{gm}\right)_{i-1}}{\left(\frac{Theta0}{gm}\right)_{0} + \left(\frac{Theta1}{gm}\right)_{0}}$$

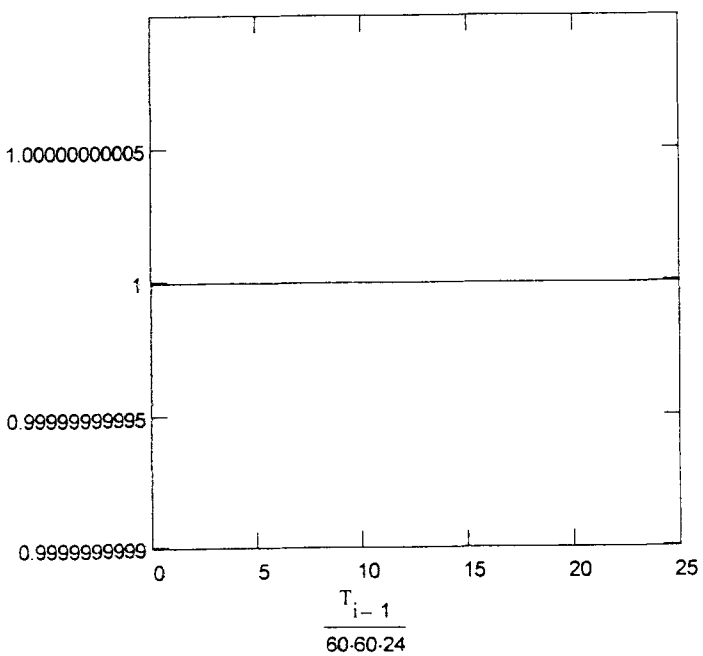

WRITEPRN("wheeting4.prn") := S

Appendix C. Mathcad Program Listing – CFLOW

Model Development

Governing Equations

Liquid transport

$$\frac{d}{dt}m_l = \frac{d}{dx}\left(\rho_w \cdot K\left(m_l\right)\cdot\frac{d}{dx}\Psi\left(m_l\right)\right) + s_l$$

Vapor Transport

$$\frac{d}{dt}m_v = \frac{d}{dx}\left(f_a\left(m_l\right)\cdot D_{vap}\left(m_l\right)\cdot\frac{d}{dx}p_{wv}\left(m_l, m\right)\right) + s_v$$

Solute Transport

$$\frac{d}{dt}m = \frac{d}{dx}\left(D_e\left(m_l\right)\cdot\frac{d}{dx}m - \frac{m}{m_l}\cdot v_l\right) + s_c$$

Global Constants

Constants (Pitzer's Method)

$N_o := 6.0221367 \cdot 10^{23}$	Avagodro's number
$k := 1.380658 \cdot 10^{-16}$	Boltzmann's constant, erg/deg
$e := 4.803 \cdot 10^{-10}$	absolute electronic charge, e.s.u
$M_w := 18.0016$	molecular weight of water
$R := 8.3143$	gas constant, joule/K/mole

Model Parameters

Media Properties

$\theta_r := 0.001$	residual water content, m^3/m^3
$\theta_s := 0.75$	saturated water content, m^3/m^3
$\alpha := 14$	empirical fitting parameter, 1/m
$n_{vg} := 1.195$	empirical fitting parameter
$m_{vg} := 1 - \frac{1}{n_{vg}}$	empirical fitting parameter
$K_{sat} := 500\ \frac{cm}{day}\cdot\frac{sec}{m}$	saturated hydraulic conductivity, m/s

Experimentally determined data for the water retention of selected media. These values only represent very approximate averages for the different textural classes.

Soil Texture	θ_r	θ_s	a,1/cm	n	K_s,cm/d		Bulk Density,mg/m^3
Sand	0.045	0.43	0.145	2.68	712.8	1.5105	
Loamy Sand	0.057	0.41	0.124	2.28	350.2	1.5635	
Sandy Loam	0.065	0.41	0.075	1.89	106.1	1.5635	
Loam	0.078	0.43	0.036	1.56	24.96	1.5105	
Silt L.	0.034	0.46	0.01	1.37	6	1.431	
Sandy Clay Loam	0.067	0.45	0.02	1.41	10.8	1.4575	
Clay Loam	0.1	0.39	0.059	1.48	31.44	1.6165	
Silty Clay Loam	0.095	0.41	0.019	1.31	6.24	1.5635	
Sandy Clay	0.089	0.43	0.01	1.23	1.68	1.5105	
Silty Cl.	0.1	0.38	0.027	1.23	2.88	1.643	
Clay	0.07	0.36	0.005	1.09	0.48	1.696	
1:1 Peat:Ver.	0.326	0.75	0.14	1.818	500	0.13	
1:1 Peat:Ver (2)	0.454	0.85	0.064	2.042	500	0.19	
Ref. Silt Loam	0.243	0.515	0.028	1.411	10	-	
1:1 Peat:Ver.	0	0.75	0.1967	1.008	500	0.17	m=0.1858

Solution Parameters

Pitzer's parameters (Zemaitis et al. 1986, Pytkowicz, 1979)

KBr: β_0=0.0569 β_1=0.2212 C_ϕ=-0.00180 max molarity=5.5

NaBr: β_0=0.0973 β_1=0.2791 C_ϕ=0.00136 max molarity=4

NaCl: β_0=0.075 β_1=0.2664 C_ϕ=0.00127 max molarity=6

KCl: β_0=0.04835 β_1=0.2122 C_ϕ=-0.00084 max molarity=4.8

NH_4NO_3: β_0=-0.0154 β_1=0.1120 C_ϕ=-0.00003 max molarity=6

Na_2CO_3: $4/3\beta_0$=0.2530 β_1=3.128 $2^{[5/2]/3}C_\phi$=-0.09057 max molarity=1.5

$NaNO_3$: β_0=0.0068 β_1=0.1783 C_ϕ=-0.00072 max molarity=6

$\beta_0 := 0.0569$ $\beta_1 := 0.2212$ $C_\phi := -0.00180$ parameters dependent on solute

$B := 1.2$ $\alpha_1 := 2.0$ parameters independent of solute

$\nu := 2$ number of ions resulting from one molecule of electrolyte

Solubility= 5.5 solubility in water, moles/kg of water

Other Parameters

$T := (273.15 + 20)$ absolute temperature, deg Kelvin

$\rho_w := 998.2$ density of water at T, kg/m^3

$D_o := 78.54$ static dielectric constant of water, at T

$Po_{wv} := 17.30 \cdot 10^{-3}$ saturation water vapor density, atT, kg/m^3

$V_w := 1.805 \cdot 10^{-5}$ partial molar volume of water atT, m^3/mole

$D_{wv} := 2.42 \cdot 10^{-5}$ diffusion coefficient of water vapor in air atT, m^2/s

$D_{eff} := 2.4 \cdot 10^{-9}$ effective diffusion coefficient of solute in an aqeous solution atT, m^2/s

$x := 0.25$

Nodal Data and Iteration Criteria

nodes := 40 number of nodes

dx := 0.004 uniform node spacing, m

Subroutines and Functions

Water retention function,van-Genuchten (1980)

$$\theta(h) := \theta_r + \frac{\theta_s - \theta_r}{\left[1 + (\alpha \cdot h)^{n_{vg}}\right]^{m_{vg}}}$$

$$\Psi(\theta) := \begin{cases} \frac{1}{\alpha} \cdot \left[\frac{1}{\left(\frac{\theta - \theta_r}{\theta_s - \theta_r} \right)^{\frac{1}{m_{vg}}}} - 1 \right]^{\frac{1}{n_{vg}}} & \text{if } \theta \geq \theta_r + 0.00000000000000001 \cdot \theta \leq \theta_s \\ \Psi\left(\theta_r + 0.00000000000000001\right) & \text{if } \theta < \theta_r + 0.00000000000000001 \\ 0 & \text{if } \theta > \theta_s \end{cases}$$

Mualem (1976)-van Genuchten (1980) conductivity function

$$K_{vg}(h) := \begin{cases} K_{sat} \cdot \frac{\left[1 - (\alpha \cdot h)^{n_{vg}-1} \cdot \left[1 + (\alpha \cdot h)^{n_{vg}}\right]^{\frac{1}{n_{vg}}} - 1\right]^2}{\left[1 + (\alpha \cdot h)^{n_{vg}}\right]^{\frac{n_{vg}-1}{2 \cdot n_{vg}}}} & \text{if } h \leq \Psi\left(\theta_r\right) \\ K_{vg}\left(\Psi\left(\theta_r\right)\right) & \text{otherwise} \end{cases}$$

Internodal Conductivities - Harmonic Mean / Geometric Mean

$$KK_{1,K_2} := \frac{2 \cdot K_1 \cdot K_2}{K_1 + K_2} \qquad KK_{1,K_2} := \begin{cases} \frac{K_1 + K_2}{2} & \text{if } K_1 \neq 0 \cdot K_2 \neq 0 \\ 0 & \text{otherwise} \end{cases}$$

Vapor diffusion coefficient

$$D_{vap}(m_l) := \begin{cases} D_{wv} \cdot \theta_s - \frac{m_l}{\rho_w}^{0} & \text{if } \frac{m_l}{\rho_w} > 0 \\ D_{wv} \cdot \theta_s - \theta_r \cdot \frac{m_l}{\rho_w \cdot \theta_r} & \text{otherwise} \end{cases}$$

Air filled porosity

$$f_a(m_l) := \theta_s - \frac{m_l}{\rho_w}$$

Effective ion diffusion coefficient

$$D_{eff} = 2.4 \cdot 10^{-9}$$

$$D_e(m_l) := D_{eff} \left[\frac{\left(\frac{m_l}{\rho_w} \right)}{\theta_s} \right]^{\frac{4}{3}} \cdot \theta_s^{\frac{10}{3}} \qquad D_e(m_l) := \frac{D_{eff}}{2} \cdot \left(\frac{m_l}{\rho_w} \right)^{1} \qquad D_e(m_l) := D_{eff} \frac{m_l}{\rho_w} \cdot \left(\frac{m_l}{\rho_w \cdot \theta_s} \right)^{x}$$

Pitzer's Method (Pitzer, 1973)

$$D_e(0.04 \cdot \rho_w) = -2.75 \cdot 10^{-11}$$

$$D_e(\theta_s \cdot \rho_w) = 1.5 \cdot 10^{-9}$$

Debeye-Huckel osmotic coefficient

$$A_m(T) := \frac{1}{3} \cdot \sqrt{\frac{2 \cdot \pi \cdot N_o \cdot \rho_w}{10^6}} \cdot \left(\frac{e^2}{D_o \cdot k \cdot T} \right)^{\frac{3}{2}}$$

Osmotic Coefficient for 1:1 electrolytes

$$A_m(T) = 0.4005$$

$$\phi(m_2) := -\left[\frac{A_m(T) \cdot \sqrt{m_2}}{1 + B \cdot \sqrt{m_2}} \right] + m_2 \cdot \beta_0 + \beta_1 \cdot \exp\left(-\alpha_1 \cdot \sqrt{m_2}\right) + m_2^2 \cdot C_\phi + 1$$

m_2 is the molality of the solution, moles/kg

Osmotic Potential

$$\Psi_{s}(m_2) := \phi(m_2) \cdot \frac{R \cdot T \cdot v \cdot m_2 \cdot M_w}{1000 \cdot V_w}$$

Calculation of the water vapor density, ρ_{wv}

water vapor density at molality m_2

$$p_{wv}(m_2, m_1) := \begin{cases} \Psi_{matric} \leftarrow \Psi(m_1) \cdot \rho_w^{-1} \cdot \rho_w \cdot 9.807 \\ \Psi_{total} \leftarrow \Psi_s(m_2) + \Psi_{matric} \\ \exp\left(\frac{-\Psi_{total} \cdot V_w}{R \cdot T}\right) \cdot Po_{wv} \quad \text{if } m_2 \geq 0 \\ Po_{wv} \quad \text{otherwise} \end{cases}$$

Solution Properties (Graphical)

molality := 0, 0.1 .. Solubility

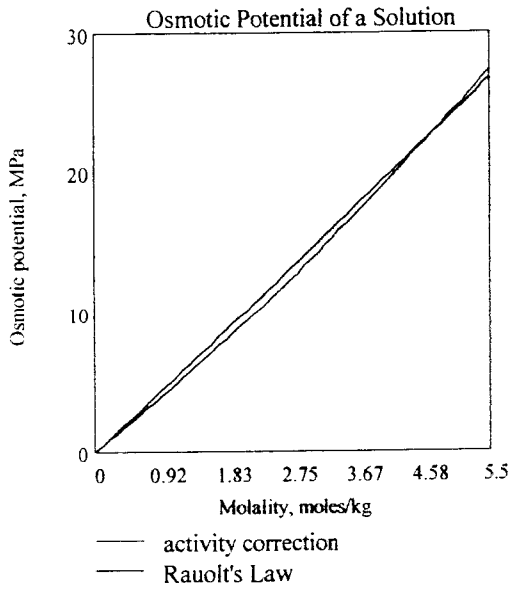

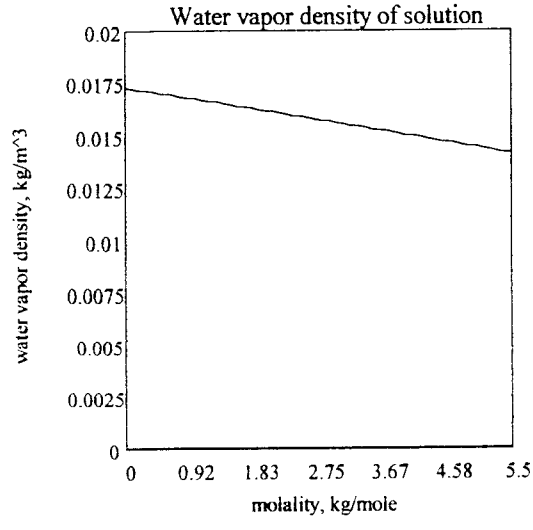

Media Properties (Graphical)

theta := 0.01, 0.011 .. θ_s - 0.001

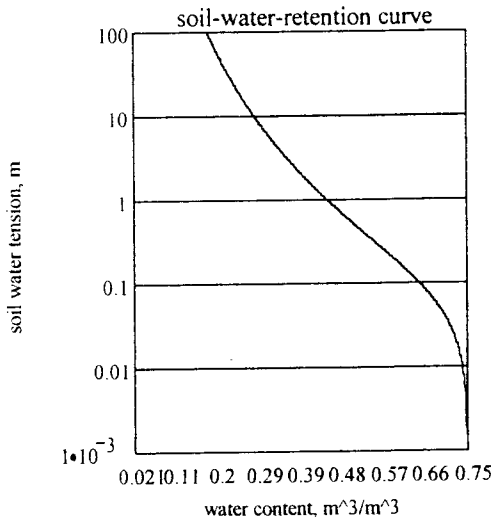

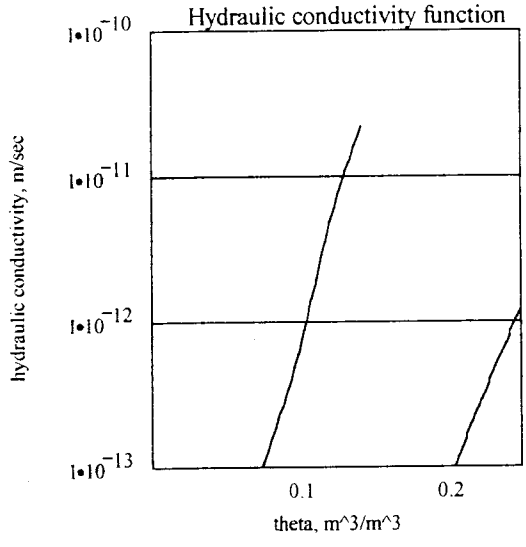

$m_l := 0 \cdot \rho_w .. \theta_s \cdot \rho_w$

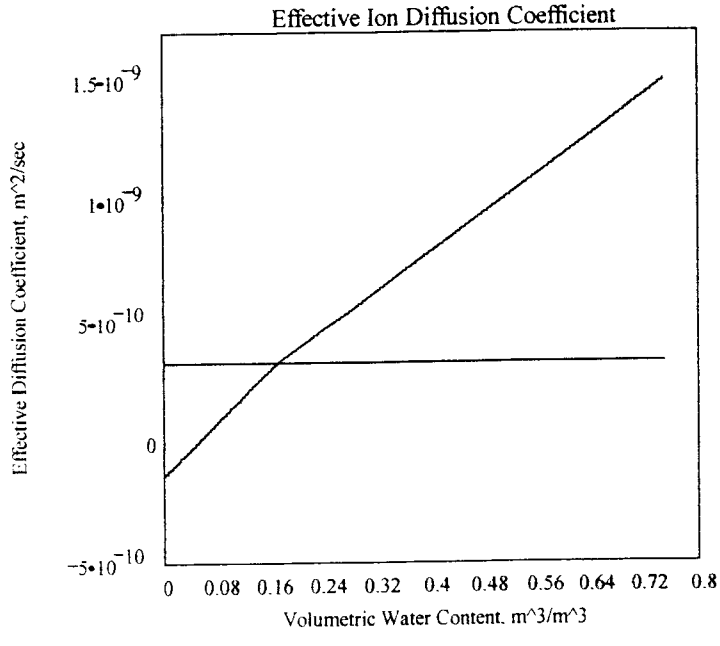

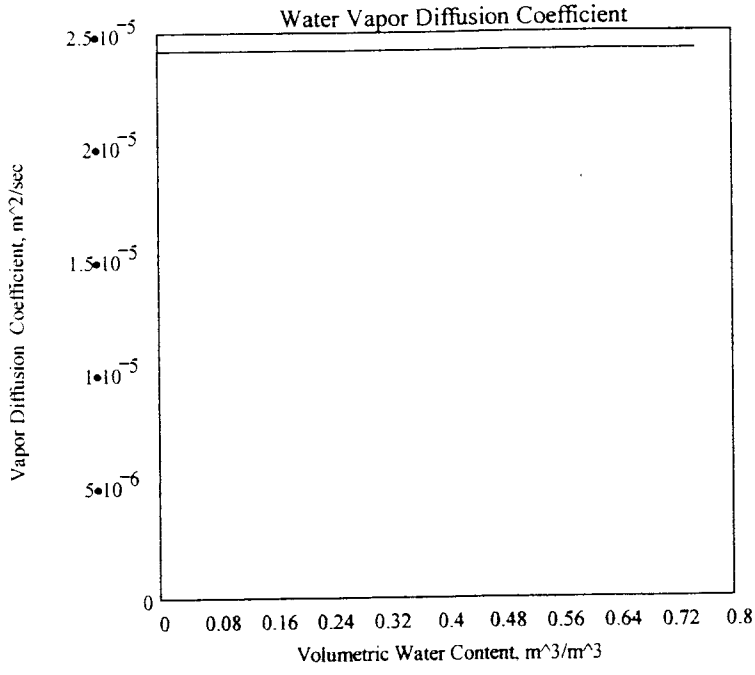

Finite Difference Equations (Explicit Formula)

Initial conditions

$i := 1 .. nodes$

$m_{l_i} := 0.17 \cdot \rho_w$ — Mass of the liquid water, kg/m^3

$\theta_i := m_{l_i} \cdot \rho_w^{-1}$ — Volumetric Water Content, m^3/m^3

$\Psi_{\tau_i} := \Psi(\theta_i)$ — Matric Potential, m

$K_i := K_{vg}(\Psi_{\tau_i})$ — Liquid hydraulic conductivity, m/s

$m_{s_i} := 0$ — Molality [mole/kg]

$p_{vap_i} := p_{wv}(m_{s_i}, m_{l_i})$ — water vapor density, kg/m^3

$D_{e_i} := D_e(m_{l_i})$ — Effective Ion Diffusion Coefficient, m^2/s

$m_{v_i} := p_{vap_i} \cdot f_a \cdot m_{l_i}$ — Mass of the water vapor, kg/m^3

$D_{vap_i} := D_{vap}(m_{l_i})$ — Vapor Diffusion Coefficient, m^2/s

$V_i := 0$ — Mean pore water velocity, m/s

Boundary Conditions

$m_{l_0} := 0 \qquad m_{l_{nodes+1}} := 0$

$\theta_{nodes+1} := 0$

$\Psi_{\tau_{nodes+1}} := 0 \qquad \Psi_{\tau_0} := 0$

$K_{nodes+1} := 0 \qquad K_0 := 0$

$m_{v_0} := 0 \qquad m_{v_{nodes+1}} := 0$

$D_{vap_{nodes+1}} := 0$

$m_{s_0} := 0 \qquad m_{s_{nodes+1}} := 0$

$p_{vap_{nodes+1}} := 0$

$D_{e_{nodes+1}} := 0$

Finite Difference Approximation Equations

LFDLiquid$(m_l, dt) :=$ | for $i \in 0..nodes+1$

$\theta_i \leftarrow m_{l_i} \cdot \rho_w^{-1}$

$\Psi_{\tau_i} \leftarrow \Psi(\theta_i)$ Volumetric Water Content, m^3/m^3

$K_i \leftarrow K_{vg}(\Psi_{\tau_i})$ Matric Potential, m

$K_0 \leftarrow 0$ Liquid hydraulic conductivity, m/s

$K_{nodes+1} \leftarrow 0$

$\Psi_{\tau_0} \leftarrow 0$

$\Psi_{\tau_{nodes+1}} \leftarrow 0$

$m'_l \leftarrow m_l$

for $i \in 1..nodes$

$$m_{l_i} \leftarrow \frac{K(K_{i+1}, K_i) \cdot dt \cdot \rho_w \cdot (\Psi_{\tau_i} - \Psi_{\tau_{i+1}})}{dx^2} + \frac{K(K_{i-1}, K_i) \cdot dt \cdot \rho_w \cdot (\Psi_{\tau_i} - \Psi_{\tau_{i-}}}{dx^2} + m'_{l_i}$$

m_l

Vapor Transport Equation

$$\text{FDVapor}(m_l, m_v, m_s, dt) := \left|\begin{array}{l} \text{for } i \in 1..\text{nodes}+1 \\ \quad \left|\begin{array}{l} p_{vap_i} \leftarrow p_{wv}(m_{s_i}, m_{l_i}) \\ D_{vap_i} \leftarrow D_{vap}(m_{l_i}) \end{array}\right. \\ m'_v \leftarrow m_v \\ D_{vap_0} \leftarrow 0 \\ D_{vap_{nodes+1}} \leftarrow 0 \\ \text{for } i \in 1..\text{nodes} \\ \quad m_{v_i} \leftarrow \dfrac{-K(D_{vap_{i+1}}, D_{vap_i}) \cdot dt \cdot f_a(m_{l_i}) \cdot (p_{vap_i} - p_{vap_{i+1}})}{dx^2} \ldots \\ \qquad + \dfrac{K(D_{vap_{i-1}}, D_{vap_i}) \cdot dt \cdot f_a(m_{l_i}) \cdot (p_{vap_{i-1}} - p_{vap_i})}{dx^2} \ldots \\ \qquad + m'_{v_i} \\ m_v \end{array}\right.$$

Water vapor density, kg/m^3

Vapor Diffusion Coefficient, m^2/s

Coupled Liquid - Vapor Water Balance Equations

Couples liquid and vapor phase flow and maintains water balance.

1. Calculates the mass of the water vapor based on the pore space in the media as m'_v.
2. If m_v is less than the the water vapor calculated as a result of diffusion, mv than subtract the difference between mv and m'v from the liquid water at the node (i.e. liquid is evaporated into the vapor). Otherwise the difference is added to the liquid water at the node (i.e vapor is condensed into the liquid).
3. Check to make sure the liquid water content doesn't fall to less than the residual water content.
4. Check to make sure the liquid water content doesn't increase to higher than the saturated water conte

Calculate Water Vapor based on pore space

$$\text{VaporCalc}(m_l, m_v, m_s) := \left|\begin{array}{l} \text{for } i \in 1..\text{nodes} \\ \quad \left|\begin{array}{l} \rho_{wv} \leftarrow p_{wv}(m_{s_i}, m_{l_i}) \\ m_{v_i} \leftarrow \rho_{wv} \cdot \theta_s - \dfrac{m_{l_i}}{\rho_w} \end{array}\right. \\ m_v \end{array}\right.$$

WaterBalance $m_l, m_v, m_s :=$

for $i \in 1..nodes$

$\rho_{wv} \leftarrow p_{wv}(m_{s_i}, m_{l_i})$

$m'_{v_i} \leftarrow \rho_{wv} \cdot \theta_s - \frac{m_{l_i}}{\rho_w}$

$m_{l_i} \leftarrow -\rho_{wv} \cdot \theta_s - m_{v_i} - m_{l_i} \cdot \frac{\rho_w}{-\rho_{wv} + \rho_w}$ if $m_{v_i} > m'_{v_i}$

$m_{l_i} \leftarrow \rho_{wv} \cdot \theta_s - m_{v_i} - m_{l_i} \cdot \frac{\rho_w}{\rho_{wv} - \rho_w}$ if $m_{v_i} < m'_{v_i}$

$m_{l_i} \leftarrow m_{l_i}$ if $m_{v_i} = m'_{v_i}$

m_l

Mean pore water velocity

FDVelocity $m_l :=$

for $i \in 0..nodes + 1$

$\theta_i \leftarrow m_{l_i} \cdot \rho_w^{-1}$

$\Psi_{\tau_i} \leftarrow \Psi(\theta_i)$

$K_i \leftarrow K_{vg}(\Psi_{\tau_i})$

$K_0 \leftarrow 0$

$K_{nodes+1} \leftarrow 0$

$\Psi_{\tau_0} \leftarrow 0$

$\Psi_{\tau_{nodes+1}} \leftarrow 0$

for $i \in 1..nodes$

$$v_{l_i} \leftarrow \frac{K(K_{i+1}, K_i) \cdot (\Psi_{\tau_{i+1}} - \Psi_{\tau_i})}{dx} + \frac{K(K_{i-1}, K_i) \cdot (\Psi_{\tau_i} - \Psi_{\tau_{i-1}})}{dx}$$

$$v_{l_1} \leftarrow \frac{2 \cdot K(K_1, K_2) \cdot (\Psi_{\tau_2} - \Psi_{\tau_1})}{dx}$$

v_l

Solute Transport Equation

FDSolute $m_l, m_s, v_l, dt :=$

for $i \in 0..nodes + 1$

$D_{e_i} \leftarrow D_e \, m_{l_i}$

$m'_s \leftarrow m_s$

$m_{s_1} \leftarrow$ Solubility

for $i \in 2..nodes$

$$m_{s_i} \leftarrow \frac{K\, D_{e_{i+1}}, D_{e_i} \cdot dt \cdot m'_{s_{i+1}} - m'_{s_i}}{dx^2} \ldots + \frac{K\, D_{e_{i-1}}, D_{e_i} \cdot dt \cdot m'_{s_{i-1}} - m'_{s_i}}{dx^2} \ldots + v_{l_i} \cdot \frac{m'_{s_{i+1}} - m'_{s_{i-1}} \cdot dt}{2 \cdot dx} \ldots + m'_{s_i}$$

m_s

Main Loop Parameters

$nodes = 40$ Number of Nodes

$dx \cdot m = 4 \cdot 10^{-3} \cdot m$ Node spacing, m

$maxtime = 25 \cdot \frac{day}{sec}$ Maximum simulation time, seconds

$maxtimesec = 2.16 \cdot 10^{6} \cdot sec$ Maximum simulation time, days

$delta := 60 \cdot 240$ Time step, seconds

$$Runtime = \frac{maxtime}{delta} \cdot nodes \cdot 20 \cdot \frac{sec}{10000}$$

$Runtime = 0.2 \cdot min$ Estimated Runtime

Main Loop $f(m_l, m_v, m_s) :=$

$m'_l \leftarrow m_l$

$m'_s \leftarrow m_s$

$dt \leftarrow delta$

for $step \in 1 .. \frac{maxtime}{dt}$

$m_{s_1} \leftarrow Solubility$

$m_l \leftarrow FDLiquid(m_l, dt)$

$m_v \leftarrow FDVapor(m_l, m_v, m_s, dt)$

$v_l \leftarrow FDVelocity(m_l)$

$m_l \leftarrow WaterBalance(m_l, m_v, m_s)$

$m_v \leftarrow VaporCalc(m_l, m_v, m_s)$

$m_s \leftarrow FDSolute(m_l, m_s, v_l, dt)$

$m'_l{}^{\langle \frac{step}{6} \rangle} \leftarrow m_l$ if $mod(step, 6) = 0$

$m'_s{}^{\langle \frac{step}{6} \rangle} \leftarrow m_s$ if $mod(step, 6) = 0$

$v'_l{}^{\langle \frac{step}{6} \rangle} \leftarrow v_l$ if $mod(step, 6) = 0$

$[m_l \; m_v \; m_s \; m'_l \; m'_s \; v'_l]$

$m_{s_1} := Solubility$

Solution $:= f(m_l, m_v, m_s)$

$k := 0 .. 14$

FRAME := 0 .. 24

TIME = 0 •day

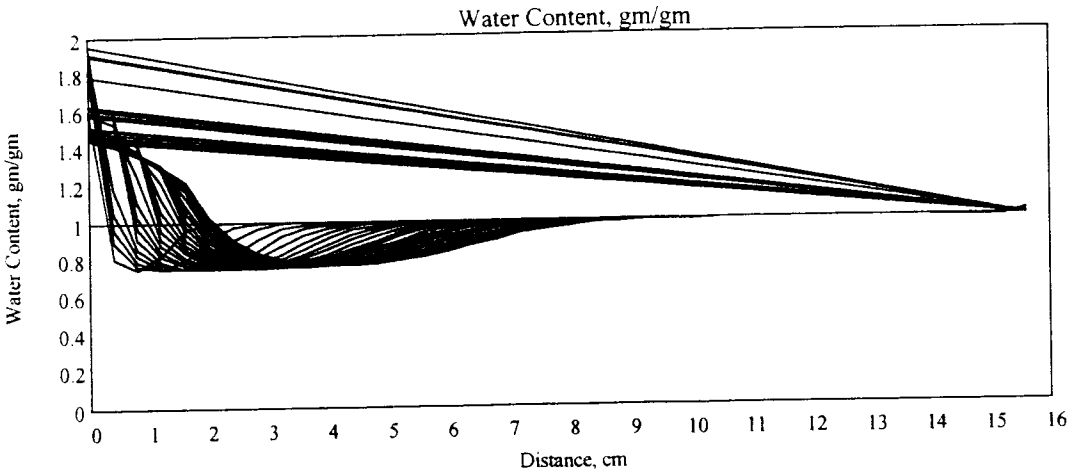

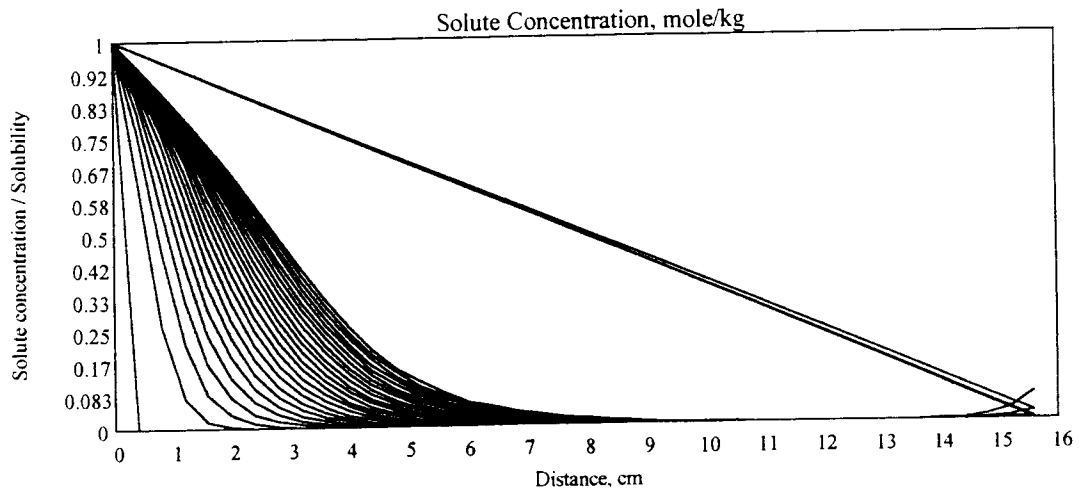

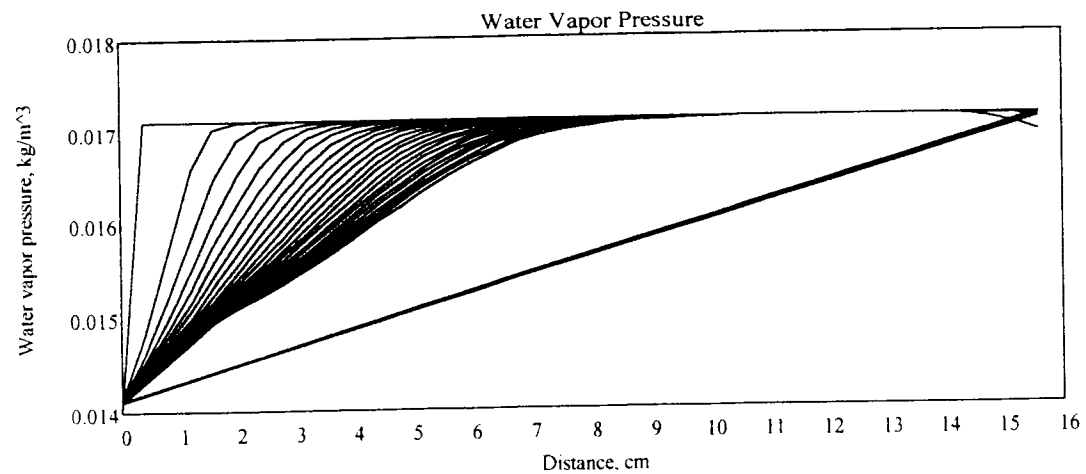

Appendix D. Using Short Soil Moisture Probes with High Bandwidth Time Domain Reflectometry Instruments

by

Shaun F. Kelly, John S. Selker and James L. Green

Technical Note published in *Soil Science Society of America Journal*. 59:97-102. 1995.

Abstract

Time domain reflectometry (TDR) is used to measure moisture content and salinity of soils. Most TDR systems have a bandwidth of 2.5 GHz or less, limiting the precision of measurements using short probes. The primary objective of this research was to develop and test short probes for use with a high bandwidth (20 GHz) TDR instrument. The secondary objective was to determine moisture content in highly conductive media by insulating the probes with Teflon heat shrinkable tubing. Laboratory packed test cells with probe lengths of 0.025, 0.05 and 0.075 m were used for the primary research objective,and 0.075 m probes for the secondary objective. Linear relationships between the apparent refractive index and volumetric moisture content were developed for each probe length and type. The accuracy of the probes was ±0.0125, ±0.05, ±0.025, and ±0.035 m^3/m^3 for the 0.075, 0.075(insulated), 0.05, and 0.025 m probes respectively. Moisture measurements in highly conductive media were possible using insulated probes.

Introduction

During the last decade, the use of time domain reflectometry (TDR) has rapidly attained widespread use among researchers in soils, agriculture, forestry, engineering and environmental studies to measure volumetric soil moisture and bulk soil electrical conductivity (e.g., Topp et al. 1980; Topp and Davis 1985; Dasberg and Dalton 1985; Dalton and van Genuchten 1986; Constanz and Murphy 1990; Arulanandan 1991; Wraith and Baker 1991; Kachanoski 1992; Pelletier and Tan 1993). This increase in use has been paralleled by numerous advances in practical techniques, technology and conceptual

understanding (Topp et al. 1990), including systems for remote automatic monitoring of probes (Baker and Allmaras 1990; Heimovaara and Bouten 1990; Herkelrath et al. 1991) and improved methods for calibration and signal analysis (Yanuka et al. 1988; Roth et al. 1990; Van Loon et al. 1990; Dirksen and Dasberg 1993; Wraith et al. 1993).

Attenuation of the signal by the soil can limit the maximum probe length. Combinations of high water content and high salinity lead to high electrical conductivity of the media causing dissipation of the voltage pulse before it is reflected back to the source making it necessary to use short probes. The lower limit of probe length is determined by the bandwidth of the TDR system, which is collectively determined by the instrument and noise introduced by the probe, connections and cable. Electronic instruments are traditionally specified in terms of a rated bandwidth, which is the range of frequencies from DC or zero to the highest frequency component of the signal which the instrument can measure. Since the TDR instrument is usually intended for pulse analysis it is more significant to specify a limiting rise time, where rise time is defined as the time required for a pulse to rise from 10 to 90 % of its final value. A convenient relationship between instrument bandwidth, B in megahertz, and rise time, t_r in microseconds, is given in Eq. [142] (Oliver and Cage, 1971).

$$B = K / t_r, \quad K \approx 0.35 \qquad [142]$$

Thus, instruments with a typical bandwidth specified at 2.5 GHz and 20 GHz are capable of measuring signals with rise times of 140 ps and 17.5 ps respectively.

A common TDR system to determine water content of soils is the Tektronix 1502B (2.5 GHz bandwidth) with probe lengths $\geq$ 0.15 m (Topp and Davis, 1985;

Zegelin et al. 1989; Kachanoski et al., 1990; Heimovaara and Bouten, 1990; Wraith et al. 1993). The practical lower limit of probe length for water measurements using a Tektronix 1502 has been about 0.1 m with a reported uncertainty of ±0.02 m^3/m^3 (Keng and Topp 1983; Dalton and van Genuchten, 1986). Malicki et al. (1992) reported using 0.054 m probes read with a TDR moisture meter operating with a 250 ps rise-time pulse. Heimovaara (1993) found that probes less than 0.05 m in length could not be used with cable lengths greater than 3.2 m because of increased rise times of the signal.

The principle objective of this research was to develop and test short high resolution probes for use with a high bandwidth TDR instrument to measure moisture content in laboratory columns. The secondary objective of this research was to investigate the use of insulating the probes for measuring soil moisture contents made in highly conductive media with high solute concentrations present.

Material and Methods

For laboratory column experiments on ion diffusion currently underway by the authors, it was necessary to design short TDR probes (< 0.075 m long) capable of high resolution measurements of water content and salinity. These measurements required the elimination of the spurious noise introduced through connectors and baluns present in previous probe designs. These needs were the motivation behind our principle objective to design short, high resolution TDR probes. High quality gold plated Sub-Miniature, type A (SMA) connectors rated to 18 GHz were used throughout the system in place of bayonet connectors (BNC) with typical frequency responses of 2.5 GHz. SMA connectors increase the repeatability of the measurements as connections are

disconnected and reconnected more accurately than with a BNC connection (J. Kennedy, Technical engineer, Tektronix Inc., Beaverton OR. 1992, personal communication). Signal quality was best when factory assembled high quality coaxial cable assemblies matching the rated bandwidth of the instrument were used rather than cable assemblies built in our lab from type RG-58/59 coaxial cable and off the shelf SMA or BNC connectors. A 1.25 m long flexible 50 ohm coaxial cable (Tektronix part # 174-1428-00) with male SMA connectors on both ends were used to make measurements.

The balun was eliminated from the system by running the coaxial cable directly to the soil probe (Figure 32). Systems using two parallel probes commonly use a balun to attach coaxial cable to parallel TV wire (Topp and Davis, 1985). Noise introduced along the parallel TV cable connected to the probe causes problems when used with short probes by degrading the signal, thus making it difficult to interpret. Sometimes the balun is incorporated directly into the probe (Spaans and Baker 1993) or a three wire probe design (Zegelin et al. 1989) is used to ensure a balanced signal on the probe. In the present research a balanced signal was not found to be required to obtain usable signals, therefore no balun was used. A three wire probe was constructed by replacing the mounting screw (Figure 32) with a third probe wire and the resulting signal showed no noticeable increase in signal clarity. It was found to be more advantageous to securely fasten the probe to the ring to prevent movement of the probe wires in the media, which could result in measurement errors due to air gaps (Annan 1977).

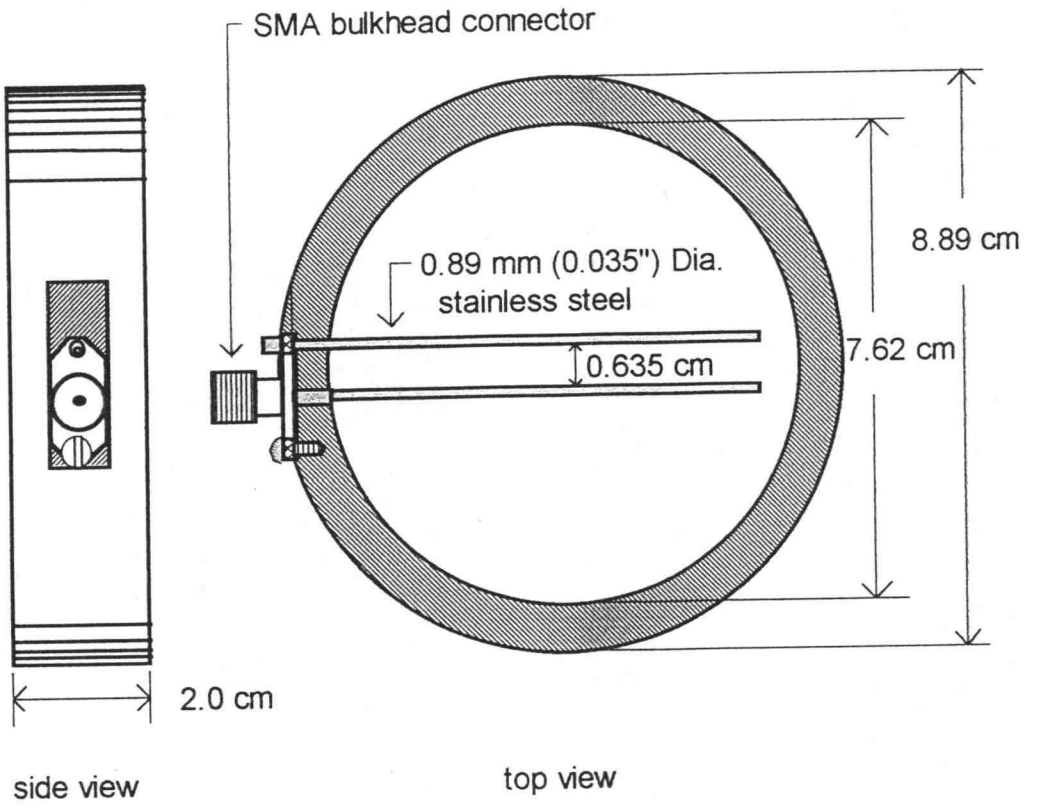

Figure 32. Short TDR probe and acrylic rings.

The bandwidth of the TDR system and rise time of the pulse generated affect the quality of the signal to be analyzed. A Tektronix 11801 digital sampling oscilloscope with an SD-24 TDR sampling head was used to generate, display and determine measurements from the TDR signal. This system is a 20 GHz digital sampling oscilloscope, generating a TDR pulse with a rise time of 25 ps at the connector on the instrument. This instrument allowed sharp pulses to be generated along the probe and high resolution storage and display of the resulting signal. The signal could then be analyzed directly using algorithms built into the oscilloscope or stored digitally and transferred via a GPIB interface to a personal computer to be further analyzed.

The probes, shown in Figure 32, were made from 0.889 mm diameter stainless steel wire and plated with 14K gold to facilitate soldering. The two probe wires were soldered to a commercially available SMA bulkhead connector (ITT Type 50-645-4524-310) that could be connected directly to the coaxial cable from the TDR system. One probe wire was soldered directly to the center conductor and the second probe wire was soldered to the connector body using a brass bushing. Probes with wire lengths of 0.075, 0.05 and 0.025 m were constructed and tested. The bulkhead connector was machined to fit a mating surface in an acrylic ring, as shown in Figure 32, through which the probe extends into the media placed in the ring. Rings, one and two cm in height, were constructed from acrylic tubing (7.62 cm ID x 8.89 cm OD) and machined to accept the TDR probes and secured to the ring using size 3-48 brass machine screws.

Test cells were constructed from 2 cm high rings, as shown in Figure 32, by attaching a flat acrylic plate on the bottom with silicone caulk. The test cells were packed with Accusand Grade 40/50 silica sand (Unimin Corp., ID) to a dry bulk density of 1.75 g

cm^{-3} and leveled off. Six test cells were prepared using two probes at each length of 0.025, 0.05 and 0.075 m by inserting each probe through a ring and into the media. Initially, the media was saturated with deaired water and test cells were allowed to equilibrate overnight sealed in plastic containers. The following calibration procedure was devised by assuming that an equilibrium moisture content would exist in the cell after allowing the cell to equilibrate for 24 h in sealed plastic containers to maintain a high relative humidity at the surface of the cell. At low moisture contents, the pore sizes are assumed small enough that capillary rise brings the system to a relatively constant moisture content within the 2 cm height of the ring within 24 h. At high moisture contents, gravity redistribution of the water can result in uneven of moisture contents within the 2 cm height of the ring. It is assumed that even though there exists a higher volumetric moisture content at the base of the cell than the top of the cell, the probe, inserted at the 1 cm height, will measure the average moisture content in the cell which is equal to the moisture content determined gravimetrically. Calibration was carried out by alternately leaving the test cell open to the atmosphere to evaporate water and then resealing the plastic container to allow the cell to come to an equilibrium moisture content throughout the cell, after which the test cell was weighed and TDR measurements made. A final measurement was determined after oven drying the test cell. In this manner a complete calibration curve could be obtained in about 10 days. Additional calibrations were made using six test cells fitted with 0.075 m probes in a 1:1 by volume peat vermiculite media. The media was then wetted with solutions of distilled water, 0.5, 0.1, 0.01 and 0.001 M KBr solutions. Successive measurements were then carried out in the manner described above.

The secondary objective of this research was investigated by insulating a probe from the media with Teflon heat shrink tubing, (Small Parts Inc., FL, part # D-SMT-22). To measure the transit time of a pulse, direct electrical contact between the probe and the media need not be maintained. By placing a thin layer of electrical insulating material between the probe and the media the pulse may be maintained along the length of the probe when measurements are made in highly conductive media with high solute concentrations present. Two test cells were fitted with 0.075 m probes; one insulated and one non-insulated. The test cells were filled with Grade 30/40 Accusand and saturated with a 0.5 M KBr solution, and calibration was carried out in the manner described above.

To illustrate the advantages of using the high bandwidth TDR system, actual traces of 0.025, 0.05 and 0.075 m probes mounted in acrylic rings in air from the high bandwidth, 20 GHz, TDR sampling system are shown in Figure 33 and compared with a trace from a 0.075 m probe in air from the commonly used Tektronix 1502B (2.5 GHz) set at a maximum horizontal resolution shown in Figure 34. By comparing the traces in Figure 33 and Figure 34 it is clear that more accurate timing measurements can be made when using short probes with the 20 GHz bandwidth system than with the 2.5 GHz system. Using the 20 GHz system, the resulting signal loss through the coaxial cable, connectors and probe is about 10 ps and accurate timing measurements were made with probe lengths down to 0.025 m.

The travel time of the pulse along the probe is then determined by finding the inflection points as the pulse encounters changing impedance along the probe. These points were initially found by shorting the probe as it enters the inside of the ring and at

the end of the ring as shown in Figure 35. Subsequent measurements were made by finding these same points on each pulse. By using this method to calculate the travel time (T_d), the length of the probe (L) can be calculated from the apparent velocity (v) using Eqs. [143] and [144] (Topp et al. 1980) when the probe wires are surrounded by a media with known dielectric properties; air (dielectric constant, K_a = 1.0) and water (dielectric constant, K_a = 80.50 @ 20°C).

$$v = 2L / T_d \qquad [143]$$

$$v \approx c / \sqrt{K_a} \qquad [144]$$

The actual measured of all probe lengths were found to agree to less than 0.3 mm of the probe length calculated from Eqs. [143] and [144] using pulse travel times measured in air and water.

Once the pulse travel time for each probe length is determined in air (T_{air}), Eqs. [143] and [144] are combined to form Eq. [145] and K_a is calculated after measuring the travel time, T_d in the unknown media.

$$K_a = (T_d / T_{air})^2 \qquad [145]$$

The apparent refractive index, n_a is then calculated from Eq. [146] (Heimovaara, 1993), which is the ratio of the velocity of the pulse in air, c = 2.998 × 10^8 m/s, to the apparent velocity of the pulse in the soil.

$$n_a = \sqrt{K_a} = T_s / T_{air} \qquad [146]$$

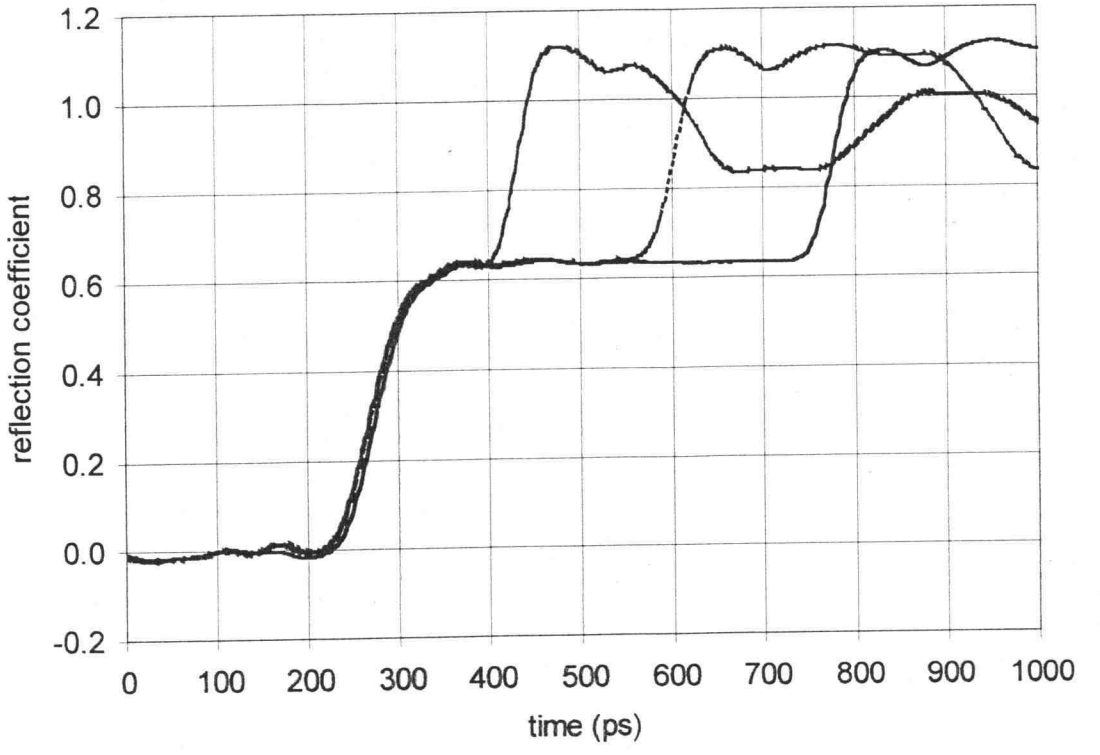

Figure 33. Actual trace from the 20 GHz TDR sampling system using a high resolution 0.025, 0.05 and 0.075 m probe in air.

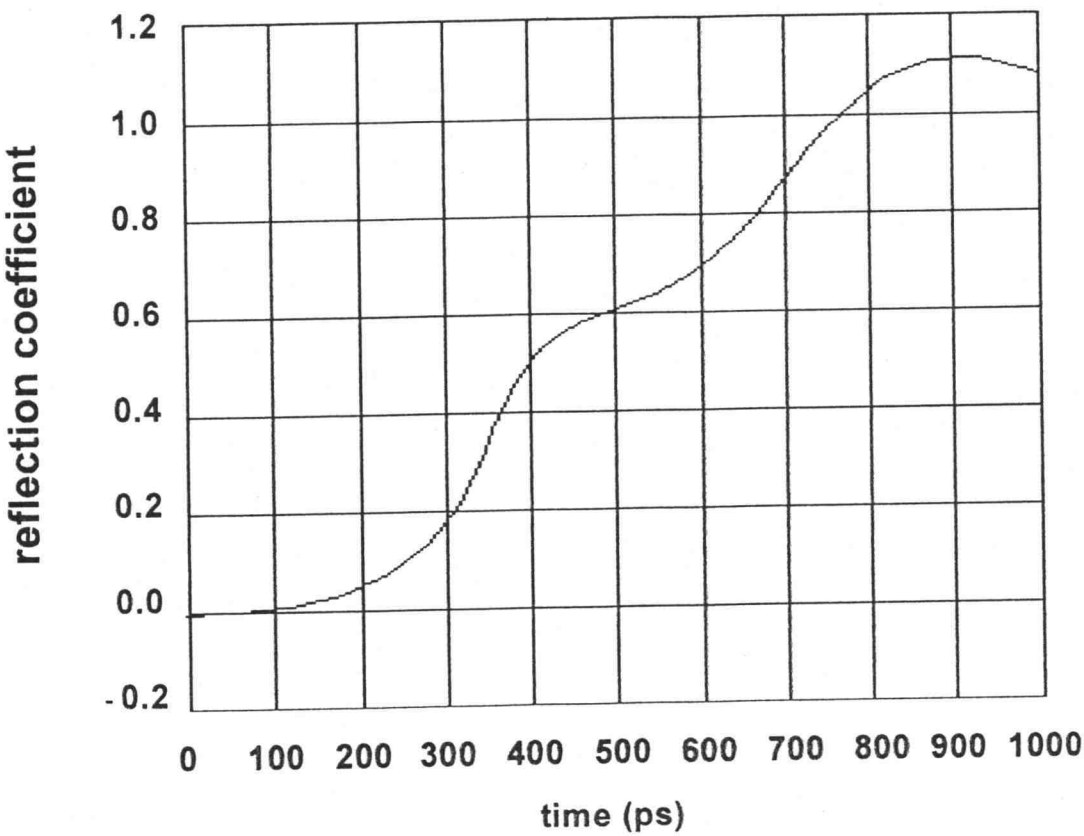

Figure 34. Actual trace from Tektronix 1502B set at maximum resolution (0.1 ft) using a high resolution 0.075 m. probe in air.

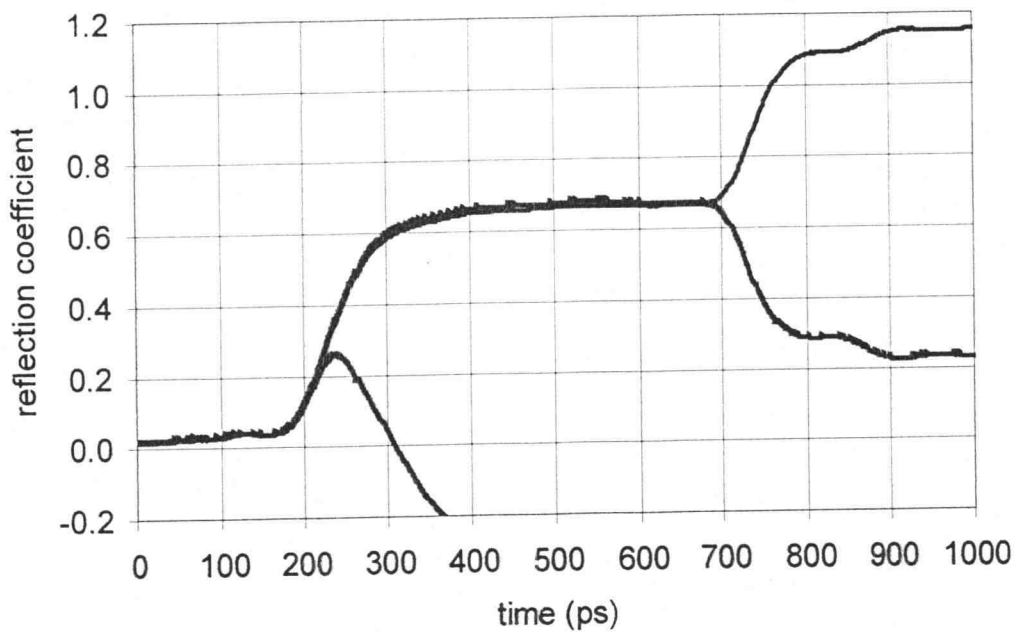

Figure 35. A 0.075 m probe in air is shorted where the probe enters the inside of the ring (T_{start} = 225 ps) and at the end of the probe (T_{end} = 690 ps) to determine the travel time (T_d = 465 ps) , along the length of the probe inside the ring ($L_{in\ ring}$ = 0.0695 m).

The apparent velocity was shown to be linearly related to volumetric moisture content (Herkelrath et al. 1991; Heimovaara 1993) and is a convenient method to develop calibration curves.

Results and Discussion

Results from the tests with the 0.075, 0.05 and 0.025 m probes are shown in Figure 36. The relationship between the measured dielectric constant and volumetric moisture content as determined by Topp et al. (1980) and generally used in practice is

$$\theta_v = -5.3 \times 10^{-2} + 2.92 \times 10^{-2} K_a - 5.5 \times 10^{-4} K_a^2 + 4.3 \times 10^{-6} K_a^3 \qquad [147]$$

K_a is the measured dielectric constant and θ_v is the volumetric moisture content. Eq. [147] is also plotted in Figure 36. The dielectric constants calculated from travel times using Eq. [145] at various moisture contents deviate significantly from the relationship described by Eq. [147]. The results are consistent with Eq. [147] which show that the relative change in K_a at low moisture contents is much less than at higher water contents. This leads to a decreased measurement sensitivity at low moisture contentss when compared to high moisture contents.

Due to the deviations from Eq. [147] and the decreased measurement sensitivity, it was found advantageous to relate the apparent refractive index, n_a to volumetric moisture content, θ_V. Figure 37 -Figure 39 show a linear relationship between n_a and θ_V for the 0.075, 0.05 and 0.025 m probes in Grade 40/50 Accusand. Individual regression lines were determined for each probe length and compared to a common regression line obtained by pooling the data from all probe lengths. The individual regression lines

provided a better estimate for volumetric moisture content (F - statistic (2,42) = 15.60). For a given measured apparent refractive index, 90% prediction intervals for volumetric moisture content were calculated for probes of each length separately (Weisberg, 1985). For the most accurate moisture determinations it is recommended that a separate calibration be performed with each combination of probe length and soil. The calibration procedure described in the materials and methods section was found to be relatively quick and easy, especially considering the increased gain in measurement precision when compared to using a pooled calibration or Eq. [147].

The average prediction interval increased with decreasing probe length. For 0.075, 0.05 and 0.025 m probes, the average prediction intervals were ±0.0125, ±0.025, and ±0.035 m^3/m^3 respectively. The critical timing measurements necessary for determination of moisture content were able to be made precisely, even with probe lengths as short as0.025 m using the high bandwidth TDR instrument. The decrease in precision with probe length was due to air gaps, probe scale and wall effects. The air gap problem becomes more serious with shorter probes of smaller diameter (Annan 1977) and any slight movement of the probe could cause an air gap to occur, decreasing the apparent refractive index. As the probe size approaches the scale of the soil particles, the sampling volume becomes smaller and the pore water interacts with the probe in the same way it would with the soil, causing jumps in the measured apparent refractive index as the soil dries or wets. To prevent air gaps between the probe and the soil it was necessary to secure the probe to the acrylic ring. The effect of the acrylic where the probe enters the soil was found to be relatively insignificant for the longer, 0.075 m probes but increased

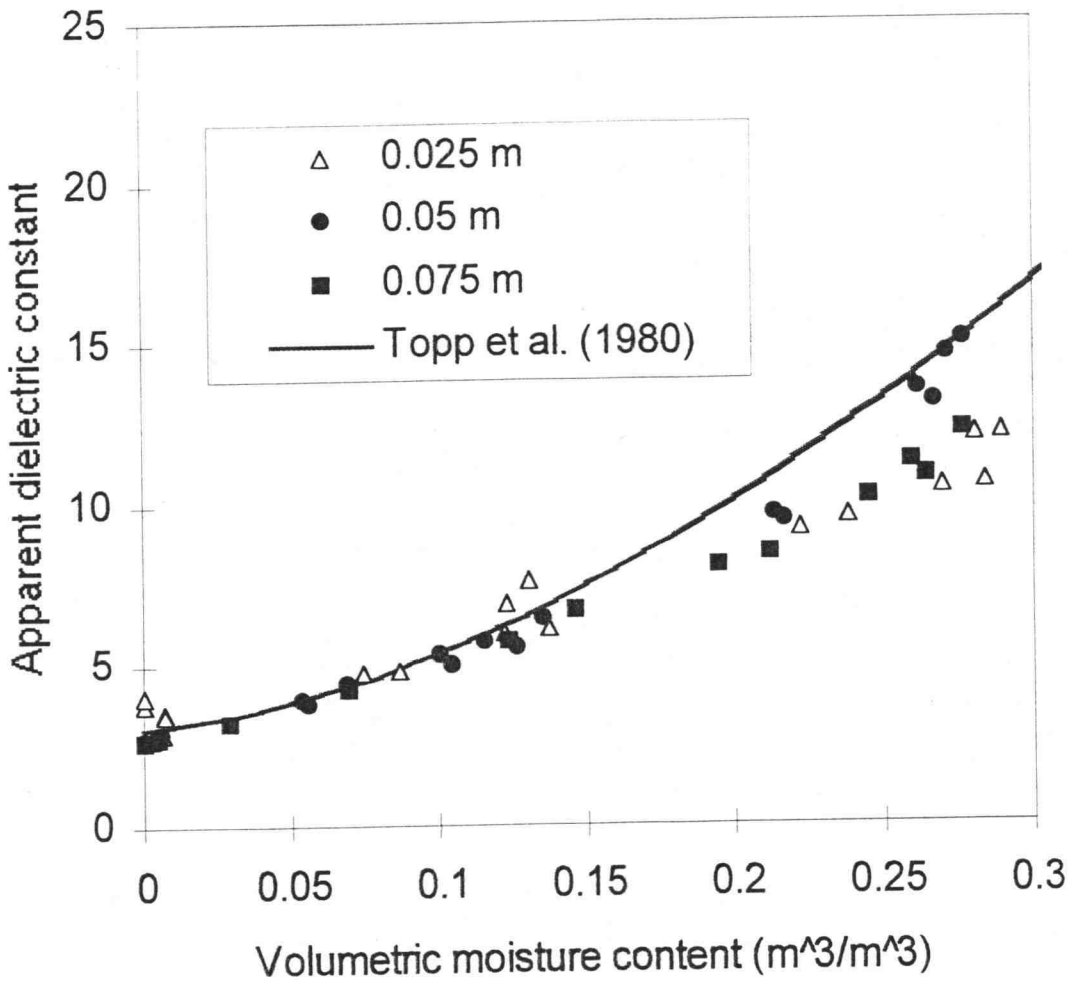

Figure 36. Calibration of 0.075, 0.05 cm and 0.025 m probes, K_a vs. volumetric moisture content, in Grade 40/50 Accusand compared with Topp et al. (1980), Eq. [147].

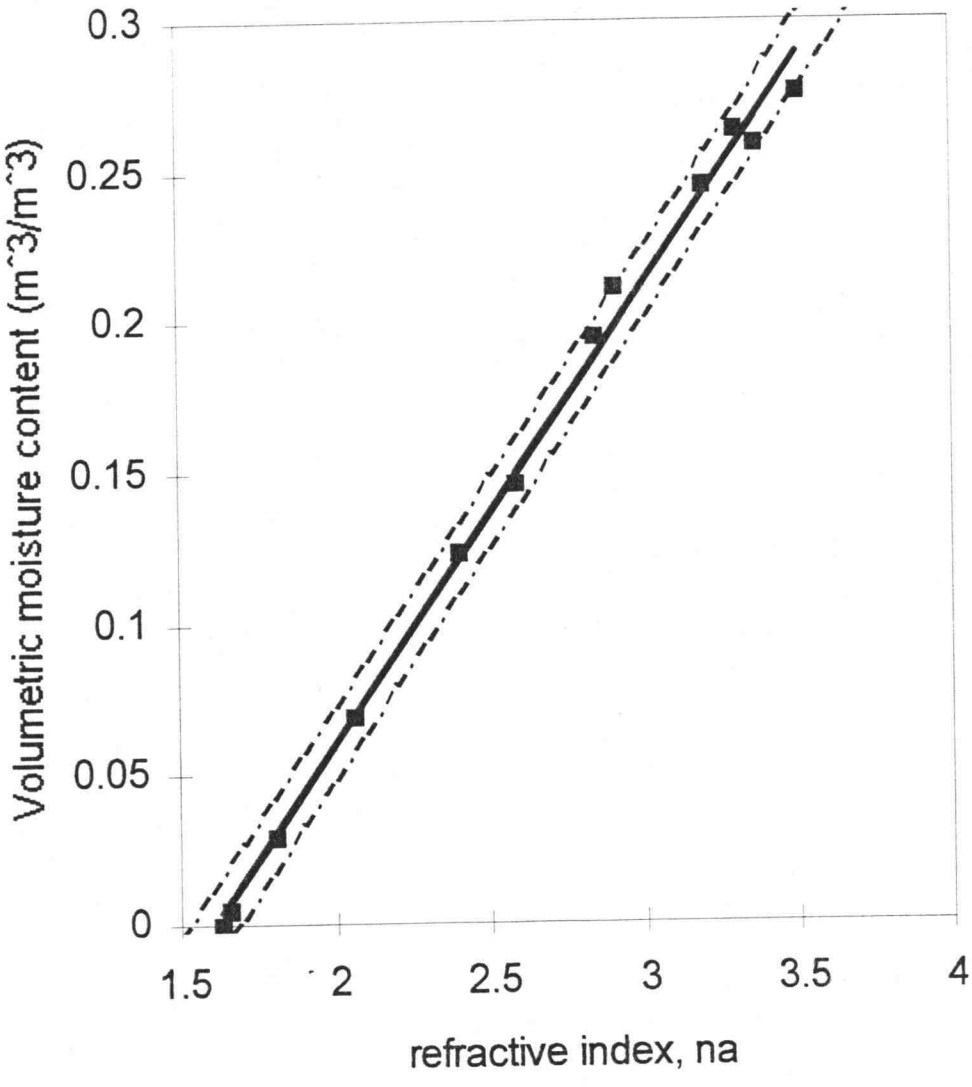

Figure 37. Calibration of 0.075 m probes, apparent refractive index, n_a vs. volumetric moisture content, θ_v, in Grade 40/50 Accusand. Standard Error = 0.007 m^3/m^3; slope = 0.153; intercept = -0.246 m^3/m^3. Dashed lines enclose a 90% prediction interval for θ_v for a given value of n_a.

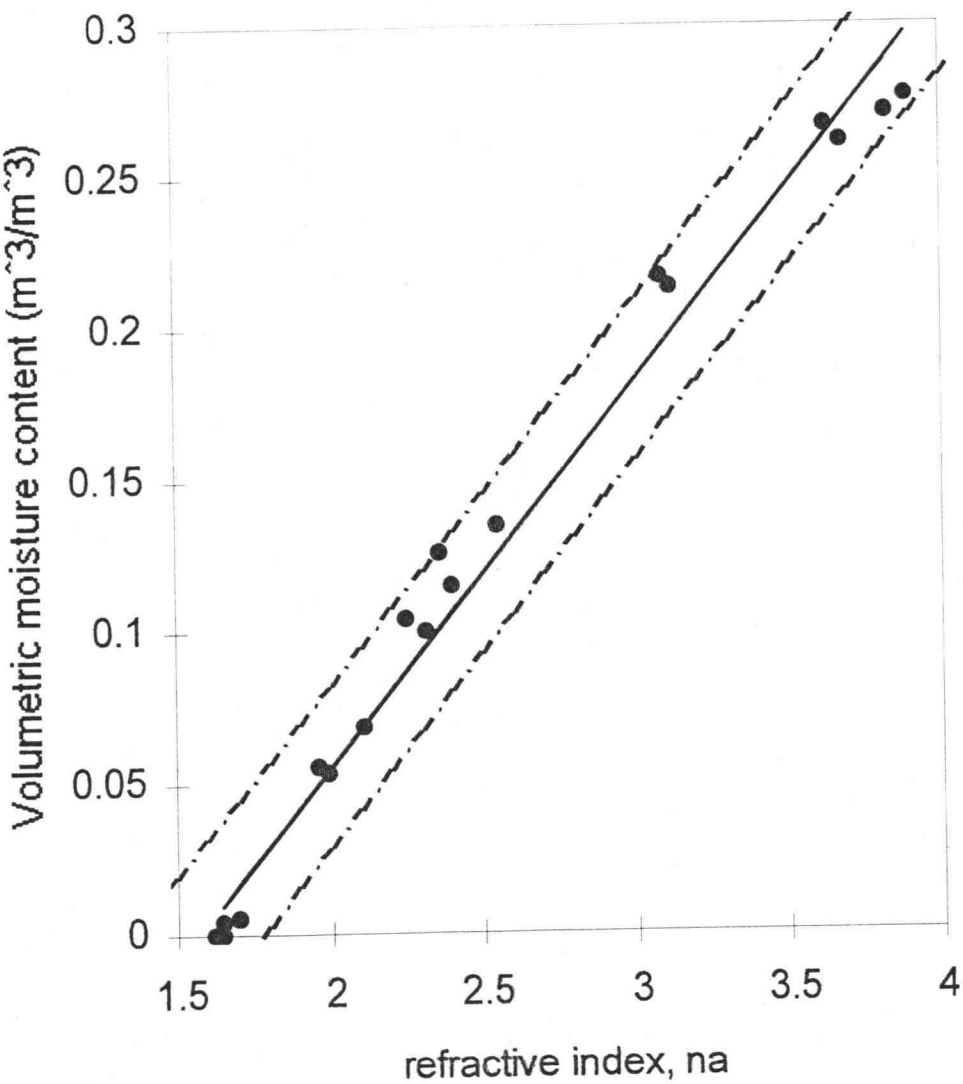

Figure 38. Calibration of 0.05 m probes, apparent refractive index, n_a vs. volumetric moisture content, θ_v, in Grade 40/50 Accusand. Standard Error = 0.015 m^3/m^3; slope = 0.128; intercept = -0.200 m^3/m^3. Dashed lines enclose a 90% prediction interval for θ_v for a given value of n_a.

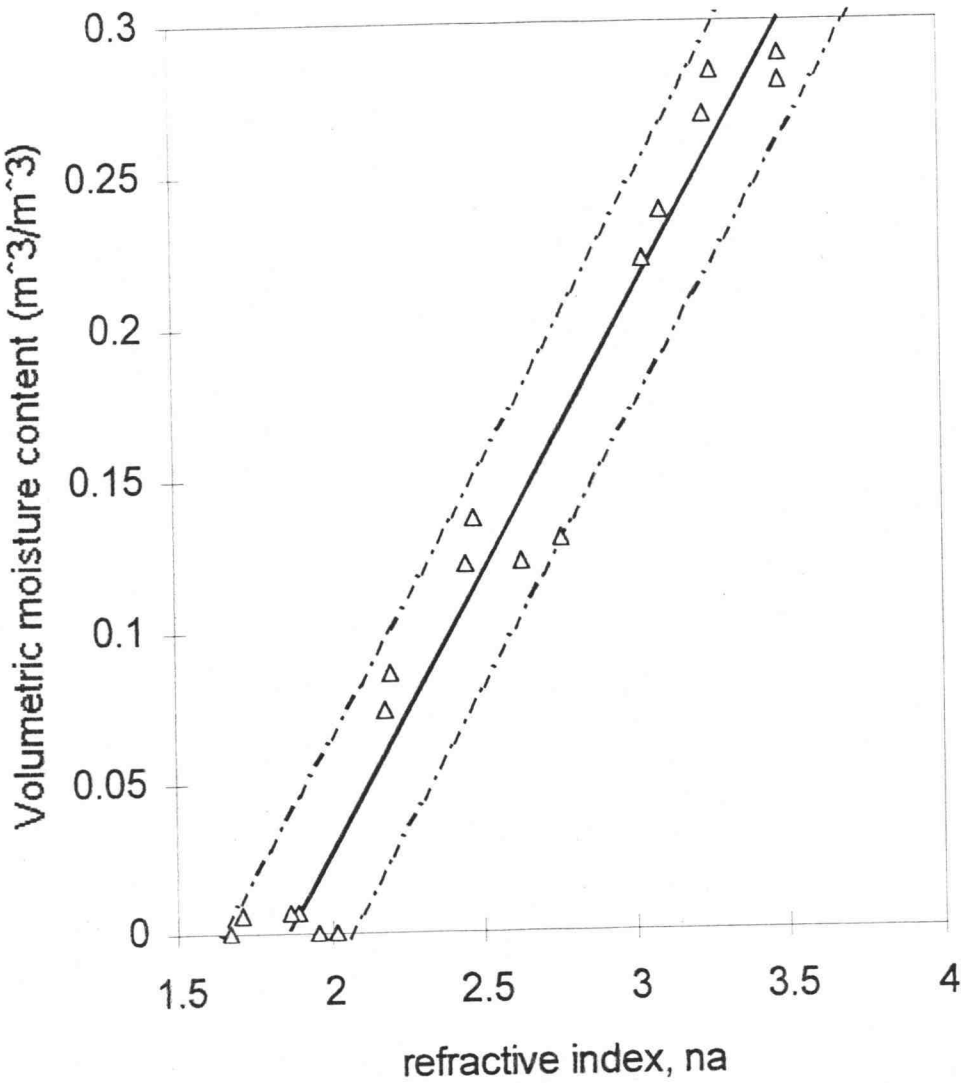

Figure 39. Calibration of 0.025 m probes, apparent refractive index, n_a vs. volumetric moisture content, θ_v, in Grade 40/50 Accusand. Standard Error = 0.021 m^3/m^3; slope = 0.185; intercept = -0.344 m^3/m^3. Dashed lines enclose a 90% prediction interval for θ_v for a given value of n_a.

as probe length decreased because a greater proportion of the apparent refractive index is due to the acrylic. Separate calibrations are carried out for each probe length to keep this effect constant.

Similar results were obtained with the peat:vermiculite media as shown in 0.025 m using the high bandwidth TDR instrument. The calibration curve for our probes, apparent refractive index versus volumetric moisture content, depended on the length of the probe and whether the probe was insulated with Teflon heat shrink. For the most accurate moisture determinations it is recommeded that a separate calibration be performed with each combination of probe length and soil. An evaporation technique to calibrate probes was developed and found to be a relatively quick and easy method for calibration of short probes in the laboratory. The use of Teflon insulated probes makes the application of TDR soil moisture measurements in highly conductive media possible.

Figure 40, but gave a different relationship between n_a and θ_v than the Accusand. In practice, the water content of this media rarely drops below 25 m^3/m^3 so to more accurately determine moisture content we only use the calibration data obtained above 25 m^3/m^3. The relationship for the peat:vermiculite media is linear between moisture contents of 25 to 80 m^3/m^3. The data plotted in 0.025 m using the high bandwidth TDR instrument. The calibration curve for our probes, apparent refractive index versus volumetric moisture content, depended on the length of the probe and whether the probe was insulated with Teflon heat shrink. For the most accurate moisture determinations it is recommeded that a separate calibration be performed with each combination of probe length and soil. An evaporation technique to calibrate probes was developed and found to

be a relatively quick and easy method for calibration of short probes in the laboratory. The use of Teflon insulated probes makes the application of TDR soil moisture measurements in highly conductive media possible.

Figure 40 was obtained using media wetted with KBr solutions ranging from 0 M to 0.5 M KBr, further verifying that moisture measurements are independent of bulk conductivity of the media. At moisture contents below 25 m^3/m^3 the relationship between n_a and θ_v deviated slightly from this line. This is most likely due to bound water in this highly organic media.

The results of the secondary objective are summarized in Figure 41 and Figure 42. A bare 0.075 m probe was inserted in sand moistened with 0.5 M KBr to 0.15 m^3/m^3 moisture by volume . The time of travel was impossible to determine because of the loss of signal due to conductivity of the sand (Figure 41). When the Teflon was applied, the dielectric constant of the media was determined and a separate calibration curve was obtained as shown in Figure 42. The accuracy of the insulated 0.075 m probe was ±0.05 m^3/m^3 using 90% prediction intervals. We found that insulating the probes by dipping the probes in epoxy resins and using PVC heat shrink tubing was inferior to the use Teflon heat shrink tubing. The Teflon heat shrink tubing formed a uniformly thick, constant dielectric layer over the entire probe length that remained intact the duration of the lab testing. Further testing needs to be carried out to determine how the insulation would endure field use in undisturbed soils. The use of Teflon insulated probes makes the application of TDR soil moisture measurements in highly conductive media possible.

Conclusions

Short high resolution probes for use with a high bandwidth TDR instrument were developed and tested. The critical timing measurements necessary for determination of moisture content were able to be made precisely, even with probe lengths as short as0.025 m using the high bandwidth TDR instrument. The calibration curve for our probes, apparent refractive index versus volumetric moisture content, depended on the length of the probe and whether the probe was insulated with Teflon heat shrink. For the most accurate moisture determinations it is recommeded that a separate calibration be performed with each combination of probe length and soil. An evaporation technique to calibrate probes was developed and found to be a relatively quick and easy method for calibration of short probes in the laboratory. The use of Teflon insulated probes makes the application of TDR soil moisture measurements in highly conductive media possible.

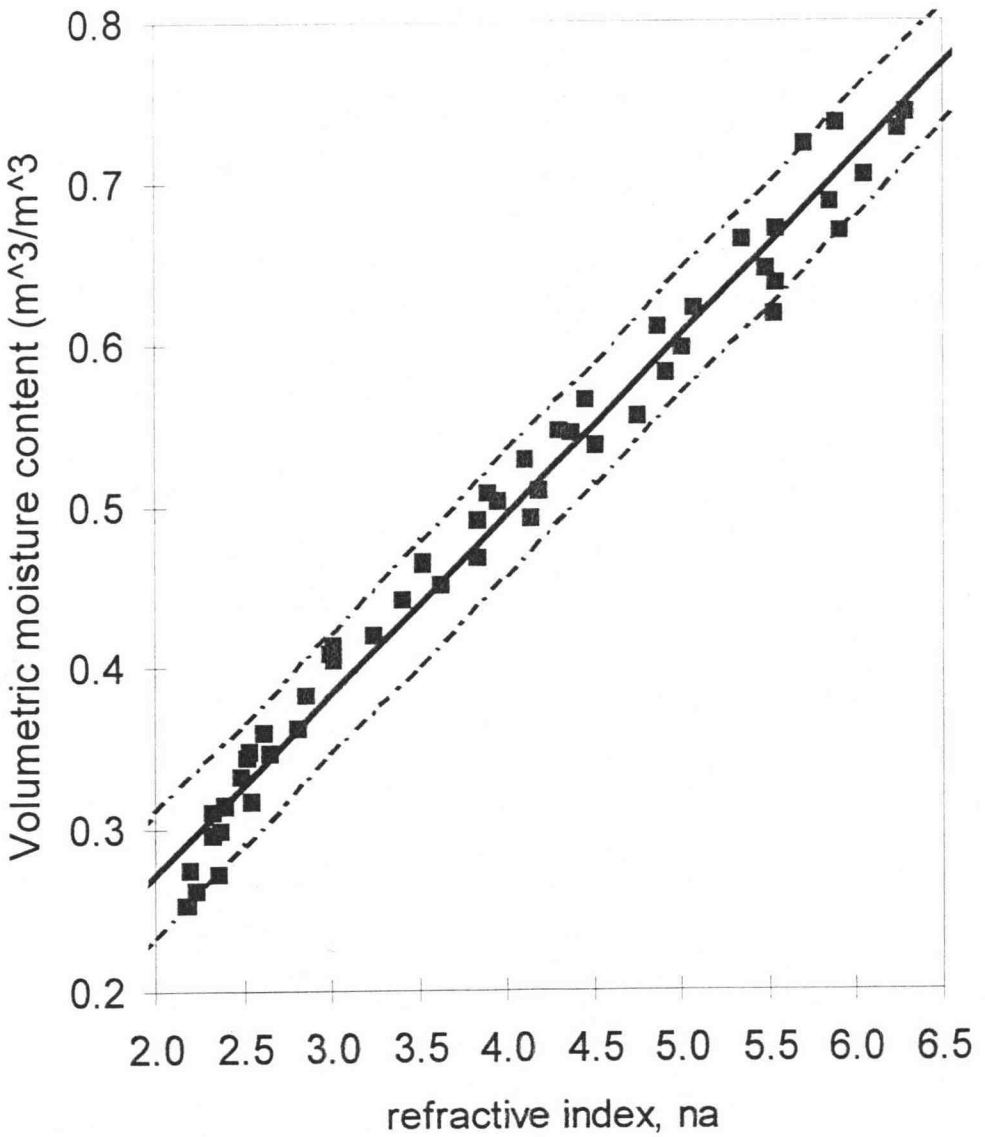

Figure 40. Calibration of 0.075 m. probes, apparent refractive index, n_a vs. volumetric moisture content, θ_v, in potting media containing 1:1 by volume peat:vermiculite. Standard Error = 0.022 m^3/m^3; slope = 0.111; intercept = -0.497 m^3/m^3. Dashed lines enclose a 90% prediction interval for θ_v for a given value of n_a.

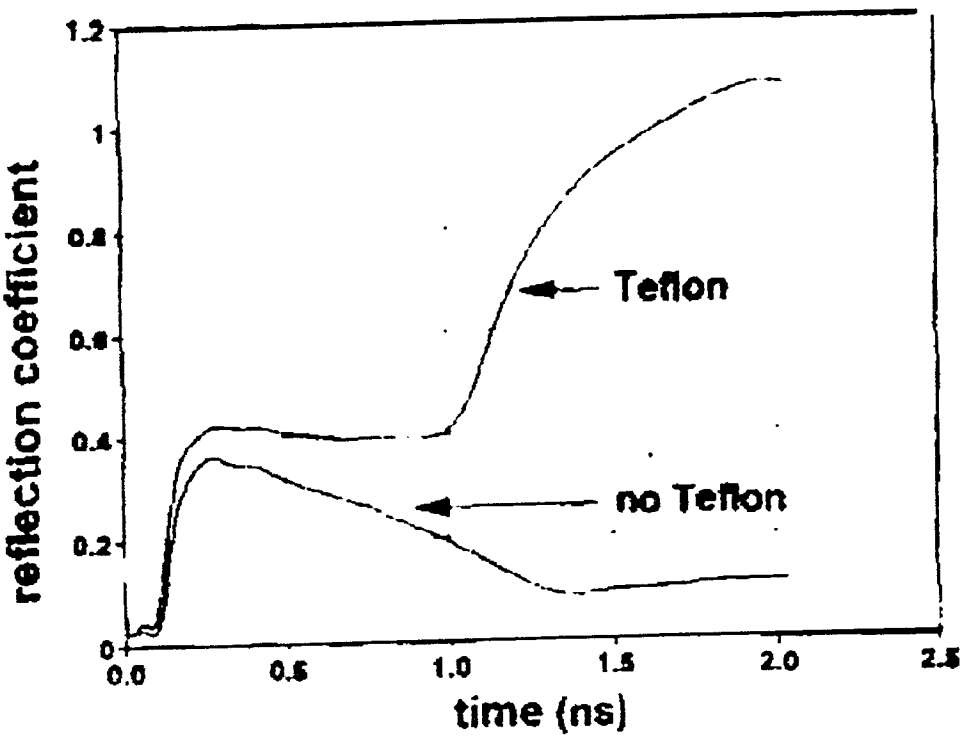

Figure 41. Using Teflon heat shrink tubing to maintain pulse readability. 0.075 m probe in Grade 30/40 silica sand wetted with 0.5 M KBr solution to a 0.15 m^3/m^3 volumetric moisture content.

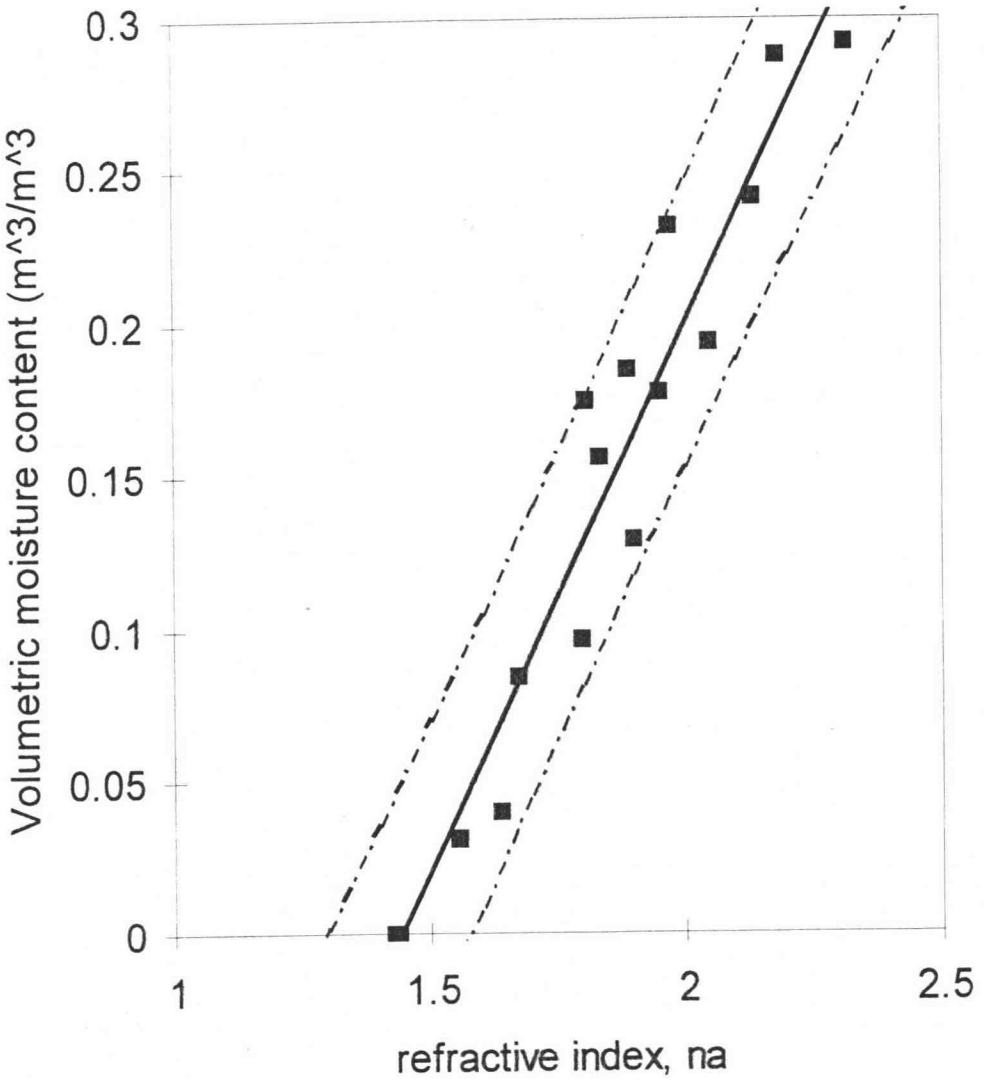

Figure 42. Calibration of 0.075 m probes insulated with Teflon heat shrink tubing, apparent refractive index n_a vs. volumetric moisture content, θ_v, in Grade 30/40 Accusand. Standard Error = 0.026 m^3/m^3; slope = 0.358; intercept = -0.517 m^3/m^3. Dashed lines enclose a 90% prediction interval for θ_v for a given value of n_a.

References

Annan, A. P. 1977. Time-domain reflectometry -- Air-gap problem for parallel wire transmission lines. Report of Activities, Part B; Geol. Surv. Can., Paper 77-1B. pps 59-62.

Arulanandan, K. 1991. Dielectric method for prediction of porosity of saturated soil. Journal of Geotechnical Engineering. 117(2):319-330.

Baker, J. M. and R. R. Allmaras. 1990. System for automating and multiplexing soil moisture measurement by time domain reflectometry. Soil Sci. Soc. Am. J. 54(1):1-6.

Constantz, J. and Fred Murphy. 1990. Monitoring moisture storage in trees using time domain reflectometry. J. Hydrol. 119:31-42.

Dalton, F. N. and M. Th. van Genuchten. 1986. The time-domain reflectometry method for measuring soil water content and salinity. Geoderma. 38:237-250.

Dasberg, S. and F. N. Dalton. 1985. Time domain reflectometry field measurements of soil water content and electrical conductivity. Soil Sci. Soc. Am. J. 49:293-297.

Dirksen, C. and S. Dasberg. 1993. Improved calibration of time domain reflectometry soil water content measurements. Soil Sci. Soc. Am. J. 57:660-667.

Heimovaara, T. J. 1993. Design of triple-wire time domain reflectometry probes in practice and theory. Soil Sci. Soc. Am. J. 57:1410-1417.

Heimovaara, T. J. and W. Bouten. 1990. A computer-controlled 36-channel time domain reflectometry system for monitoring soil water contents. Water Resources Research. 26(10):2311-2316.

Herkelrath, W. N., S. P. Hamburg and Fred Murphy. 1991. Automatic, real-time monitoring of soil moisture in a remote field area with time domain reflectometry. Water Resources Research. 27(5):857-864.

Kachanoski, R. G., E. Pringle, and A. Ward. 1992. Field measurement of solute travel times using time domain reflectometry. Soil Sci. Soc. Am. J. 56:47-52.

Kachanoski, R. G., I. J. Van Wesenbeeck, P. Von Bertoldi, A. Ward, and C. Hamlen. 1990. Measurement of soil water content during three-dimensional axial-symmetric water flow. Soil Sci. Soc. Am. J. 54:645-649.

Keng. J. C. W. and G. C. Topp. 1983. Measuring water content of soil columns in the laboratory: A comparison of gamma ray attenuation and TDR techniques. Can. J. Soil Sci. 63: 37-43.

Malicki, M. A., R. Plagge, M. Renger and R. T. Walczak. 1992. Application of time-domain reflectometry (TDR) soil moisture miniprobe for the determination of unsaturated soil water characteristics from undisturbed soil cores. Irrig. Sci. 13:65-72.

Oliver, B. M. and J. M. Cage. 1971. Electronic measurements and instrumentation. p. 372-373. McGraw-Hill Inc., New York, NY.

Pelletier, G and C. S. Tan. 1993. Determining irrigation wetting patterns using time domain reflectometry. HortScience 28(4):338-339.

Roth, K., R. Schulin, H. Fluhler, and W. Attinger. 1990. Calibration of time domain reflectometry for water content measurement using a composite dielectric approach. Water Resources Research. 26(10):2267-2273.

Spaans, E. J. A. and J. M. Baker. 1993. Simple baluns in parallel probes for time domain reflectometry. Soil Sci. Soc. Am. J. 57:668-673.

Topp, G. C., J. L. Davis, and A. P. Annan. 1980. Electromagnetic determination of soil water content: measurements in coaxial transmission lines. Water Resources Research. 16(3):574-582.

Topp, G. C. and J. L. Davis. 1985. Measurement of soil water content using time-domain reflectometry (TDR): A field evaluation. Soil Sci. Soc. Am. J. 49:19-24.

Van Loon, W. K. P., E. Perfect, P. H. Groenevelt. and B. D. Kay. 1990. A new method to measure bulk electrical conductivity in soils with time domain reflectometry. Can. J. Soil Sci. 70:403:410.

Weisberg, S. 1985. Applied linear regression. Second edition. John Wiley and Sons. NewYork.

Wraith, J. M. and J. M. Baker. 1991. High-resolution measurement of root water uptake using automated time-domain reflectometry. Soil Sci. Soc. Am. J. 55:928-932.

Wraith, J. M., S. D. Comfort, B. L. Woodbury, and W. P. Inskeep. 1993. A simplified waveform analysis approach for monitoring solute transport using time domain reflectometry. Soil Sci. Soc. Am. J. 57:637-642.

Yanuka M., G. C. Topp, S. Zegelin, and W. D. Zebchuk. 1988. Multiple reflection and attenuation of time domain reflectometry pulses: Theoretical considerations for applications to soil and water. Water Resources Research. 24(7):939-944.

Zegelin, S. J., I. White, and D. R. Jenkins. 1989. Improved field probes for soil water content and electrical conductivity measurement using time domain reflectometry. Water Resources Research. 25(11):2367-2376.